UNCLASSIFIED

AD NUMBER
AD113062
CLASSIFICATION CHANGES
TO unclassified
FROM secret
AUTHORITY
ARDC ltr, 3 Feb 1958

THIS PAGE IS UNCLASSIFIED

NOTICE: THIS DOCUMENT CONTAINS INFORMATION AFFECTING THE NATIONAL DEFENSE OF THE UNITED STATES WITHIN THE MEANING OF THE ESPIONAGE LAWS, TITLE 18, U.S.C., SECTIONS 793 and 794. THE TRANSMISSION OR THE REVELATION OF ITS CONTENTS IN ANY MANNER TO AN UNAUTHORIZED PERSON IS PROHIBITED BY LAW.

SECRET

AD 113062

BELL Aircraft CORPORATION

BUFFALO 5, NEW YORK

TECHNICAL DATA

N. F. Meullen, Project Aerodynamicist

Design Group	Aero-Thermal Group
W. J. Gill	C. M. Schmidt
R. O. Brigham	A. H. Blessing
T. W. Egan	D. J. Gibson
	A. J. Hanawalt

Approved Emmons
P. C. Emmons

REPORT NO. D143-945-033

BRASS BELL - RECONNAISSANCE
AIRCRAFT WEAPON SYSTEM
AERODYNAMICS DESIGN
VOLUME II

COPY NO. DATE October 31, 1956

This document contains 180 pages

56AA 60178

SECRET

Form G6-[illegible]S Rev 655

AFFIX TO DOCUMENT

BELL IDENTIFICATION NO. [illegible]

BELL

THE ATTACHED DOCUMENT CONTAINS

SECRET

INFORMATION

AND AS SUCH IT MUST BE

RECORDED—On a Classified Document Register and Marked with the assigned Bell Identification number when you originate, reproduce or receive a classified document. See Bell Aircraft Corporation Security Manual.

STORED—Minimum requirements call for a steel file cabinet equipped with a steel bar and three-position combination dial type padlock.

TRANSMITTED—In double sealed opaque containers. The classified information shall be protected from direct contact with the inner cover by a sheet or by folding inward. Only the inner container shall indicate the classification Both the inner and outer cover shall indicate the addressee and addressor.

By U S registered mail, air or surface, by appropriately cleared messenger designated by the company or by protected commercial express, air or surface, under billing which assures the highest degree of protective handling.

RECEIPTED FOR—Classified Document Receipt, Form G6-32, must be enclosed within the inner wrapper for all SECRET matter dispatched outside Bell Aircraft Corporation Niagara Frontier Division facilities. Hand Receipt, Form G6-42, must be used for all transmittals of SECRET matter between individuals or by company mail service within Bell Aircraft Corporation Niagara Frontier Division facilities.

ADDITIONAL SECURITY INFORMATION

(1) Bound documents—Classified books or pamphlets, the pages of which are permanently and securely bound together so that the pages thereof cannot be removed without damage or mutilation, shall be marked with the classification assigned to the document at the top and bottom on the outside of the front cover and back cover, title, first and last pages and all printed, typed, or written pages which contain classified information, including the reverse side, if used.

(2) Correspondence and unbound documents—Correspondence and other documentary material not permanently and securely bound together shall be marked with the appropriate classification at the top and bottom of each page which contains classified information, including the cover page, if used. The marking shall be placed so that it will not be hidden from view when the pages are clipped or stapled together.

(3) Letters of Transmittal—A letter transmitting defense information shall be marked with a classification at least as high as the highest classified inclosure. Letters of Transmittal, when appropriate, shall indicate that upon removal of classified inclosures such letters will be downgraded or declassified

(4) National Defense Stamp. Documents containing classified defense information furnished authorized persons other than those of or in the employ of, agencies of the Department of Defense shall bear a notation substantially as follows."

"This document contains information affecting the national defense of the United States, within the meaning of the Espionage Laws, Title 18, U.S.C., Sections 793 and 794, the transmission or revelation of which in any manner to an unauthorized person is prohibited by law."

(5) "Restricted Data". In addition to the markings prescribed above, "Restricted Data" will be marked in capital letters, "Restricted Data - Atomic Energy 1954" not less than 1/4 inch in height

SECTION 4.0

UNPOWERED FLIGHT

4.1 INTRODUCTION

The major portion of the ground to ground range of the Brass Bell vehicle is attained during the hypersonic glide at altitudes above 100,000 feet. Hence, design problems concerned with hypersonic and low density conditions are encountered chiefly during this unpowered portion of flight.

Though there has recently arisen some doubt as to whether a maximum aerodynamic lift to drag ratio path actually results in the maximum glide range the method of calculation of maximum range in this report will continue to assume it does. Although the range calculated in this manner may not be a maximum, it will still provide a convenient order of magnitude comparison of range attained by the two vehicles under consideration. Likewise, the ranges will be compared on the basis of untrimmed maximum lift to drag ratio. Although the two ranges so calculated may be slightly in error, it is felt the incremental range (which is more important as a basis of comparison) will be more accurate.

Similarly, wherever comparative studies of the two configurations are made, it is assumed the error incurred by using rather simple methods of analysis is equally applicable to both. Thus, it should still be possible to draw qualitative conclusions regarding the relative merits of each configuration.

In the general studies and investigations pertaining to the design problems associated with a Brass Bell type vehicle in unpowered flight, an

attempt has been made to uncover rather than to solve. Such studies are intended to serve as the means whereby hypersonic design experience and methods can be accumulated and developed for application to the future work associated with a Brass Bell vehicle. In some instances, they may even be so general in nature as to be applicable to hypersonic design studies of other than a Brass Bell vehicle. These later studies are included herein for such usefulness as they may serve.

4.2 EFFECT OF NOSE DROOP ON THE AERODYNAMIC CHARACTERISTICS OF THE FINAL STAGE

Previous work, as shown in Reference 4.2.1, indicated that the "undrooped" conical nose might be subjected to considerably higher temperatures near the nose-afterbody juncture (because of the possible onset of turbulent flow in this region) than would a conical nose that was "drooped" so that its bottom meridian was continuous with the bottom of the cylindrical afterbody. This five degree nose droop reduced the temperatures on the bottom of the nose by reducing the local Reynolds number so that the likelihood of the appearance of turbulent flow, at the high Mach numbers, on the bottom of the nose was lessened. In the aforementioned reference some discussion was included concerning the aerodynamic disadvantages attendant with a drooped nose design but no data was presented. This preliminary study was undertaken to provide data concerning this facet of the aerodynamic design and to point out, once again, the belief that combining the best components will necessarily yield the best over-all design is often a mistaken one.

The configuration chosen for investigation was the proposed "external" type final stage with a 60 inch diameter fuselage and in the glide configuration, i.e., the tanks and motors have been jettisoned. This configuration was selected because the nose portion was relatively smaller for this configuration than the nose portion of the 78 inch diameter "internal" type final stage. Thus, the relative effect of drooping this nose should be less than that caused by drooping the nose of the "internal" type final

stage. The fore and aft wing position was varied so that the effect of nose droop as affected by neutral point location could also be studied.

The lift of the nose, wing, and afterbody were calculated as explained in Section 3.3 of Reference 4.2.1 for the "external" type final stage with the undrooped nose. The nose lift for the configuration with the nose droop of five degrees was calculated by using its center line angle of attack which was obviously five degrees less than the remainder of the configuration. The total lift coefficients of these two configurations, i.e. nose droop of zero degrees and five degrees, at Mach numbers of 4.0, 8.0, 12.0, and 16.0, are presented in Figures 4.2-1, 4.2-2, 4.2-3, and 4.2-4. As can be seen the positive lift coefficients of the configuration with a nose droop of five degrees were less than that of the configuration with zero degrees of nose droop. This difference would be more marked for the "internal" type final stage as the nose being proportionally larger would be carrying even a greater percentage of the total lift.

The lifts of the various components were integrated about Station 552 in order to calculate the pitching moment. This was done using two wing positions: first, leading edge of the wing MAC at Station 450; second, leading edge of the wing MAC at Station 476. These calculated pitching moments were plotted versus lift so that the effect of nose droop on longitudinal stability could be studied. From Figures 4.2-5, 4.2-6, 4.2-7, and 4.2-8 it can be seen that nose droop had only a slight effect on the aircraft's static margin at both wing positions. However, as the Mach number increased so that nonlinear effects became more apparent it was found that

five degree nose droop slightly increased both the instability (more positive dC_m/dC_L) at low C_L's and the stability (more negative dC_m/dC_L) at high C_L's above that calculated for the configuration with the undrooped nose. Perhaps the most striking difference between the two configurations was evidenced by the large diving moment imparted by the drooped nose.

This was the main disadvantage attendant with the drooped nose. An aircraft flies, ordinarily, in a trimmed condition (i.e., moments held at zero by control surfaces). Therefore, the exact calculation of aircraft performance must incorporate the trim values of lift and drag. It is obvious that this large increase in diving moment, as caused by the drooped nose, requires appreciably larger control surface deflections with the attendant larger drag penalties. Thus, the slight advantage a drooped nose configuration might possess in untrimmed lift-drag ratio would be quickly erased in more correctly considered case of trimmed lift-drag ratios.

Values of trim lift coefficients were calculated and are presented for Mach numbers of 4.0 to 16.0 in Figures 4.2-9, 4.2-10, 4.2-11, and 4.2-12. (These trim lift values were calculated assuming the control lift force to act at 87 perent of the MAC of the wing.) It can be seen that the trimmed flight of the drooped nose configuration required approximately 1.5 degrees more angle of attack than the undrooped nose configuration flying at the same altitude. Although the temperature was reduced locally on the nose it would be increased everywhere else on the drooped nose configuration. When total heat influx was considered, it appeared likely that the undrooped nose configuration actually required the least coolant weight per unit of

time. Additional studies to verify this conclusion with regard to coolant weight should be undertaken. However, on the basis of the larger control deflections required to trim the drooped nose configuration at high speed flight conditions it was decided at this point in the design investigation, to favor the undrooped nose configuration.

4.2 REFERENCES

4.2.1 Postle, R. S., et al: MX-2276 Reconnaissance Aircraft Weapon System - Aerodynamics, Bell Aircraft Corporation Report No. D143-945-024, December 1, 1955

4.2 SYMBOLS

$\bar{c}$	MAC of exposed wing panel
C_L	Lift coefficient, L/qS_{ref}
$C_{L_{trim}}$	Trim lift coefficient
C_m	Pitching moment coefficient, $M/qS_{ref}\bar{c}$
L	Lift force, pounds
M	Pitching moment, lost pounds
M	Mach number
q	Dynamic pressure, pounds per square foot
S_{ref}	Reference area, area of exposed wing panels, square feet
α	Angle of attack, degrees

SECRET

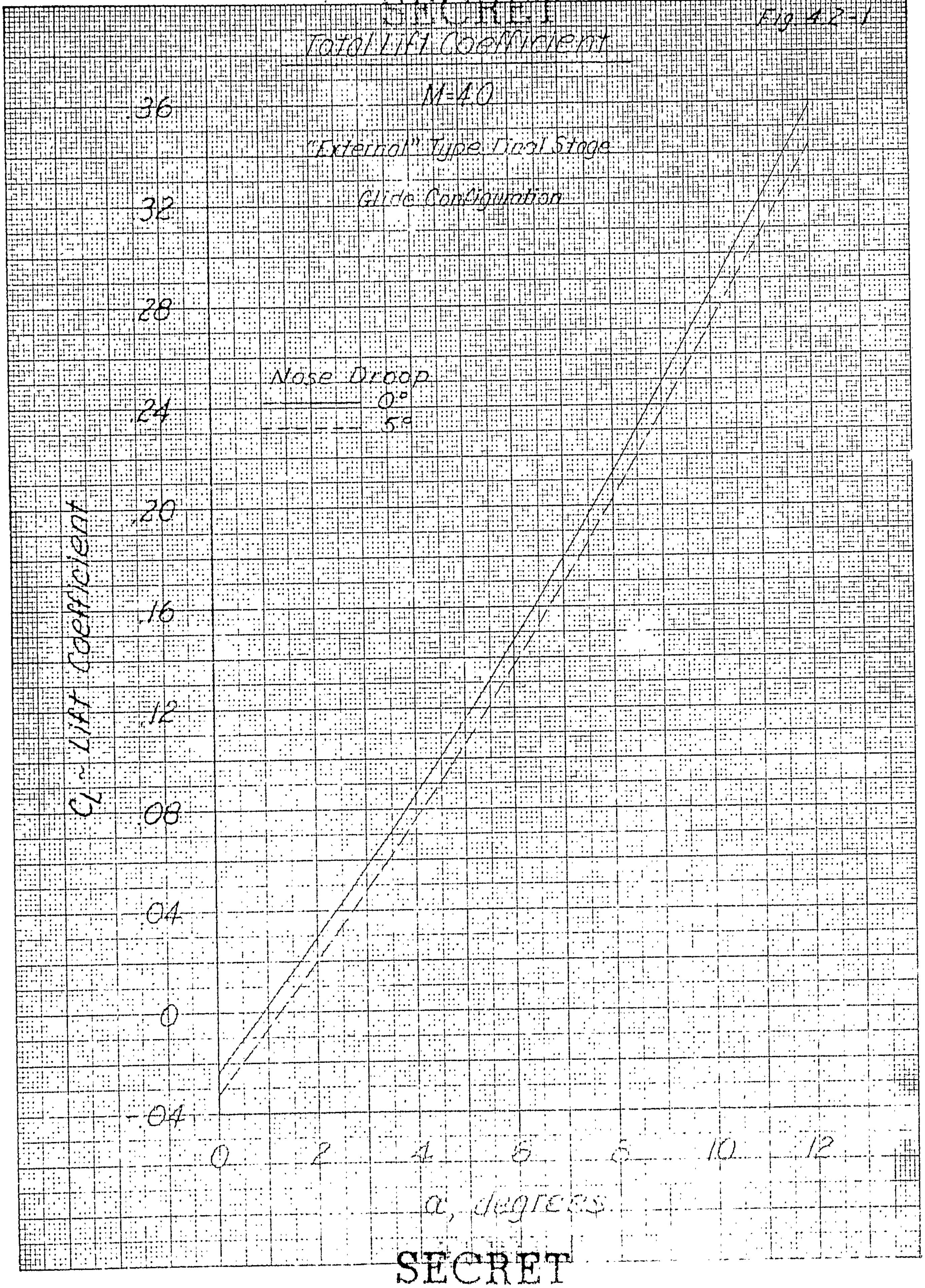

SECRET

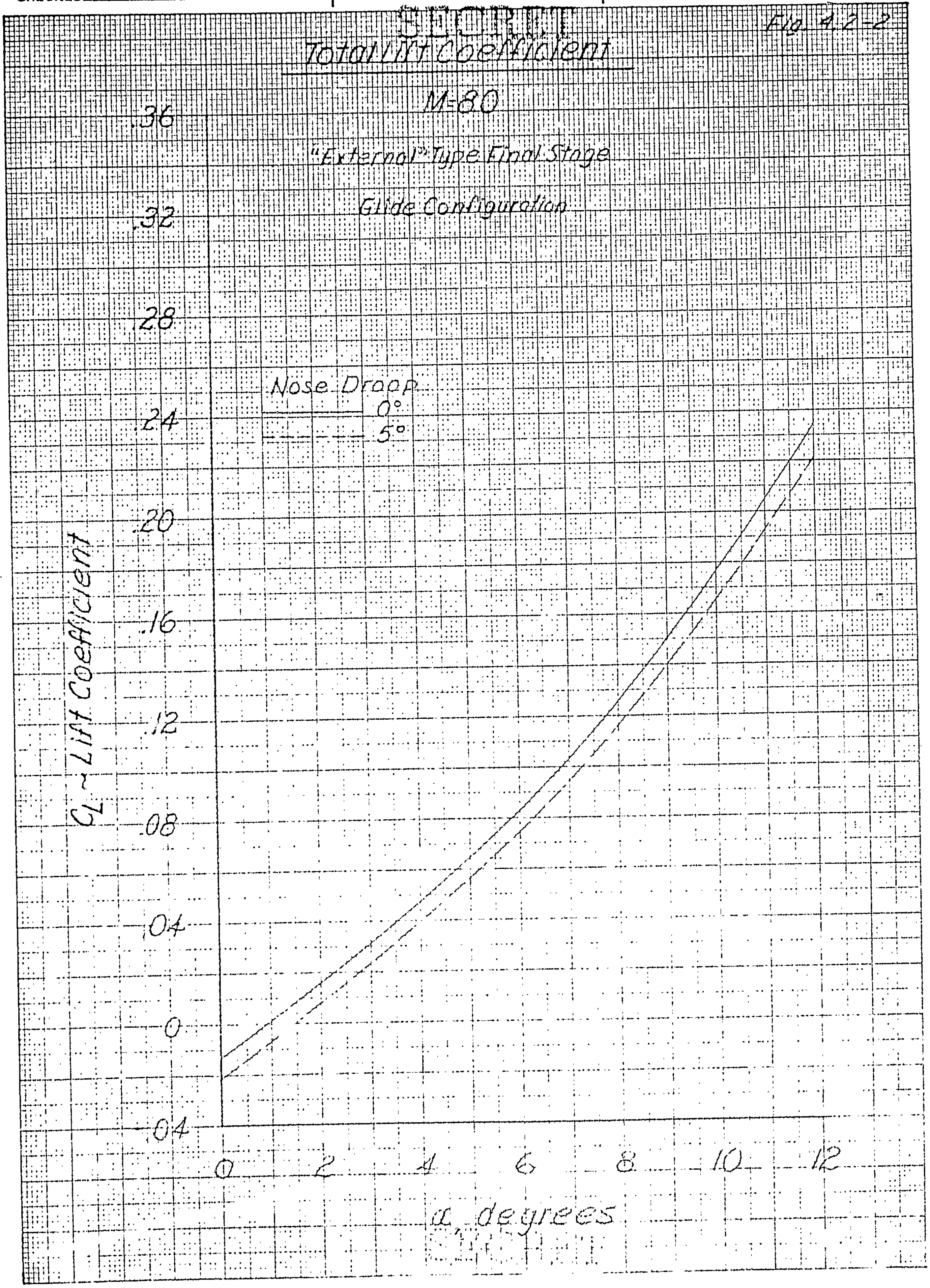
Fig. 4.2-2
Total Lift Coefficient
M-80
"External" Type Final Stage
Glide Configuration
Nose Droop
0°
5°
.36
.32
.28
.24
.20
.16
.12
.08
.04
0
-.04
C_L ~ Lift Coefficient
0
2
4
6
8
10
12
α, degrees

SECRET

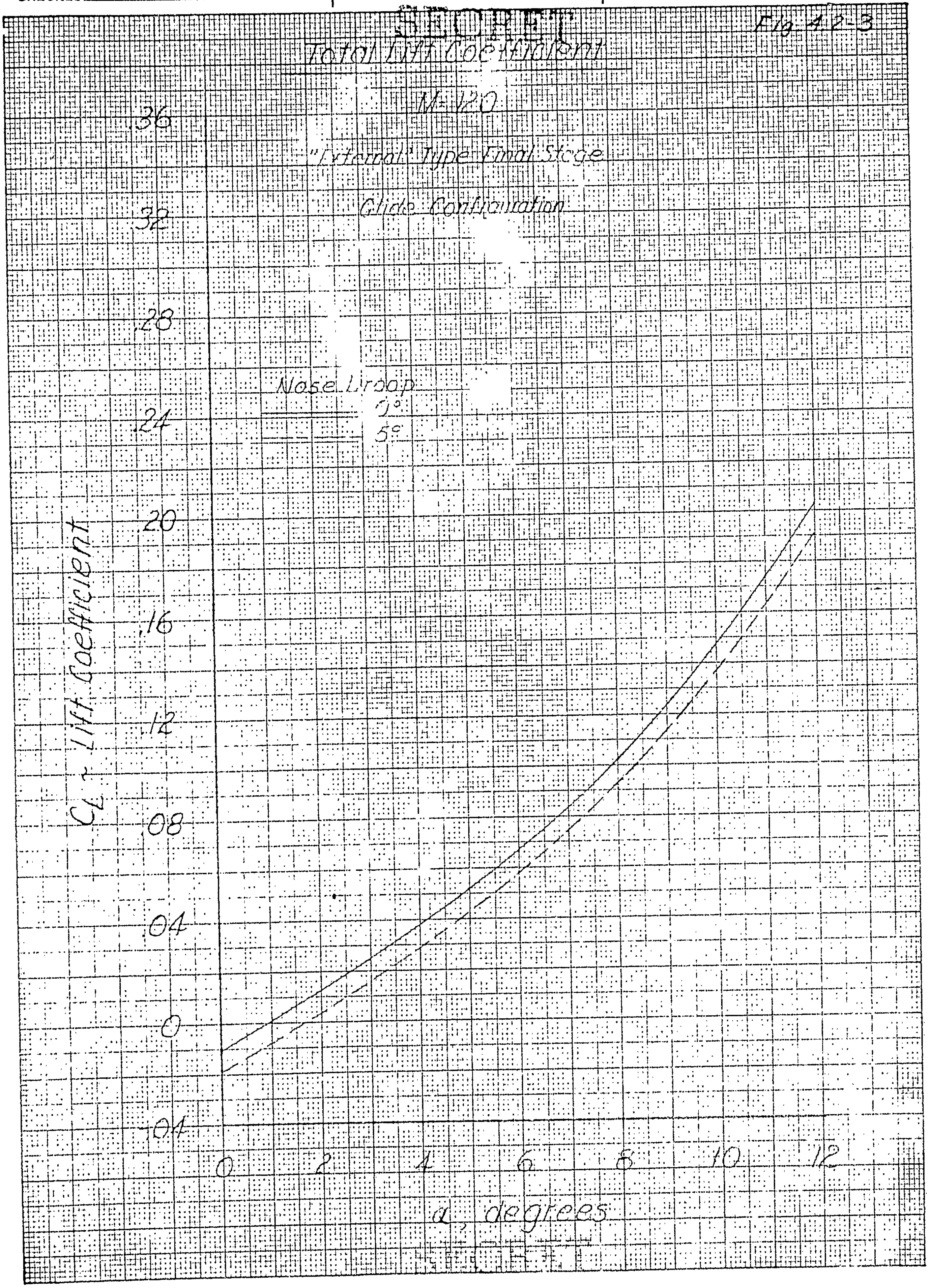
Fig 4.2-3
Total Lift Coefficient
M-120
"External" Type Final Stage
Glide Configuration
Nose Droop
0°
5°
C_L ~ Lift Coefficient
.36
.32
.28
.24
.20
.16
.12
.08
.04
0
-.04
0
2
4
6
8
10
12
α, degrees

SECRET

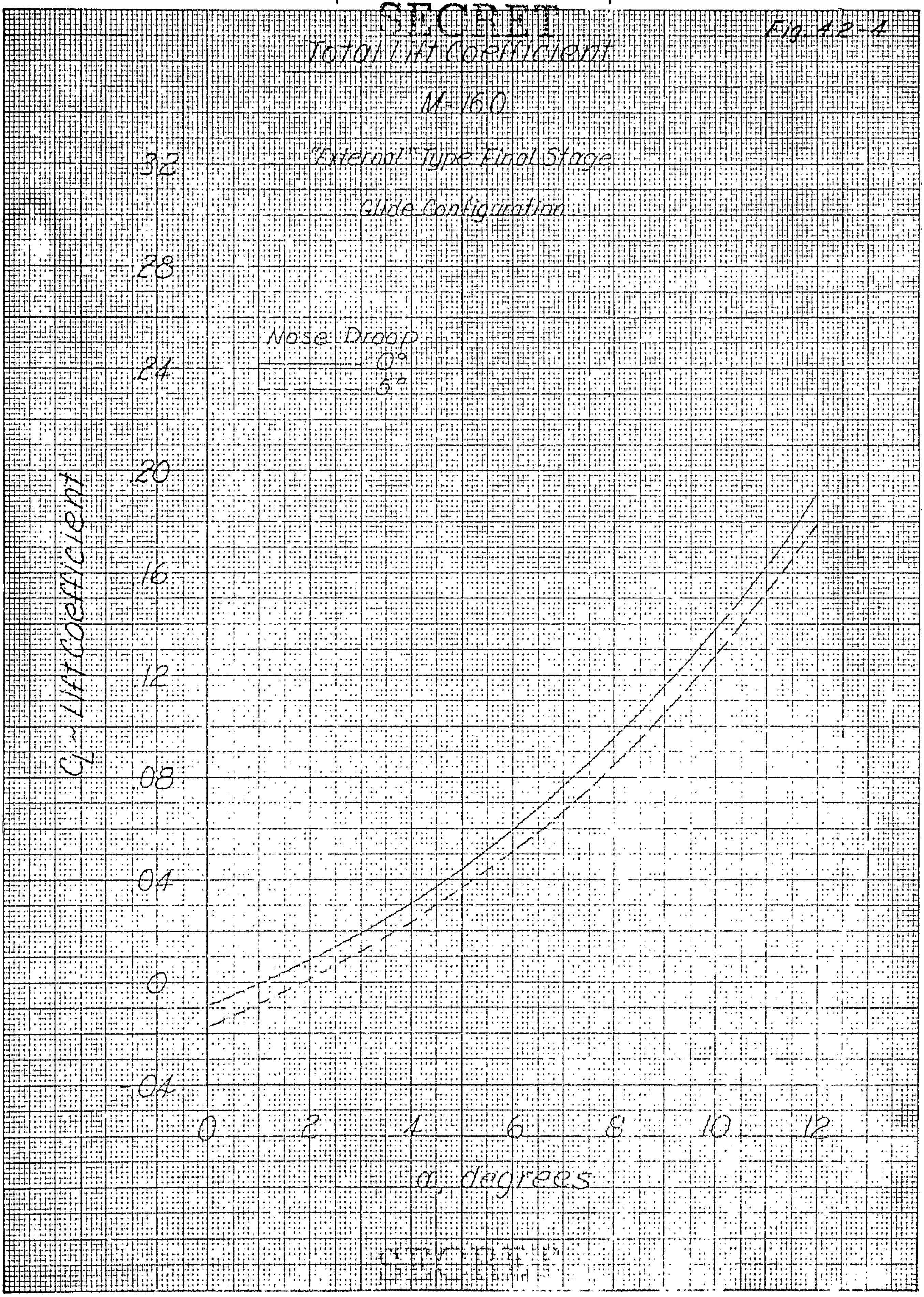

SECRET

SECRET

Fig. 4.2-5

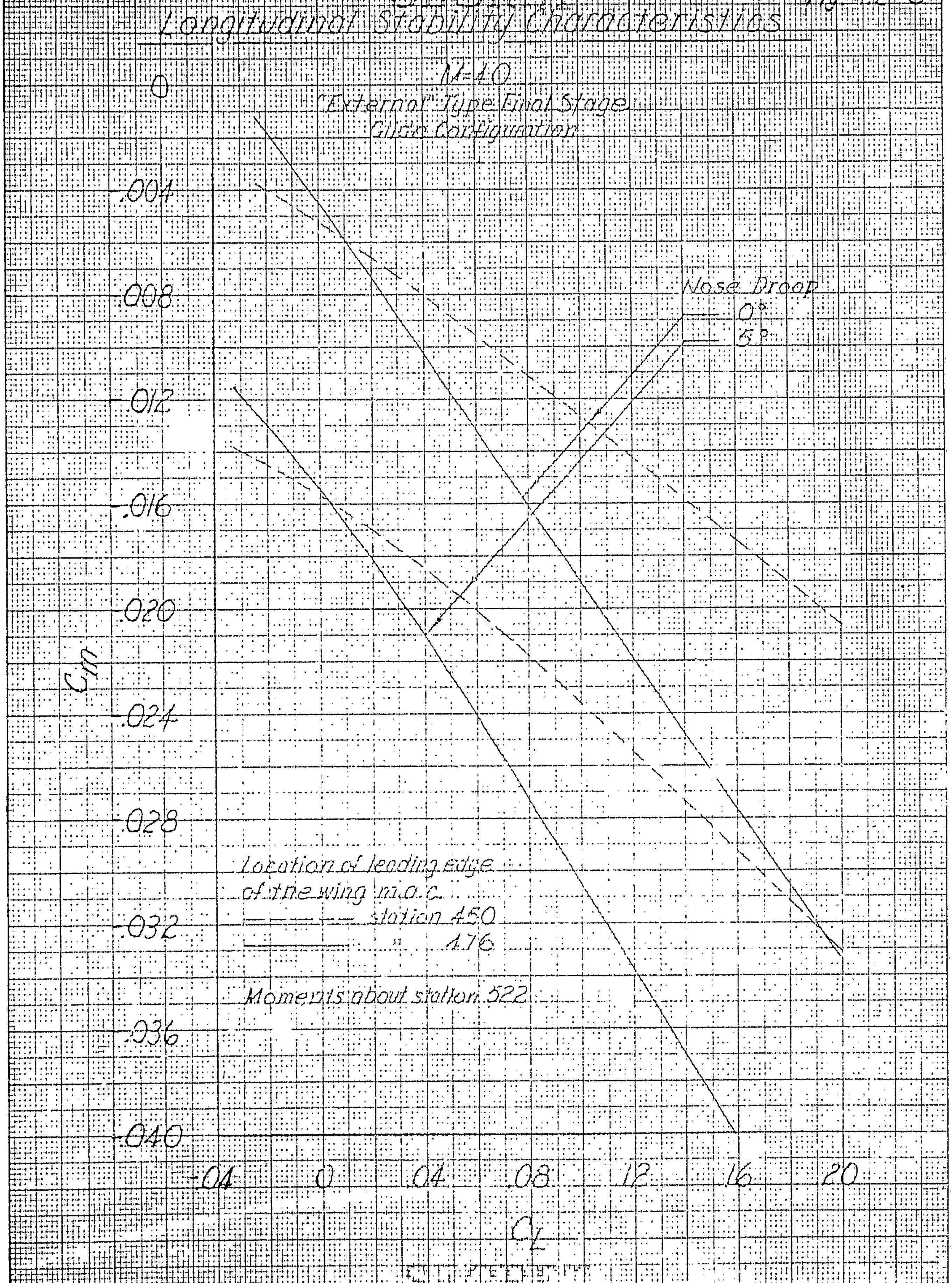

SECRET

Fig 42-6

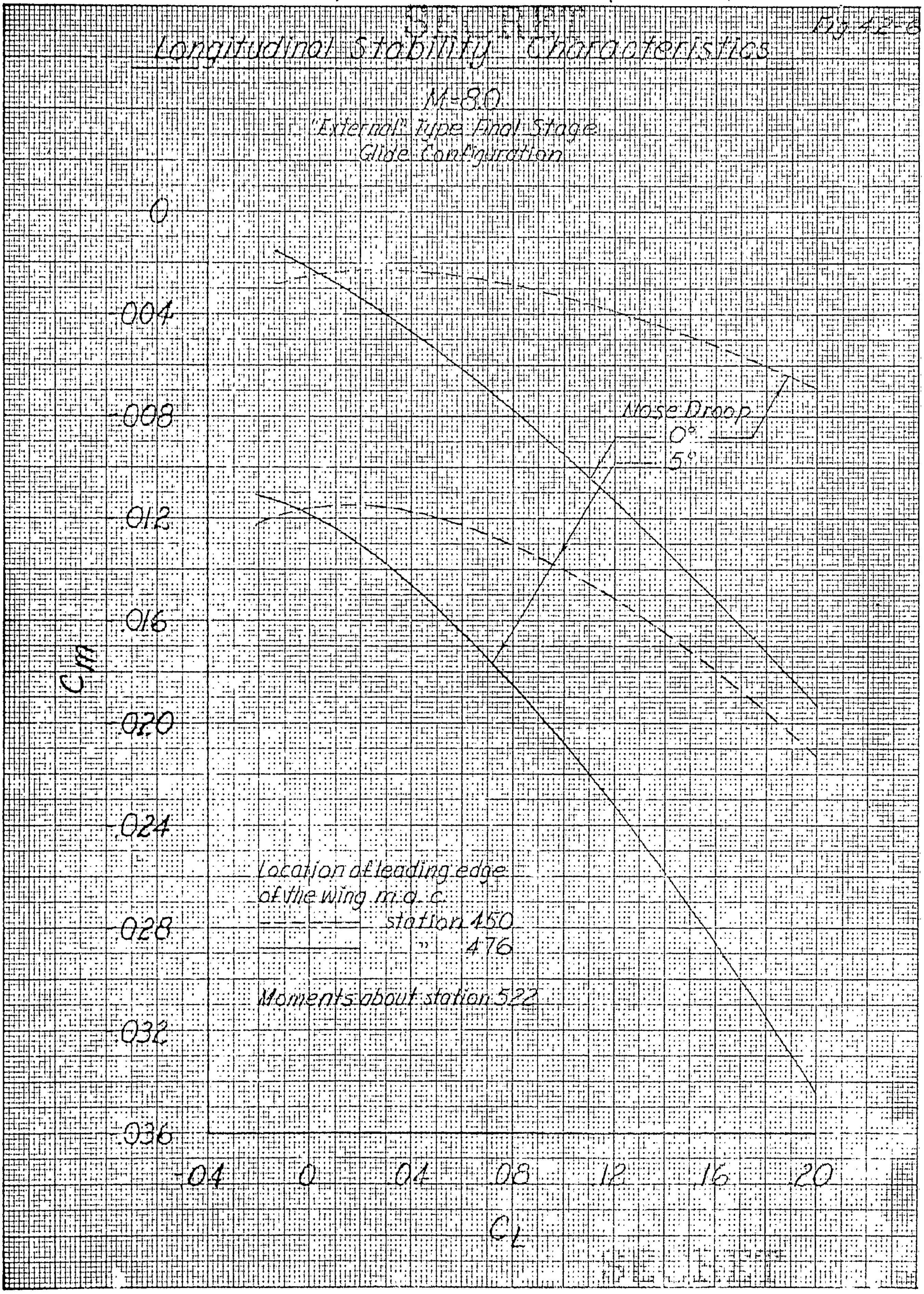
Longitudinal Stability Characteristics
M=.80
"External" Type Final Stage
Glide Configuration
0
-.004
-.008
-.012
-.016
-.020
-.024
-.028
-.032
-.036
Cm
Nose Droop
0°
5°
Location of leading edge
of the wing m.a.c.
station 450
" 476
Moments about station 522
-.04
0
.04
.08
.12
.16
.20
C_L

SECRET

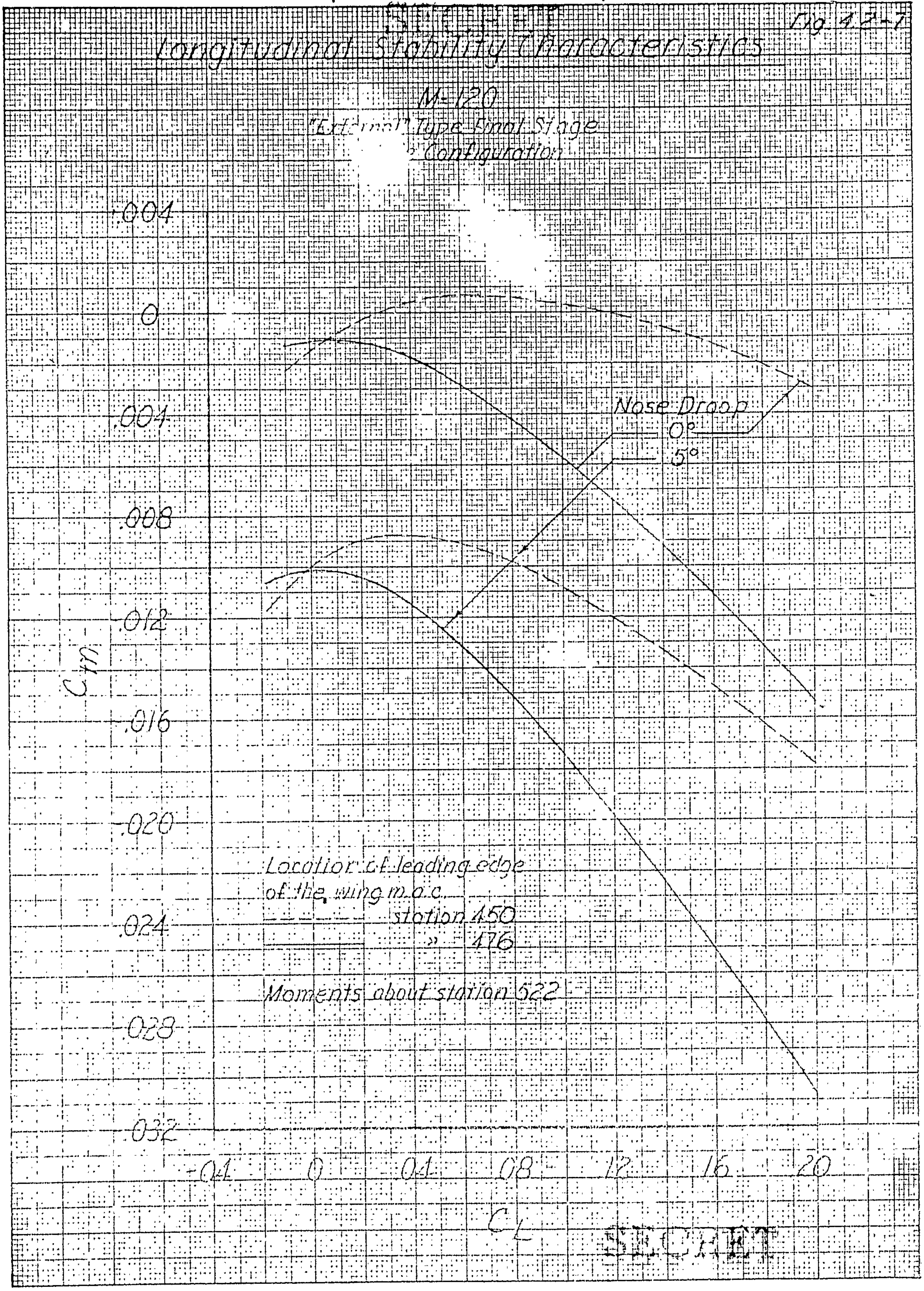

SECRET

SECRET

Fig. 4.2-8

Longitudinal Stability Characteristics

M-160

"External" Type Final Stage
Glide Configuration

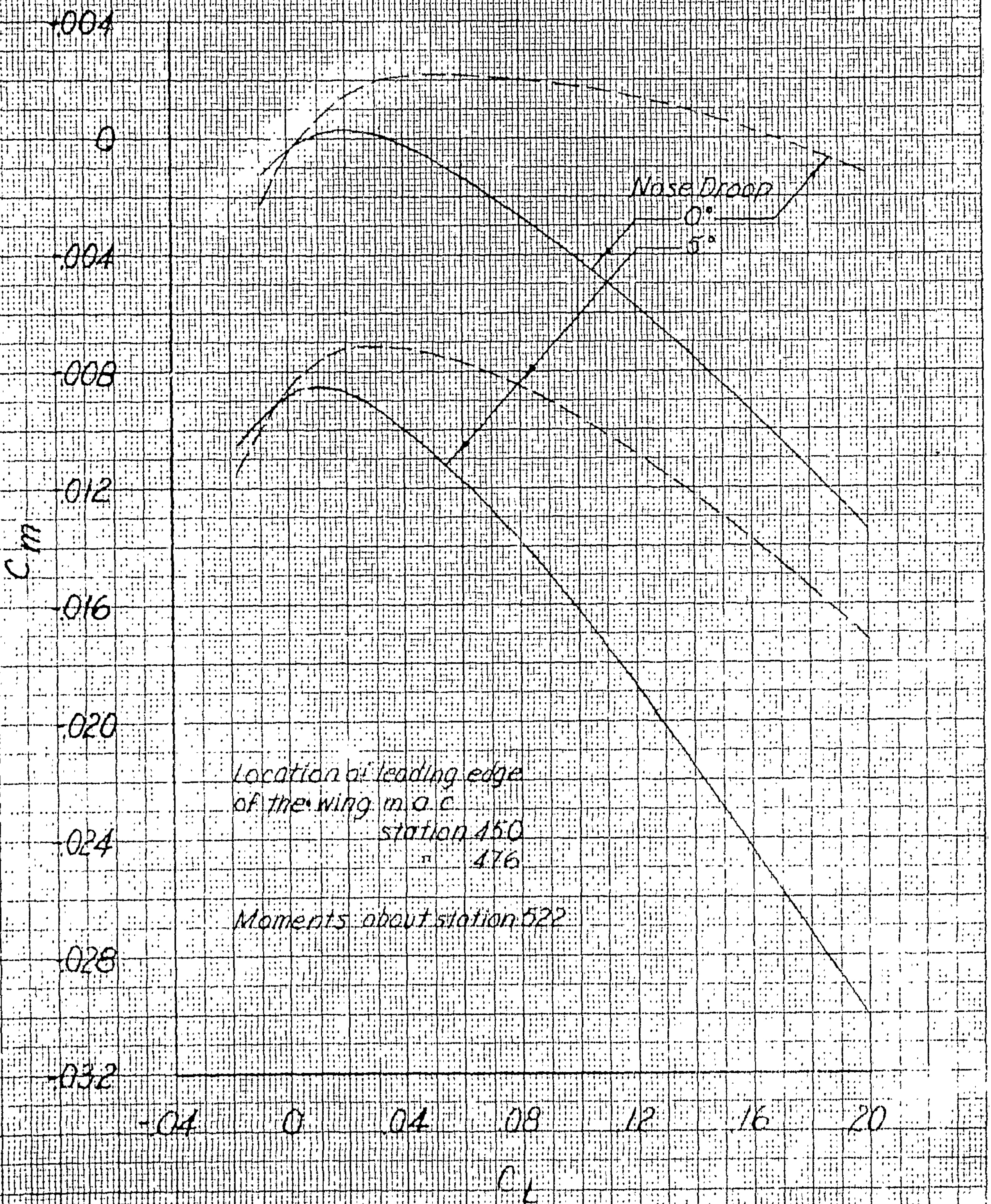

SECRET

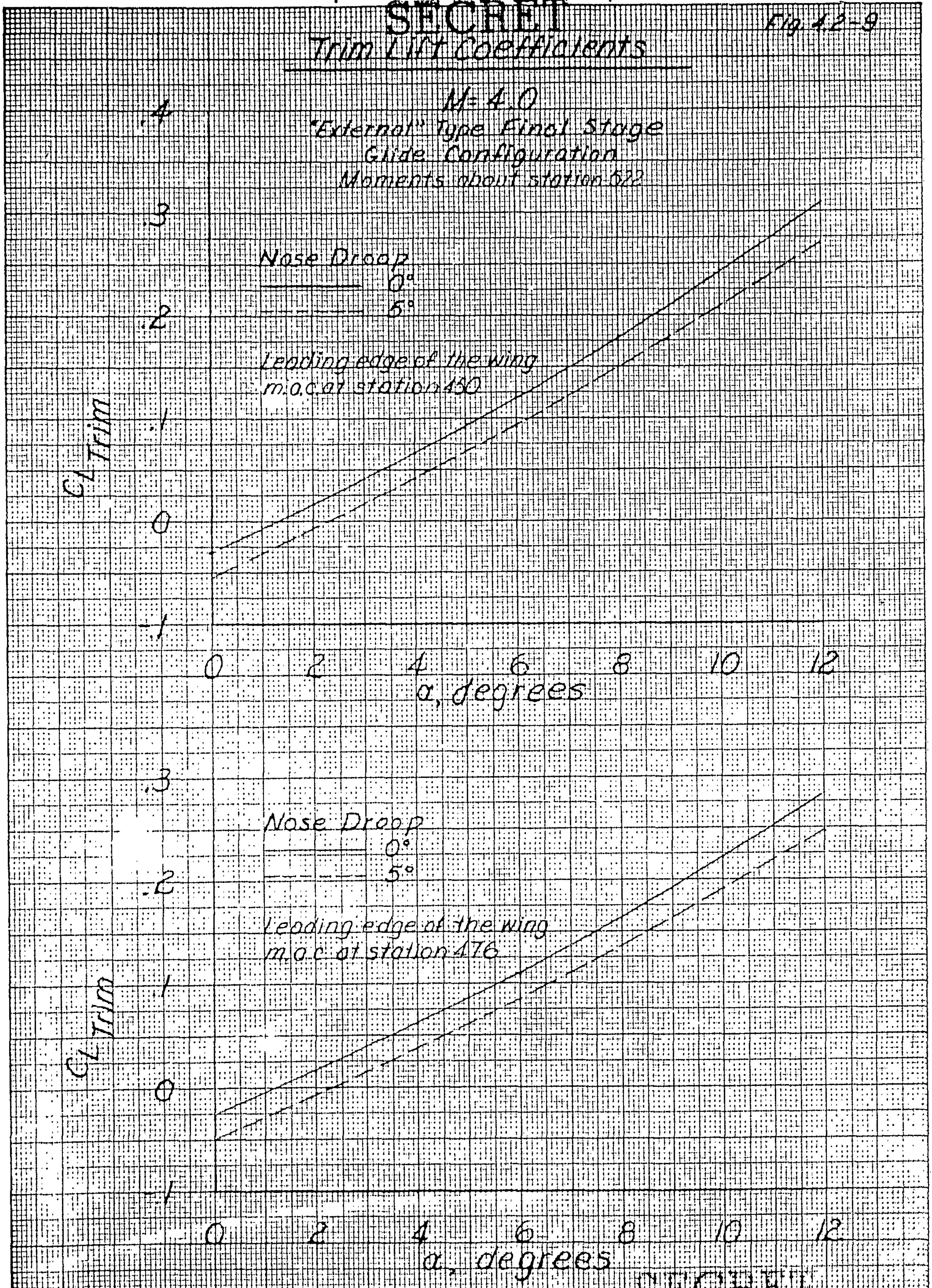

SECRET

SECRET

Fig. 4.2-10

Trim Lift Coefficients

M = 8.0
"Externol" Type Final Stage
Glide Configuration
Moments about station 522

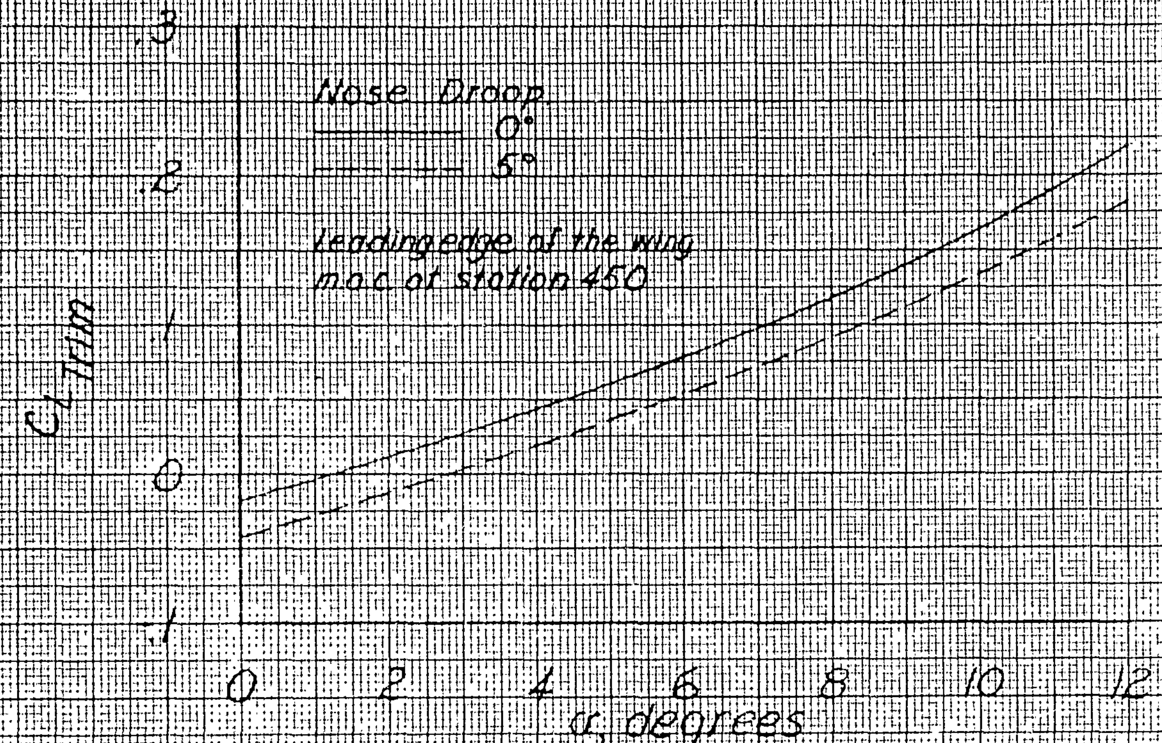

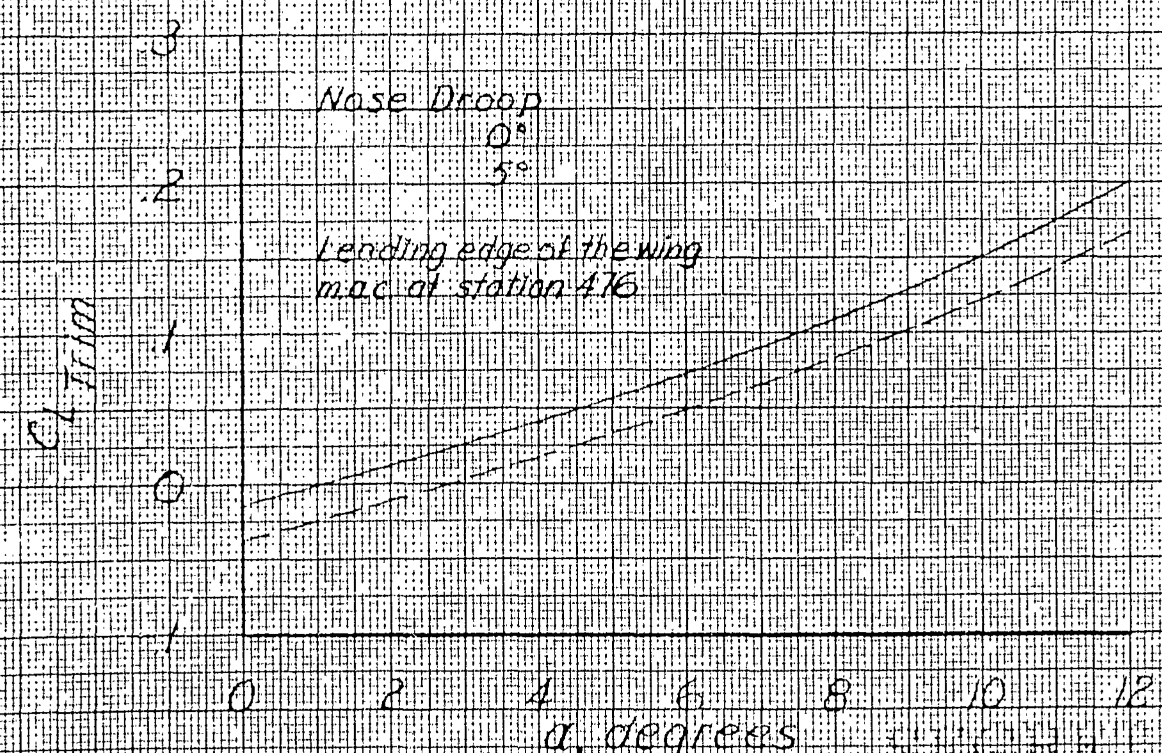

SECRET

Fig. 4.2-11

Trim Lift Coefficients

M=12.0
"External" Type Final Stage
Glide Configuration
Moments about station 522

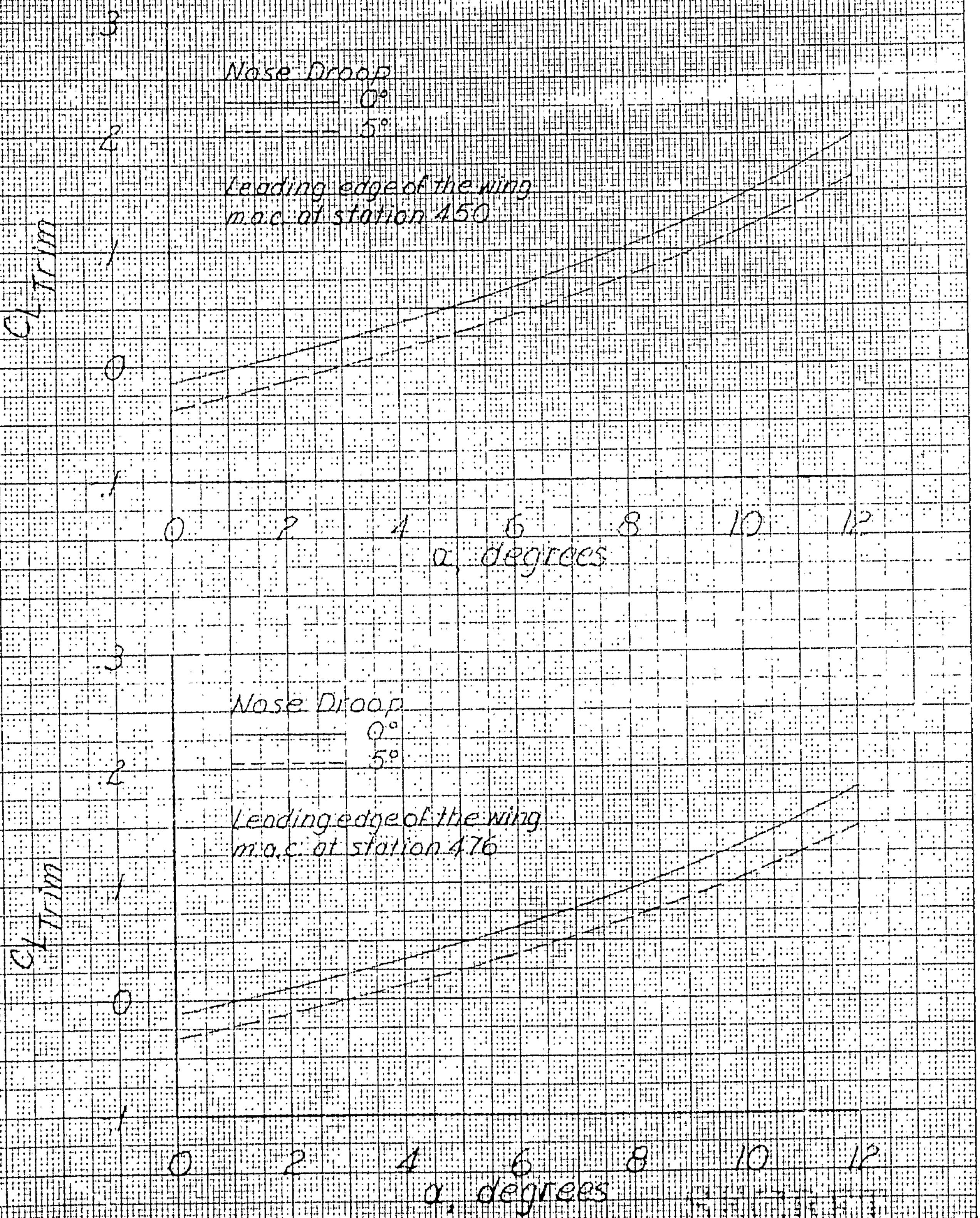

SECRET

SECRET

Fig. 4.2-12

Trim Lift Coefficients

M=16.0
"External" Type Final Stage
Glide Configuration
Moments about station 522

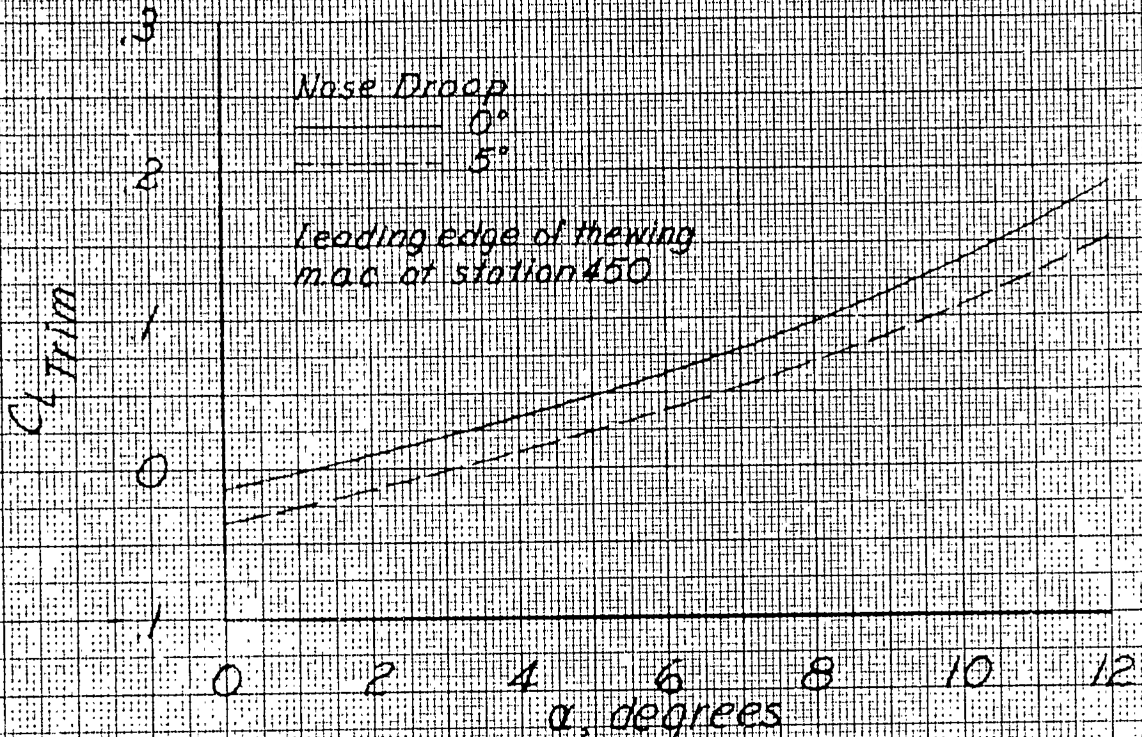

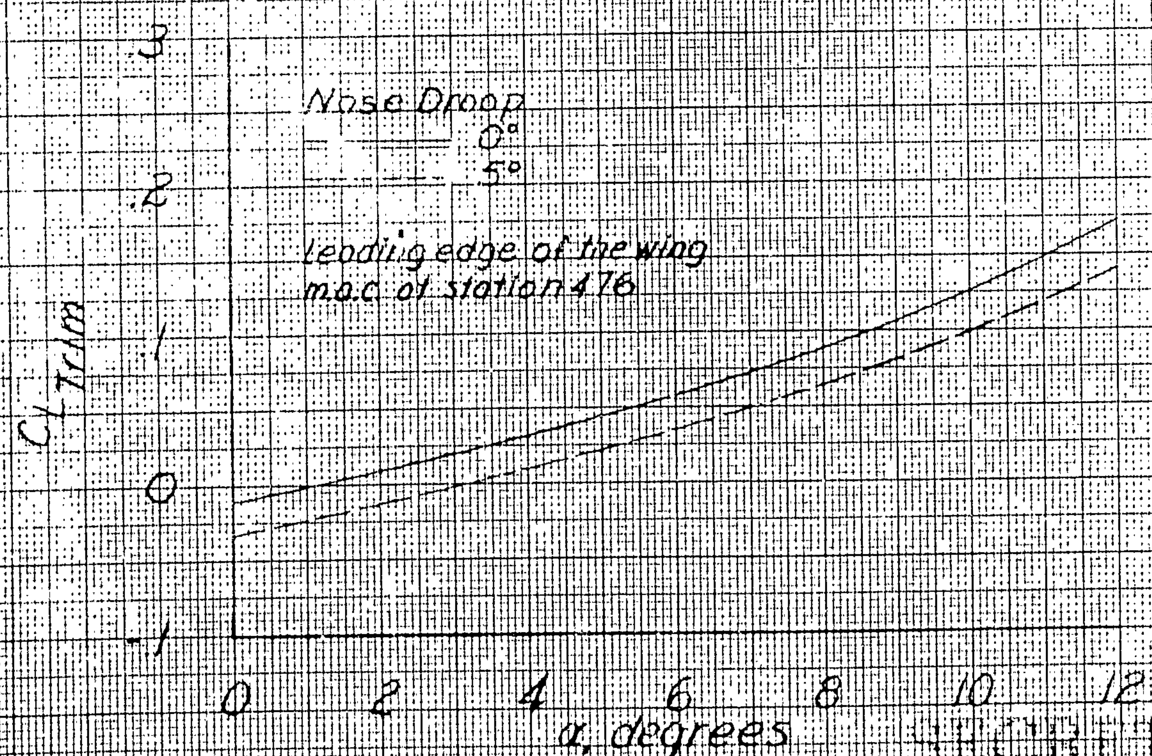

SECRET

4.3 AIRFOIL THICKNESS RATIO

In previous design work the thickness ratio of the airfoil, in a streamwise direction, has been taken as .04. During the course of those present analyses, a possibility of reducing the thickness ratio to .03 was discovered. This could be accomplished by a permissible reduction in the primary structural thickness ratio of the airfoil. Thus, the external thickness ratio could be reduced to .03 while holding the insulation thickness constant or the external thickness ratio could be held constant at .04 and the insulation thickness increased.

By increasing the depth of insulation in the wing, a reduction in the weight of coolant per square foot might be possible. On the other hand, reduction of the external thickness ratio might result in improved aerodynamic characteristics. This preliminary investigation of such possible improvements due to reduction in airfoil thickness ratio was performed using conventional two dimensional shock-expansion methods to calculate the pressures over an airfoil with an eight foot chord and thickness ratios of .03 and .04. The leading edge of this airfoil has a .5 inch diameter, the bottom surface is flat; and the top surface is composed of wedge from the leading edge to the 35 percent chord point followed by a flat surface aft to the trailing edge.

The section lift characteristics were calculated for Mach numbers of 4.0, 8.0, 12.0, and 16.0 and appear in Figures 4.3-2 and 4.3-2. The .03 airfoil had greater lift at a given angle of attack than the .04 airfoil due primarily to the decreased wedge angle on the upper surface. This lift

advantage decreased with both increasing α and Mach number as might be expected. It can be seen from these figures that the drag due to lift at a constant C_L would be less for the .03 airfoil. However, in the range of α's of interest (six degrees to eight degrees) this difference is negligible. Some slight advantage from less pressure drag plus base drag could be attributed to the .03 airfoil, but the importance of these factors, at the high Mach numbers where most of the range is accomplished, is insignificant in affecting the maximum L/D of the vehicle.

In Figures 4.3-3 and 4.3-4 are shown the stability characteristics of the two airfoils (moments taken about the leading edge) for Mach numbers of 4.0 to 16.0. As in the case of lift, the .03 airfoil is superior in this regard, but insignificantly so.

As a result of this study it appears that only very slight aerodynamic advantages can result by decreasing the external thickness ratio from .04 to .03 in the 4.0 to 16.0 Mach number range.

Additional studies into the aerodynamic effects of decreasing the external thickness ratio of this airfoil in the transonic and subsonic flight regimes should be conducted before final decisions can be made. In addition, the important temperature and structural weight considerations must likewise be investigated before the complete basis for comparison can be achieved. At this point in the preliminary design of glide vehicles of the proposed type, the lightest wing is still the best wing. Hence the structural considerations are presently paramount to the aerodynamic ones, which have been shown to be negligible in their importance concerning a choice between a .03 or .04 external thickness ratio.

4.3 SYMBOLS

c	Chord of the airfoil, feet
C_L	Lift coefficient
C_m	Pitching moment coefficient
M	Mach number
α	Angle of attack, degrees

SECRET

Fig 4.3-1

Section Lift Characteristics

c=8 feet

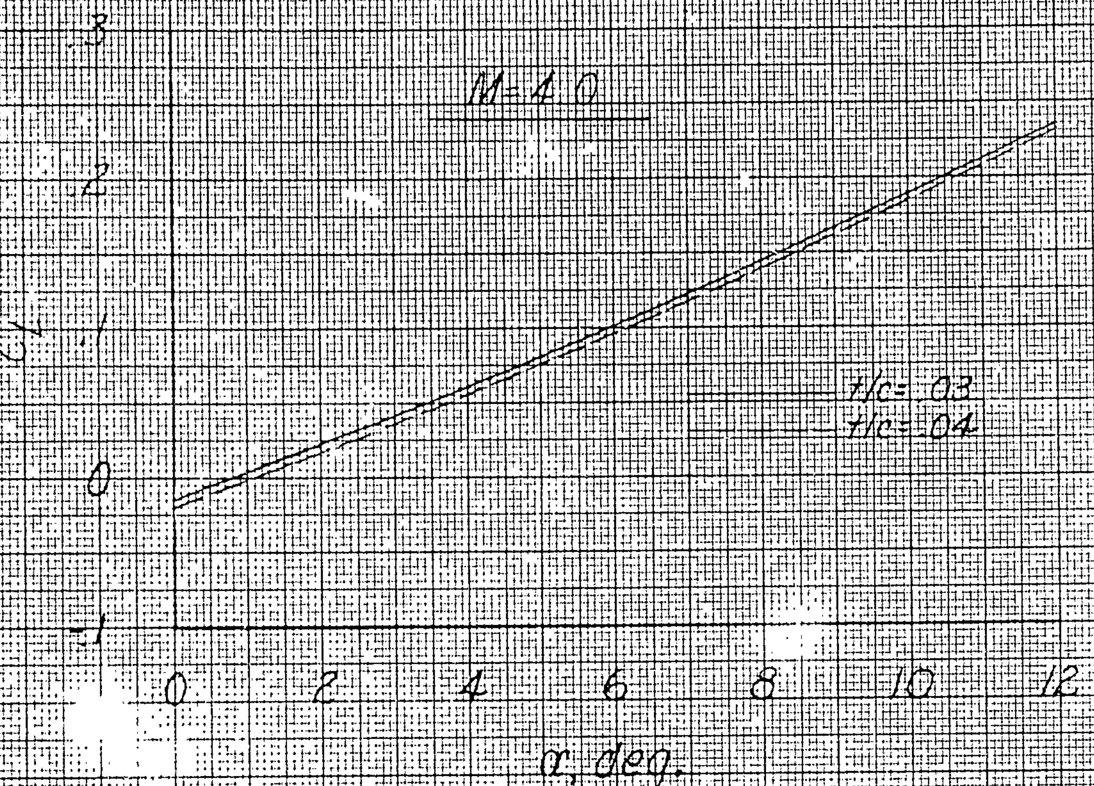

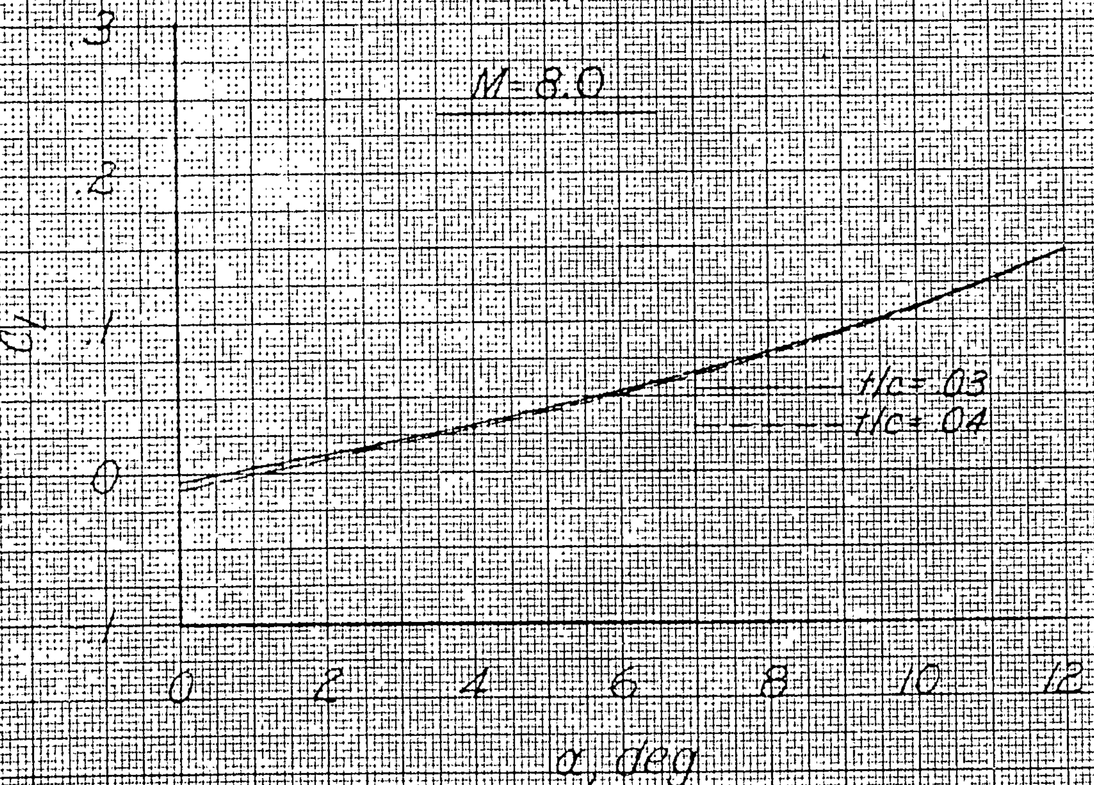

SECRET

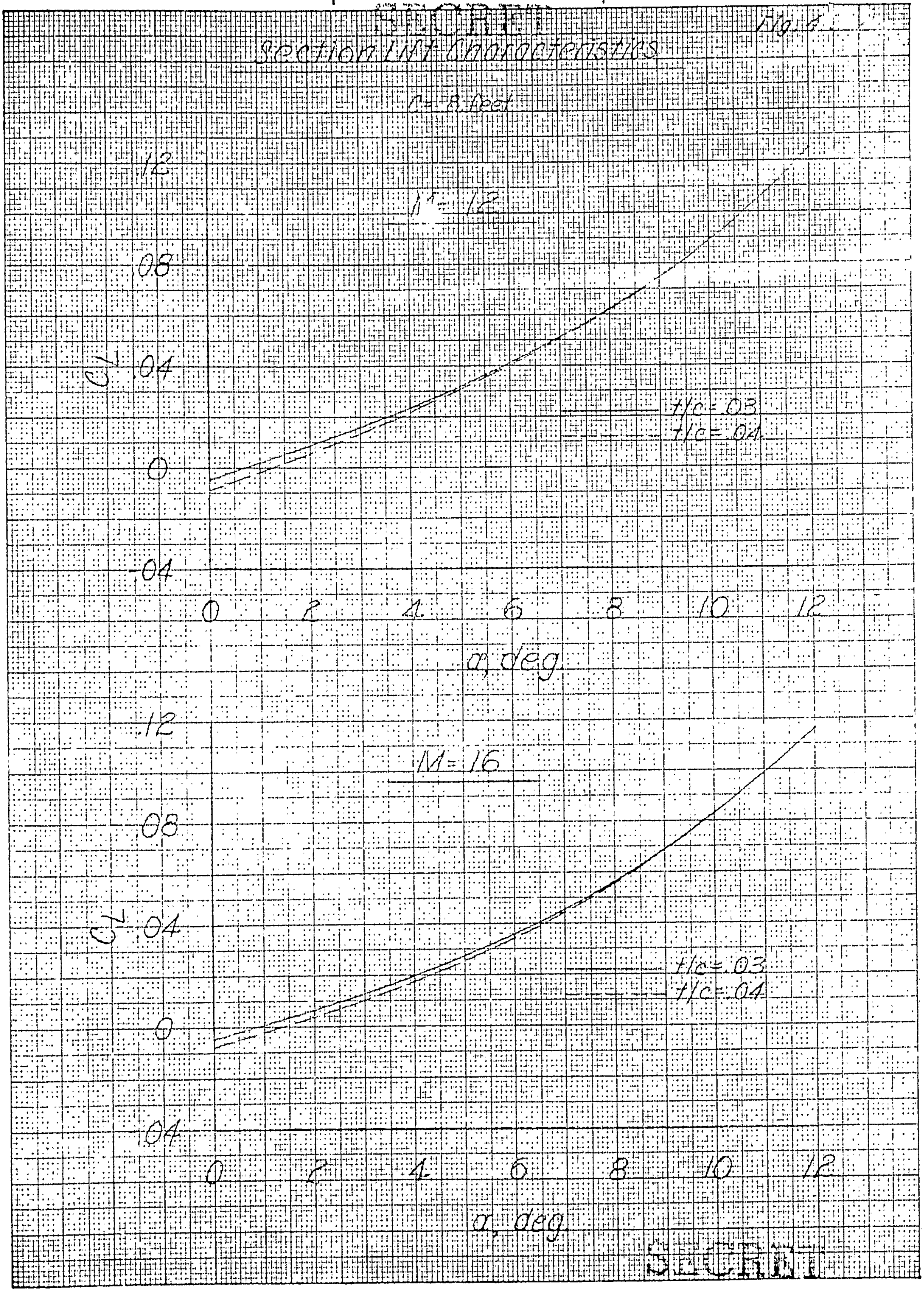
SECRET
Section Lift Characteristics
c = 8 feet
M = 1.2
.12
.08
.04
0
-.04
c_l
t/c = .03
t/c = .04
0
2
4
6
8
10
12
α, deg
M = 1.6
.12
.08
.04
0
-.04
c_l
t/c = .03
t/c = .04
0
2
4
6
8
10
12
α, deg
SECRET

SECRET

Fig 4.3-3

Section Moment Characteristics

Moments taken about the leading edge

C = 8 feet

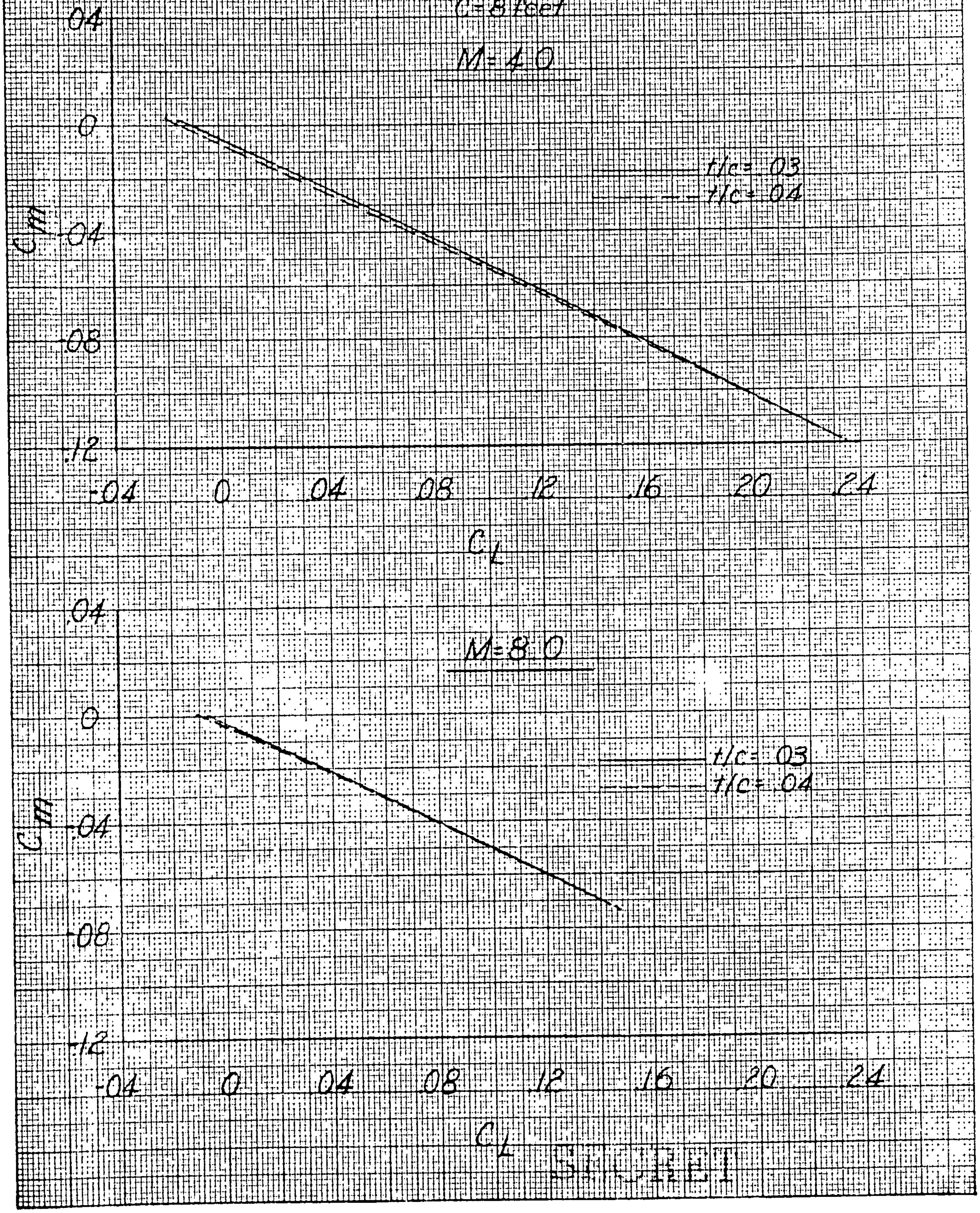

SECRET

SECRET

Fig. 4.3-4

Section Moment Characteristics

Moments taken about the leading edge

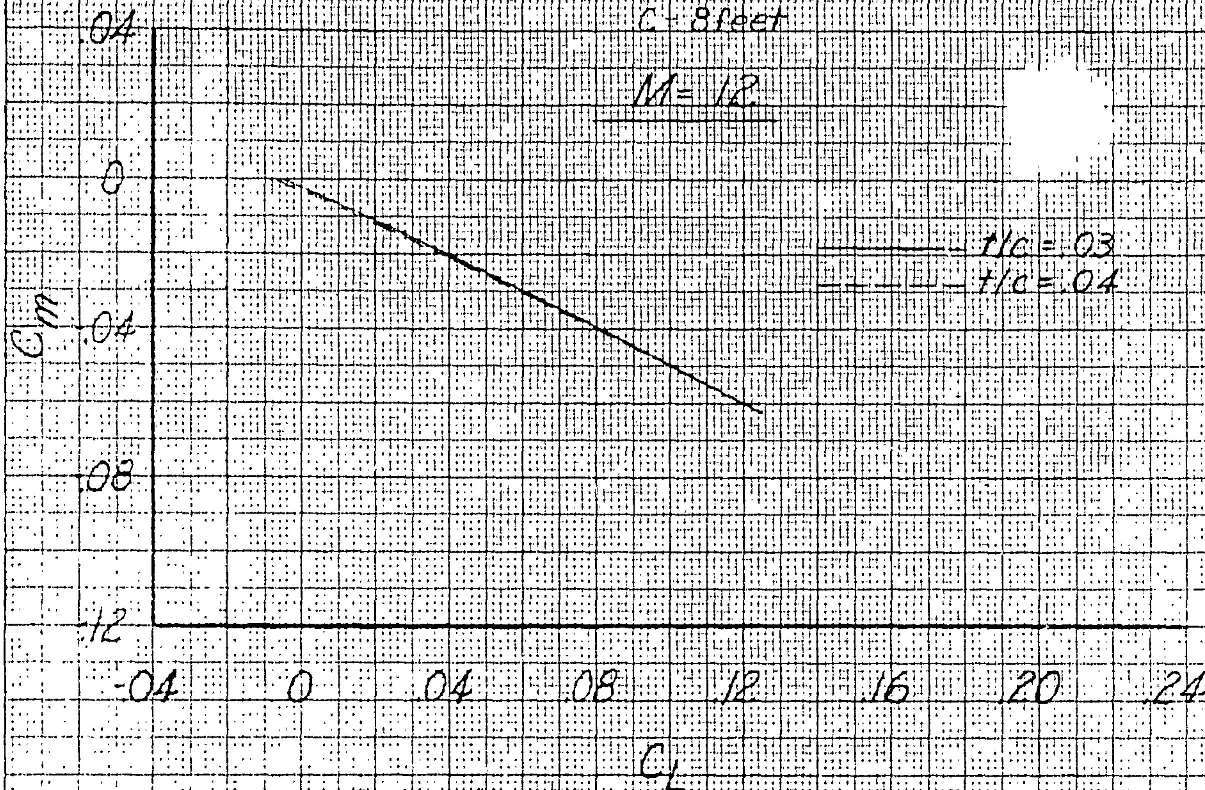

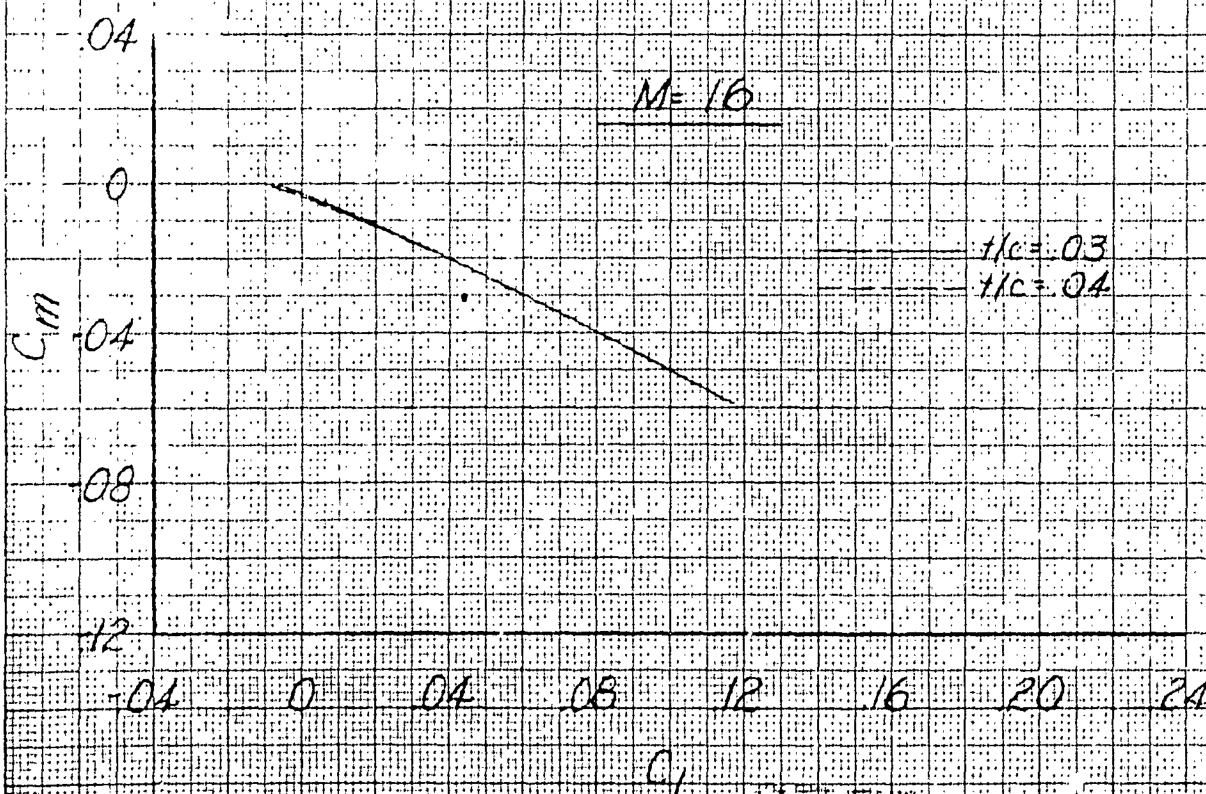

SECRET

SECRET

Classified only when data are entered

4.4 LOCATION OF THE AERODYNAMIC CENTER OF LOW ASPECT RATIO DELTA WINGS

In the design of the final stage configuration proposed in Reference 4.4.1 the subsonic wing aerodynamic center was estimated, using the empirical method proposed in Reference 4.4.2, to be located at 35 percent of the MAC of the wing. Additional study of methods and correlating data has indicated that the commonly used extrapolation of the results of Reference 4.4.3 to be in considerable error for delta wings of aspect ratios below 1.0 and taper ratios other than zero.

Comparison of the locations of the aerodynamic center of clipped delta wings as predicted by several methods and the available correlating data are shown in Figure 4.4-1. The upper plot shows the variation with aspect ratio of the location of aerodynamic center as fractions of the root chord for taper ratios of zero and .5 as predicted from the results contained in References 4.4.2 and 4.4.3. As can be seen there is good agreement between methods for delta wings with zero taper ratio, but rather poor agreement for delta wings of aspect ratios below 2.0 and a taper ratio of .50. However, the data of Reference 4.4.4 agrees very well with the aerodynamic center locations predicted by the method of Reference 4.4.2. This would seem to indicate the proposed extrapolation of the method of Reference 4.4.3 to include very low aspect ratio delta wings was in error.

In the lower plot the location of the aerodynamic center in fractions of the MAC for delta wings with zero taper ratio are presented. In general the agreement between the methods proposed in References 4.4.2, 4.4.3, and 4.4.5 is good. However, the applicable data presented in References 4.4.2

and 4.4.4 seems to agree more closely with the predictions of References 4.4.2 and 4.4.5 for aspect ratios less than 2.0.

As a result of this study it is recommended that additional subsonic testing for aerodynamic center location data of low aspect ratio clipped delta wings be conducted. However, until such data becomes available the method of Reference 4.4.2 will be employed in the prediction of this parameter.

4.4 REFERENCES

4.4.1 Postle, R. S., et al: MX-2276 Reconnaissance Aircraft Weapon System - Aerodynamics, Bell Aircraft Corporation Report No. D143-945-024, December 1, 1955

4.4.2 Rose, R. G.: A Note on the Estimation of Some Low Speed Characteristics of Delta Wings, The College of Aeronautics Report No. 68, January 1953

4.4.3 Nielsen, J. N., Kaattari, G. E., Anastasio, R. F.: A Method for Calculating the Lift and Center of Pressure of Wing-Body-Tail Combinations at Subsonic, Transonic, and Supersonic Speeds, NACA RM A53G08, November 12, 1953

4.4.4 Adler, Alfred A.: A Correlation of Theory with Experiment for Low-Aspect-Ratio Wings at Subsonic Speeds, Cornell Aeronautical Laboratory Report No. AF-743-A-4, December 1952

4.4.5 Flax, A. H. and Lawrence, H. R.: The Aerodynamics of Low-Aspect-Ratio Wings and Wing-Body Combinations, Cornell Aeronautical Laboratory Report No. CAL-37, September 1951

4.4 SYMBOLS

$\bar{c}$	Mean Aerodynamic chord of the wing, feet
c_R	Root chord of the wing, feet
c_T	Tip chord of the wing, feet
M	Mach number
X	Location of wing aerodynamic center, feet aft of the leading edge at the reference chord
AR	Aspect ratio of the wing
λ	Taper ratio of the wing, c_T/c_R

SECRET

Fig. 4.4-1

Comparison of Aerodynamic Center Locations as Predicted by Several Methods

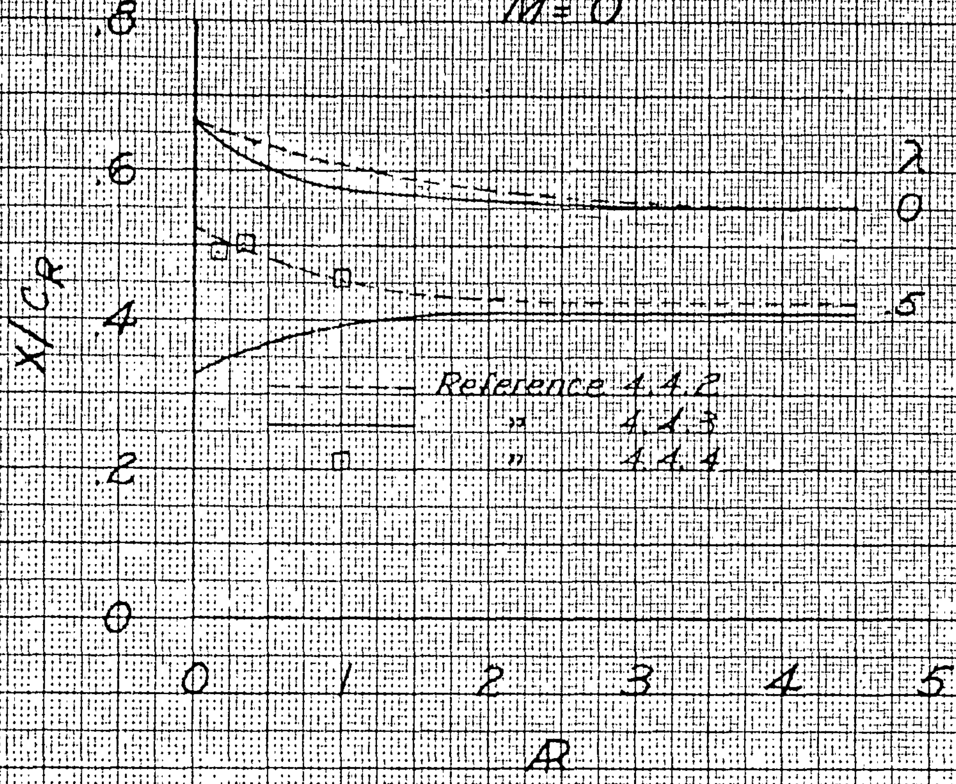

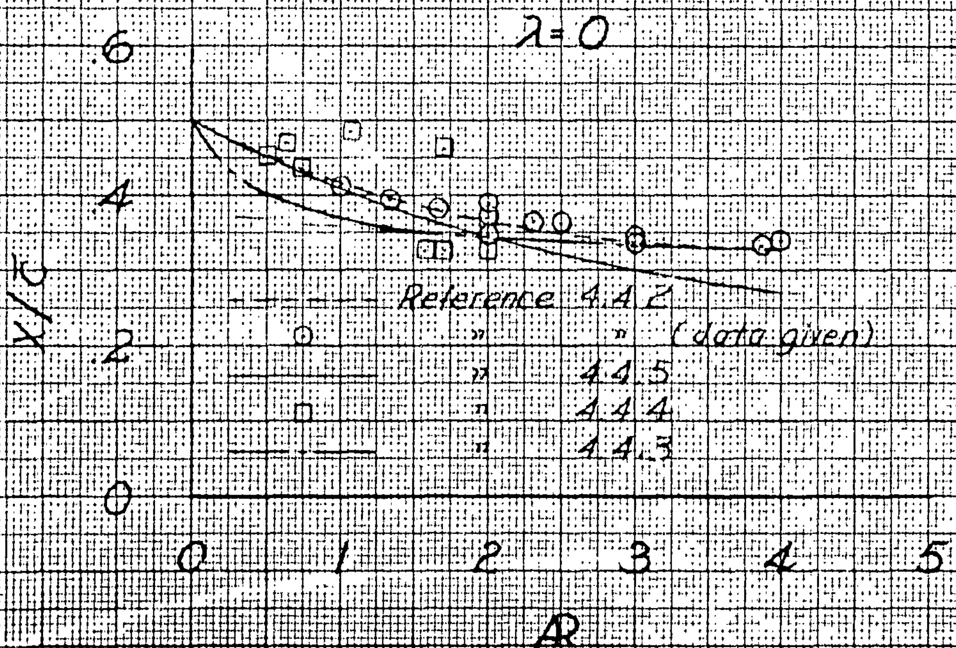

SECRET

4.5 CREW SURVIVAL

In the event of some serious malfunctioning of the aircraft the ability of the crew to reach safety must be considered. The important problem of providing the crew the highest possible chance for survival must be considered early so that the most efficient provisions for safety can be incorporated in the design.

It was obvious that the crew could not be ejected into the airstream at high altitudes and airspeeds. The natural conclusion was therefore, to investigate the problem of surrounding them with a shielding device of some sort. The amount of shielding necessary and the functions it must perform in order to protect the crew adequately can only be enumerated after a long and careful investigation. However, this preliminary investigation was undertaken to uncover order of magnitude answers that might prove helpful in initiating research and development work specifically connected with this project. The shielding device which surrounds the crew member or members can reasonably be considered as a capsule; the question remains as to whether this capsule should be part of or all of the aircraft.

Because the aerodynamic heating of the capsule airframe was by far the most serious and at the same time the least understood, of the problems involved in its design, ways had to be explored by which this heating could possibly be alleviated. From even the earliest work in which the problem of aerodynamic heating has been considered it has become apparent that both temperature and time would be determining parameters for the efficient design of practical high temperature structure. Since time was important, ways of reducing the length of time over which the structure would be

subject to elevated temperatures were considered in this preliminary study. As the best compromise between crew survival and structural design it appeared worthwhile to shorten the time between the advent of any emergency and the time when conditions permitting safe ejection of the crew from the capsule could be reached. Hence, slowing down of the capsule at high altitudes could be dismissed because the crew would have still been subjected to the dangers of high altitudes and could not be safely ejected from the capsule. Thus, it was reasoned that some sort of descending, decelerating type of flight path would be best. Naturally, the more the speed could be decreased at the higher altitudes the less serious would be the heating when the denser air of the lower altitudes was encountered. (The investigation concerning temperatures encountered during such descending flights is presented in a following section.) Increasing aerodynamic drag by increasing the lift (either negatively or positively) would have been obviously an inefficient means since every attempt has been made to make the aircraft as "clean" as possible. However, it was reasonable to expect that some type of drag brakes or devices could be extended and effectively increase the zero lift drag of the vehicle. Thus, zero lift paths were calculated for vehicles having various amounts of drag per unit mass as represented by the parameter C_DS/m (where C_D is the drag coefficient based on the reference area S and m is the mass of the vehicle).

It was assumed, for the purpose of this study, that the most critical conditions would be encountered when the descent was made from the highest possible speed and altitudes this vehicle might encounter namely, velocity equal to 18,000 feet per second and altitudes of 160,000, 180,000, and

200,000 feet. The results of these calculations of the zero lift descents are presented as time histories of velocity and altitude in Figures 4.5-1 through 4.5-6. (It was conservatively assumed that the parameter (C_DS/m) was independent of Mach number for the purpose of these calculations.) These results were calculated using the Bell Aircraft Performance Analyzer (see Reference 4.5.1). The calculation for the descent from 200,000 feet with C_DS/m = .10 resulted in dynamic pressures which were outside the present capabilities of this machine so no results appear for this case.

Several interesting things were found as a result of these calculations. It can be seen from these figures that by the time the vehicle reached an altitude of 40,000 feet its speed was practically independent of its initial altitude, and for values of $C_DS/m > .2$ was less than 1000 feet per second. At an altitude of 20,000 feet the speed was less than 860 feet per second for values of $C_DS/m > .10$. These results are presented in Figure 4.5-7.

Also presented in this figure are the maximum decelerations to which the vehicle would be subjected. It was interesting to note that the greater the value of C_DS/m the smaller the maximum deceleration encountered. Likewise, the lower the initial altitude the lower the maximum deceleration for a given value of C_DS/m. For all of the cases considered in this study the maximum deceleration was below 10 g's and with $C_DS/m > .20$ the maximum deceleration was below 8.1 g's. However, the length of time the crew would be subjected to decelerations in excess of 5 g's was found to vary from about 30 to 50 seconds with the time decreasing with increasing (C_DS/m)'s and

decreasing initial altitude. Inspection of Figure 1 of Reference 4.5.2 indicated that these times were borderline between the "zone of safety" and "zone of probable disablement" as defined in this reference as the human tolerance to transverse g's.

From this study, the importance of achieving a high value of the parameter (C_DS/m) for the crew escape "capsule" has been illustrated. Inspection of the proposed configurations revealed a reasonably high value of (C_DS/m) would be more easily obtained using the entire airframe rather than a stable capsule containing just the crew. Such a scheme would most likely mean the least addition of dead weight to the system. Thus, it would appear as a result of this study to recommend that the crew should remain with the aircraft, place the aircraft in a zero lift trajectory, and extend all drag devices. When the aircraft has reached altitudes and velocities permitting present day normal ejection procedures then the crew can leave the aircraft without additional danger.

No attempt has been made in this study to evaluate the effects of the types of emergencies on the selection of a practical means of escape. Should the emergency be of such major proportion as to cause the breakup of the aircraft then the proposed method of survival would be inadequate. Under these circumstances, there is little choice but to include an escape capsule in the aircraft design.

4.5 REFERENCES

4.5.1 Arthur, R. J., and Brigham, R. O.: The Bell Aircraft Performance Analyzer, Bell Aircraft Corporation Report No. 02-978-013, September 1, 1955

4.5.2 Goodrich, J. W.: Escape from High Performance Aircraft, WADC Technical Note 56-7, January 9, 1956

4.5 SYMBOLS

C_D	Drag coefficient, D/qS
D	Drag force, pounds
h	Altitude, feet
h_o	Initial altitude, feet
m	Mass of vehicle, slugs
S	Reference Area, square feet
V	Velocity, feet per second
V_o	Initial velocity, feet per second

SECRET

Fig 4.5-1

Zero Lift Trajectory - Velocity

h_0=160,000 feet V_0=18000 ft/sec

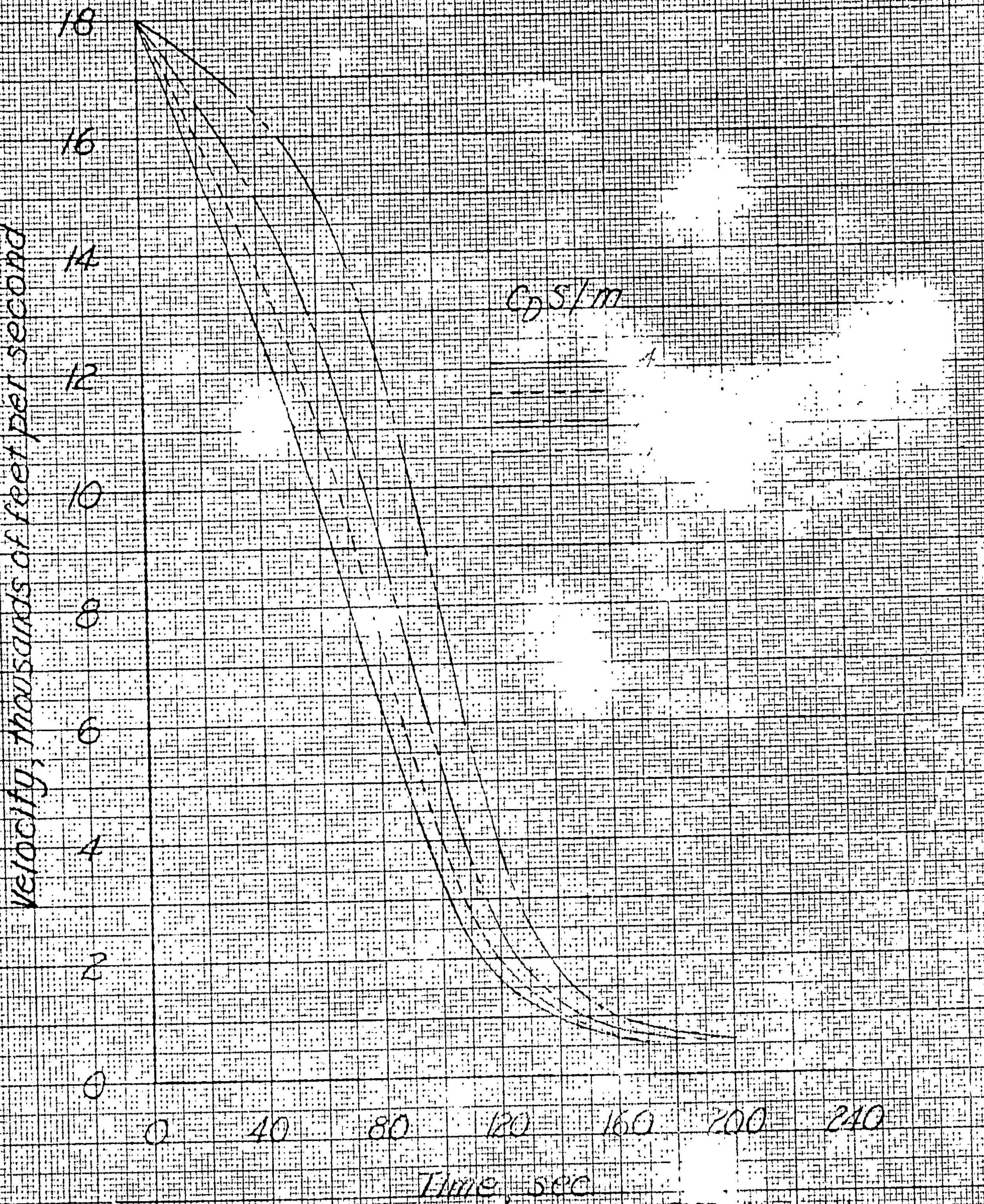

SECRET

BY________ DATE________ CHECKED________ DATE________

BELL Aircraft CORPORATION

MODEL________ PAGE 4-37
SHIP________ REPORT D143-945-033

SECRET

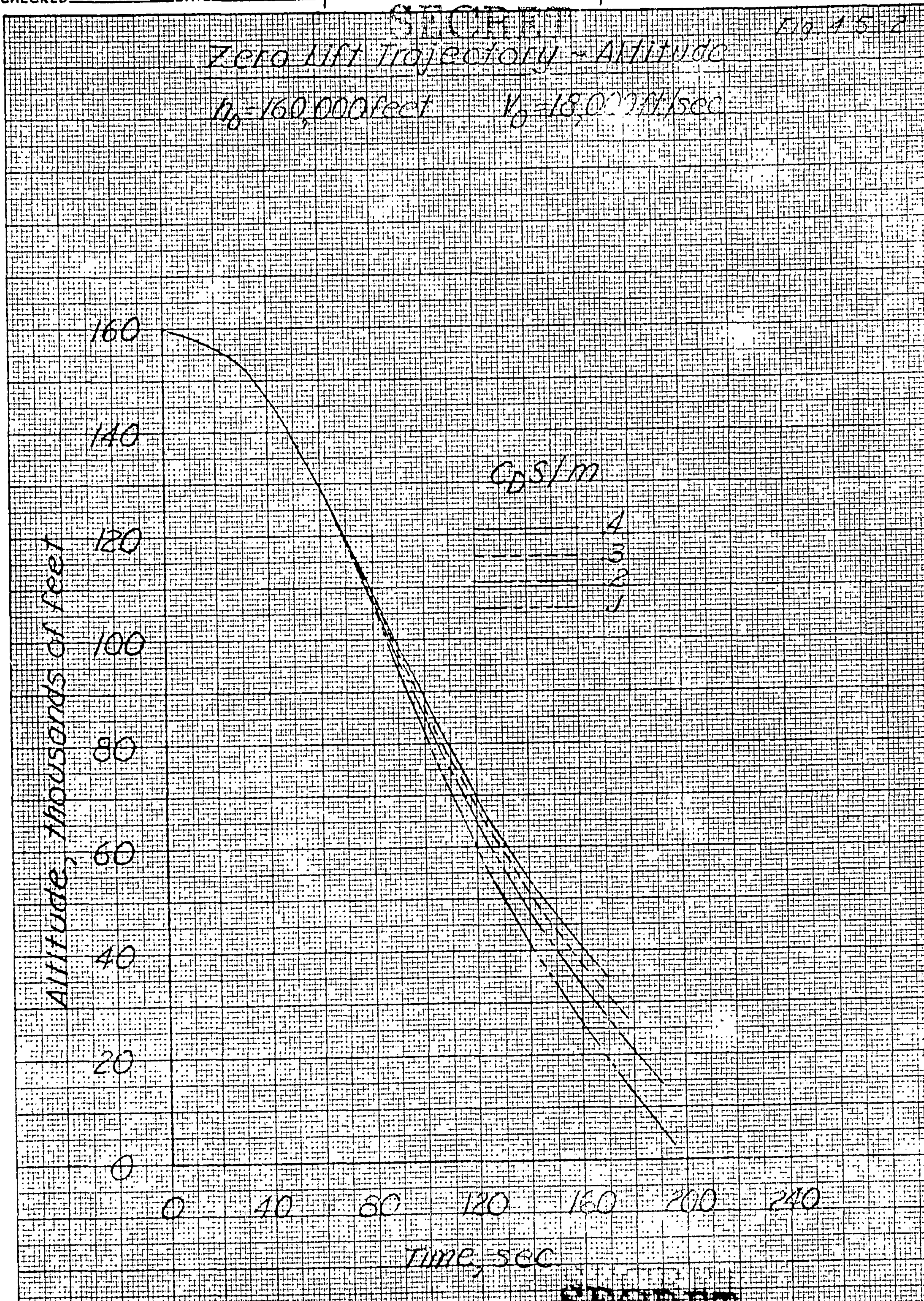

SECRET

K+E 10 X 10 TO THE CM. 359T-14
KEUFFEL & ESSER CO. MADE IN U.S.A.
ALBANENE

SECRET

Fig. 4.5-8

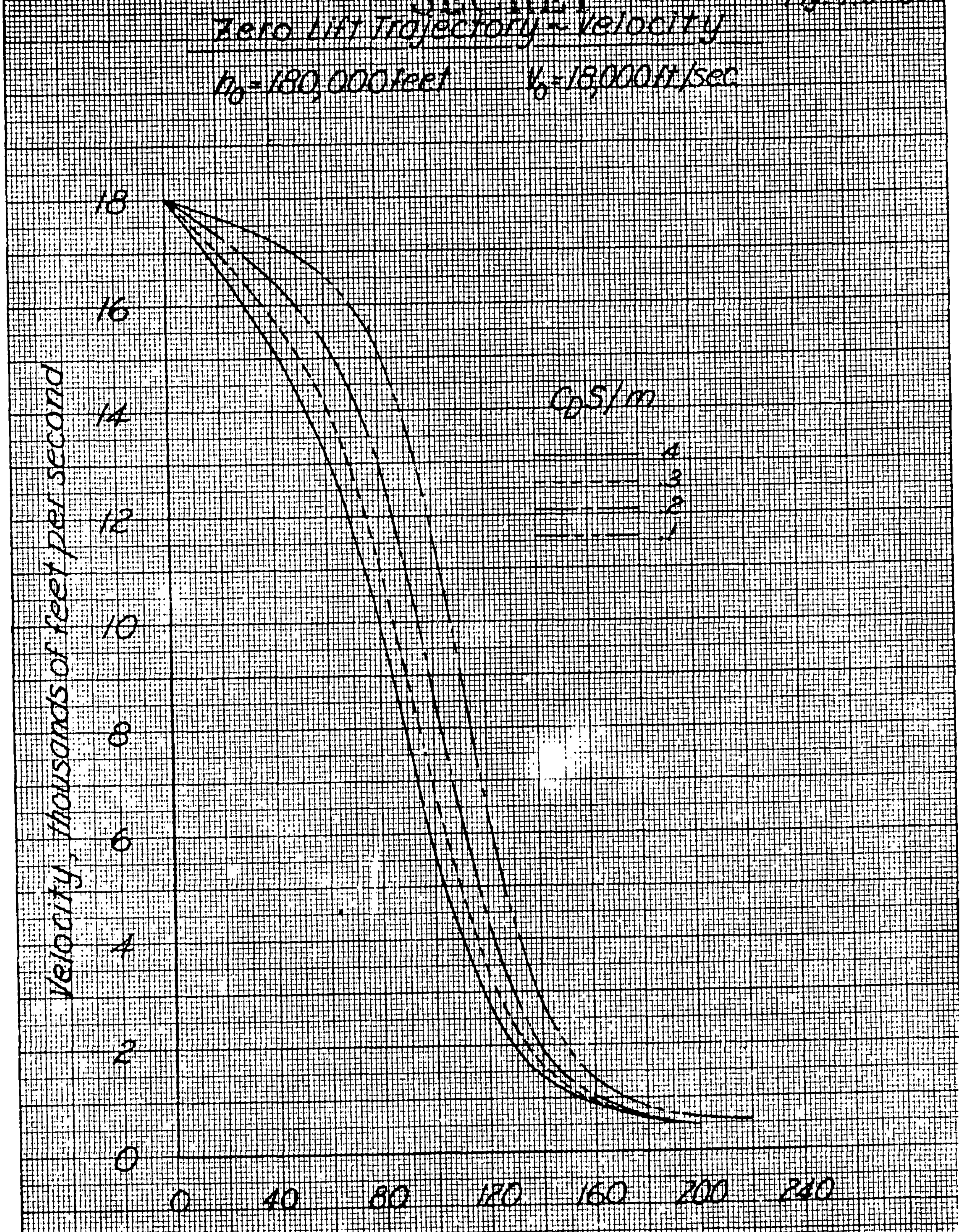

SECRET

SECRET

Fig 4.5-4

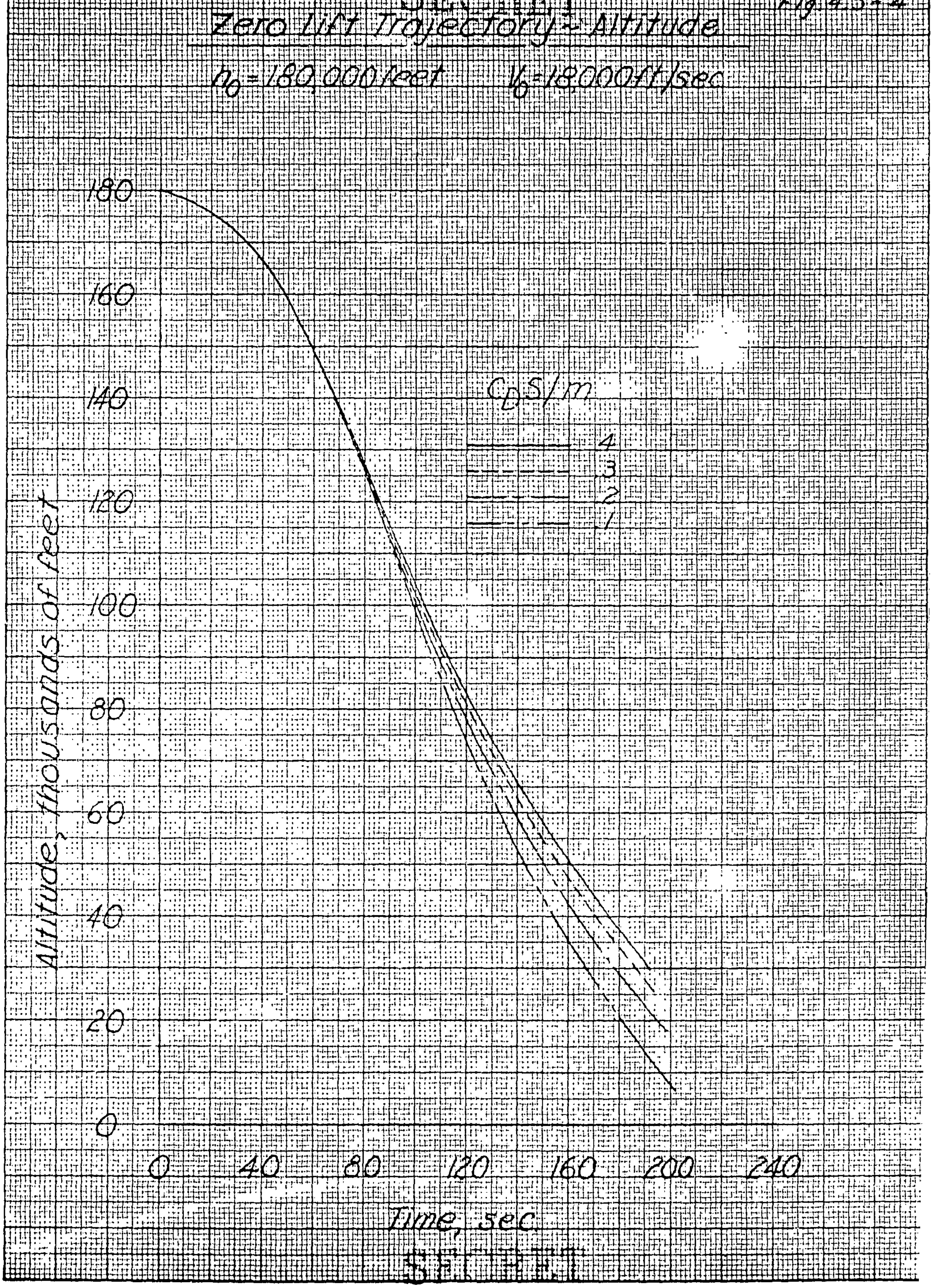

SECRET

SECRET

Fig. 4.6-5

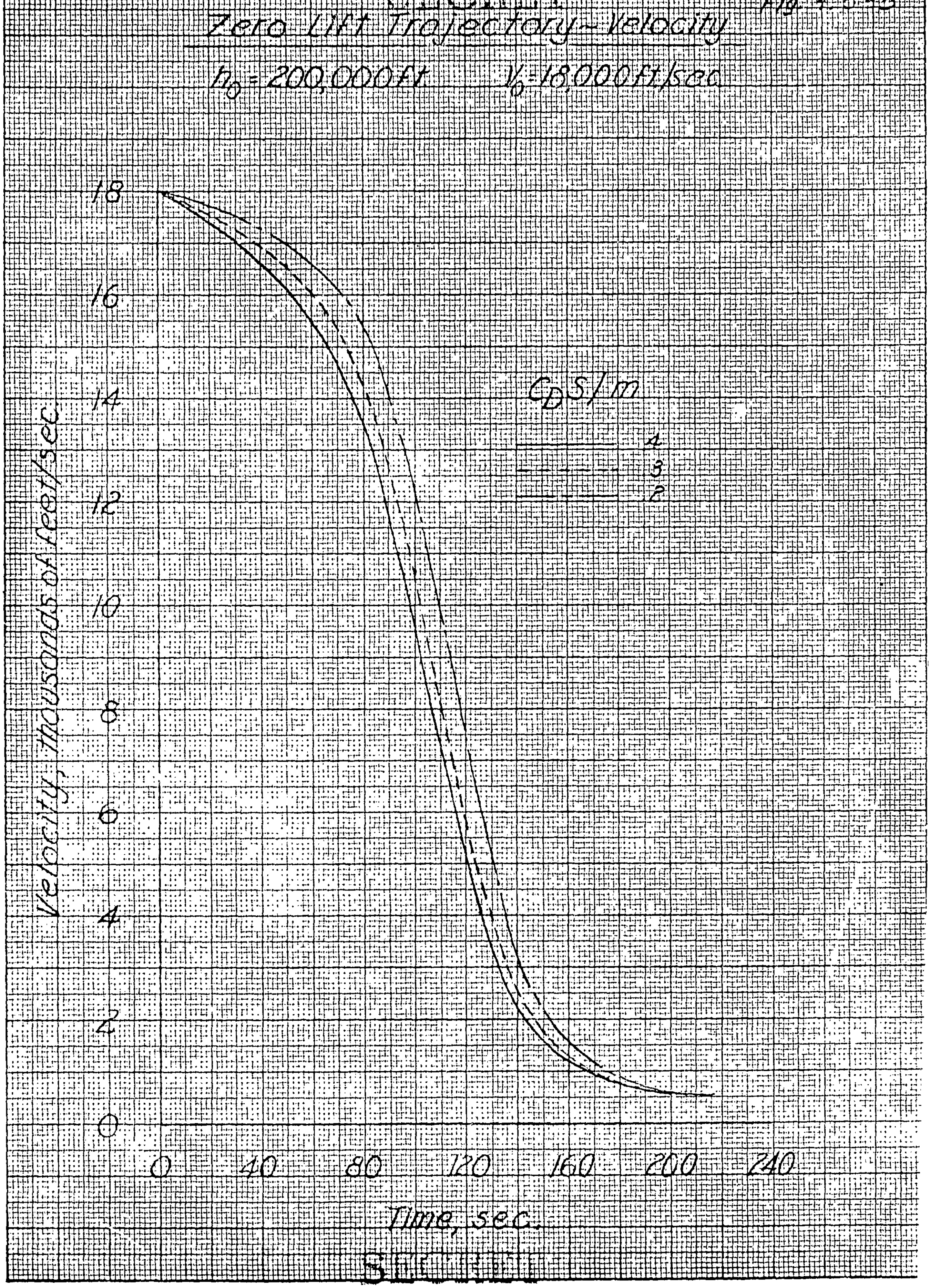

SECRET

Fig 4B-6

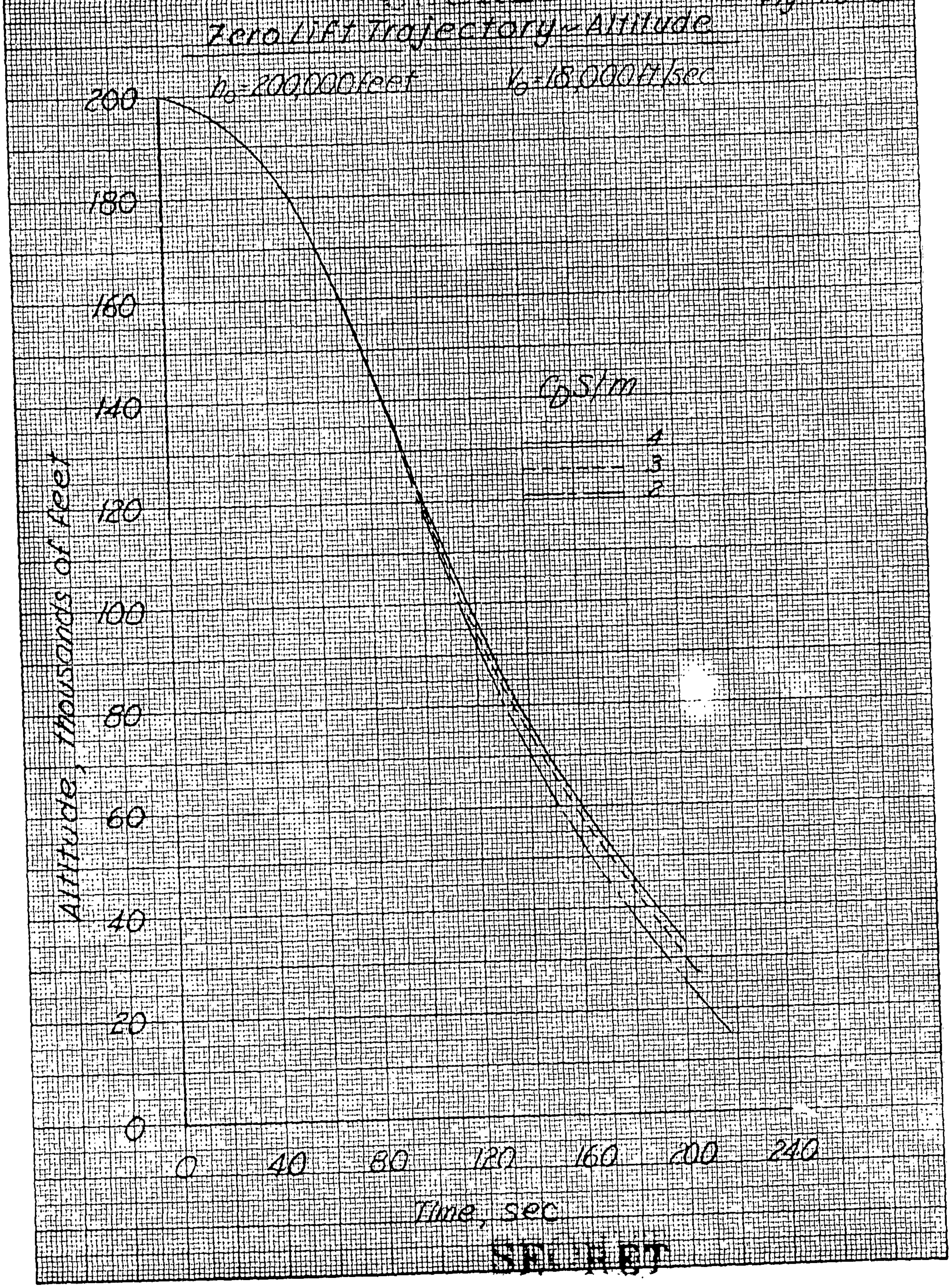
Zero Lift Trajectory - Altitude
h_0 = 200,000 feet
V_0 = 18,000 ft/sec
$C_D S/m$
4
3
2
Altitude, thousands of feet
200
180
160
140
120
100
80
60
40
20
0
0
40
80
120
160
200
240
Time, sec

SECRET

Fig. 4.5-7

Effect of $(C_D S/m)$ on Velocity of Altitude and Maximum Deceleration

$V_0 = 18{,}000$ ft/sec.

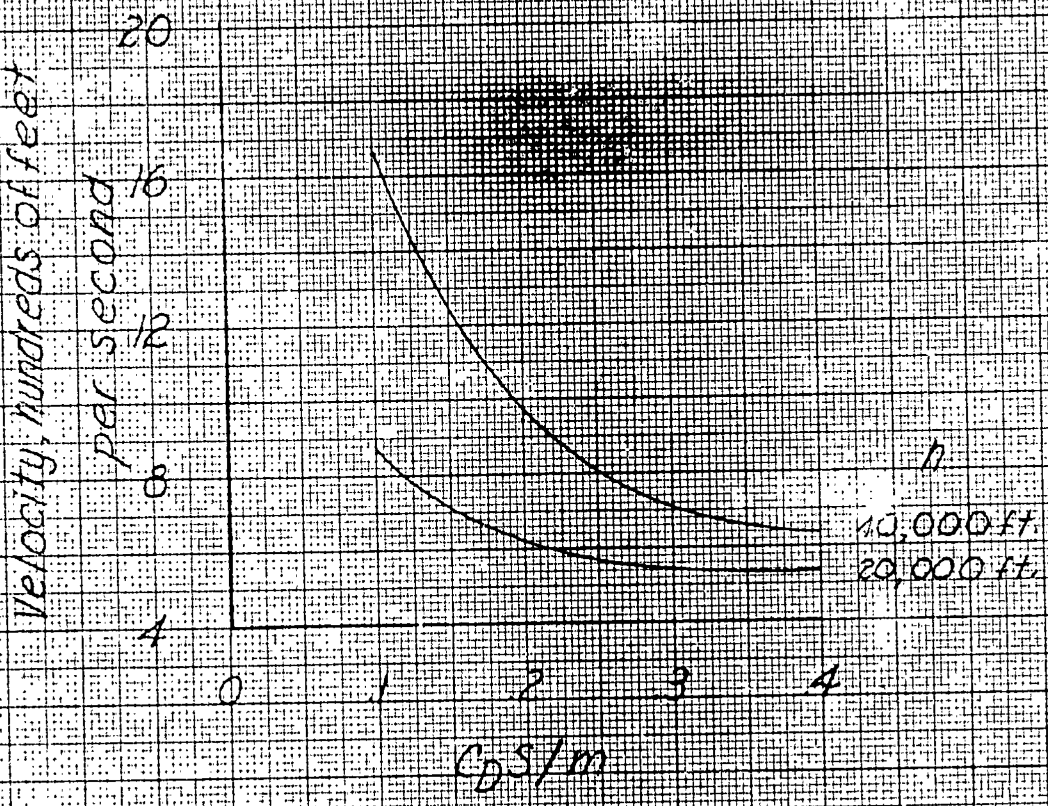

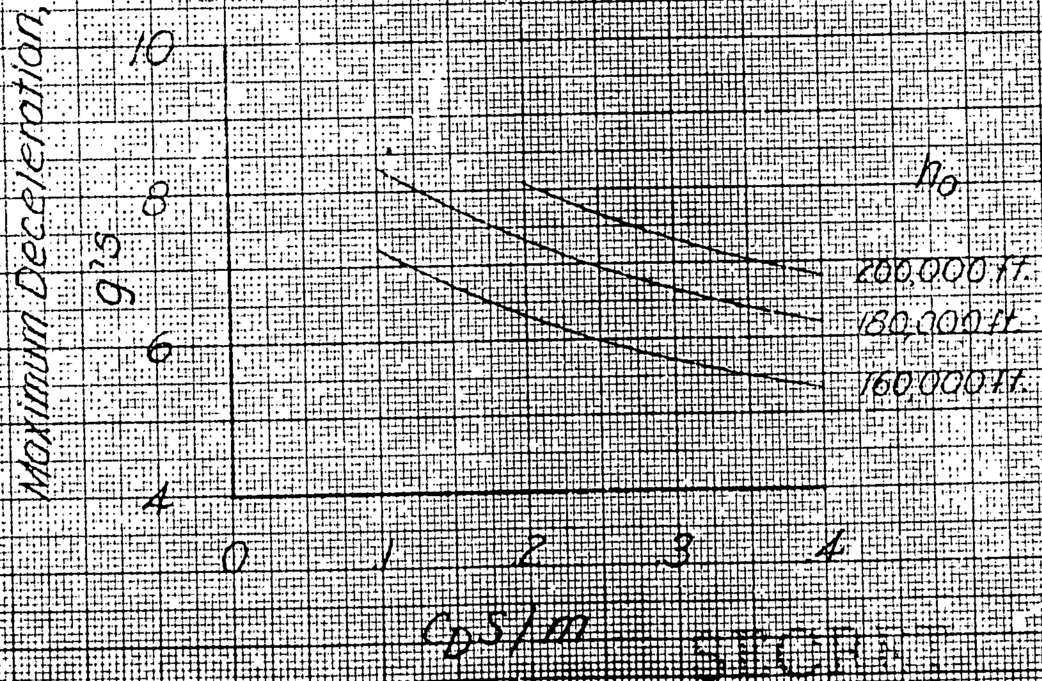

SECRET

4.6 ERRORS IN THE INITIAL GLIDE ALTITUDE

It is reasonable to expect the glider will normally start its glide at some slight variation from equilibrium conditions, i.e. $\dot{\gamma} = 0$ not equal to zero. This could be the result of errors connected with the ascent program control or simply the result of a variation between the pressure altitude and the tapeline altitude. In order to determine the possible effects and their importance to the design of such a system as proposed, this study was undertaken.

In this study it was assumed the vehicle reached the various altitudes from 160,000 feet to 200,000 feet with a velocity equal to 18,000 feet per second and a flight path angle equal to zero. This vehicle was further assumed to have a wing loading at 35 pounds per square foot of exposed wing area, L/D equal to 4.0, and C_L at maximum L/D equal to .10 (C_L also based upon exposed wing area). The time histories of altitude, flight path angle, and velocity were calculated using the Bell Aircraft Performance Analyzer (see Reference 4.6.1) for a glide vehicle starting its glide at altitudes of 160,000, 175,000, 180,000, 185,000, and 200,000 feet. (It had been originally estimated that the initial equilibrium glide conditions would be attained at 180,000 feet using tentative atmospheric data. However, these calculations shown here are based upon the latest "standard" atmosphere as presented in Reference 4.6.2. As a result the initial equilibrium conditions for this study are attained at a tapeline altitude of 177,000 feet rather than the expected 180,000 feet.)

The time histories of altitude for the various initial altitude conditions are presented in Figure 4.6-1, and in Figure 4.6-2 are shown the

corresponding time histories of flight path angle and velocity. The range covered, approximately 500 nautical miles, during this time period was just about equivalent for all the cases considered here and is not shown.

It was interesting to find the rapid convergence of altitude toward that which might be considered representative of the standard path, i.e. the path resulting from initiating the glide from the equilibrium altitude. Likewise, the tendency of both flight path angle and velocity to move towards the standard values indicated the vehicle was seeking flight conditions which would result in maximum range. Hence, it would appear that an effective means of flying the vehicle during its glide would be to sense and control the maximum L/D of the vehicle. Also any large initial corrections to attain standard glide conditions quickly appear unnecessary.

As a result of this study it would appear reasonable to require that the ascent control system place the vehicle within ±5000 feet of its initial standard altitude. An additional investigation into the variation of temperature resulting from non-equilibrium initial glide conditions is reported in a later section.

4.6 REFERENCES

4.6.1 Arthur, R. J. and Brigham, R. O.: The Bell Aircraft Performance Analyzer, Bell Aircraft Corporation Report No. 02-978-013, September 1, 1955

4.6.2 McKowen, P.: The Standard Atmosphere, Sea Level to 300,000 Feet, Bell Aircraft Corporation Aerodynamics Information Note No. 3, June 1956

4.6 SYMBOLS

C_L Lift coefficient

D Drag force, pounds

h_o Initial altitude, feet

L Lift force, pounds

$\dot{\gamma}$ Time rate of change of the flight path angle, degrees per second

SECRET

Fig. 4.6-1

Typical Time History of Altitude at the Start of the Glide

L/D = 4.0 $(C_L)_{L/D\,max} = .10$

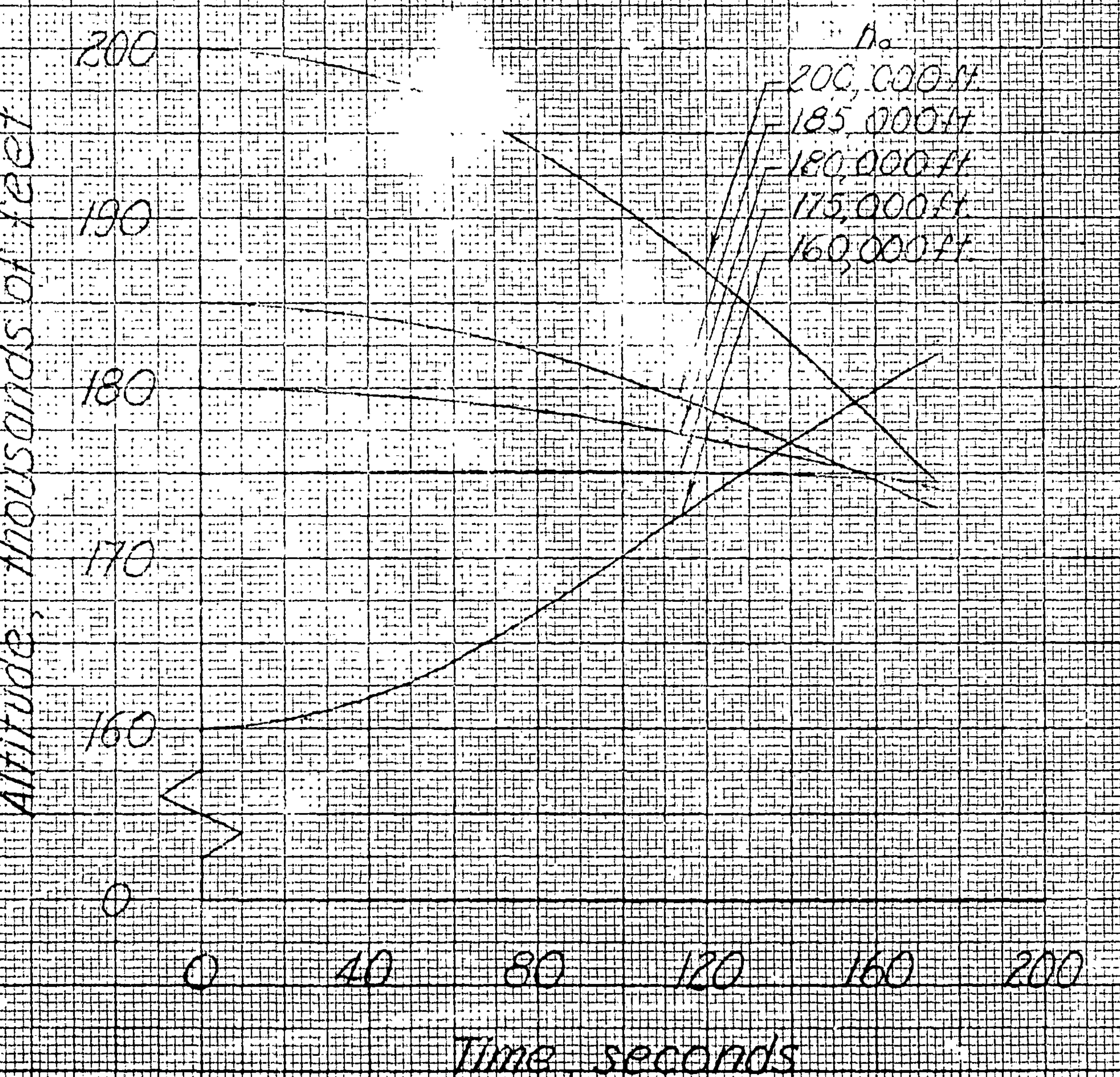

SECRET

SECRET

Fig. 4.6-2

Typical Time Histories of Flight Path Angle and Velocity at the Start of the Glide

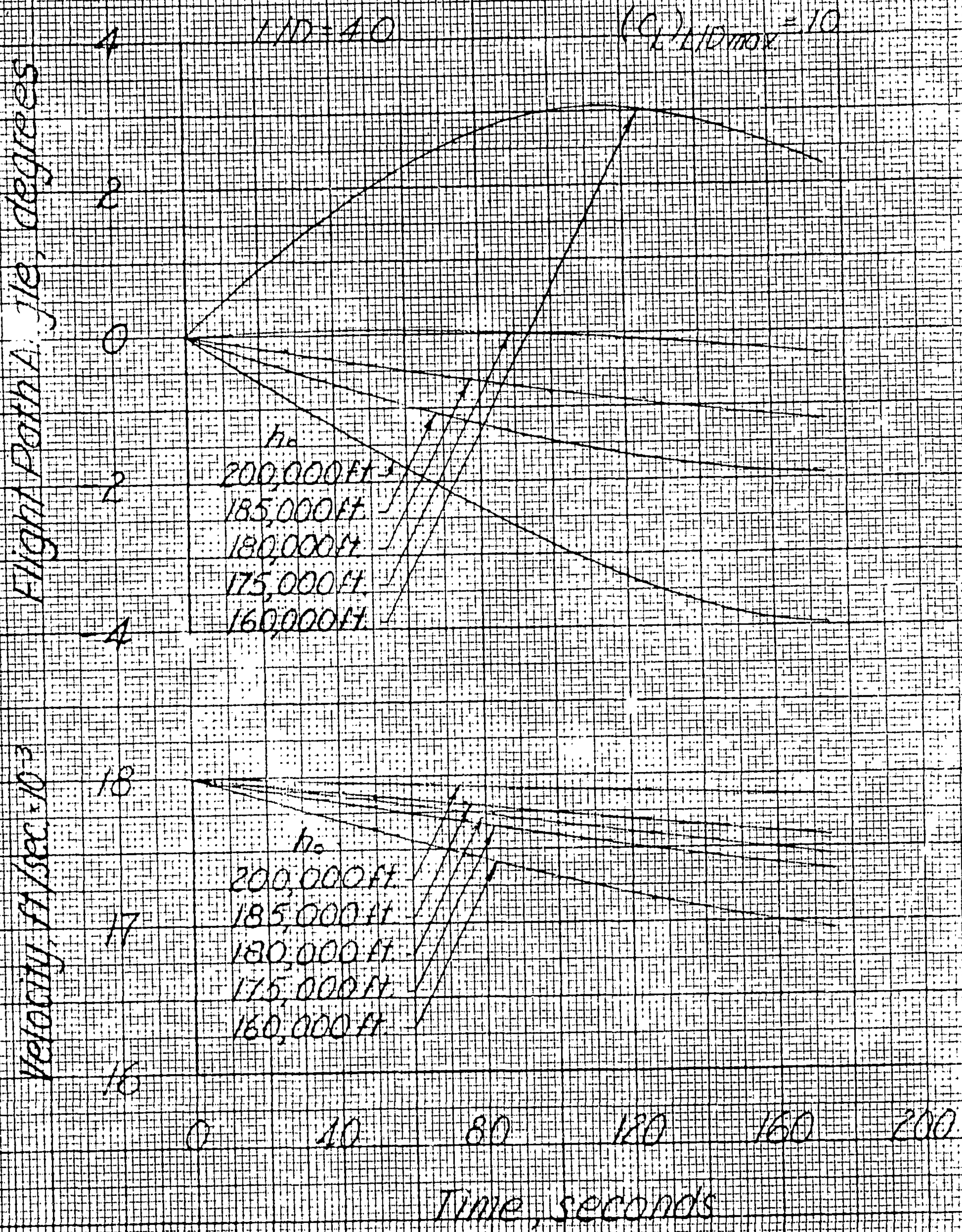

4.7 APPROXIMATING FUNCTION FOR THE LIFT TO DRAG RATIO

In the course of this design, as in many others, it became apparent that work had to be initiated before preliminary estimates of aerodynamic coefficients pertaining to specific configurations could be calculated. Not only was there a need for preliminary approximation, but in many instances a need existed for a mathematical function to represent the calculated lift-drag ratios.

This mathematical approximation for the calculated lift-drag ratio would be useful in calculating the range on digital computers and doing flight path control work. This function must be capable of exhibiting the characteristics of the lift-drag ratio, namely: a flat peak at high Mach numbers which becomes more pronounced with decreasing Mach number; a maximum value which increases with decreasing Mach number; the occurance of the maximum value of L/D at smaller angles of attack as Mach number decreases. All these obove mentioned characteristics can be approximated by the following function.

$$L/D = \frac{1}{\alpha}\left[1 - e^{-K\alpha}(1 + K\alpha)\right]$$

where L/D is the lift drag ratio

α is angle of attack expressed in radians

K is an arbitrary constant.

This function was calculated using values of K equal to 12, 15, 18, 21, and infinity. The results are presented in Figure 4.7-1. As can be seen by

calculating the proposed function with increasing values of K the characteristics of the lift-drag ratio for decreasing Mach numbers are very well approximated. Thus for the purposes of programming L/D into various calculators it would only be necessary to know the correspondence between Mach number and the arbitrary constant K.

In Figure 4.7-2 is shown the agreement between the L/D values calculated in Reference 4.7.1 and the function evaluated for K = 15. Though the general agreement is good, it would only be necessary to vary K slightly from 15 to attain excellent agreement with any calculation of L/D for a specific Mach number.

4.7 REFERENCES

4.7.1 Postle, R. S., et al: MX-2276 Reconnaissance Aircraft Weapon System - Aerodynamics, Bell Aircraft Corporation Report No. D143-945-024, December 1, 1955

4.7 SYMBOLS

D	Drag force
e	Base of natural logarithms
K	Arbitrary constant of approximating function
L	Lift force, pounds
α	Angle of attack

Fig. 47-1

Lift to Drag Ratio as Calculated using f(α, K)

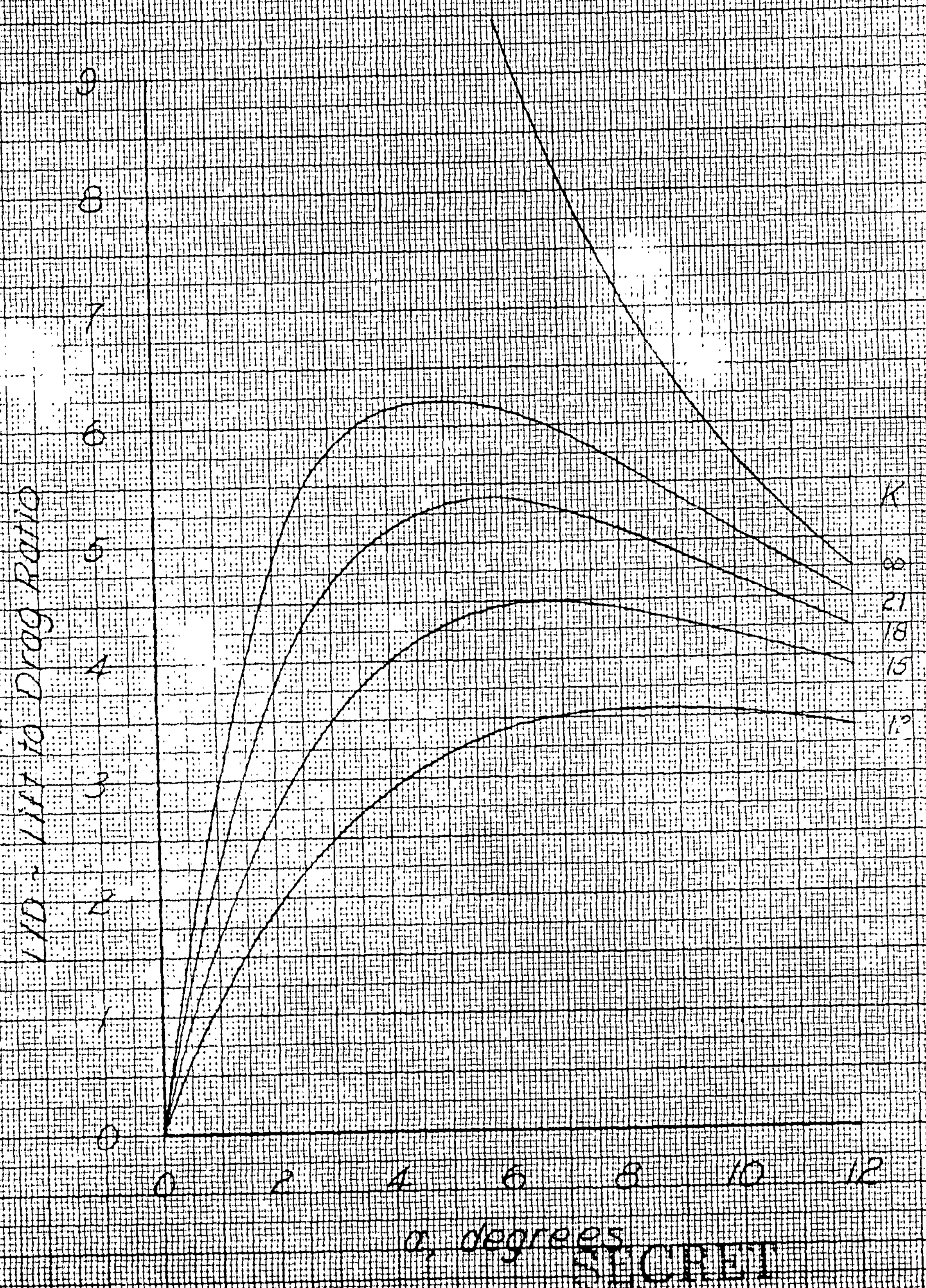

SECRET

Fig. 4.7.2

Comparison of Actual and the Approximation to Lift to Drag Ratios

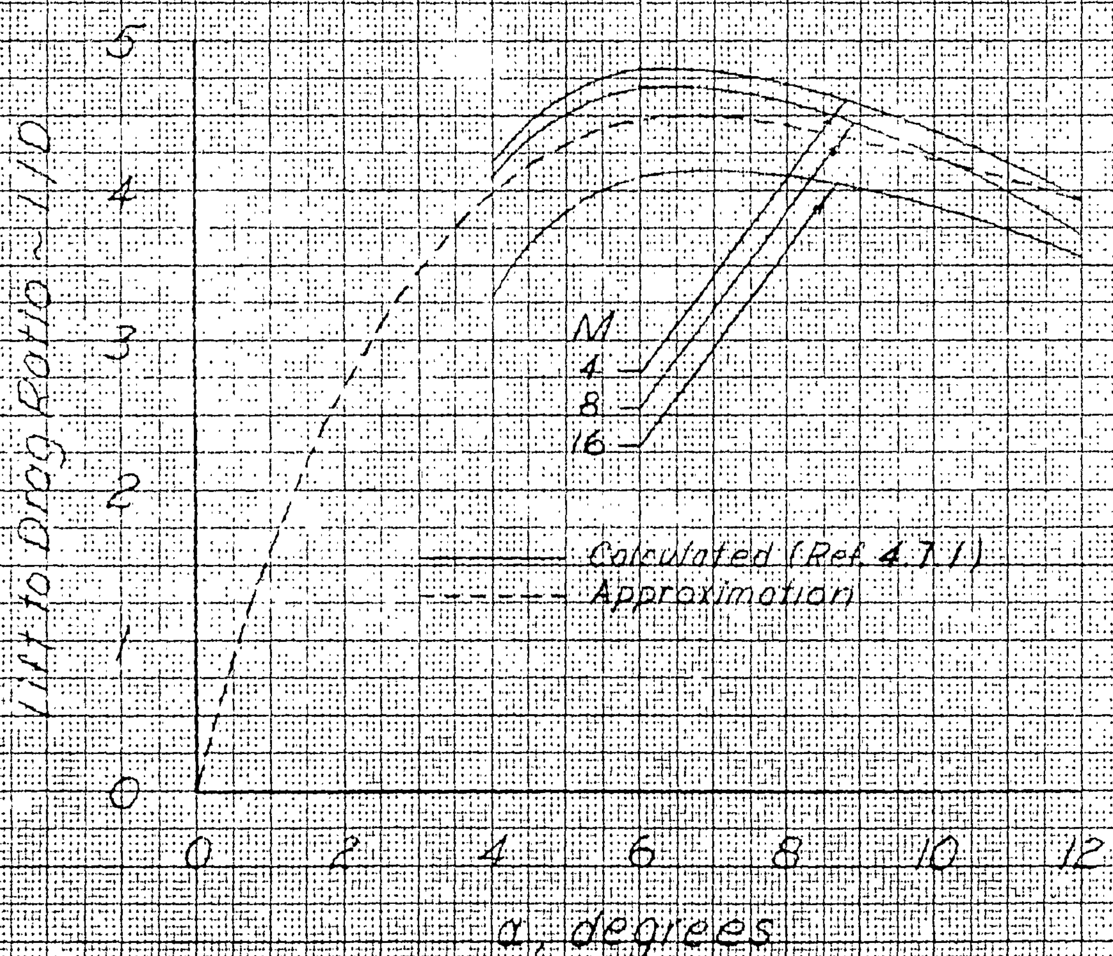

SECRET

4.8 GLIDE PERFORMANCE

The range performance of the "external" and "internal" type final stages (in glide configuration) was compared through the use of untrimmed glide range. (In a later section of this report it is shown that control deflections required for trim are of the same order of magnitude so that the glide range loss due to the additional drag of the control surfaces would be approximately the same for each glide vehicle.)

Untrimmed lift coefficients of the "internal" type and "external" type glide vehicles are presented in Figures 4.8-1 and 4.8-2. Representative untrimmed drag coefficients of these two aircraft at an altitude of 140,000 feet are shown in Figures 4.8-3 and 4.8-4. The values of lift and drag coefficients were calculated using the same methods previously described in Reference 4.8.1. Lift to drag ratios were calculated for each of the vehicles at various Mach numbers and altitudes. In Figures 4.8-5 through 4.8-7 are presented the lift-drag ratios of the "internal" type and Figures 4.8-8 to 4.8-10 show lift-drag values for the "external" type glider.

Using an empty weight of 20,200 pounds for the "internal" type glider the equilibrium altitudes for flight at various Mach numbers and angles of attack corresponding to maximum lift-drag ratio conditions were determined. These results are presented in Figures 4.8-11, 4.8-12, and 4.8-13. An empty weight of 13,700 pounds was used to determine these same flight conditions for the glide configuration at the "external" type final stage, and these are presented in Figures 4.8-14 through 4.8-16.

In Figure 4.8-17 are presented the time histories of velocity, altitude, and range of the two glide vehicles as estimated using the method

given in Reference 4.8.1. The range was calculated only during that portion of flight in which the velocity decreased from 18,000 feet per second to 4000 feet per second. As can be seen the glide range was approximately 5000 nautical miles for each vehicle. During the ascent a range of 420 to 450 nautical miles was attained (see Sections 3.4 and 3.4.1). The glide range during the descent exceeds 100 nautical miles for vehicles of this type. Thus, the ground to ground range of these two vehicles is very nearly the same, and slightly better than the 5500 nautical miles required.

4.8 REFERENCES

4.8.1 Postle, R. S., et al: MX-2276 Reconnaissance Aircraft Weapon System - Aerodynamics, Bell Aircraft Corporation Report No. D143-945-024, December 1, 1955

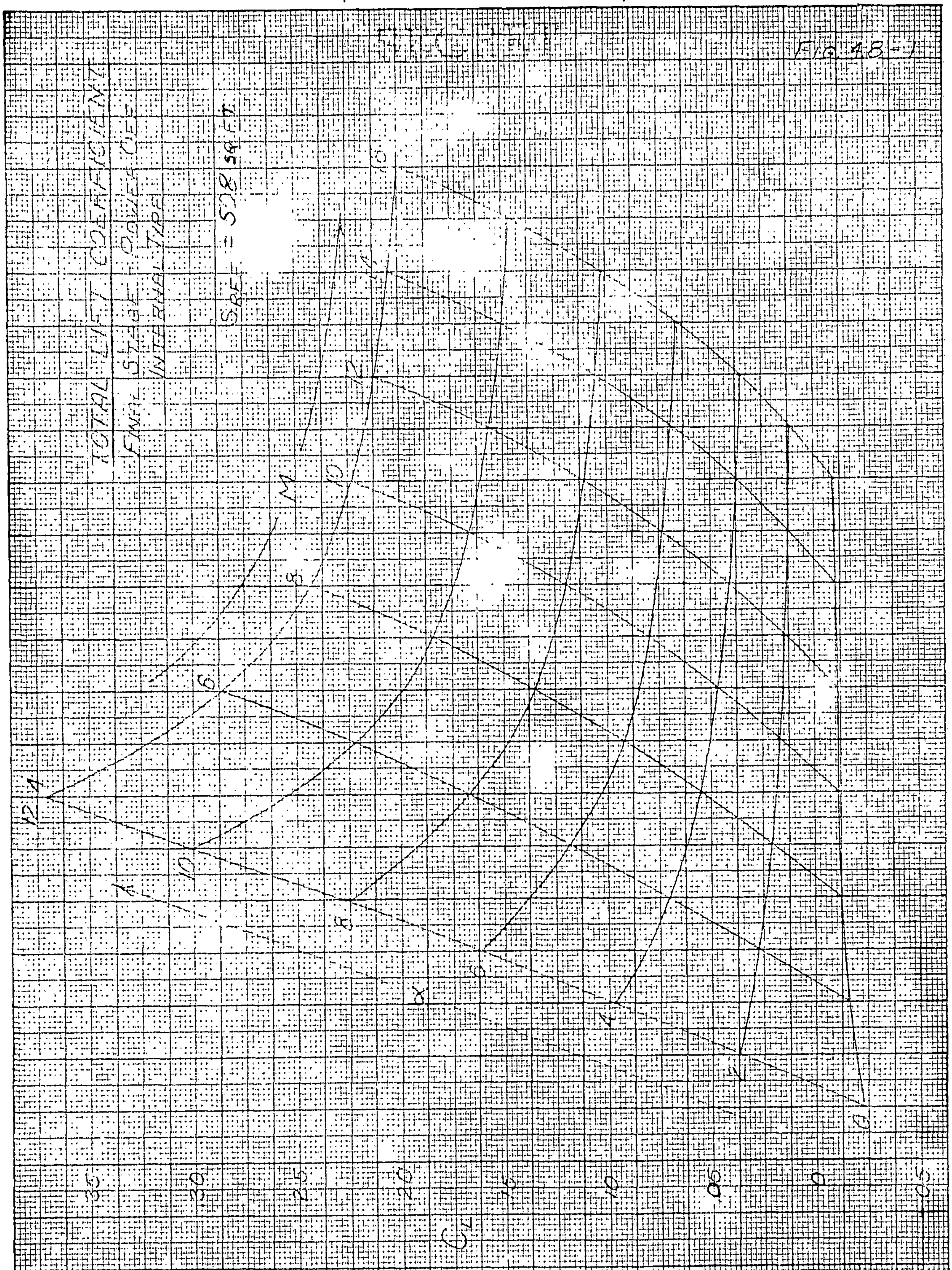
TOTAL LIFT COEFFICIENT
FINAL STAGE POWER OFF
INTERNAL TYPE
SREF = 538 SQ FT
M
α
CL

SECRET

SECRET

FIG. 48-2

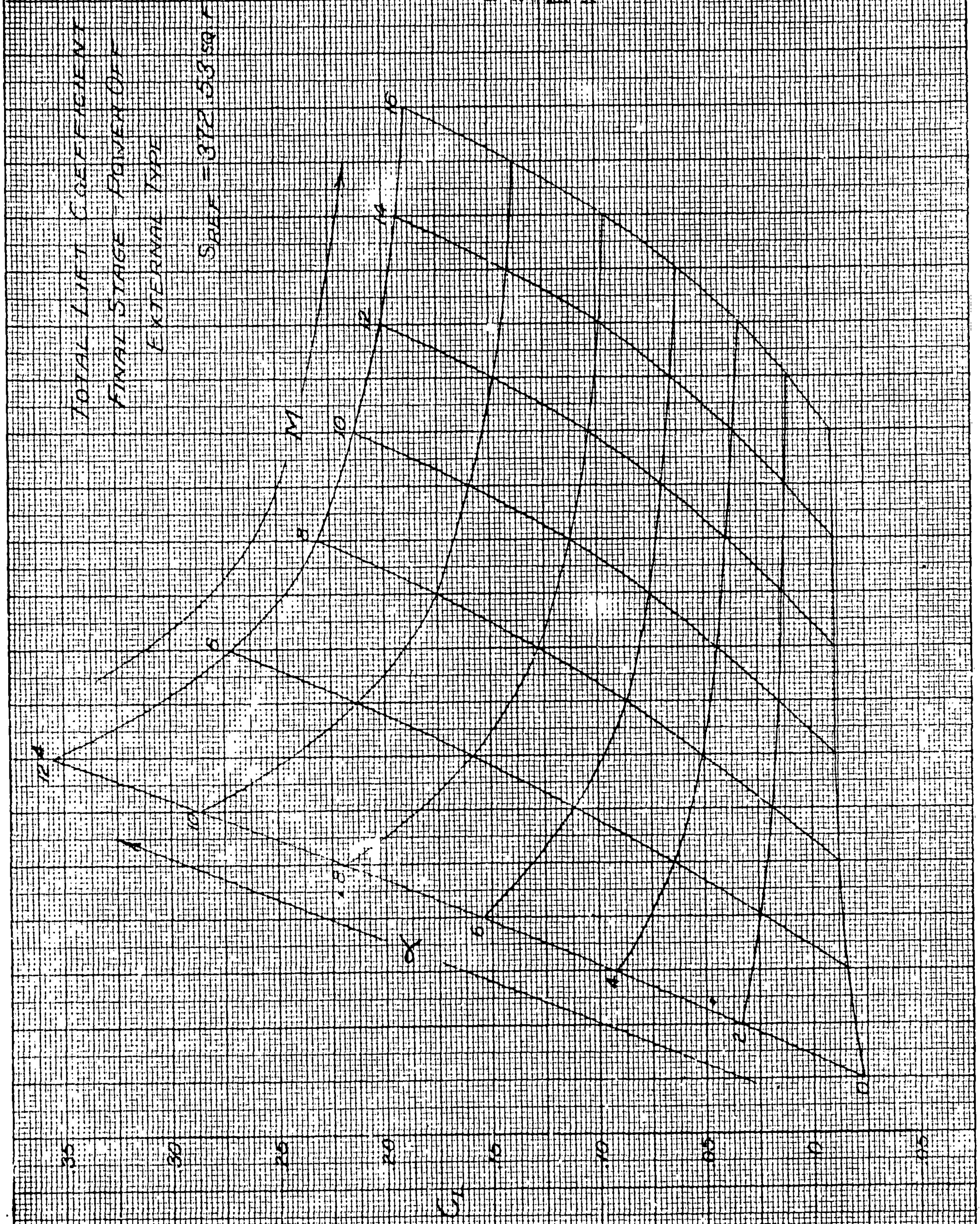

SECRET

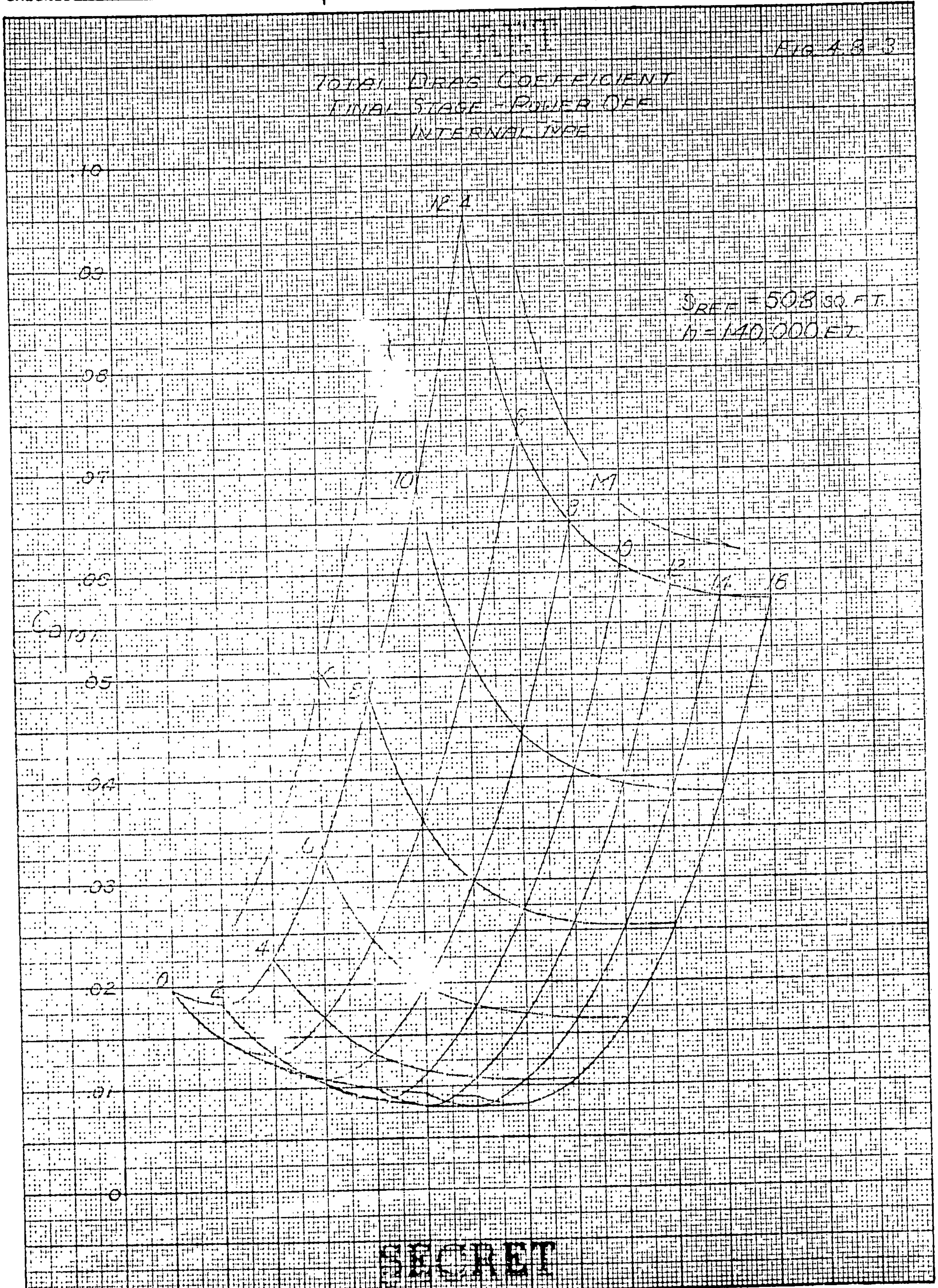
Fig 4.3-3
Total Drag Coefficient
Final Stage - Power Off
Internal Inlet
S_{REF} = 508 SQ. FT.
h = 140,000 FT.
$C_{D_{TOT}}$
.10
.09
.08
.07
.06
.05
.04
.03
.02
.01
0
M
12.4
10
6
8
9
12
14
16
4
2
0

SECRET

Fig 4.8-4

TOTAL DRAG COEFFICIENT

FINAL STAGE - POWER OFF

EXTERNAL TYPE

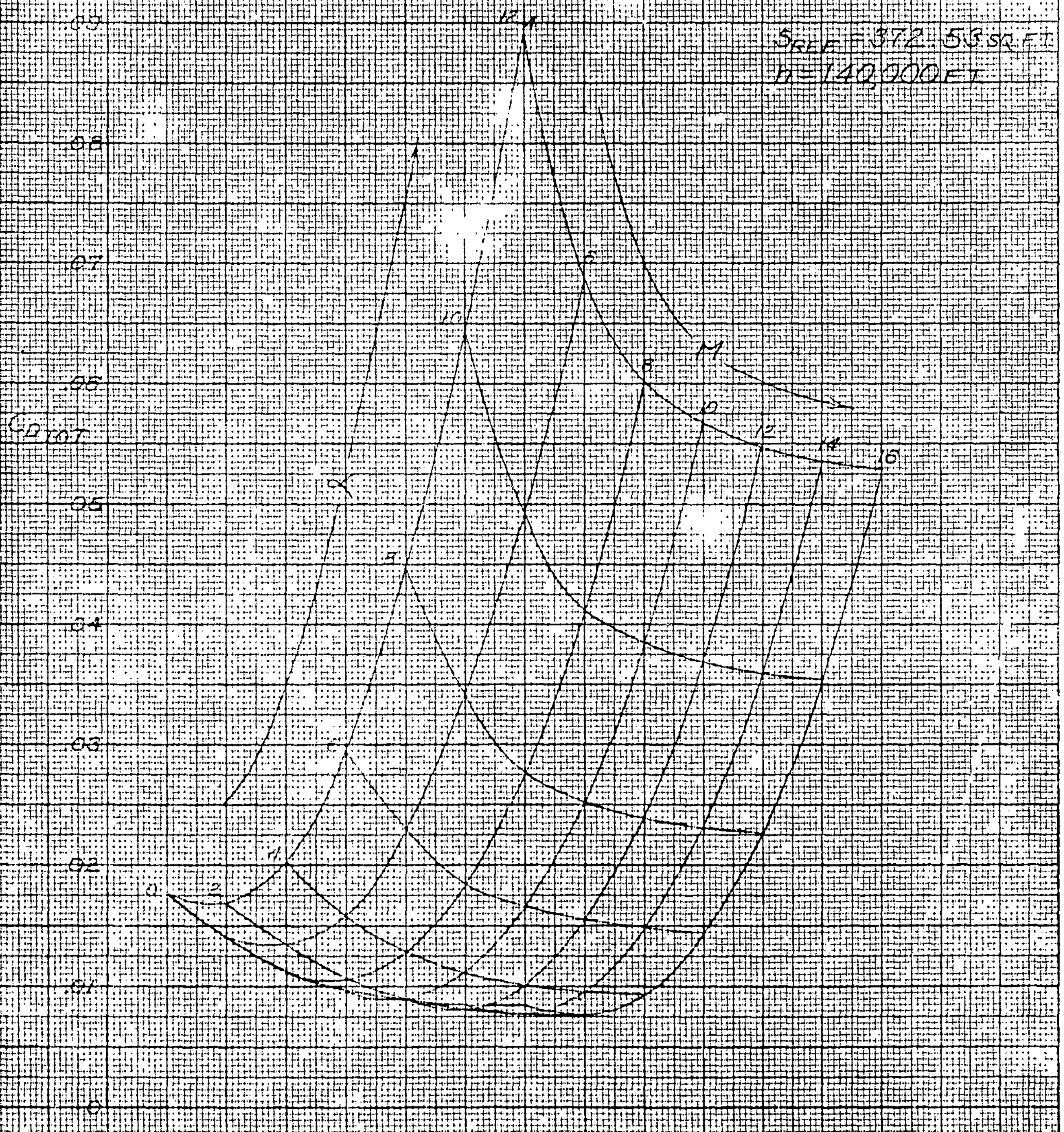

SECRET

SECRET

FIG 4.5-5

LIFT TO DRAG RATIOS - INTERNAL TYPE - POWER OFF

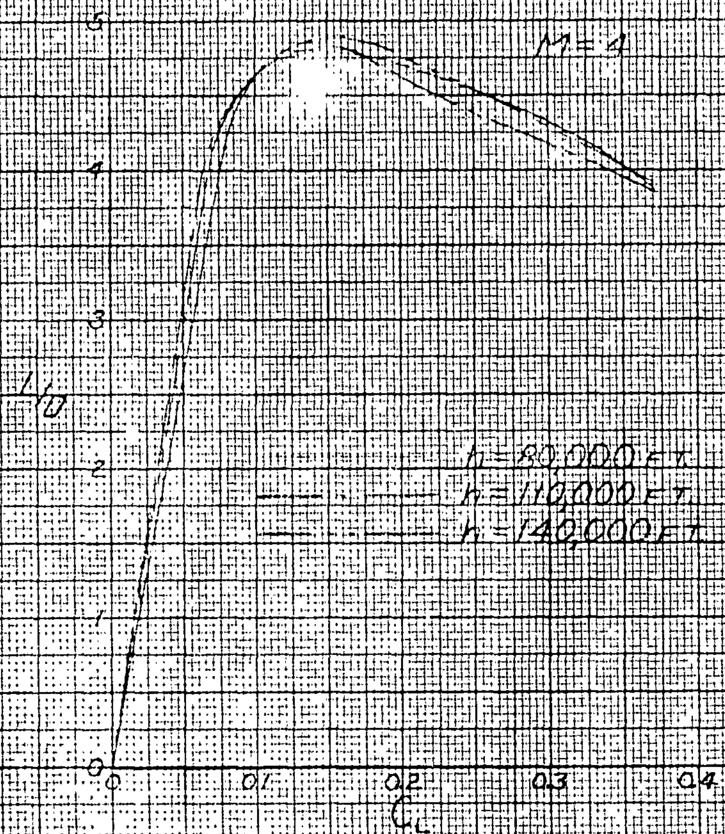

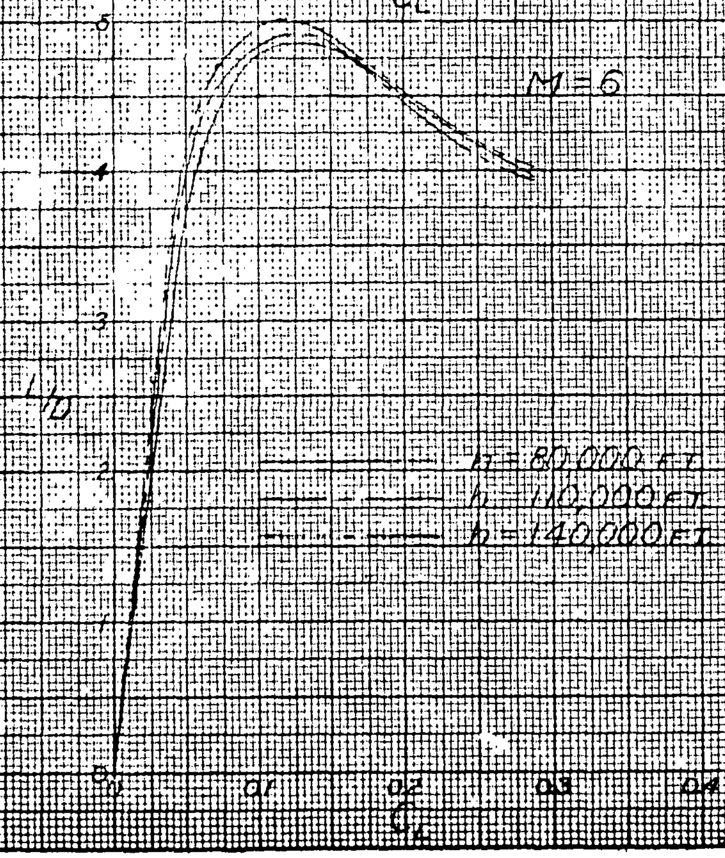

SECRET

SECRET

FIG 48-C

LIFT TO DRAG RATIOS - INTERNAL TYPE - POWER OFF

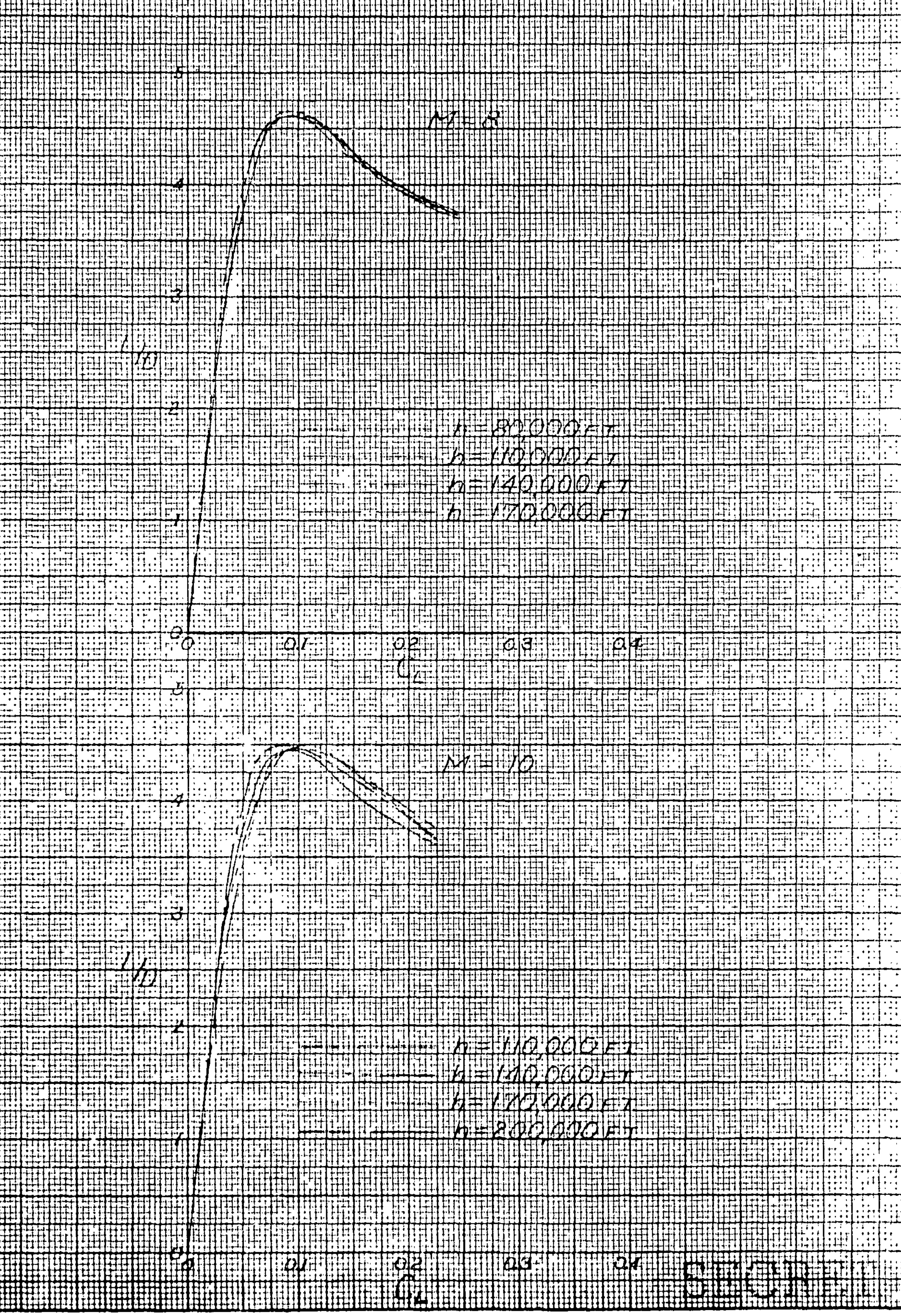

SECRET

FIG 4.6-7

LIFT TO DRAG RA[illegible] [illegible]NAL [illegible] POWER OFF

SECRET

FIG. 4.8-8

LIFT TO DRAG RATIOS - EXTERNAL TYPE - POWER OFF

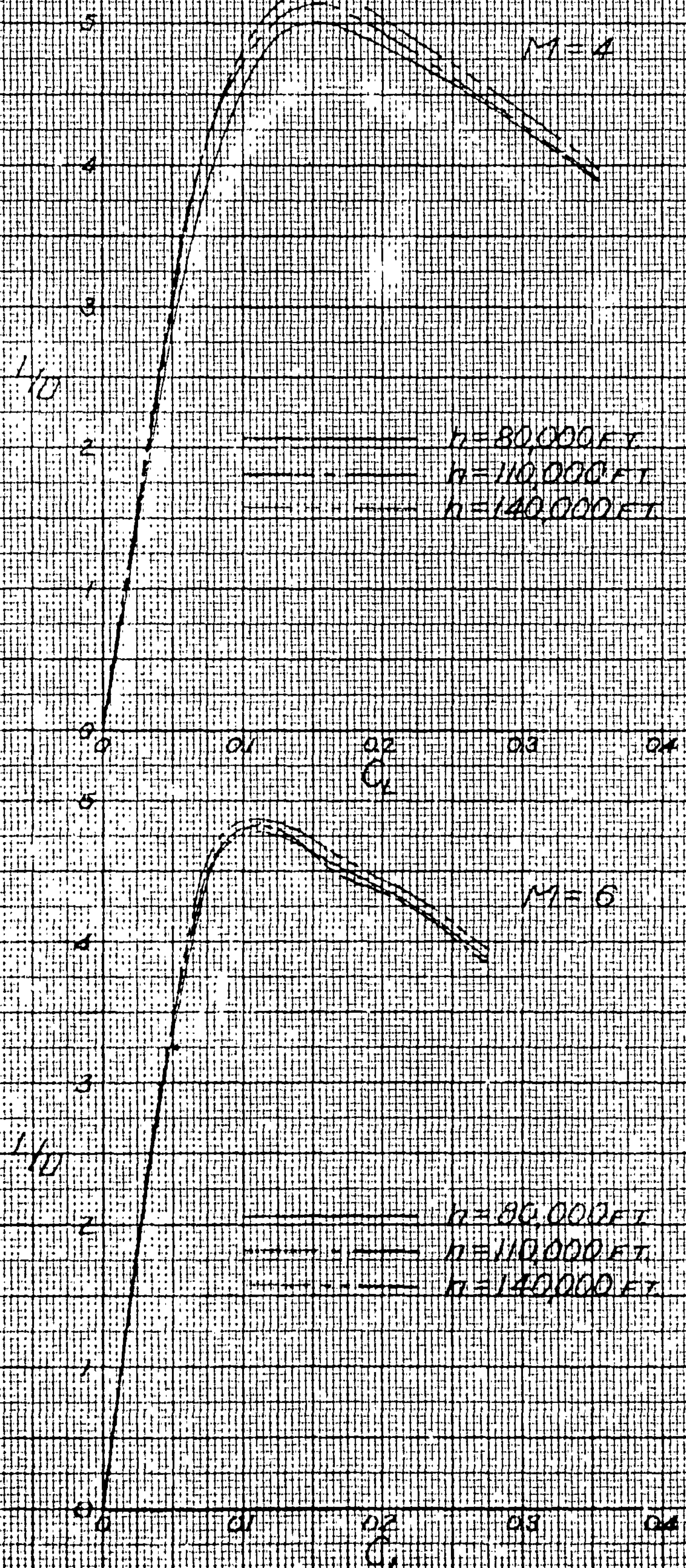

SECRET

SECRET

Fig. 4.8-?

LIFT TO DRAG RATIOS - EXTERNAL TYPE - POWER OFF

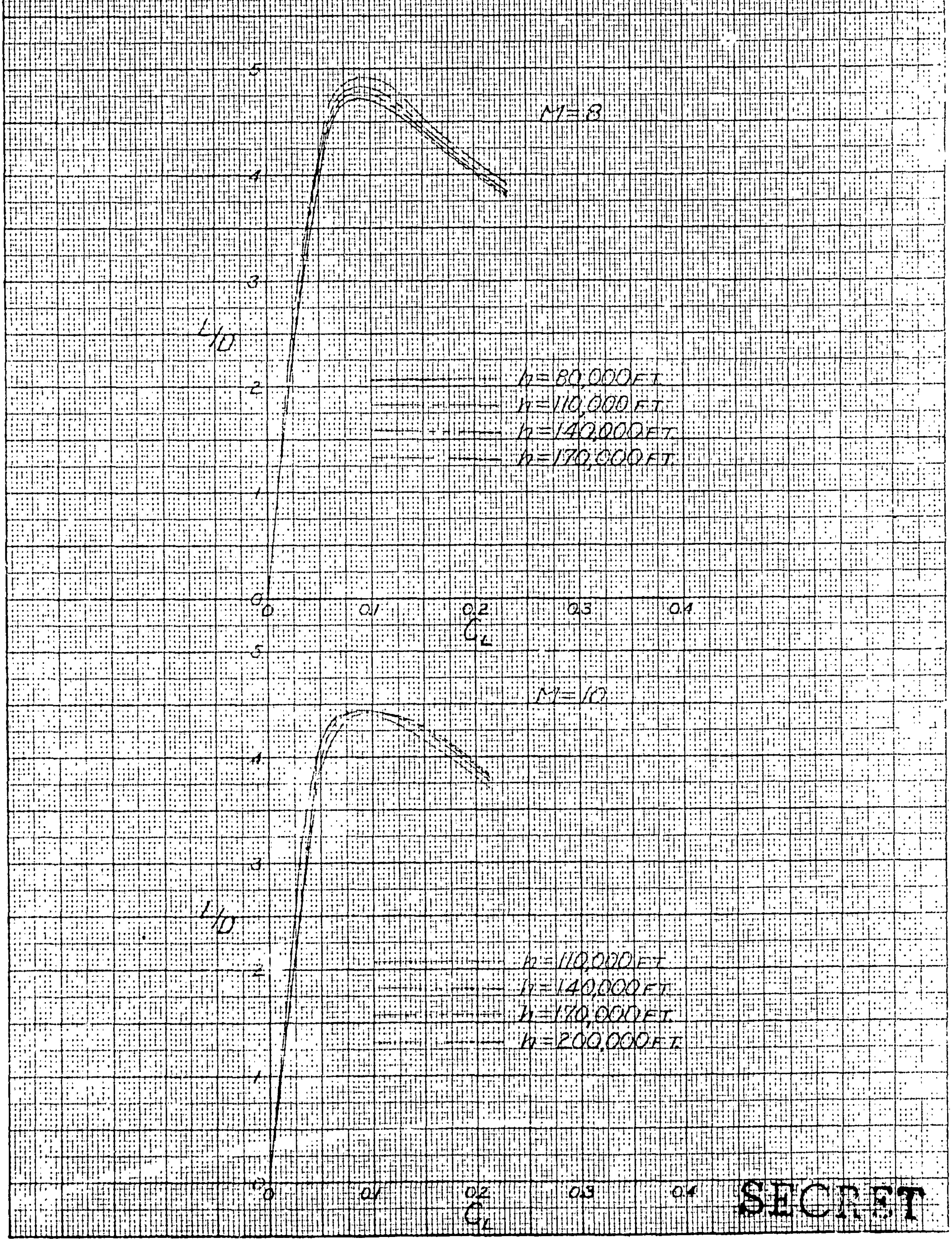

SECRET

SECRET

FIG 4.8 10

LIFT TO DRAG RATIOS – EXTERNAL TYPE – POWER OFF

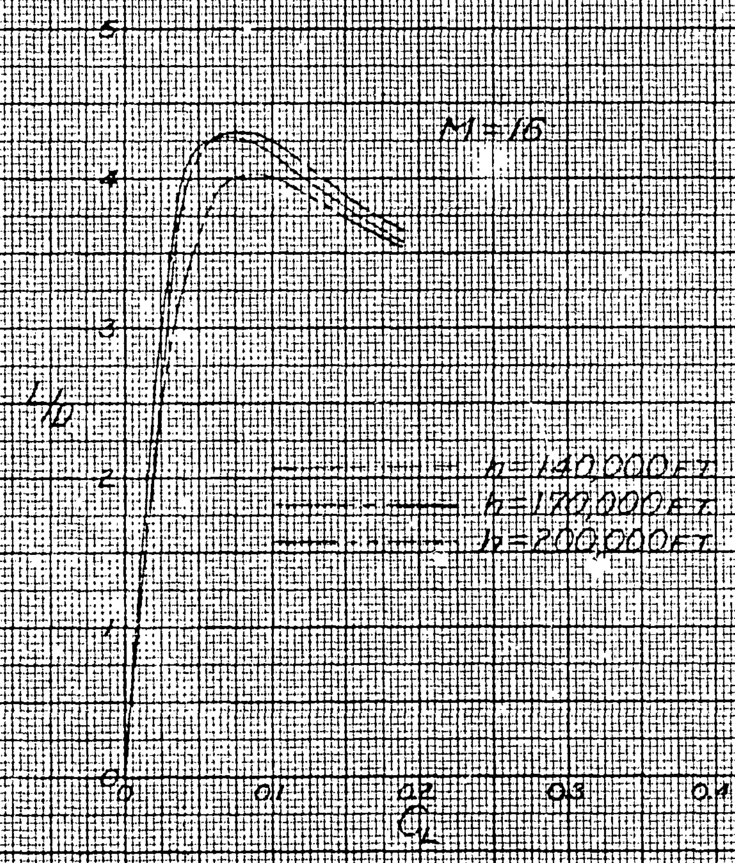

SECRET

SECRET

FIG. 4.8-11

DETERMINATION OF EQUILIBRIUM ALTITUDES
AND CORRESPONDING MAXIMUM L/D RATIOS
INTERNAL TYPE

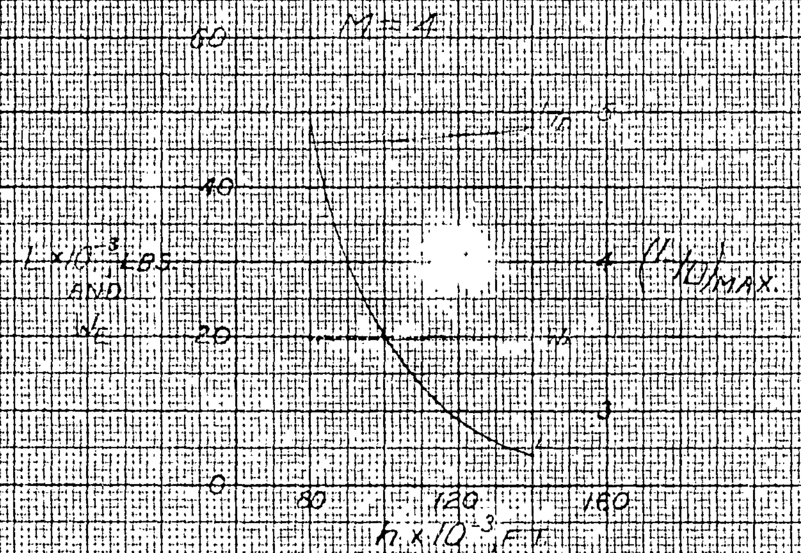

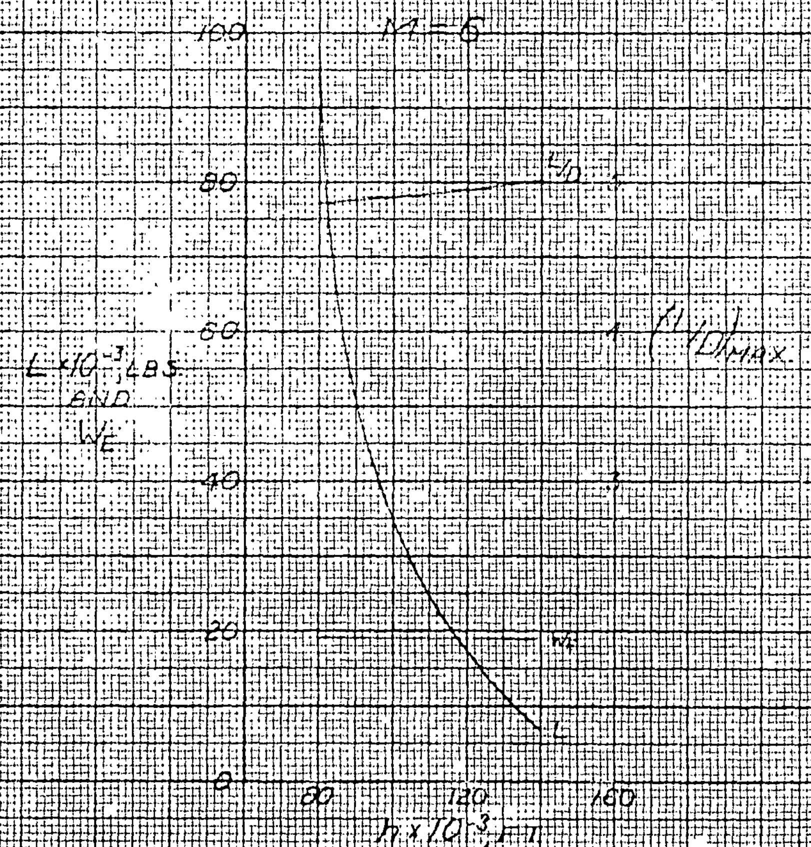

SECRET

FIG. 4.8-12

DETERMINATION OF EQUILIBRIUM ALTITUDES AND CORRESPONDING MAXIMUM L/D RATIOS

INTERNAL TYPE

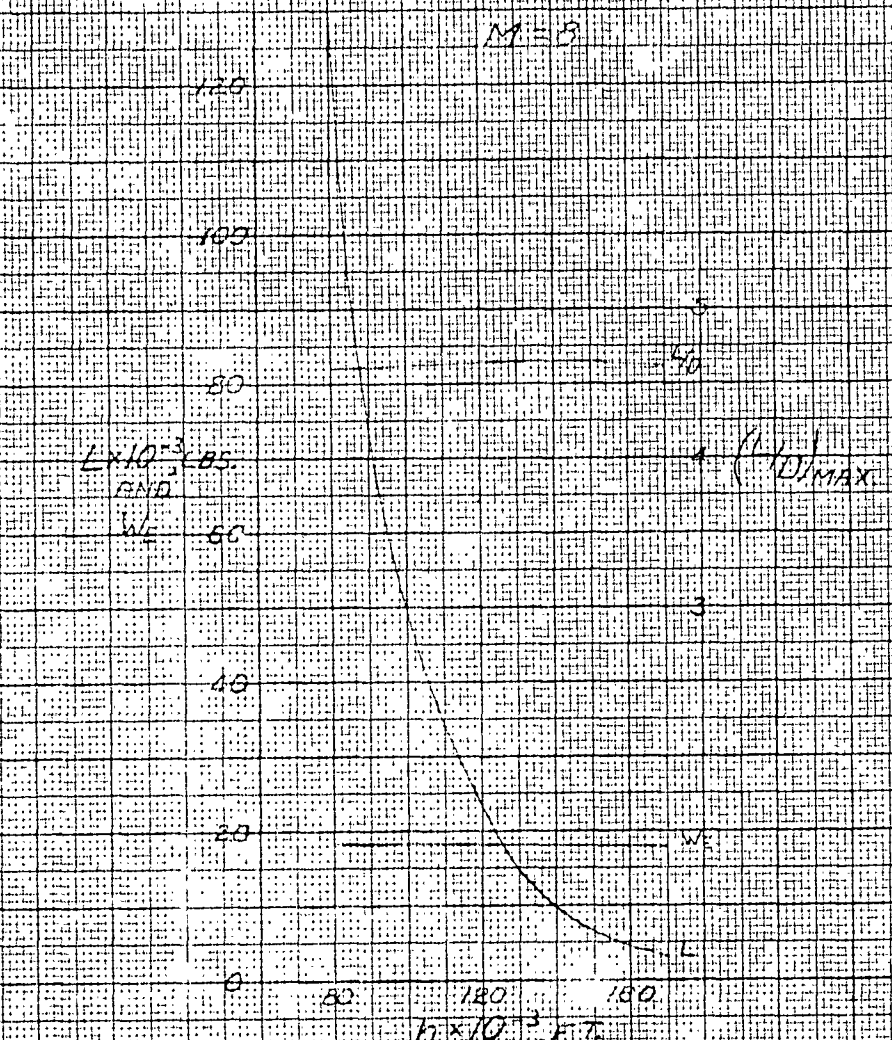

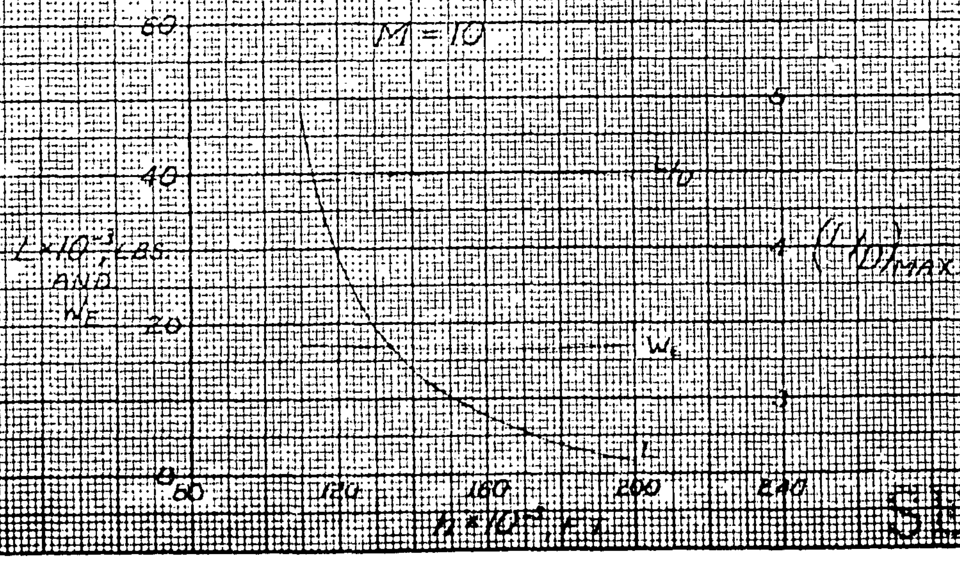

SECRET

Fig. 4.8-13

DETERMINATION OF EQUILIBRIUM ALTITUDES
AND CORRESPONDING MAXIMUM L/D RATIOS
INTERNAL TYPE

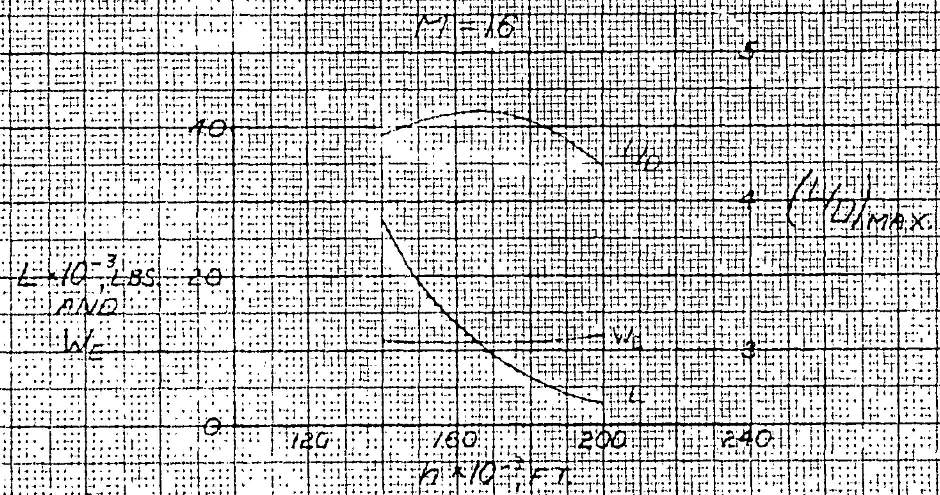

SECRET

SECRET

Fig 4.8-14

Determination of Equilibrium Altitudes and Corresponding Maximum L/D Ratios

External Type

M = 4

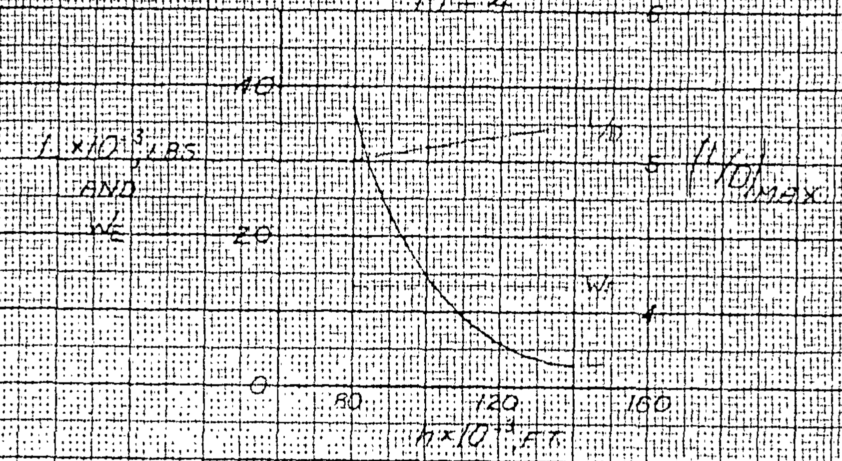

M = 6

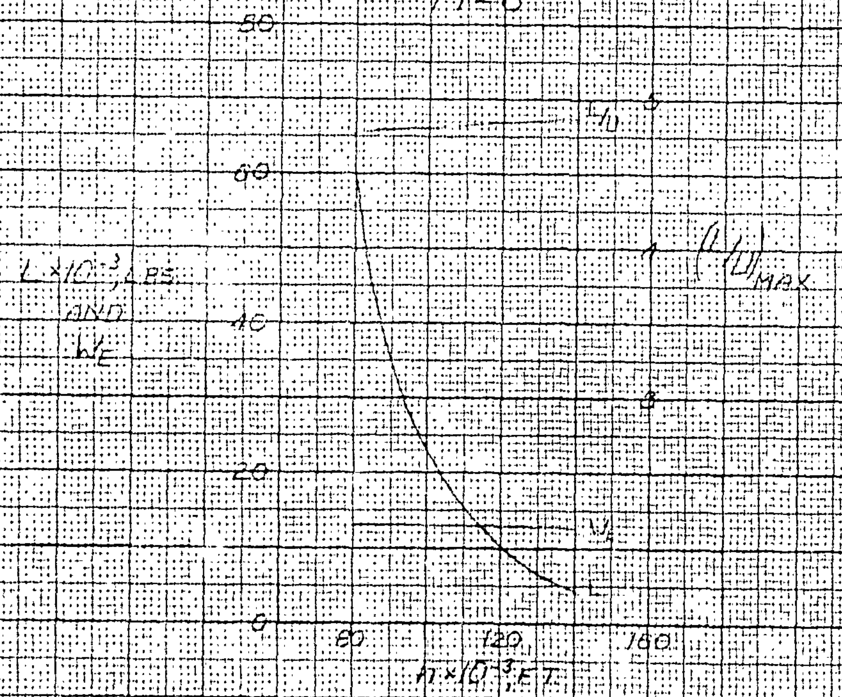

SECRET

SECRET

Fig 4.8-15

DETERMINATION OF EQUILIBRIUM ALTITUDES
AND CORRESPONDING MAXIMUM L/D RATIOS
EXTERNAL TYPE

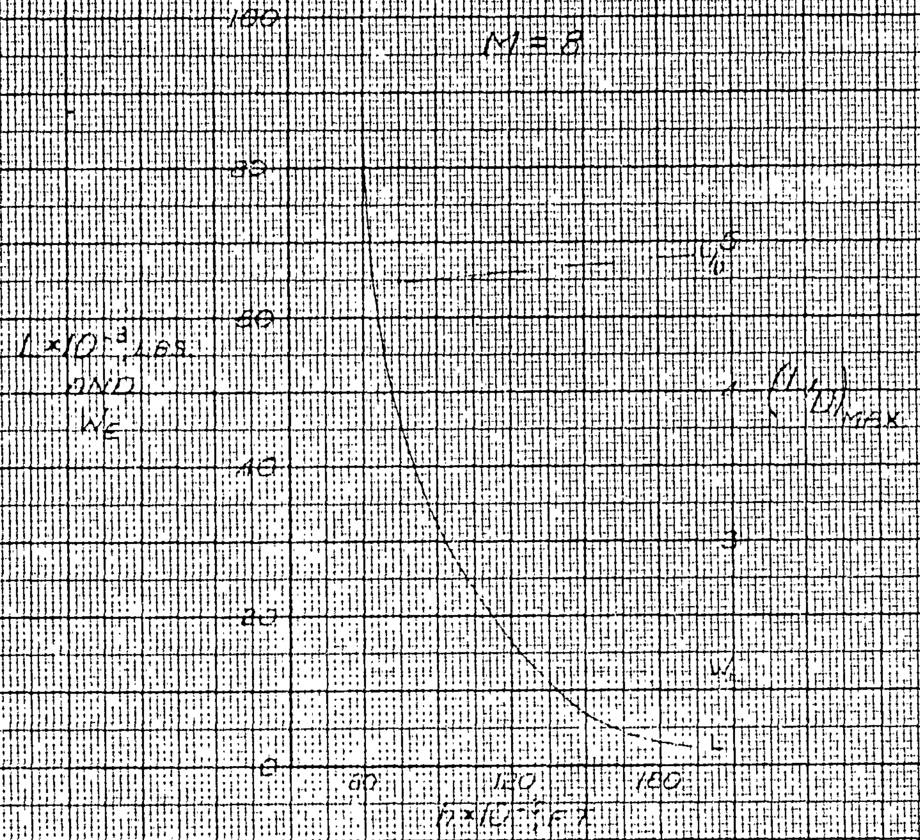

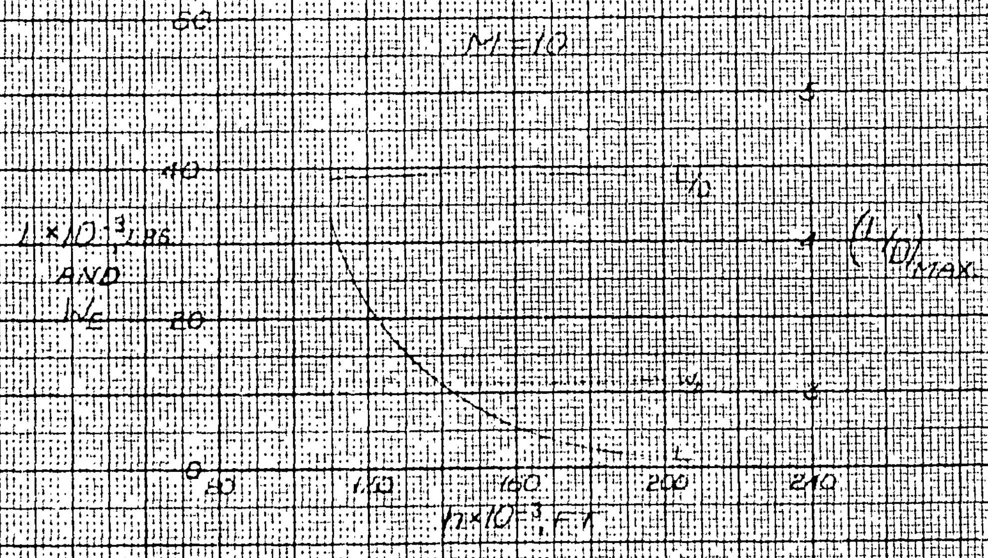

SECRET

SECRET

Fig. 4.8-16

DETERMINATION OF EQUILIBRIUM ALTITUDES
AND CORRESPONDING MAXIMUM L/D RATIOS
EXTERNAL TYPE

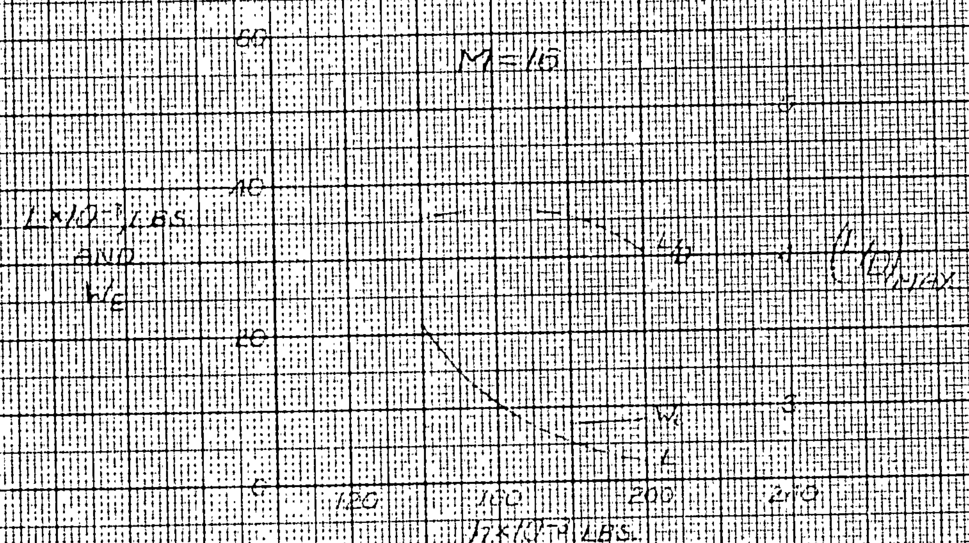

SECRET

SECRET

Time Histories of Range, Altitude, and Velocity during the Glide of the "External" and "Internal" Type Final Stages

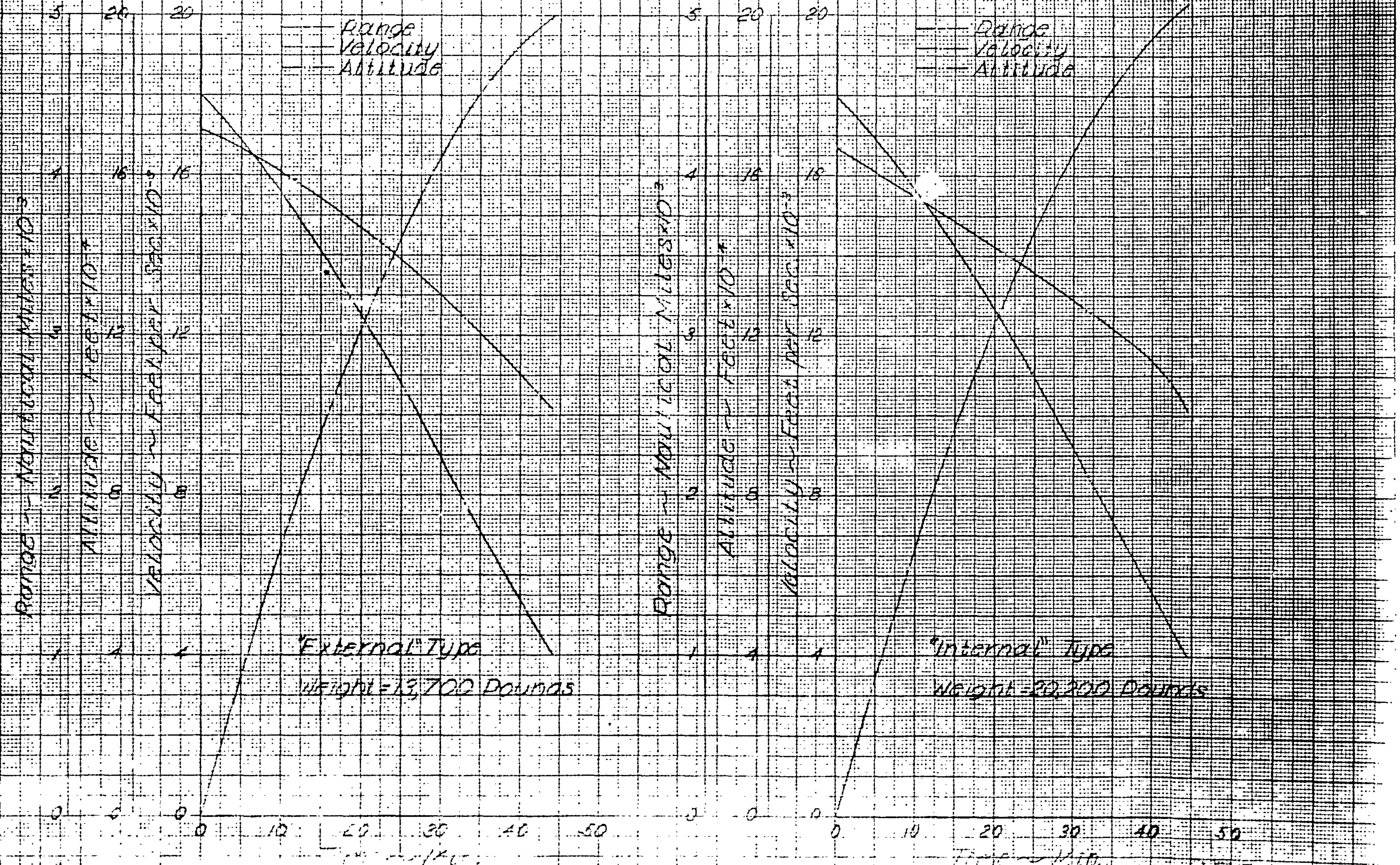

Fig. 4.8-17

4.9 STATIC LONGITUDINAL STABILITY

The high speed ($4 < M < 16$) static longitudinal stability was estimated for the two glide configurations under consideration using the methods described in Reference 4.9.1. The moments were taken about the points which had been roughly estimated to be the furthest aft locations of the center of gravity for each configuration.

In estimating the low speed ($.2 < M < .8$) stability characteristics the exposed wing lift estimated previously for the results presented in Section 3.14. This method is described in more detail in Reference 4.9.2. The wing carry-over and upwash corrections were estimated using the method presented in Reference 4.9.3. The fuselage lift and moment characteristics were calculated employing the information presented in Reference 4.9.4. As mentioned previously in Section 4.4 the method of Reference 4.4.2 would be employed to determine the aerodynamic center of the wing at subsonic speeds.

Throughout the investigation the control deflections were assumed zero. Also the center of pressures were estimated assuming inviscid, non-separated flow.

4.9.1 STATIC LONGITUDINAL STABILITY FROM MACH NUMBER 4.0 TO 16.0

The longitudinal static stability characteristics of the "internal" type final stage as estimated over the Mach number range traversed during its glide are presented in Figure 4.9-1. The moments are taken about Station 715 with the leading edge of the wing MAC placed at Station 670. The data presented in this curve was used to determine the location of the

stick fixed neutral point for constant C_L's of .06, .08, and .10. The neutral point locations corresponding to the C_L's required during the glide were also calculated. The results are presented in Figure 4.9-2. Superimposed upon this figure is the variation of the center of gravity location as it varies during the glide because of the coolant expended. As can be seen the static margin varies from about 6 percent at M = 16.0 to 16 percent at M = 4.0 at flight C_L's.

In Figure 4.9-3 are presented the stability characteristics of the glide configuration of the "external" type final stage. The stability characteristics were estimated for two wing positions. The first has the wing placed such that the leading edge of the wing MAC was located at Station 476, and the second has the leading edge of the wing MAC located at Station 450. The neutral point locations and the center of gravity locations for these two wing positions are shown in Figures 4.9-4 and 4.9-5 respectively. It should be noted that moving the wing forward also has an appreciable effect on moving the center of gravity forward. For the rearward location of the wing the static margin varies from 20 percent at M = 16.0 to 14 percent at M = 4.0 with a minimum at about M = 6.0 of 11 percent. On the other hand, the forward location of the wing reduces the stick fixed static margin to 16 percent at M = 16.0 and 10 percent at M = 4.0. For both wing positions this was only an incremental change of static margin of six percent during the glide of the "external" type whereas the change was an increment of 10 percent during the glide flight of the "internal" type.

As a result of this investigation, it is apparent that sufficient static margins during high speed flight can be achieved in the design of

either of the proposed types of vehicles. In addition, change in center of gravity location, as caused by the expulsion of coolants during the glide portion of the flight, can be used to good advantage to offset the wide variation in stability characteristics attendant with the large range of Mach number encountered during the glide.

4.9.2 STATIC LONGITUDINAL STABILITY FROM MACH NUMBER .20 TO .80

The low speed stability characteristics of the "internal" type final stage are shown in Figure 4.9-6 and the location of the stick fixed neutral points are presented in Figure 4.9-7. With the center of gravity located at Station 710 (the only changes after the complete expulsion of the coolants will be very minor as caused by lowering of landing gear, etc). The static margin is approximately 10 percent for the C_L conditions anticipated during the subsonic descent and landing.

The stability characteristics of the "external" type final stage glider are shown for the two wing positions in Figures 4.9-8 and 4.9-9. The calculated locations of the neutral points are presented in Figures 4.9-10 and 4.9-11. The static margin of the vehicle with the rearward wing location was about 10 percent at anticipated range of low speed flight C_L's from .3 to [illegible] [illegible] static margin was reduced to about two percent for the same C_L conditions when the wing was placed in the forward position. The estimated center of gravity position was at Stations 515 and 510 for the aft and forward locations of the wing respectively

SECRET

Classified only when data are entered

4.9 REFERENCES

4.9.1 Postle, R. S., et al: MX-2276 Reconnaissance Aircraft Weapon System - Aerodynamics, Bell Aircraft Corporation Report No. D143-945-024, December 1, 1955

4.9.2 Gill, W. J.: Subsonic Wing Lift; Low Aspect Ratio; Sweptback Wings, Unpublished Bell Aircraft Corporation Technical Data Report

4.9.3 Donselman, R. W.: Supersonic Wing Lift and Moments - Wing Body Combinations, Bell Aircraft Corporation Aerodynamics Research Note No. 59, October 22, 1953 (Revised to include subsonic case, February 16, 1956)

4.9.4 Youth, S. and Simon, A. D.: Determination of Performance Parameters - Subdivision BIC - Subsonic Body Lift Coefficient, Bell Aircraft Corporation Report No. 02-981-009, December 8, 1953

4.9 SYMBOLS

$\bar{c}$	Mean aerodynamic chord of the exposed wing
C_L	Lift coeffieient, L/qS
C_m	Pitching moment coefficient, $M/qS\bar{c}$
L	Lift force, pounds
M	Pitching moment, foot pounds
M	Mach number
q	Dynamic pressure, pounds per square foot
S	Exposed wing area, square feet
δ_e	Elevator deflection, degrees

SECRET

Fig 4.9-1

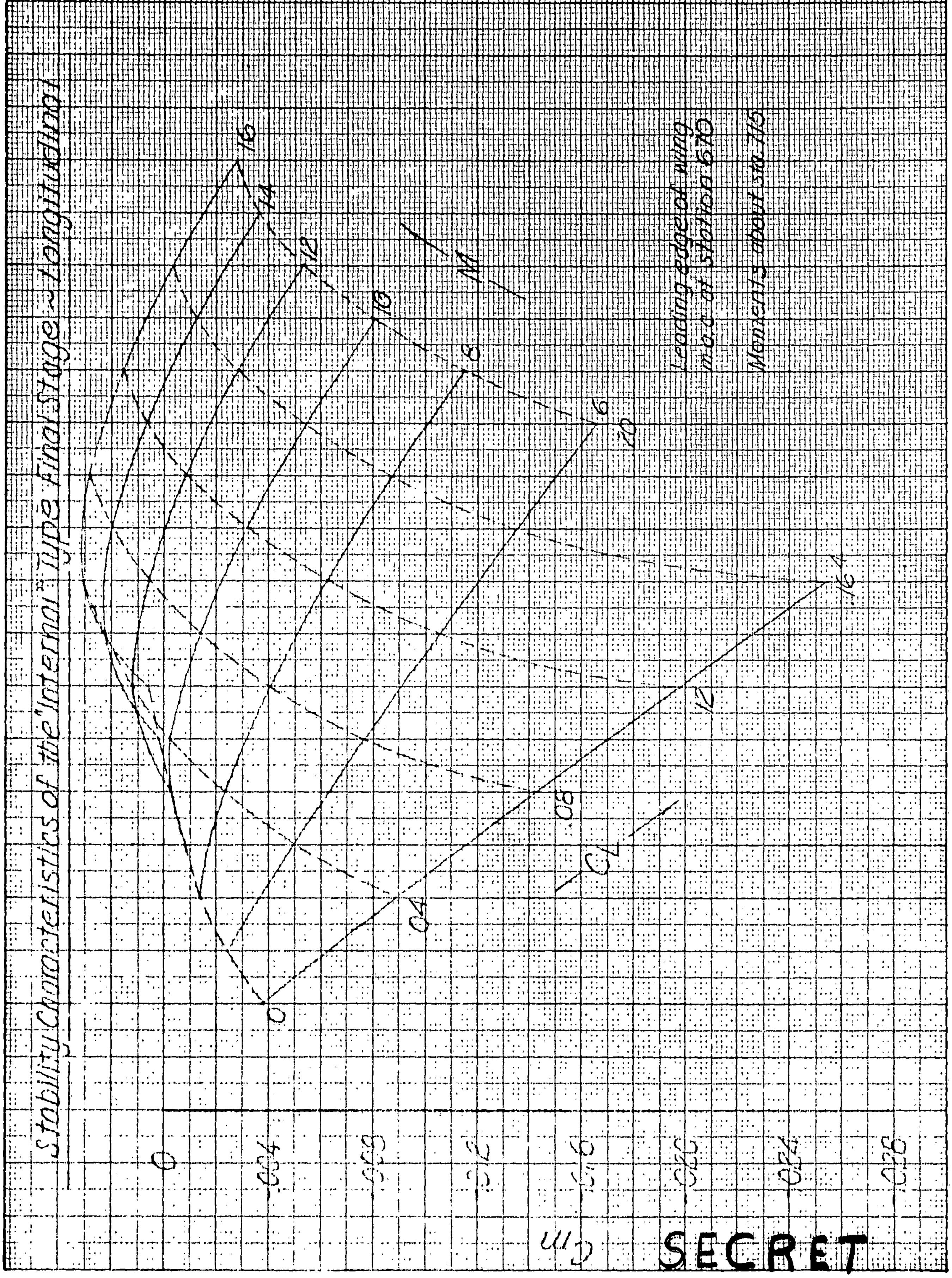

SECRET

Fig. 49-2

SECRET

Location of the Stick Fixed Neutral Point and the Center of Gravity

"Internal" Type Final Stage

$\delta_E = 0°$

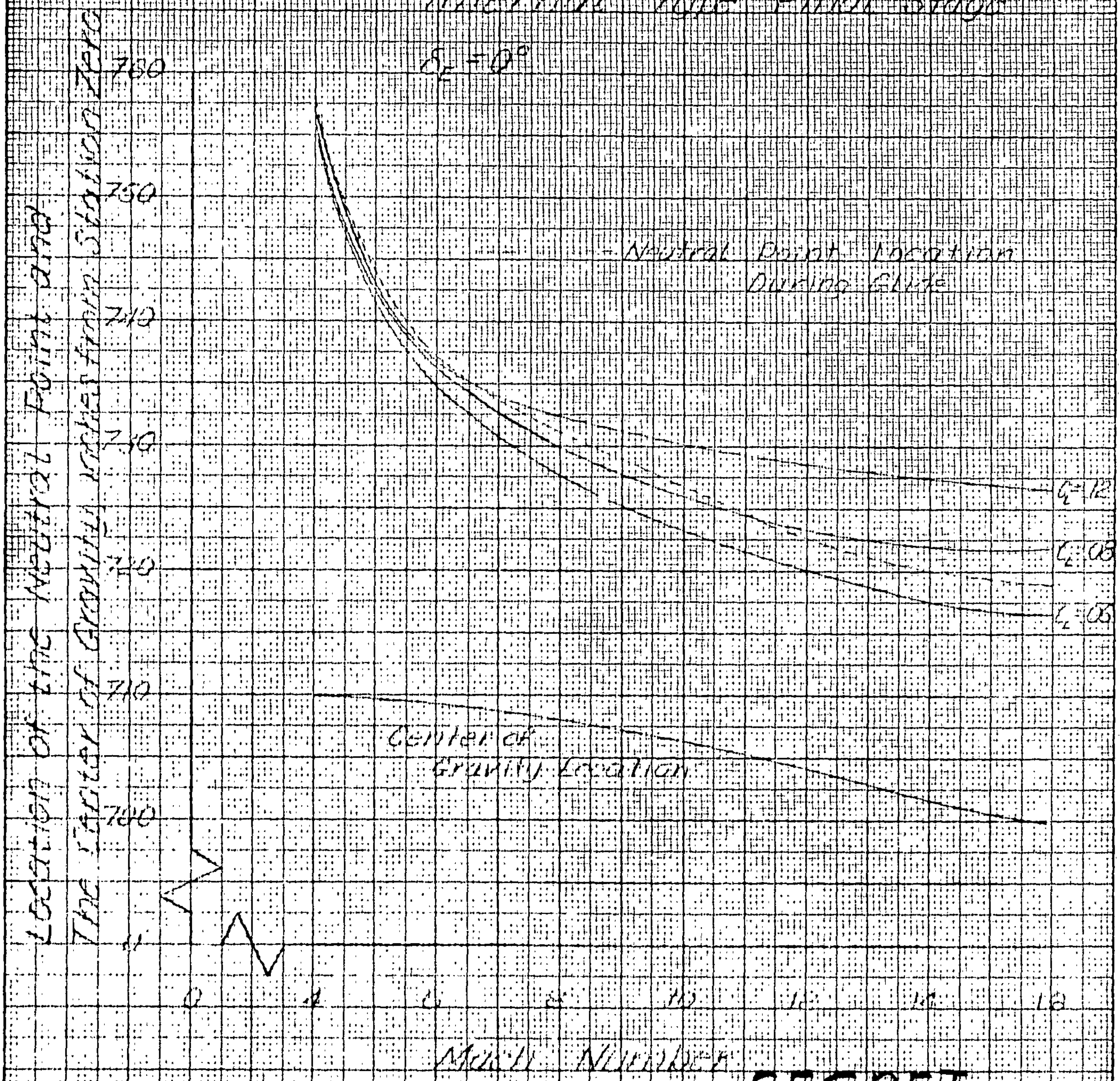

SECRET

BY ______________________ DATE ______

CHECKED ______________________ DATE ______

BELL Aircraft CORP

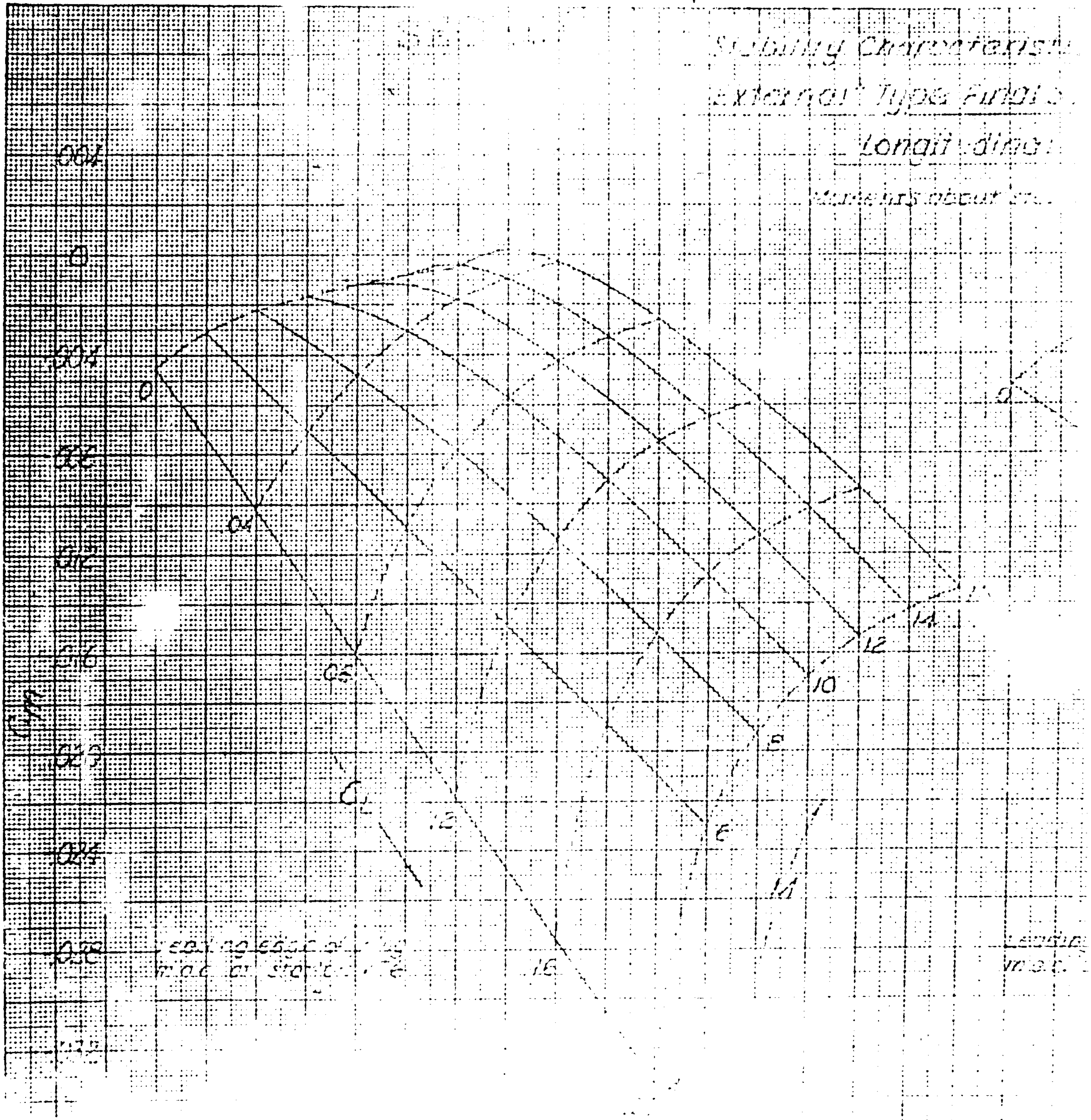

Characteristics of the
Type Final Stage ~
Longitudinal

about sta.

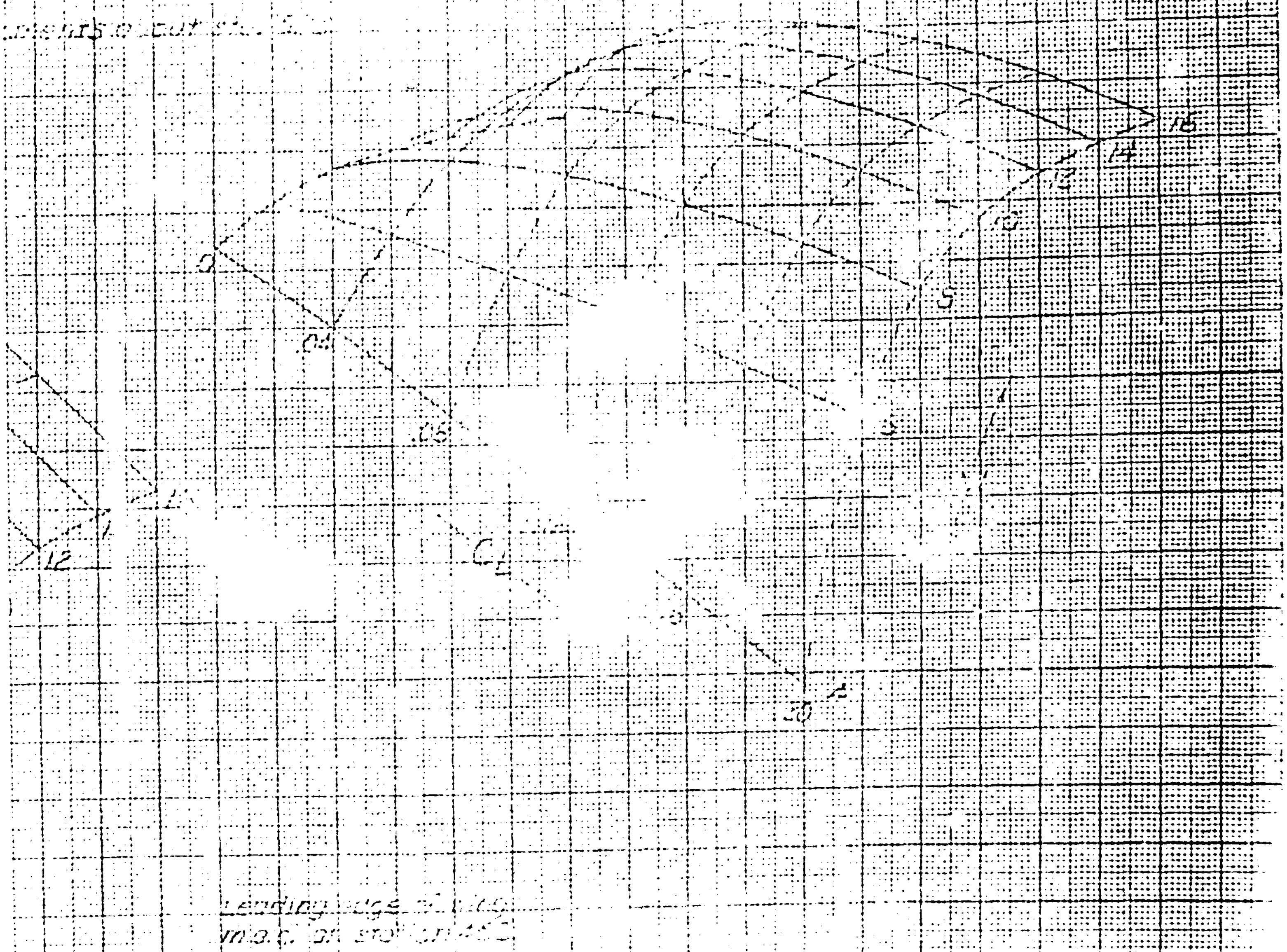

2

SECRET

Fig 4.3-4

LOCATION OF THE NEUTRAL POINT AND CENTER OF GRAVITY

EXTERNAL TYPE FINAL STAGE

$\delta_E = 0°$ GLIDE CONFIGURATION

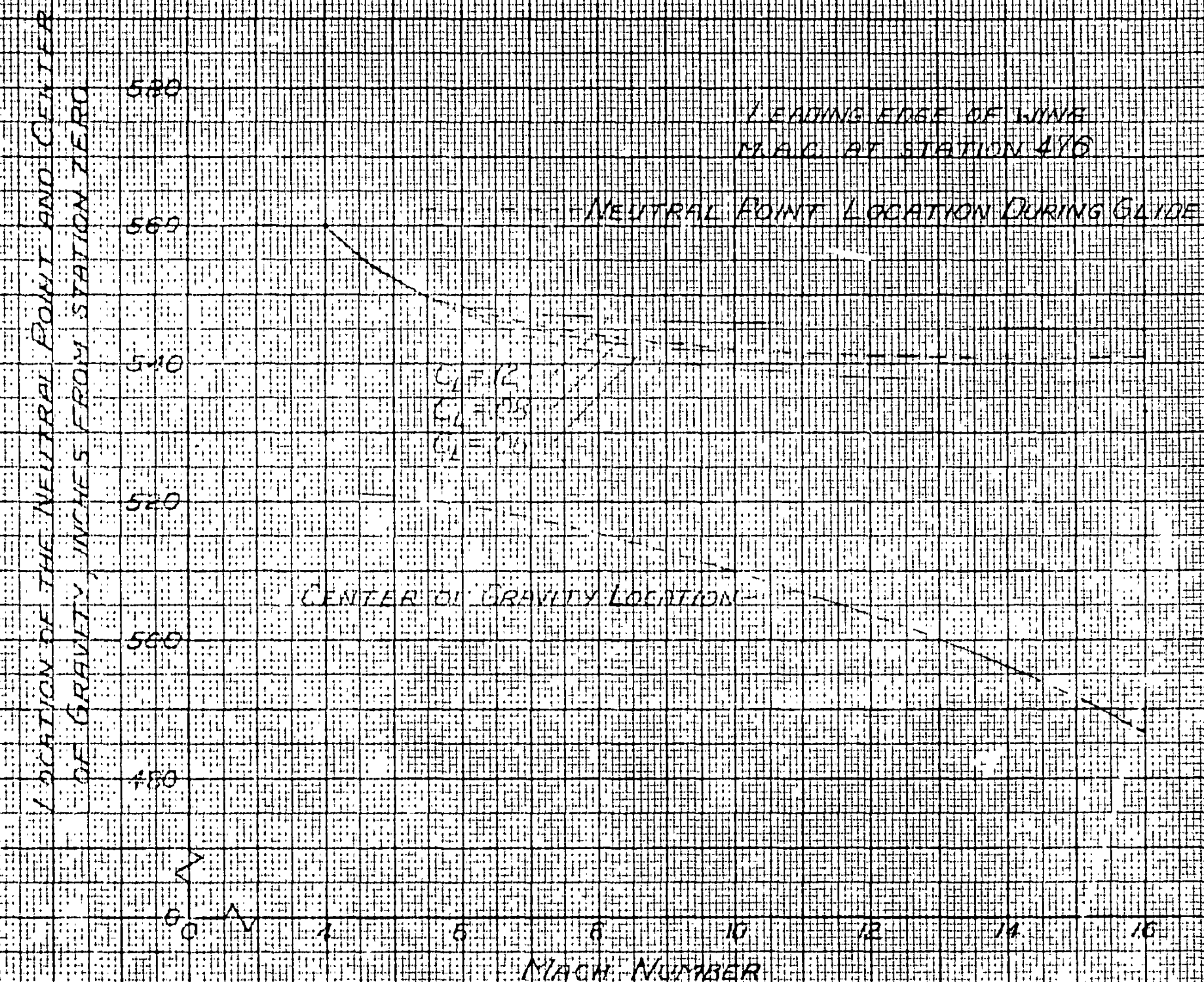

SECRET

Fig. 4.9-5

SECRET

LOCATION OF THE NEUTRAL POINT AND CENTER OF GRAVITY

EXTERNAL TYPE FINAL STAGE

$\delta_F = 0°$ GLIDE CONFIGURATION

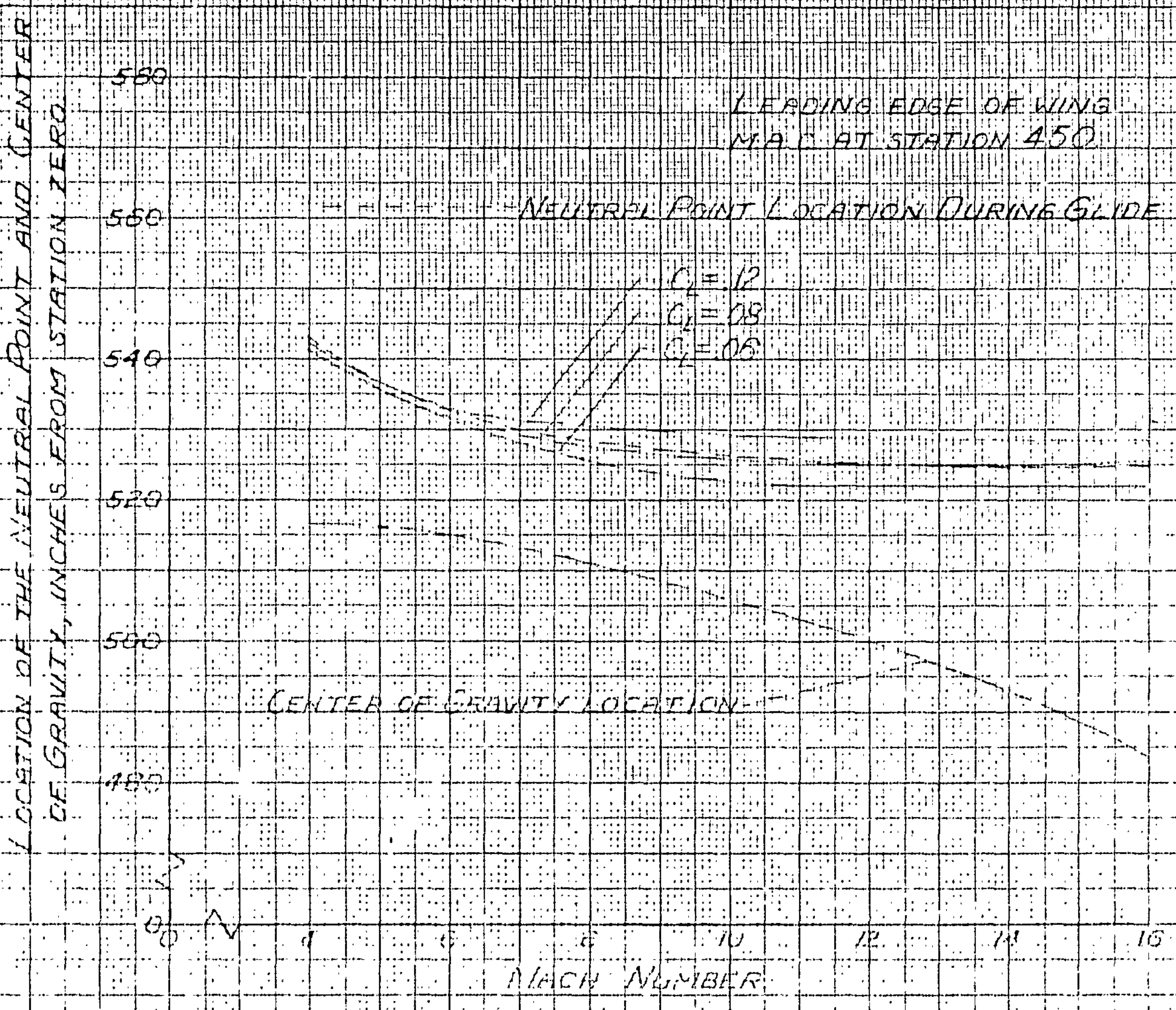

SECRET

SECRET

Fig. 4.9-6

LONGITUDINAL STABILITY CHARACTERISTICS

"INTERNAL" TYPE FINAL STAGE

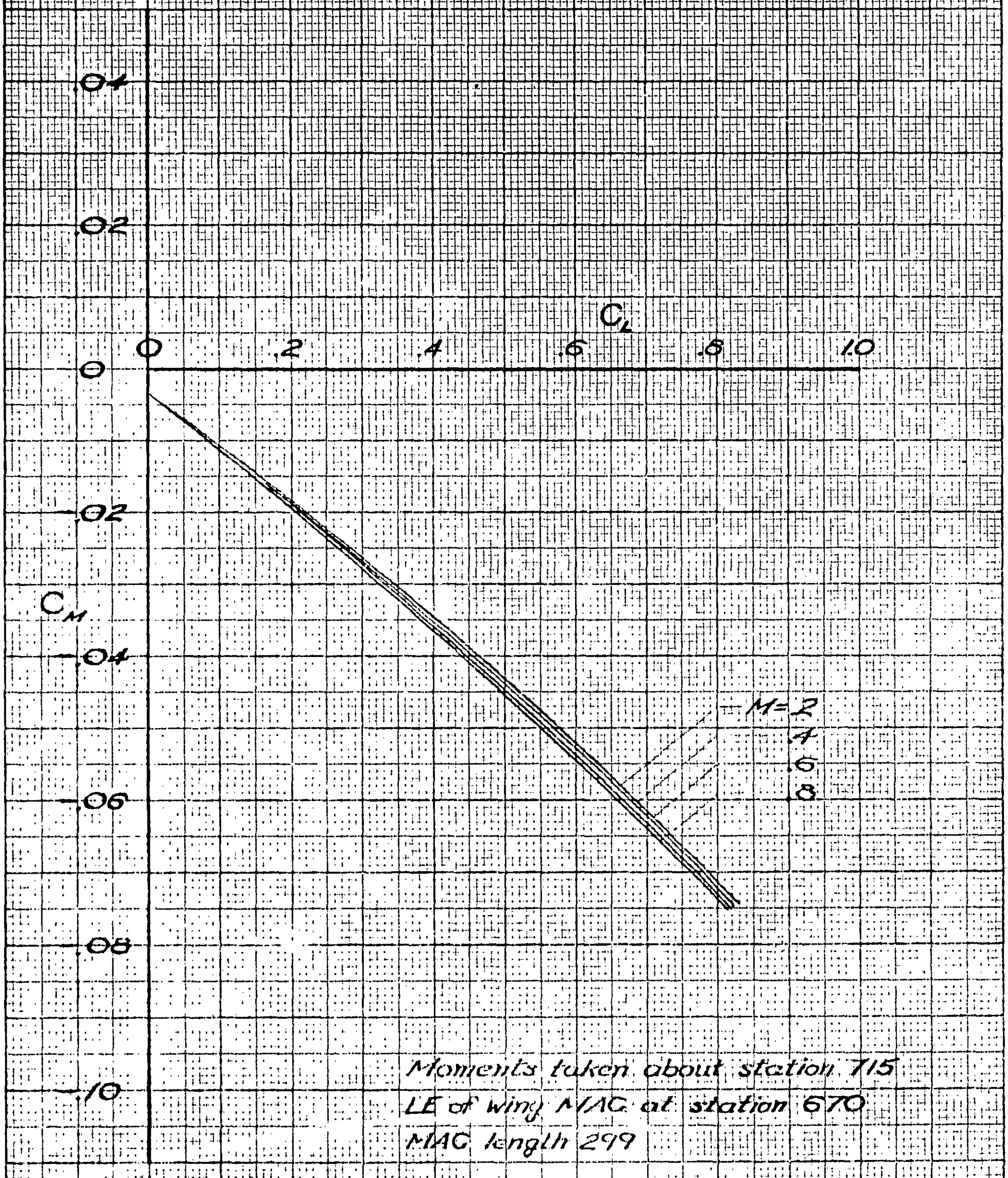

SECRET

SECRET

Fig. 4.9-7

LOCATION OF STICK FIXED NEUTRAL POINT

"INTERNAL" TYPE FINAL STAGE

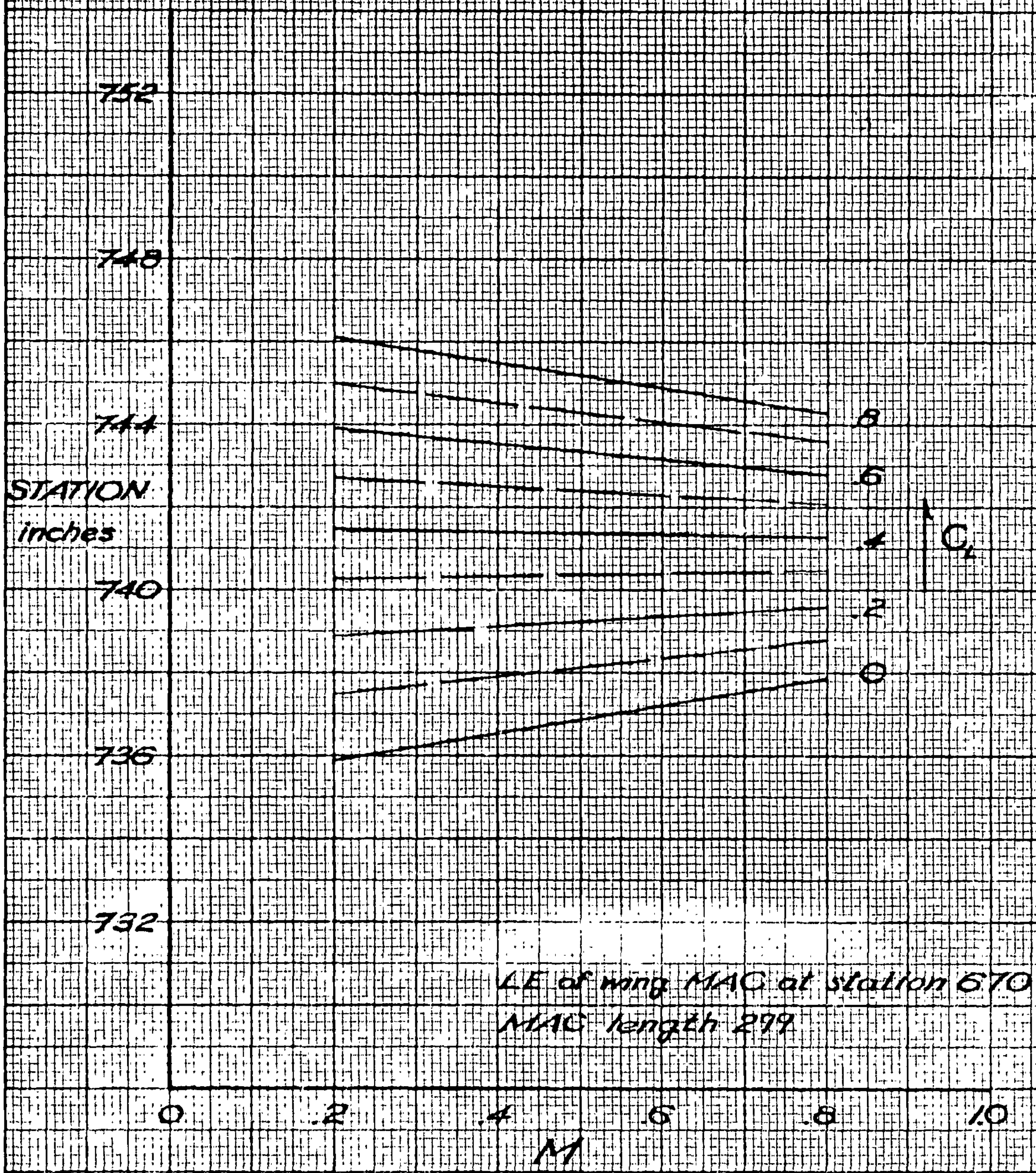

SECRET

Fig. 4.9-8

LONGITUDINAL STABILITY CHARACTERISTICS

"EXTERNAL" TYPE FINAL STAGE

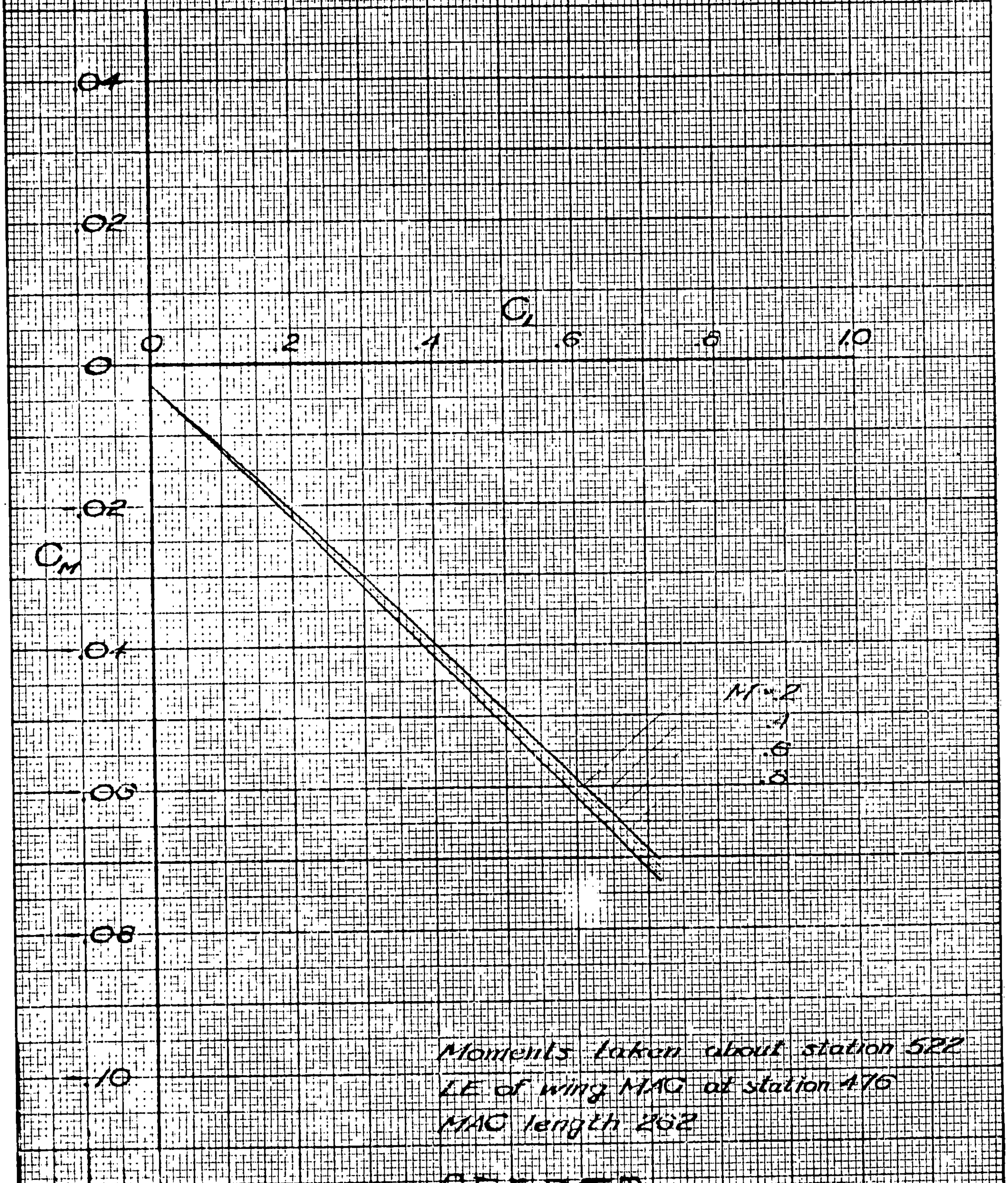

SECRET

SECRET

Fig 4.9-9

LONGITUDINAL STABILITY CHARACTERISTICS

"EXTERNAL" TYPE FINAL STAGE

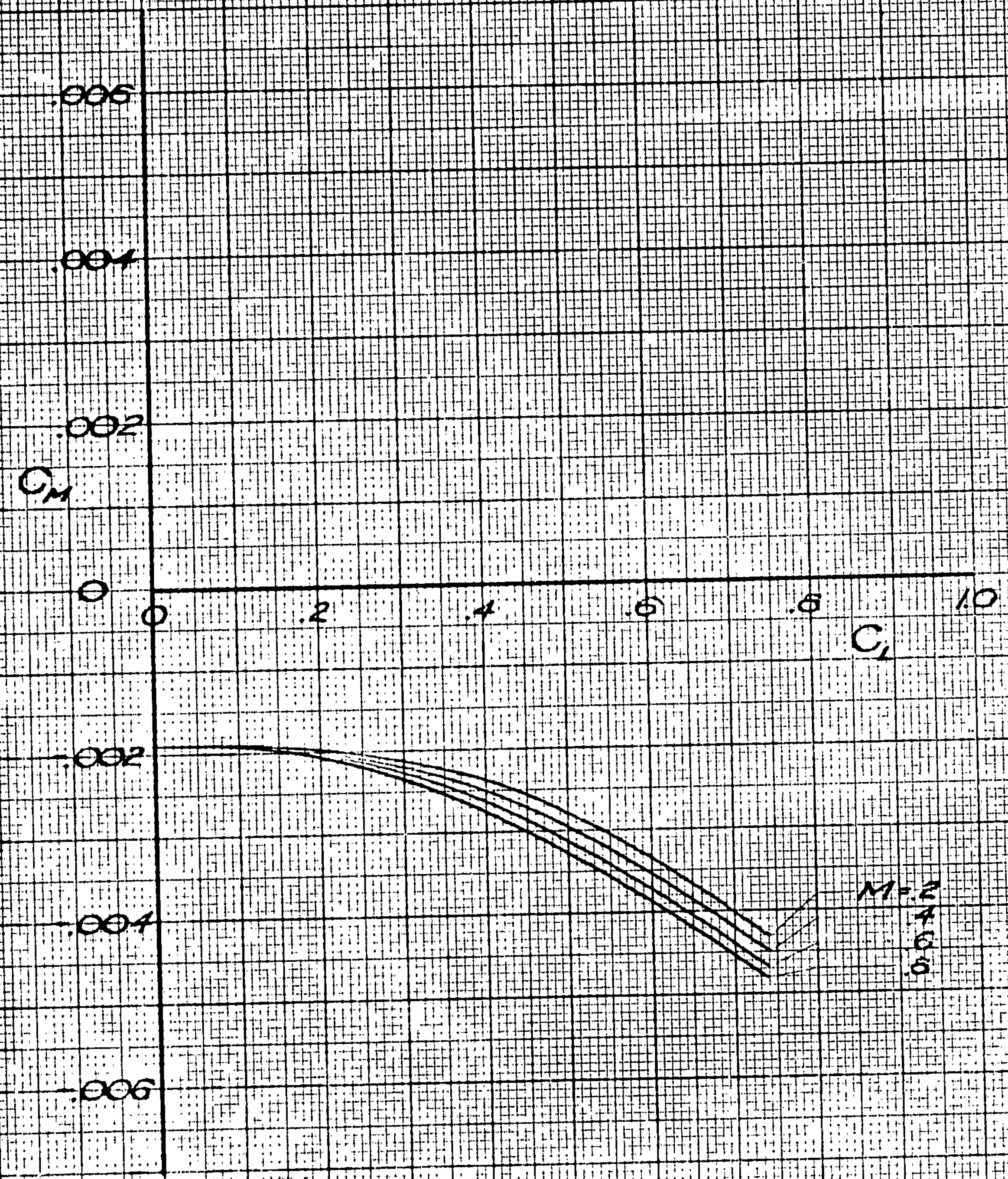

Moments taken about station 522
LE of wing MAC @ station 450
MAC length 262

SECRET

SECRET

Fig. 4.9-10

LOCATION OF STICK FIXED NEUTRAL POINT

"EXTERNAL" TYPE FINAL STAGE

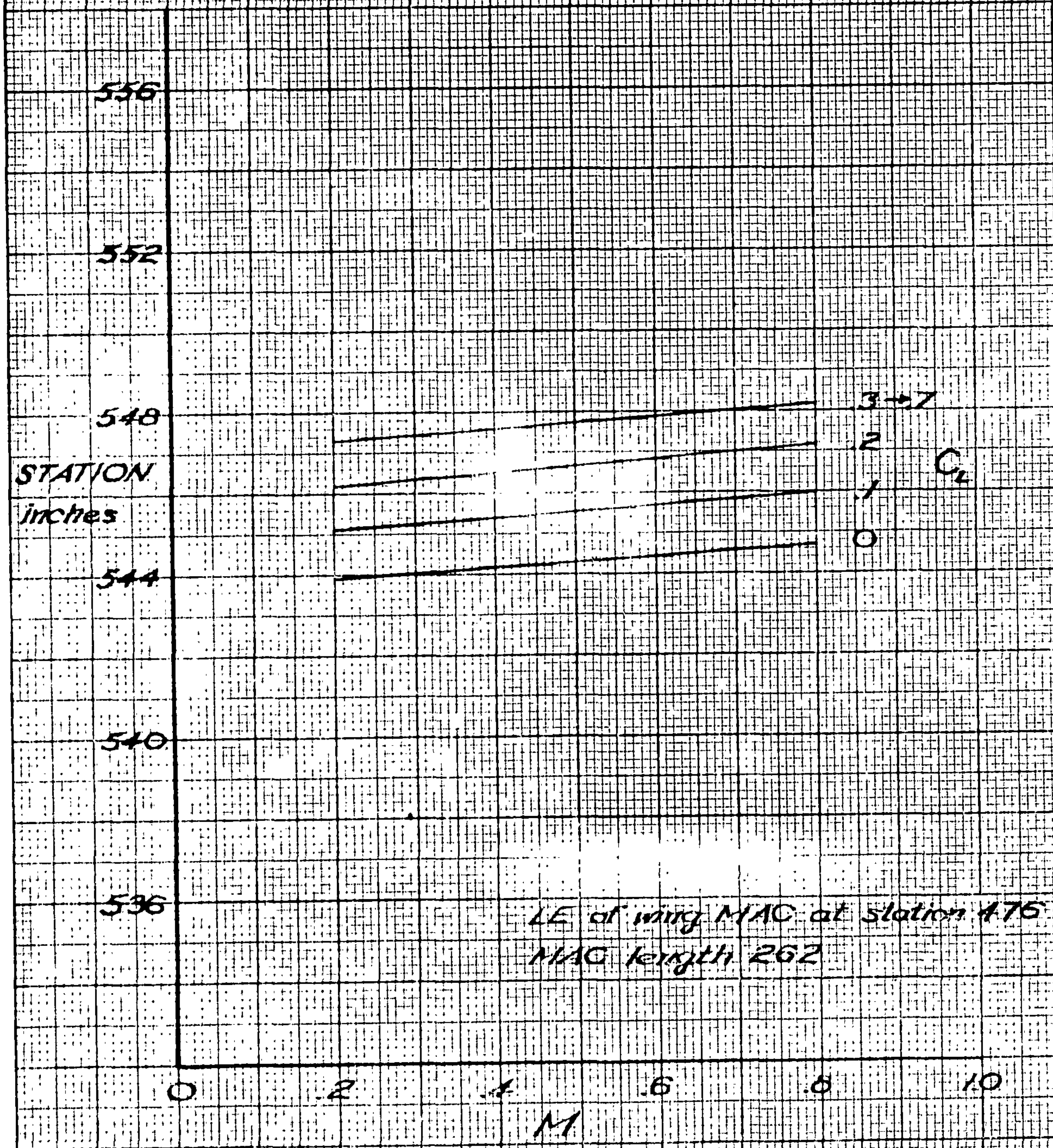

SECRET

Fig. 4.9-11

SECRET

LOCATION OF STICK FIXED NEUTRAL POINT

"EXTERNAL" TYPE FINAL STAGE

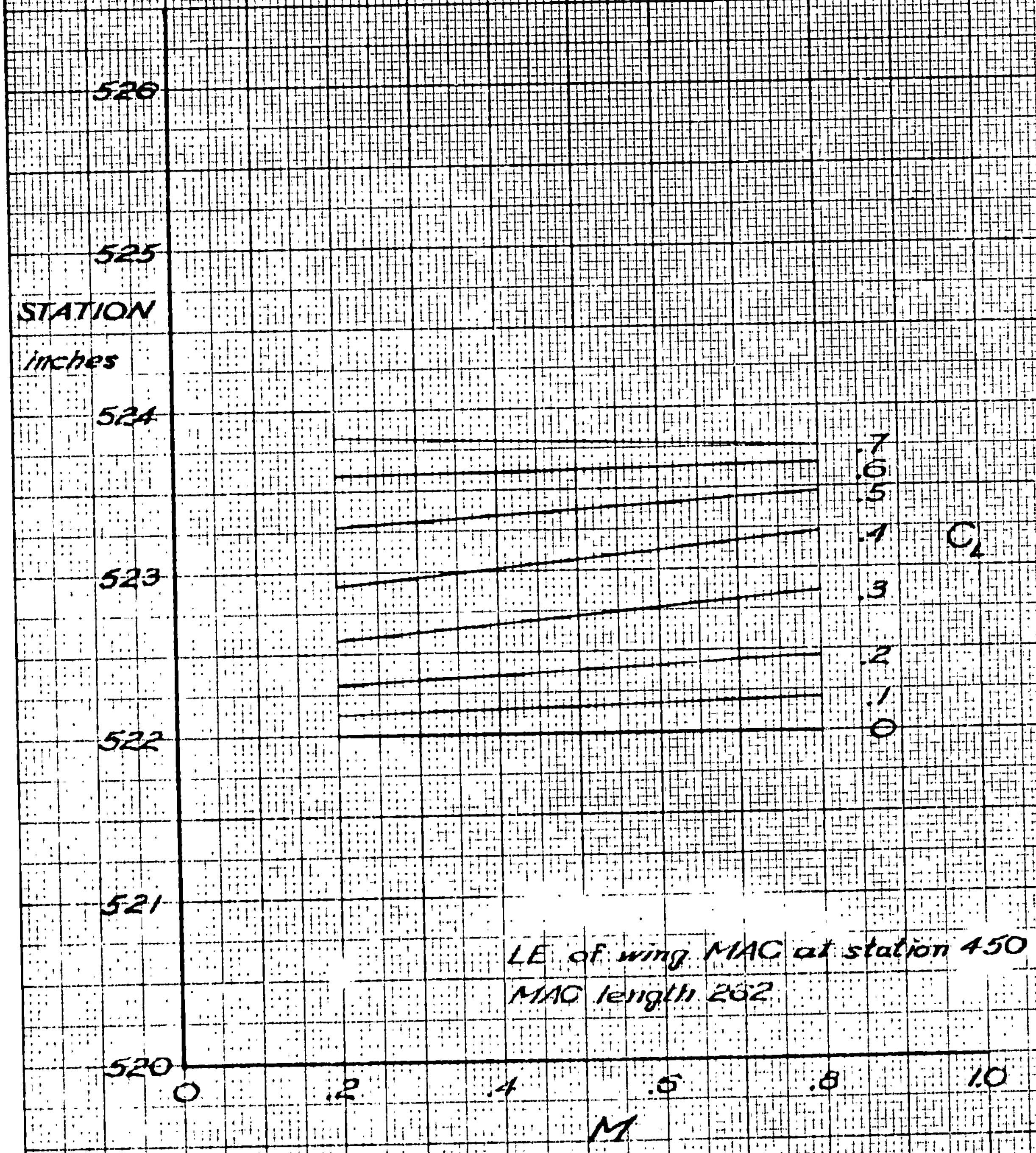

SECRET

4.10 CONTROL DEFLECTIONS FOR TRIM DURING THE GLIDE

As a means of qualitatively comparing the effects of control deflection on the glide range at the two vehicles estimates of the deflections required for trim during the glide were made.

The moment to be trimmed was calculated using the pitching moment characteristics shown in Figures 4.9-1 and 4.9-3. These moments were adjusted to the center of gravity location corresponding to the Mach number at a given time in the glide. (This variation of center of gravity with Mach number is given in Figures 4.9-2, 4.9-4, and 4.9-5.)

As a means of estimating the flap lift effectiveness a method (Reference 4.10.1) which is based upon that method proposed in Reference 4.10.2 for estimating wing characteristics was employed. In Figure 4.10-1 is shown the increment of lift due to deflecting a flap down as a function of the hypersonic similarity parameters K_{α} and K_{δ}. In Figures 4.10-2 and 4.10-3 are presented the lift due to deflecting a trailing edge flap at Mach numbers 4, 8, 12, and 16 where the wing surface is at angles of attack of 0, 6, and 8 degrees. It is interesting to note that the flap effectiveness decreased with increasing Mach number when the angle of attack was zero. The reverse was true for angles of attack of six and eight degrees. This can be understood by considering that as the Mach number increases the shock at the leading edge of the wing becomes stronger for a constant angle of attack of the surface. As a result the control surface would be acting in a region of increasing static pressure which would be considerably above that of free stream at the higher Mach numbers and thereby would increase its lift effectiveness.

The lift due to flap deflection as calculated from theory is compared with the test results of Reference 4.10.3 in Figure 4.10-4. Although the airfoil profile was not the same in the test as that used in the theory the good agreement does substantiate the order of magnitude of the theoretical results.

As the theory was based upon inviscid flow the angle of attack effects were neglected and only the results of the calculations for the zero angle of attack case were used to estimate the trim deflections required. The boundary layer effects would be most predominate during the high altitude, high Mach number flight at a Brass Bell vehicle, and as can be seen from Figures 4.10-2 and 4.10-3 using the zero angle of attack case should more than account for any loss in flap effectiveness due to viscous effects at the glide Mach number conditions.

As one of the effects of viscous flow will be to move the center of pressure forward the flap deflections were estimated by assuming the flap lift to act at the hinge line and also by assuming it to act at the mid-chord of the flap. The flap deflections required during the glide of the "internal" type glide vehicle are presented in Figure 4.10-5 and the deflections required during the glide of the "external" type glide vehicle are shown in Figure 4.10-6. In the latter case, the effect of a different wing position on trim deflections is also presented.

In order to better appreciate the difference in required control deflection the variation with glide range is shown in Figure 4.10-7. As can be

seen the deflections required for the "internal" type are well below those of the "external" for the first 4000 nautical miles of range. This would indicate a small range loss for the former configuration than the latter. It is apparent from both this investigation and the previous one (Section 4.9) that the center of gravity of the "external" type glider was too far forward at the initiation of the glide. It would have to be moved aft to more closely approximate the control requirements of the "internal" type glide vehicle and thereby reduce the range difference that presently can be accredited to its larger control deflections.

4.10 REFERENCES

4.10.1 Meullen, N. F.: Additional Lift Due to Deflecting a Flap in a Two-Dimensional Hypersonic Flow. Unpublished Bell Aircraft Corporation Aerodynamics Method Note

4.10.2 Linnell, R. D.: Two-Dimensional Airfoils in Hypersonic Flows. Journal of the Aeronautical Sciences, Volume 16, January 1949

4.10.3 Dunning, R. W. and Ulmann, E. F.: Aerodynamic Characteristics at Mach Number 4.04 of a Rectangular Wing of Aspect Ratio 1.33 Having a 6-Percent-Thick Circular-Arc Profile and a 30-Percent Chord Full Span Trailing Edge Flap. NACA RM L53D03

4.10 SYMBOLS

C_L	Change in lift coefficient due to flap deflection
K_α	Hypersonic similarity parameter, $M_o\alpha$ (α in radians)
K_δ	Hypersonic similarity parameter, $M_o\delta$ (δ in radians)
M_o	Free Stream Mach number
S_{flap}	Area of control flap
S_{ref}	Reference area for coefficients
α	Angle of attack
δ	Control surface deflection

SECRET

Fig. 4.10-1

Lift due to Deflecting Trailing Edge Flaps in Two-Dimensional Flow

M>1

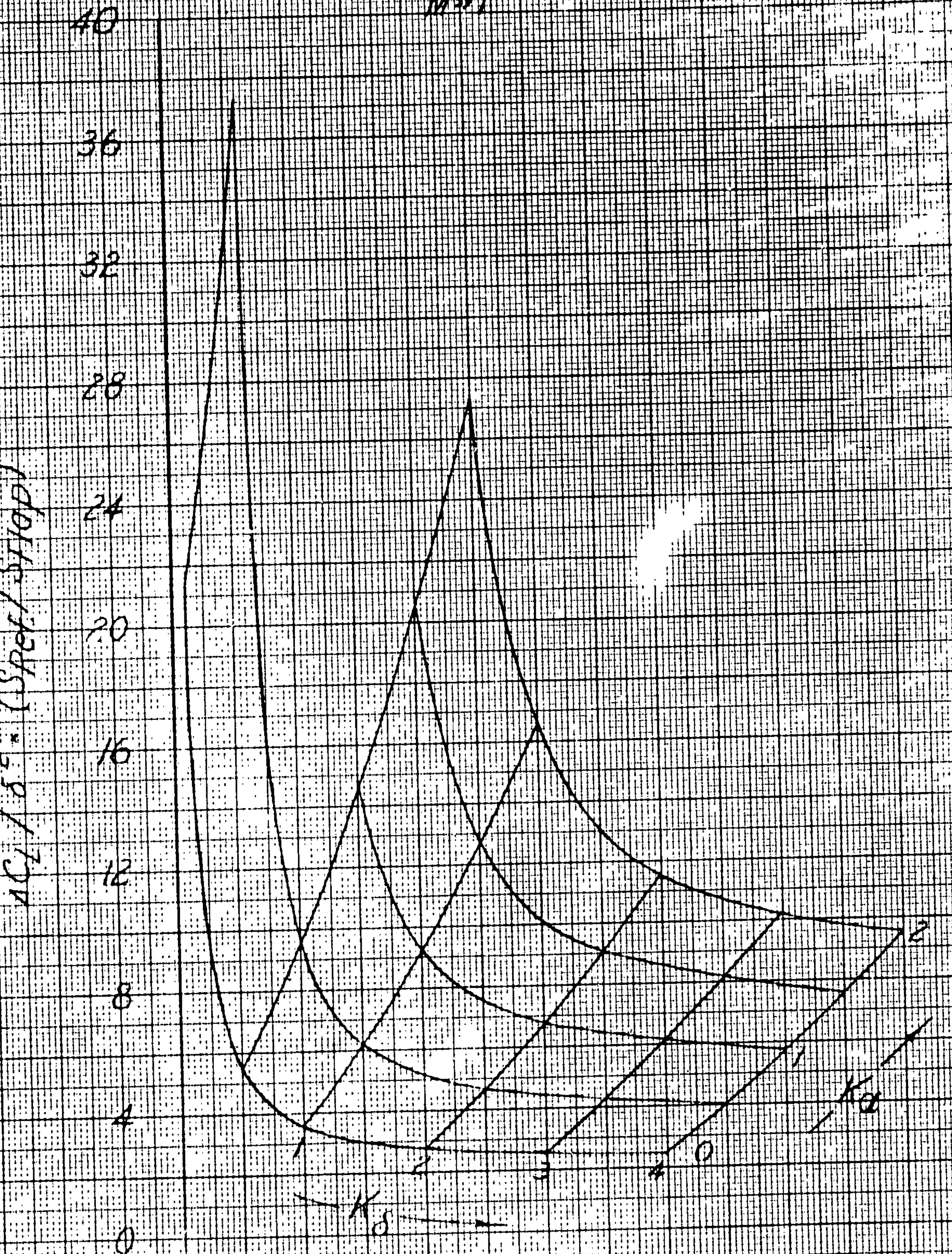

SECRET

SECRET

Fig 4.10-2

Theoretical Flap Lift

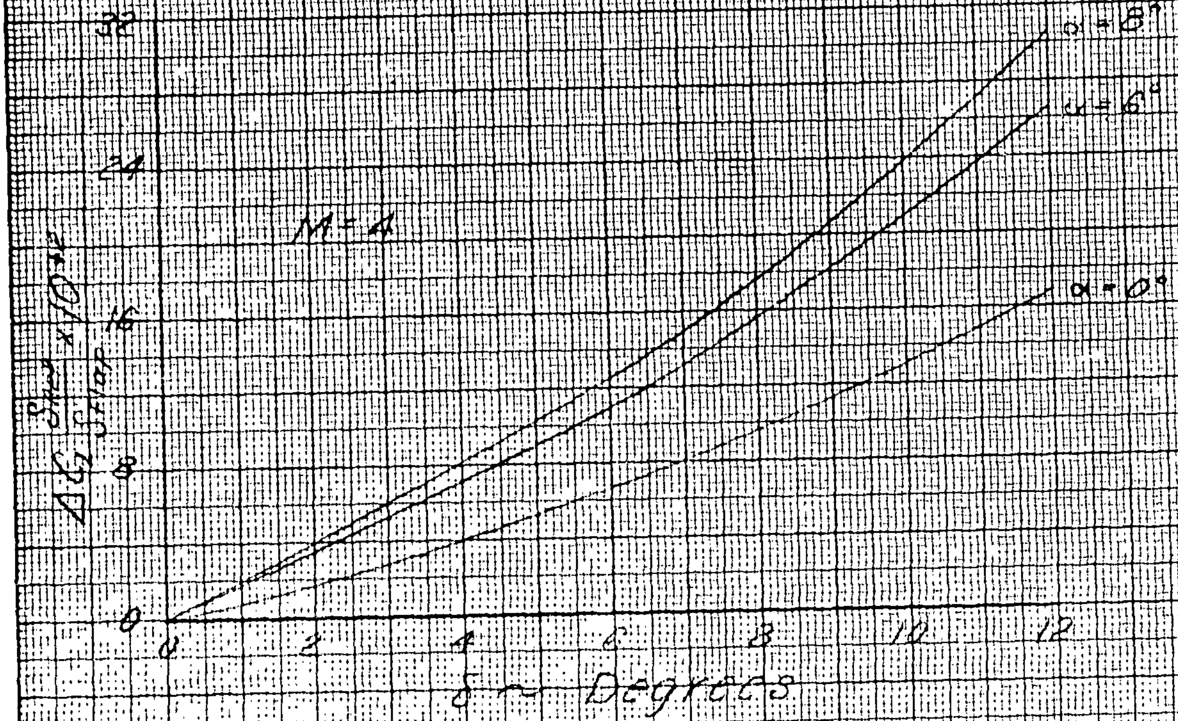

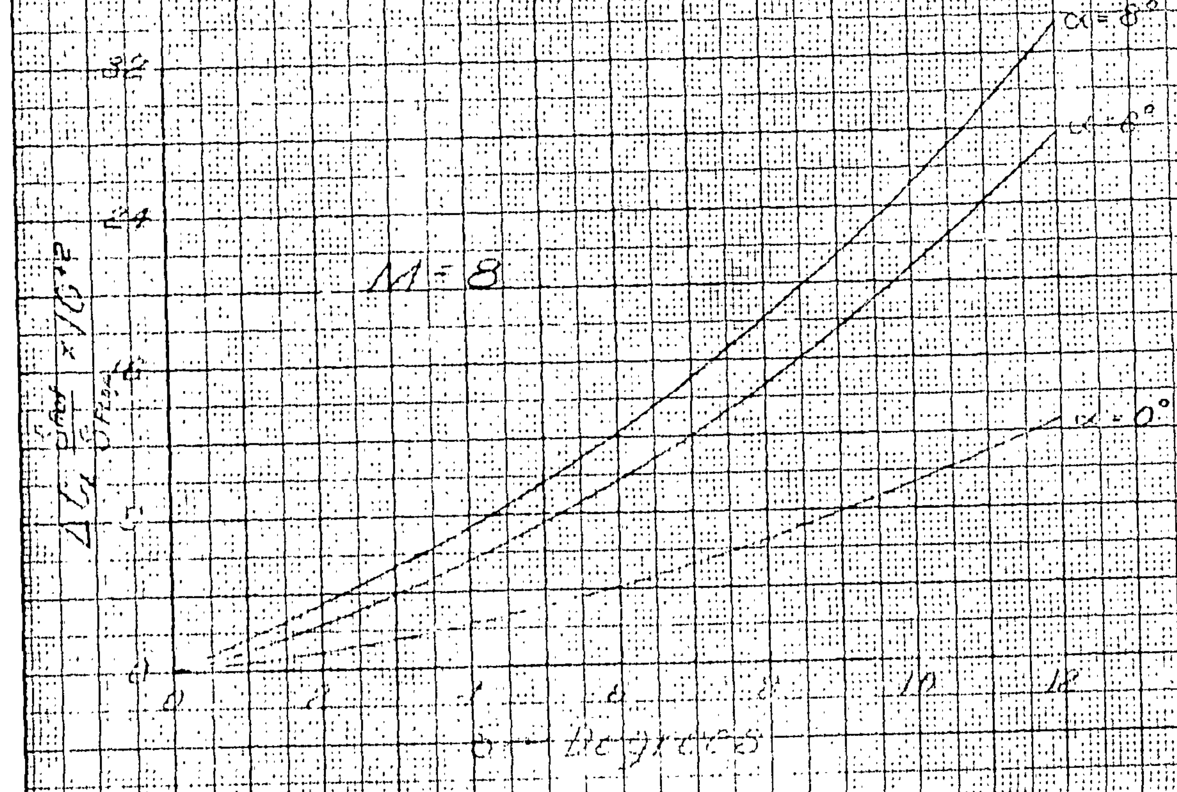

SECRET

SECRET

Fig 4.10-3

Theoretical Flap Lift

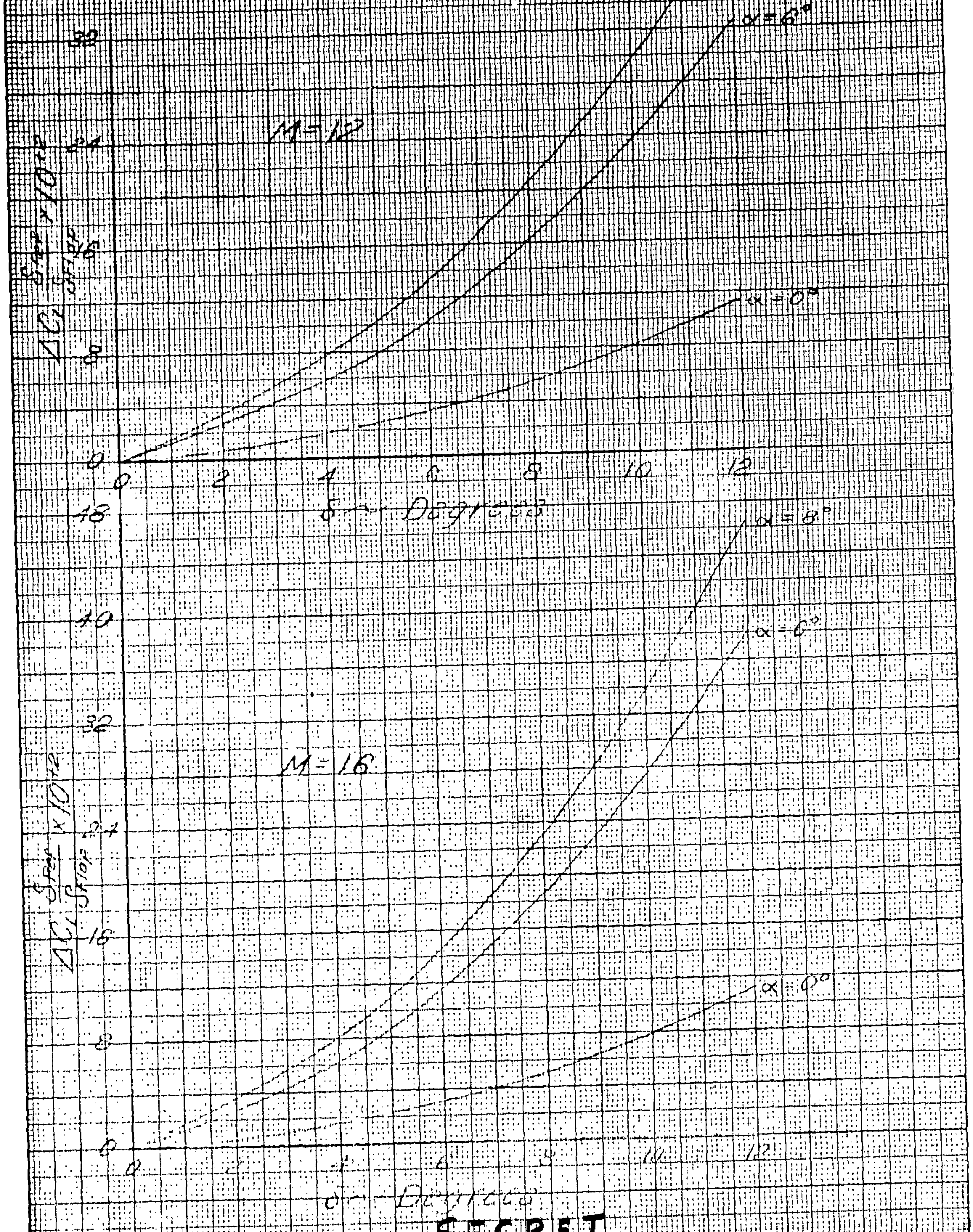

SECRET

SECRET

Fig 4.10-4

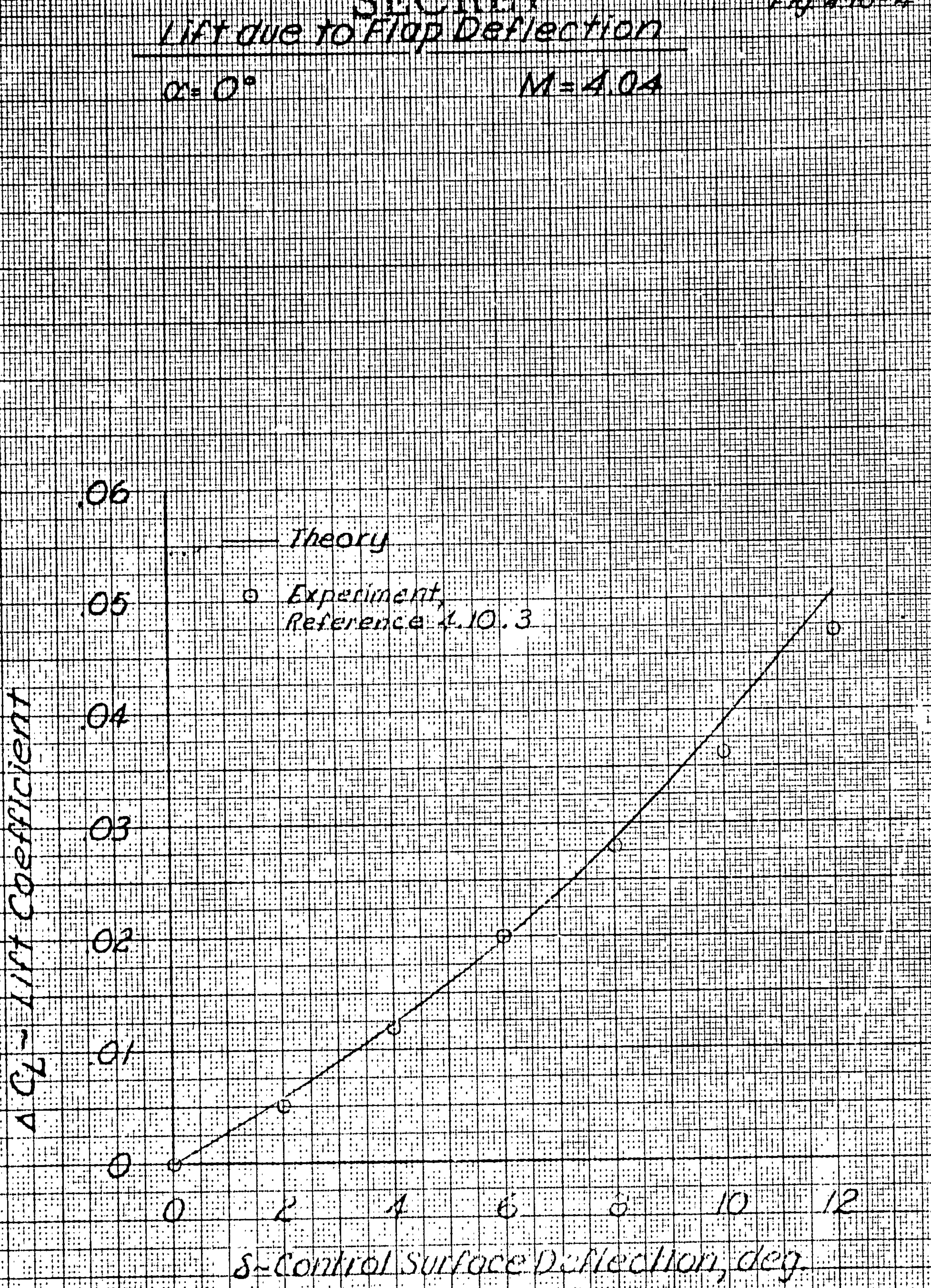

SECRET

SECRET

Fig 4.10-5

Required Flap Deflection for Trim During Glide for "Internal" Type Final Stage

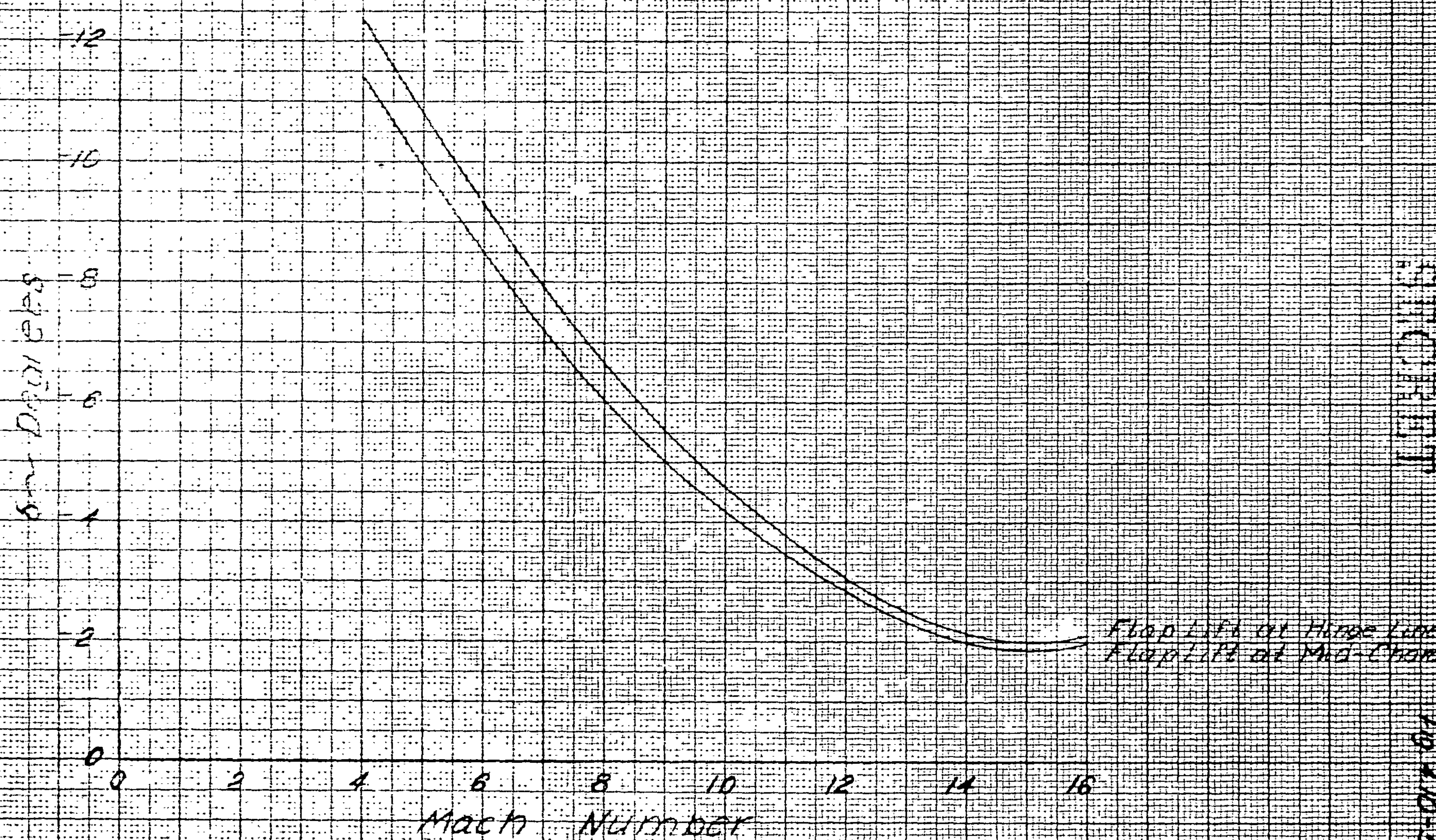

SECRET

SECRET

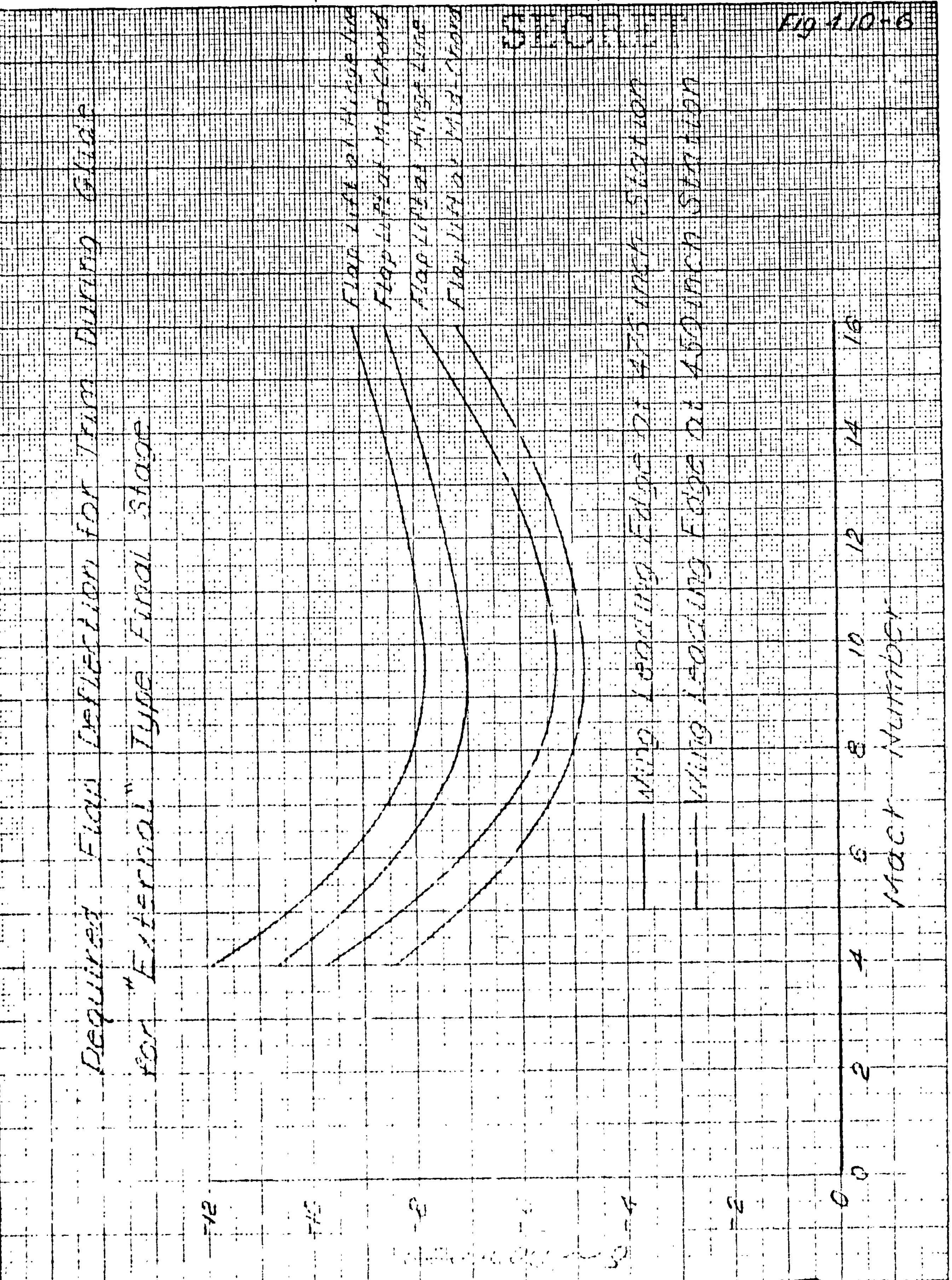

SECRET

SECRET

Fig 4.10-7

Variation of Control Deflection Required for Trim
with Range for "Internal" and "External" Type
Final Stages

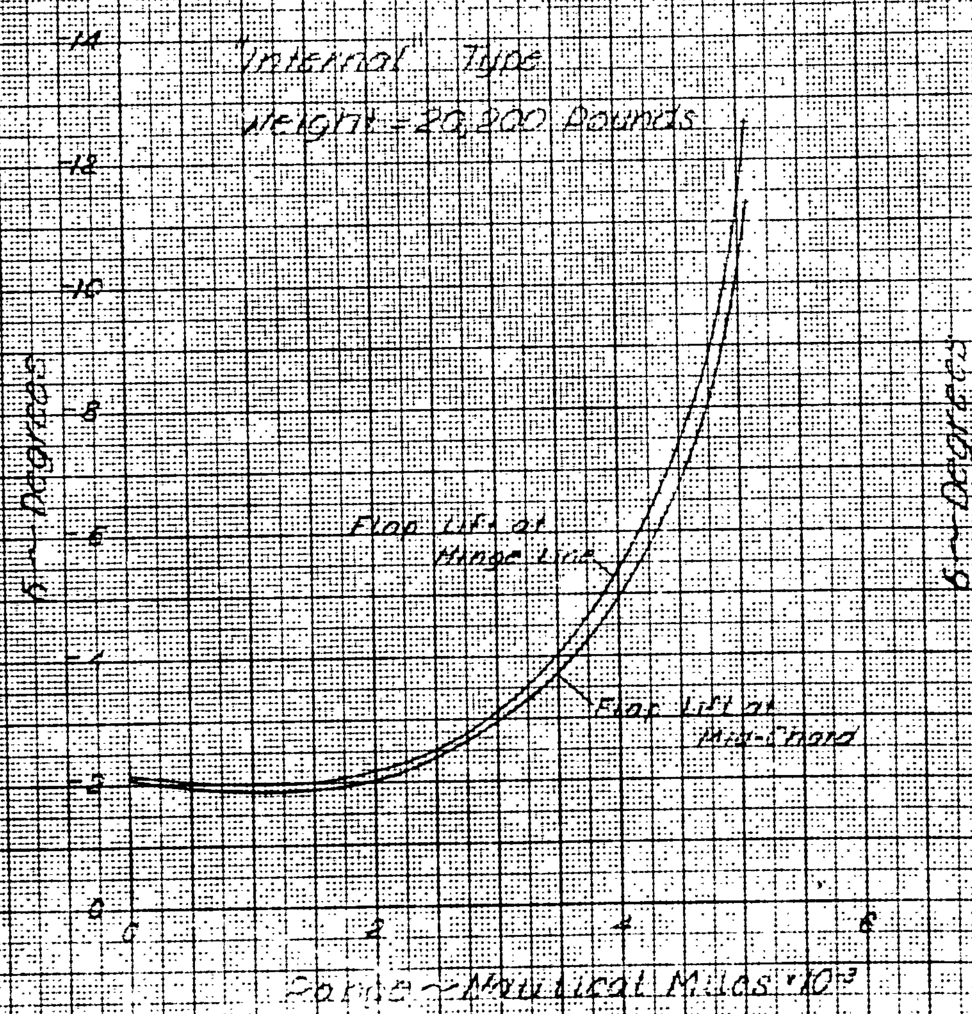

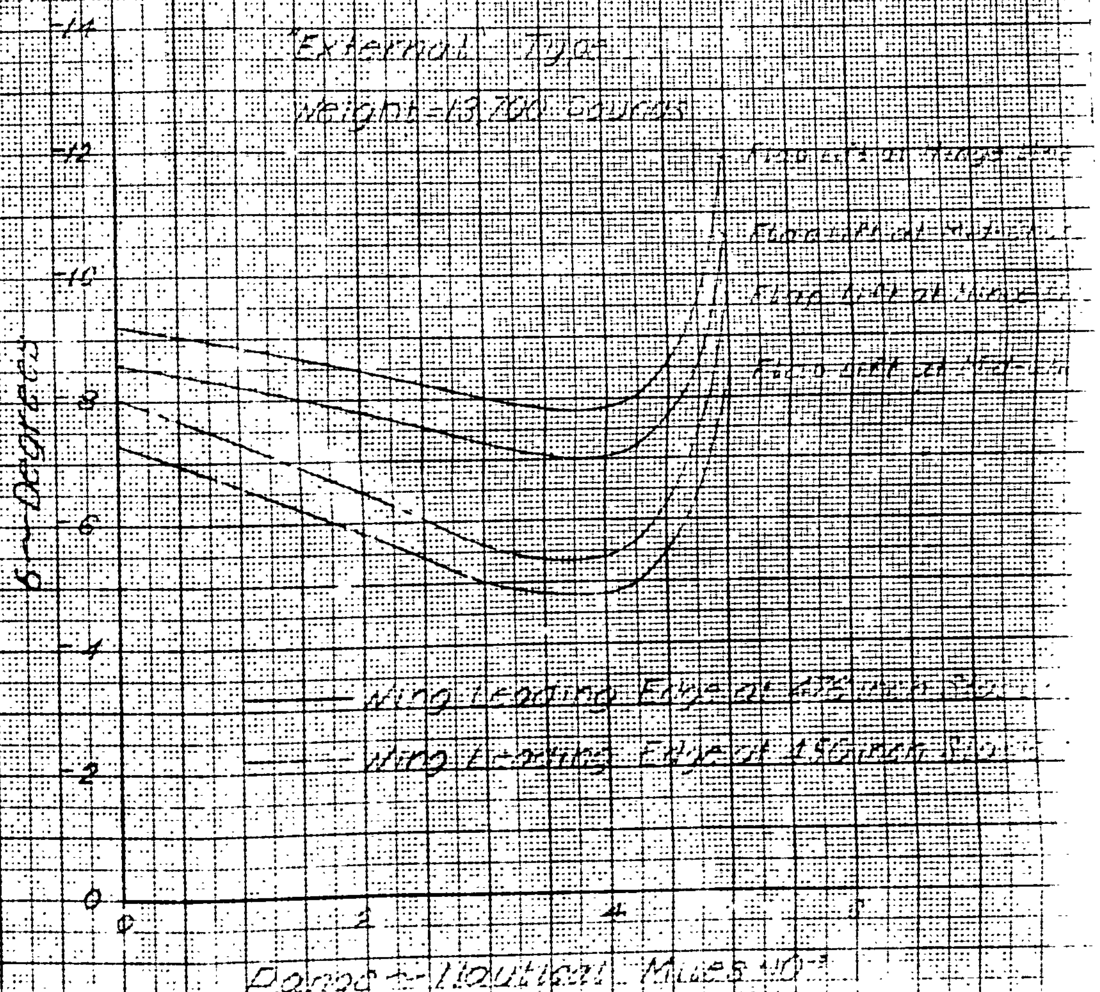

SECRET

4.11 STATIC DIRECTIONAL STABILITY

The static directional stability of the "external" and "internal" type glider configurations has been investigated over the speed range from low subsonic to M = 8.0. The "external" type configuration has a vertical tail and a ventral fin located at the most aft fuselage station. The "internal" type configuration has a vertical tail located with the trailing edge at the most aft fuselage station and two ventral fins located under the wings.

In these studies it has been assumed that the ratio of local dynamic pressure to free stream dynamic pressure (q_L/q_∞) in the region of the tail is equal to unity. This assumption is justified only for angles of attack near zero. From the data presented in Reference 4.11.1 at M = 6.9 the effect of angle of attack was shown to have an appreciable influence on the dynamic pressure ratio in the region of the tail. These data indicate the dynamic pressure ratio for an upper vertical tail approaches zero as the angle of attack increases whereas the ratio for a ventral fin may become two or three. This indicates that for equal areas a ventral fin may be many times more effective for stability than an upper vertical tail when the vehicle is operating at an appreciable angle of attack. For the present study it was desired only to find the approximate total tail areas required for static directional stability primarily for reasons of weight estimation and the assumption of q_L/q_∞ equal to one may be considered reasonable over the low angle of attack range. More detail examination at higher angles of attack may indicate that the relative proportions of vertical tail area to ventral fin area should be changed to improve the static directional stability.

SECRET

Classified only when data are entered

These studies also include the effects on static directional stability of center of gravity movement during the glide. As coolant is expelled during the glide the cg moves aft toward the landing cg. The forward cg locations during the high Mach number phases of the glide provide a stabilizing influence due to the increase in tail arm. The Mach number range below M = 8 was investigated because preliminary estimates had indicated the cg variation to be relatively small. The previous estimates of longitudinal stability (see Section 4.8) had indicate the smallest static margin at flight C_L's in the high Mach number range to be in the M = 6 to M = 8.0 regime, as a result of the relation between wing lift and cg variations during the glide. Hence it was anticipated that the least favorable tail lift - tail arm relation might likewise occur in this same Mach number range.

This investigation is intended to complement the static directional stability studies presented in Reference 4.11.2 where the M = 16 flight condition was examined with corrections included for the variation of q_L/q_∞ that occurs at angle of attack.

4.11.1 HIGH SPEED STATIC DIRECTIONAL STABILITY

The high speed yawing moment coefficient, C_n, and the slope, C_{n_β}, for the "external" type configuration with a constant center of gravity located at the landing weight cg (station 522) are presented on Figure 4.11-1 and 4.11-2 for Mach numbers from 2.0 to 8.0. These curves show that neutral static directional stability will occur at about M = 8.0. Figure 4.11-3 shows the anticipated variation of cg position with Mach number for Mach numbers less than 10.0. This curve has been used to recalculate C_n and C_{n_β}

accounting for the cg variation with Mach number and the results are shown on Figures 4.11-4 and 4.11-5. A slight positive static directional stability is then shown to be available at M = 8.0.

The same analysis has been performed on the "internal" type configuration. Figures 4.11-6 and 4.11-7 present C_n and C_{n_β}, respectively, for the landing cg (station 710). This configuration shows neutral static directional stability at about M = 3.0 for low angles of sideslip. Using the cg variation presented in Figure 4.11-8 the C_n and C_{n_β} have been recalculated and are shown on Figure 4.11-9 and 4.11-10. It is noted that the cg variation for this configuration is small and therefore has a negligible effect on the static directional stability.

The lift curve slopes and center of pressure locations for the tail surfaces at supersonic speeds have been determined from Reference 4.11.3 with corrections included for the increase in effective aspect ratio due to the presence of the body and wing.

The yawing moment coefficients for the bodies have been calculated using Reference 4.11.4.

4.11.2 LOW SPEED STATIC DIRECTIONAL STABILITY

The subsonic yawing moment coefficient and slope for the "external" type configuration are shown on Figures 4.11.11 and 4.11.12. No variation of stability with Mach number is noted. The center of gravity is constant at the landing location (station 522). This configuration exhibits positive static directional stability at subsonic speed with the basic tail group and has a slight positive stability with the vertical tail only.

The subsonic static directional stability characteristics for the internal type configuration are presented on Figures 4.11.13 and 4.11.14. The configuration with the tail group considered in these studies (designated T_6) shows positive static directional stability throughout the β range. The center of gravity is constant at the landing location (station 710).

At subsonic speeds the lift curve slope for the tail surfaces have been determined from the low speed data presented in Reference 4.11.5. From Reference 4.11.6 no change in lift curve slope is expected for Mach numbers up to .80 because the very low aspect ratio of the tail surface minimizes the compressibility effects. The center of pressure of the tail is assumed constant with Mach number up to M = .8 and has been estimated from Reference 4.11.3.

The body yawing moment coefficients have been calculated using Reference 4.11.4.

4.11 REFERENCES

4.11.1 Becker, J. V.: Aerodynamic Data Pertinent to X-15 Project; NACA Presentation at WADC. WADC 55-WCS-3707, January 18, 1955

4.11.2 Postle, R. S., et al: MX-2276 Reconnaissance Aircraft Weapons System - Aerodynamics. Bell Aircraft Corporation Report No. D143-945-024, January 2, 1955

4.11.3 Donselman, R. W.: Supersonic Wing Lift and Moment - Wing Body Combinations. Bell Aircraft Corporation Research Note No. 59

SECRET

Classified only when data are entered

4.11.4 Simon, A. D. and Youth, S.: Determination of Performance Parameters - Subsonic and Supersonic Body Lift Coefficient. Bell Aircraft Corporation Report No. 02-981-009, December 8, 1953

4.11.5 Cambell, J. P. and McKinney, M. O.: Summary of Methods for Calculating Lateral Stability and Response and for Estimating Lateral Stability Derivatives. NACA TR 1098, 1952

4.11.6 Raeisz, S. F.: Aerodynamic Parameters for Aeroelastic Analysis of Wing with Various Planforms. Bell Aircraft Corporation Research Note No. 89

SECRET

Fig. 4.11-A

YAWING MOMENT COEFFICIENT

"EXTERNAL" TYPE FINAL STAGE

SUPERSONIC

$\alpha = 0°$

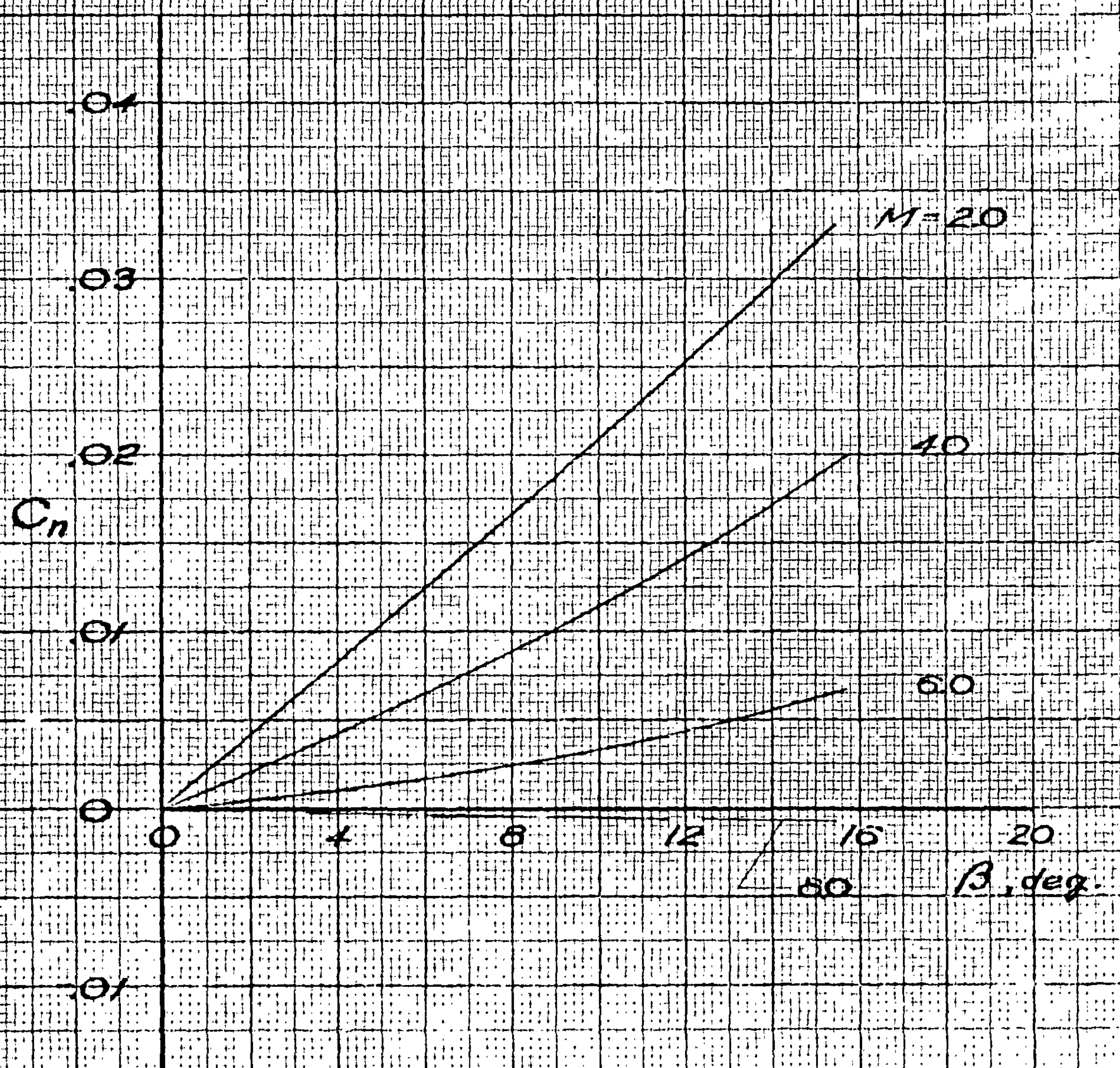

SECRET

SECRET

Fig 4.11-2

DIRECTIONAL STABILITY CHARACTERISTICS

"EXTERNAL" TYPE FINAL STAGE

SUPERSONIC
$\alpha = 0°$

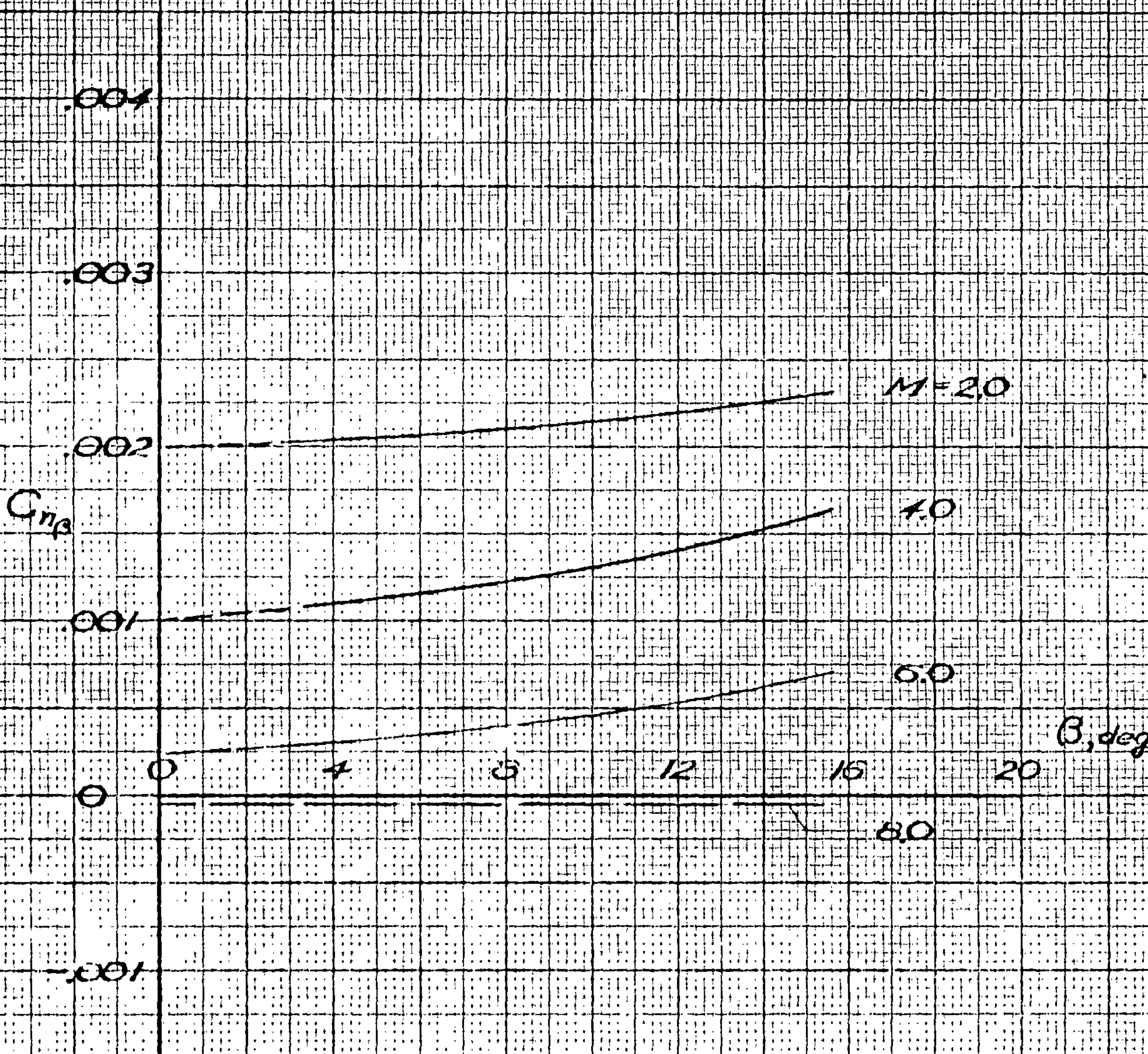

Moments taken about station 522

SECRET

SECRET

Fig 4.11-3

CENTER OF GRAVITY LOCATION

"EXTERNAL" TYPE FINAL STAGE

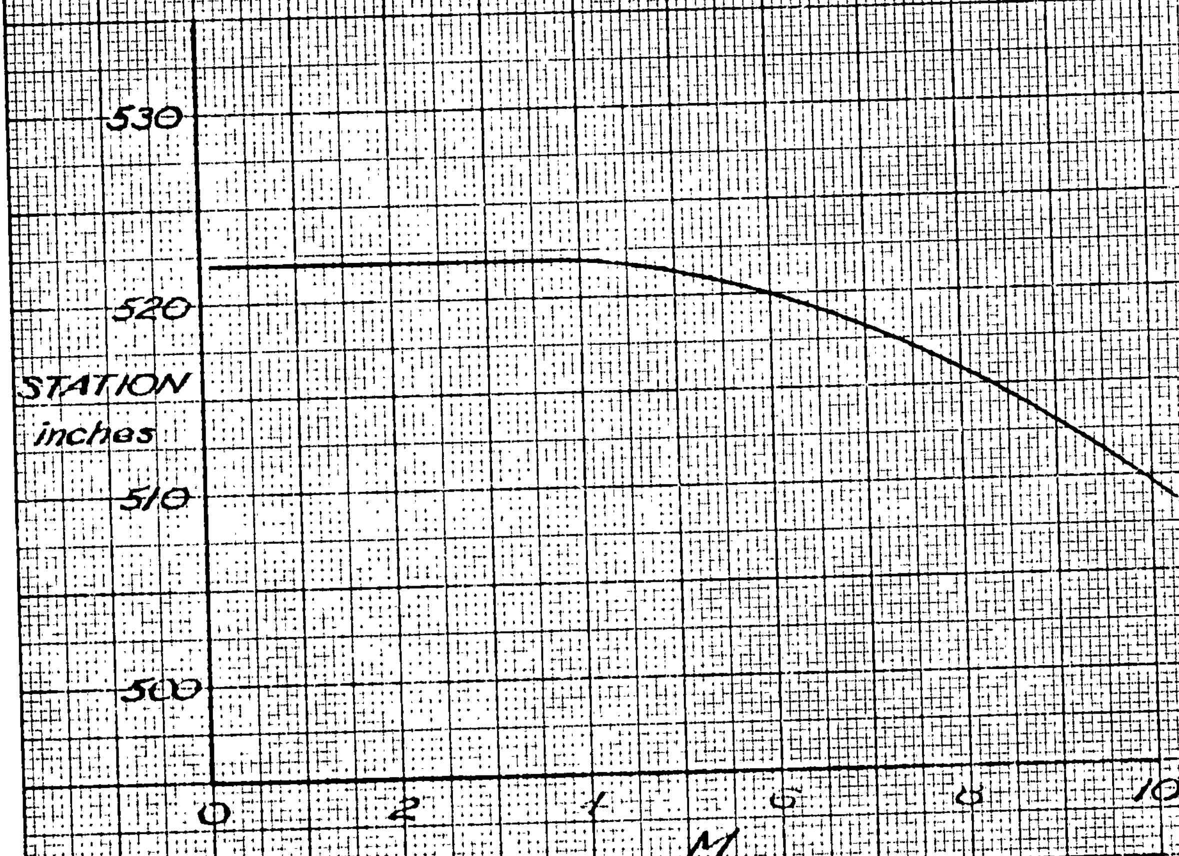

SECRET

SECRET

Fig 4.11-4

YAWING MOMENT COEFFICIENT

"EXTERNAL" TYPE FINAL STAGE

SUPERSONIC

$\alpha = 0°$

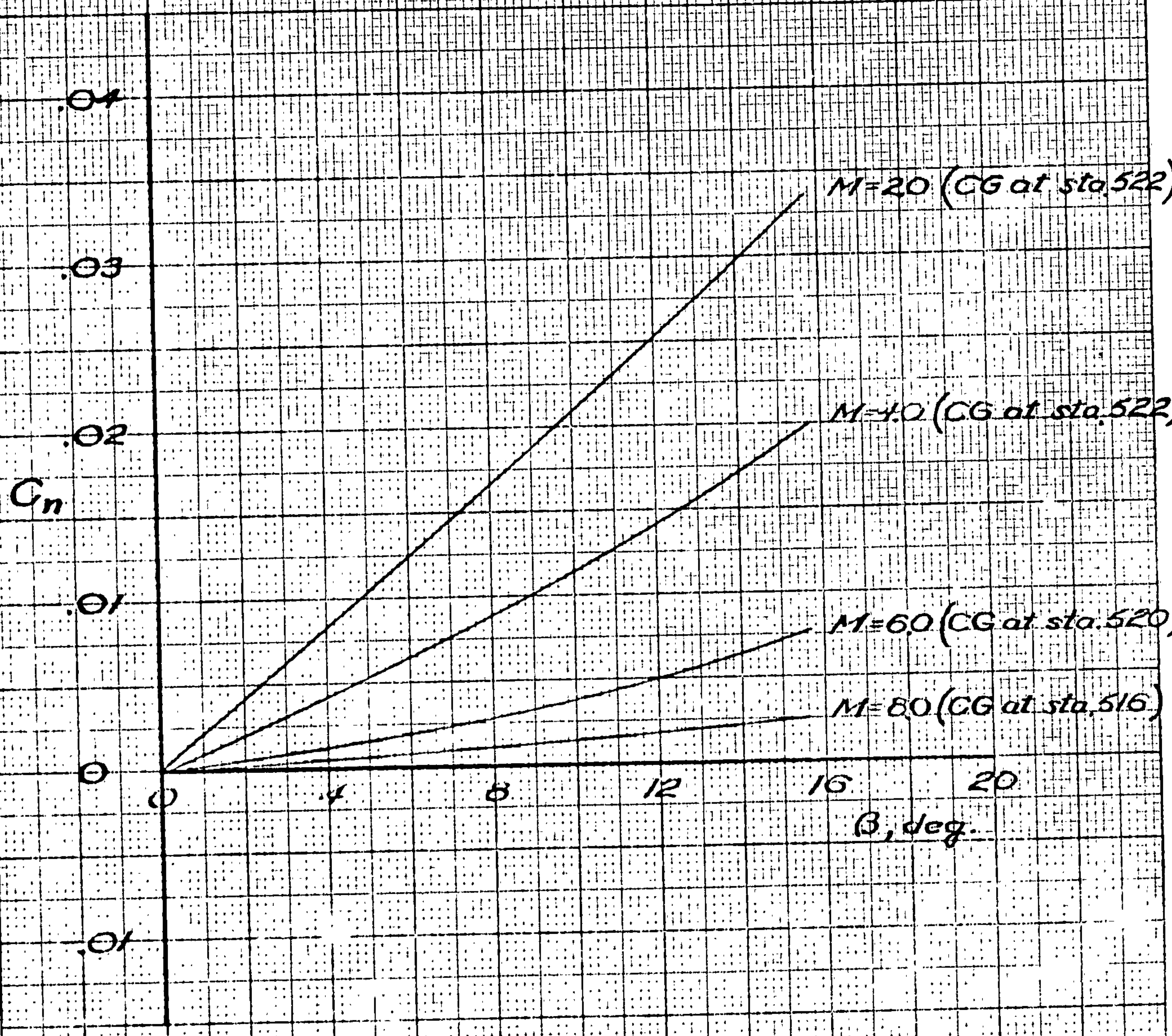

SECRET

SECRET

Fig 4.11-5

DIRECTIONAL STABILITY CHARACTERISTICS

"EXTERNAL" TYPE FINAL STAGE

SUPERSONIC
$\alpha = 0°$

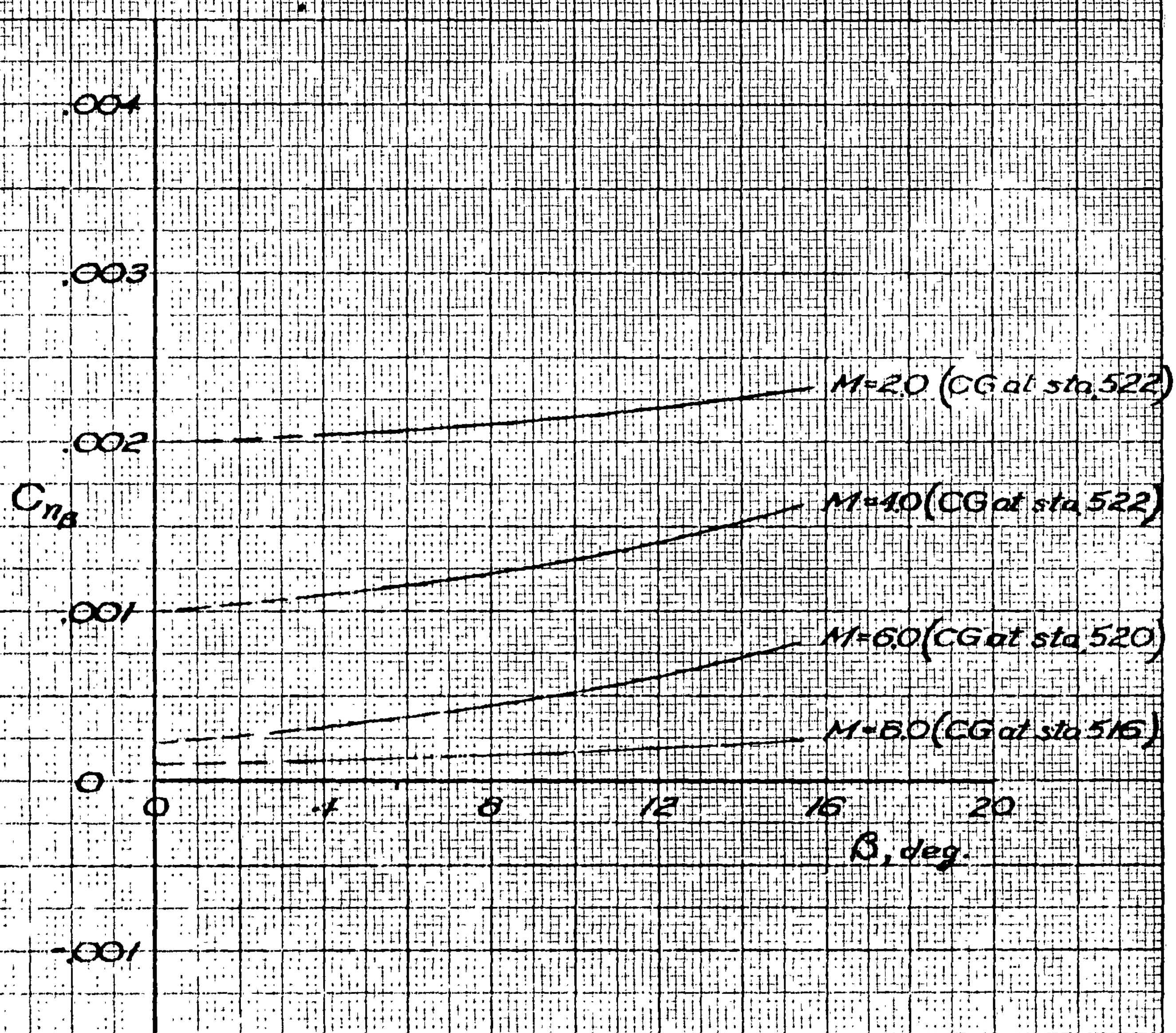

SECRET

SECRET

Fig 4.11-6

YAWING MOMENT COEFFICIENT

"INTERNAL" TYPE FINAL STAGE

SUPERSONIC

$\alpha = 0°$

Vertical Tail At Most Aft Fuselage Location
Two Ventral Fins Under The Wings

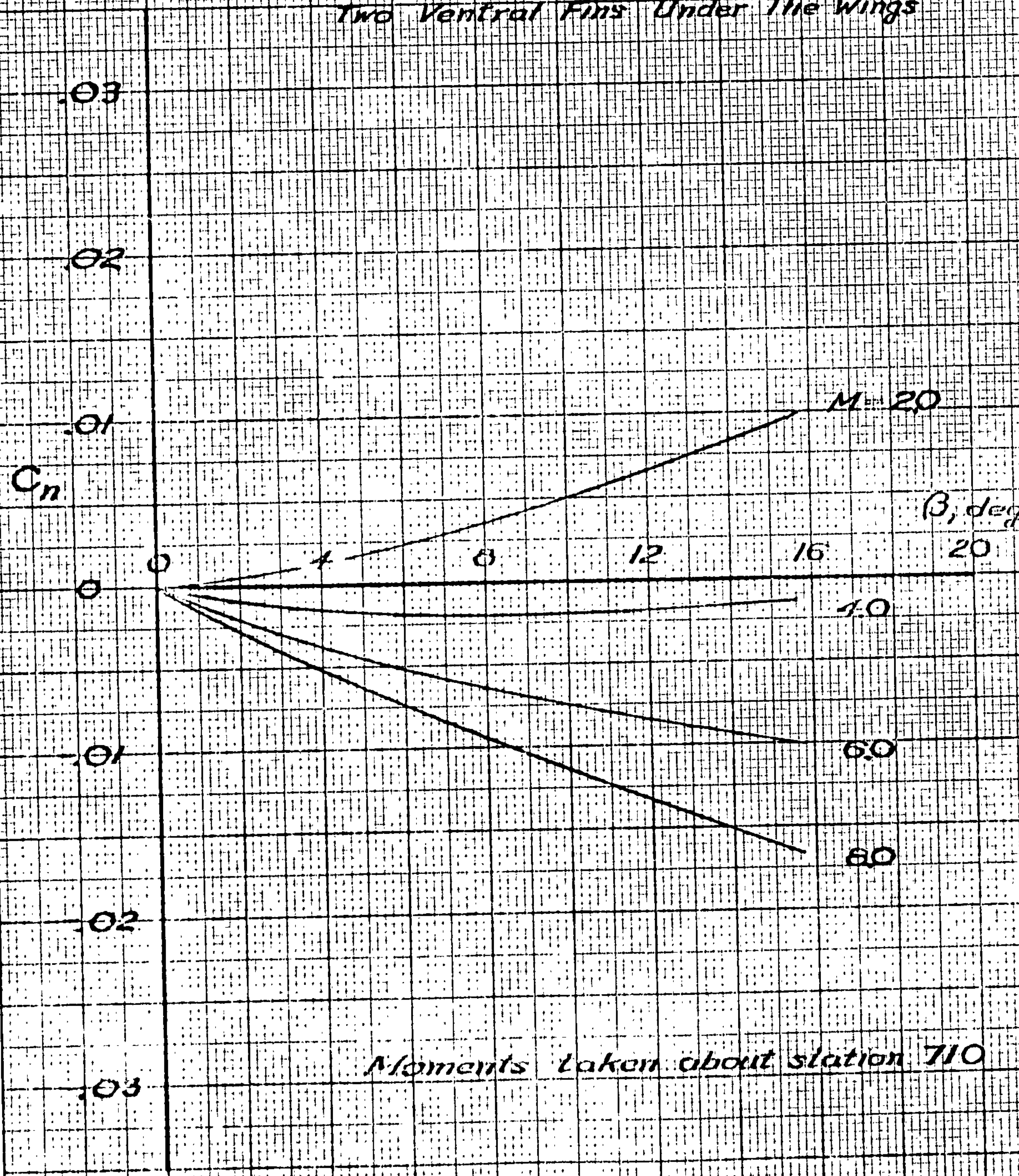

SECRET

SECRET

Fig 4.11-7

DIRECTIONAL STABILITY CHARACTERISTICS

"INTERNAL" TYPE FINAL STAGE

SUPERSONIC

$\alpha = 0°$

Vertical Tail At Most Aft Fuselage Location
Two Ventral Fins Under The Wings

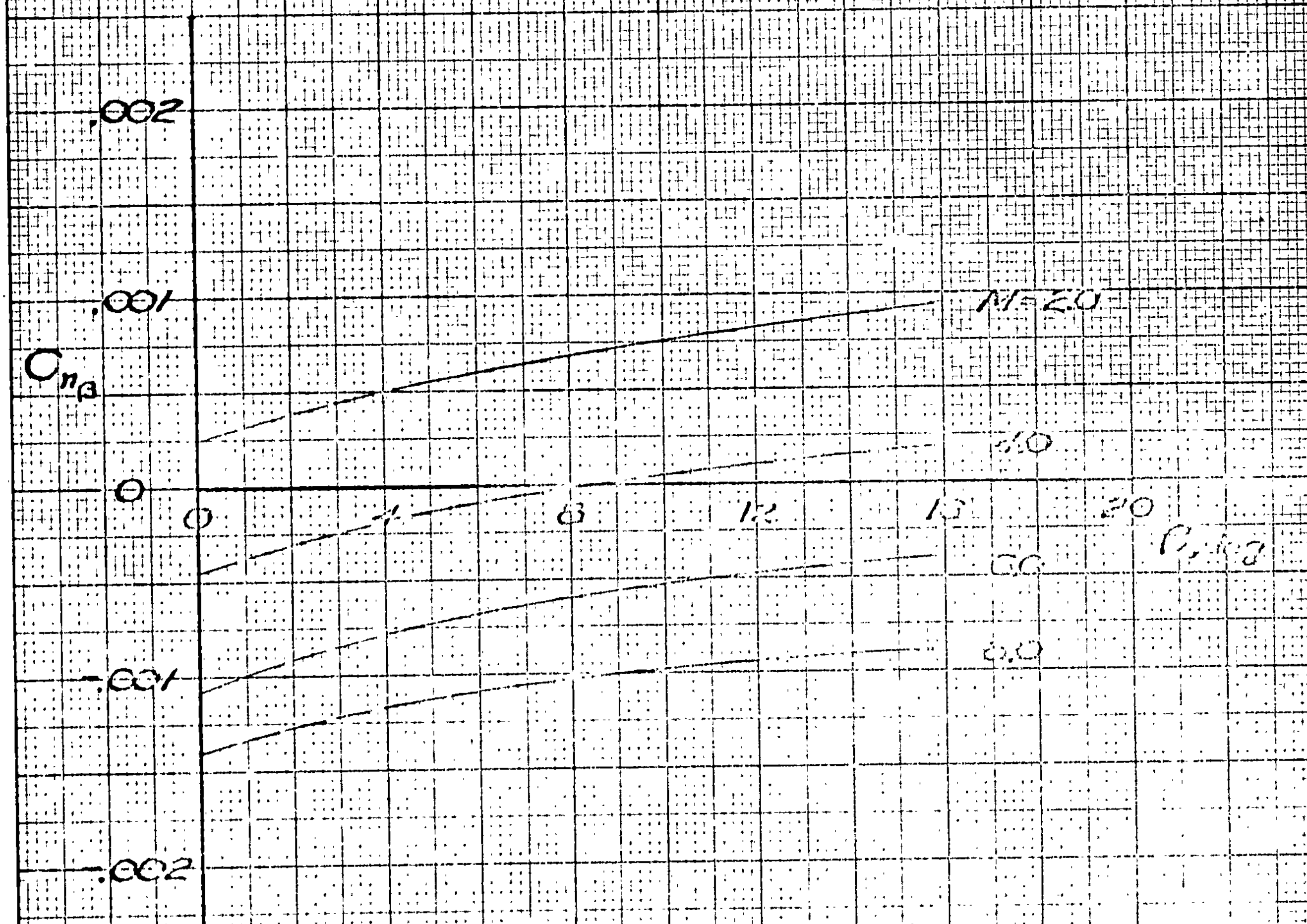

Moments taken about station 110

SECRET

SECRET

Fig 4.11-8

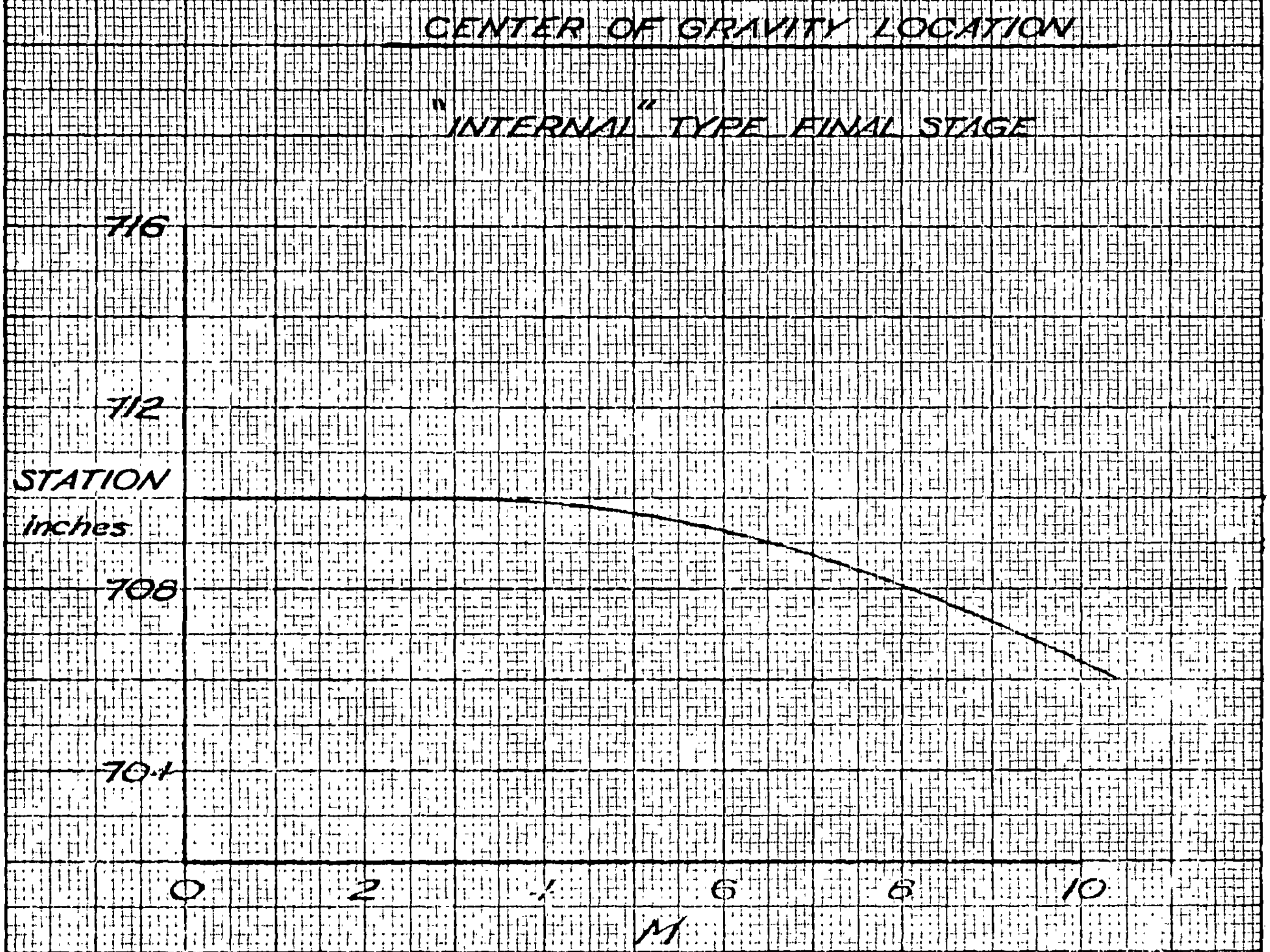

SECRET

SECRET

Fig. 4.11-9

YAWING MOMENT COEFFICIENT

"INTERNAL" TYPE FINAL STAGE

SUPERSONIC
$\alpha = 0°$

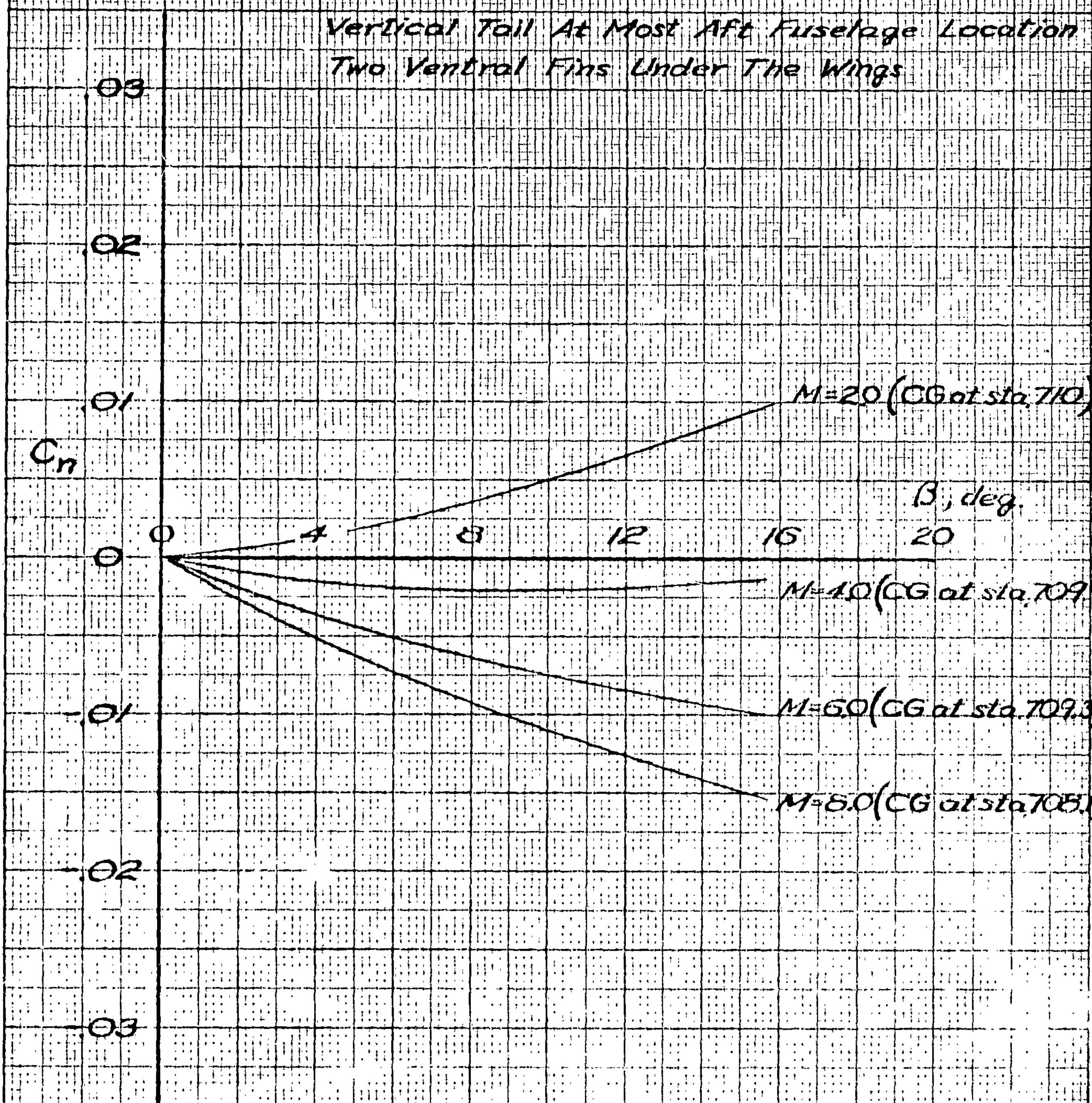

SECRET

SECRET

Fig. 4.II-10

DIRECTIONAL STABILITY CHARACTERISTICS

"INTERNAL" TYPE FINAL STAGE

SUPERSONIC
$\alpha = 0°$

Vertical Tall At Most Aft Fuselage Location
Two Ventral Fins Under The Wings

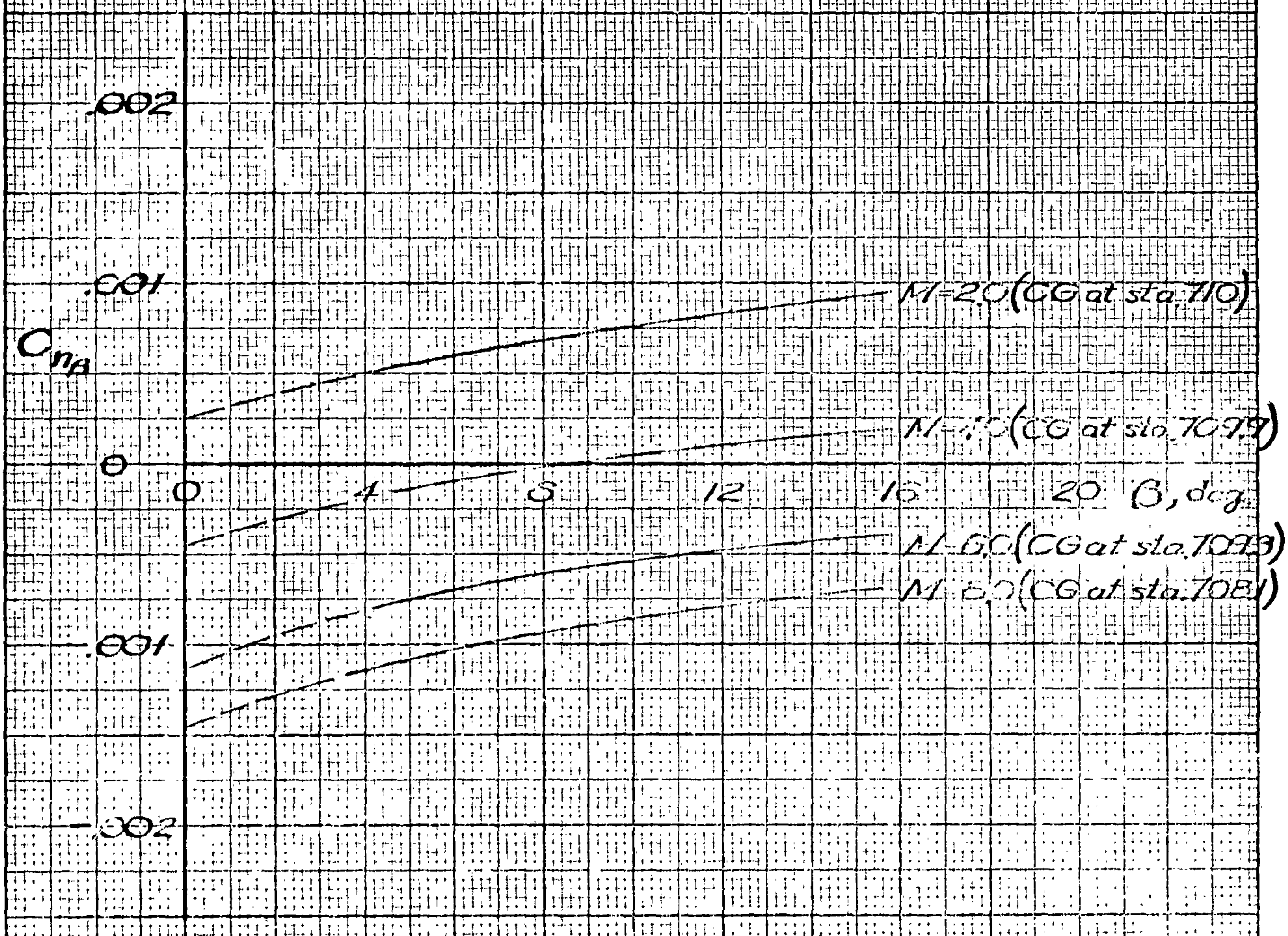

SECRET

SECRET

Fig 4.11-11

YAWING MOMENT COEFFICIENT

"EXTERNAL" TYPE FINAL STAGE

SUBSONIC

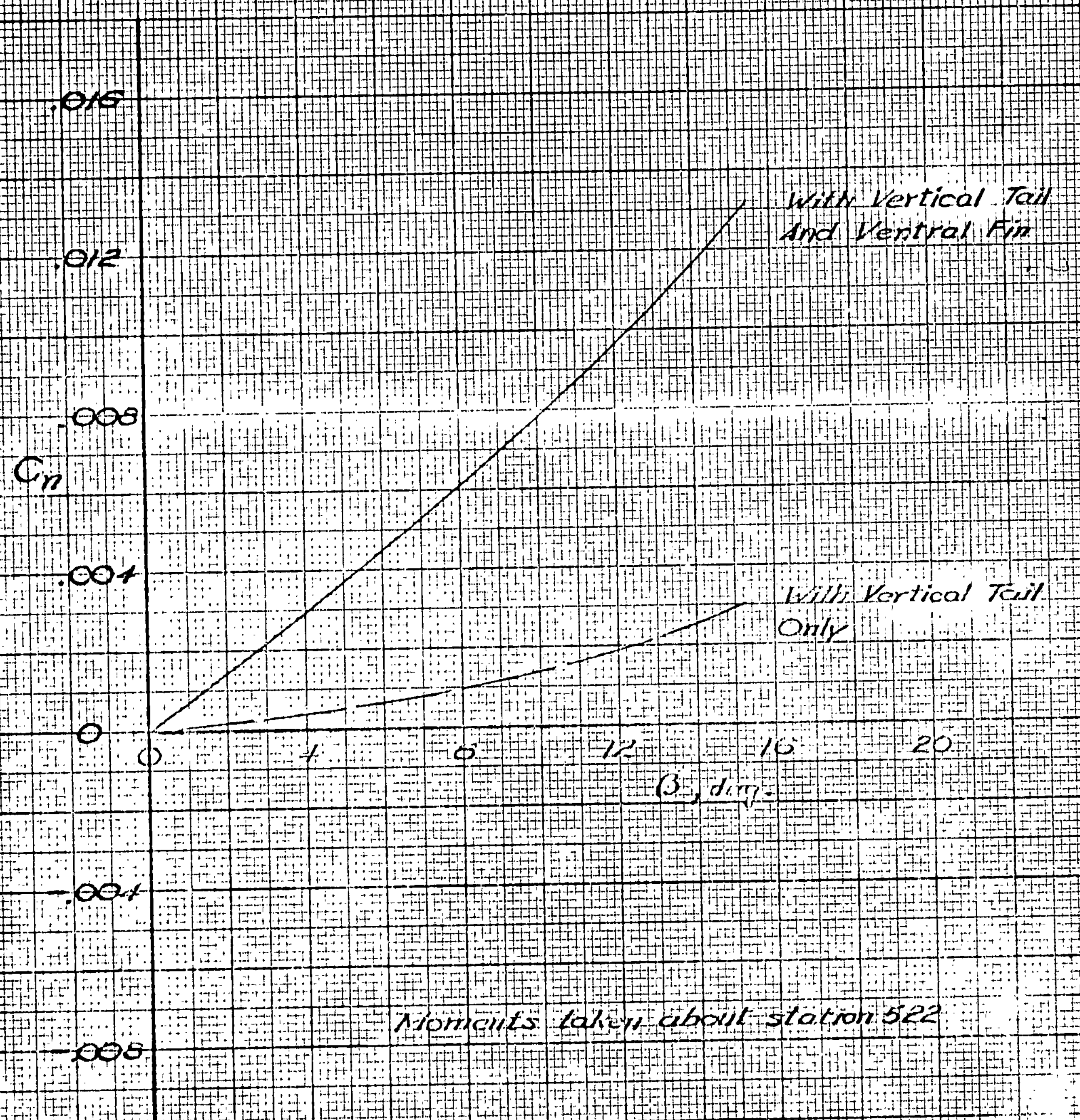

SECRET

SECRET

Fig 4.11-12

DIRECTIONAL STABILITY CHARACTERISTICS

"EXTERNAL" TYPE FINAL STAGE

SUBSONIC

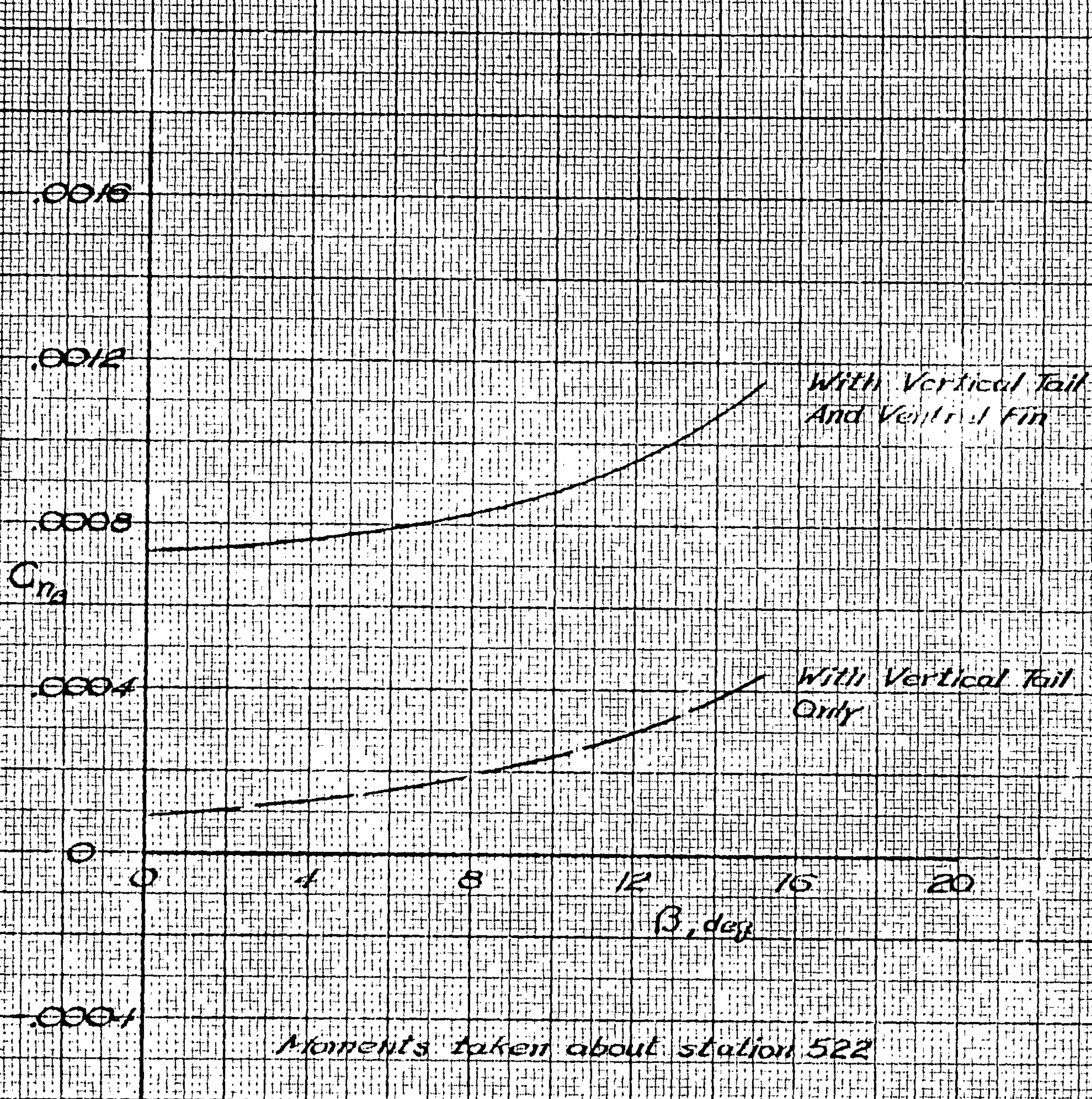

SECRET

SECRET

Fig. 4.11-13

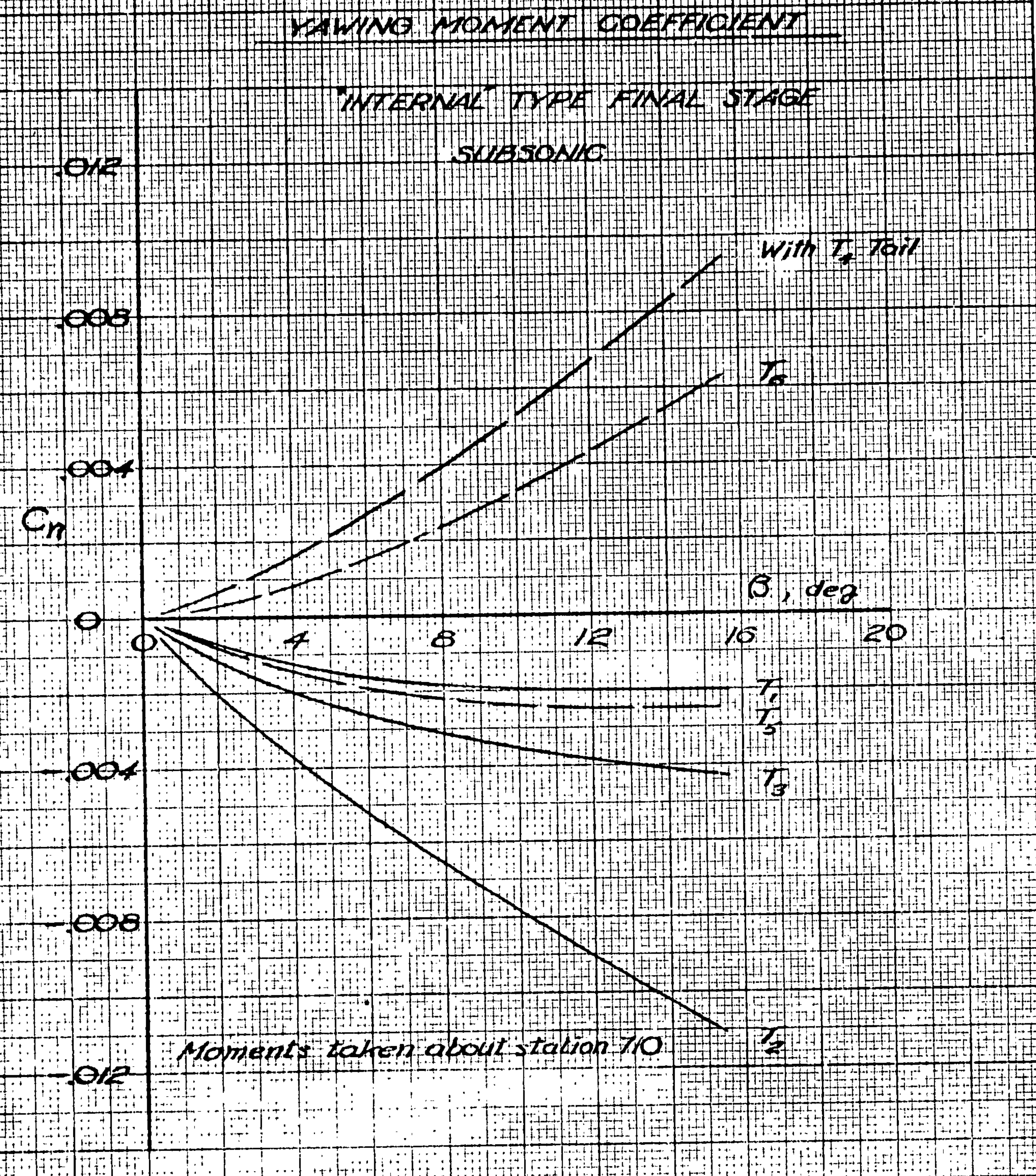

T_1	Upper Vertical Tail With Single Ventral Fin Under Fuselage
T_2	" " " " No Ventral Fin
T_3	" " " " Two Ventral Fins Under Wings
T_4	Same As T_1 With Tail At Most Aft Location (Dash Lines)
T_5	" " T_2 " " " " " " " "
T_6	" " T_3 " " " " " " " "

SECRET

SECRET

Fig. 4.11-14

DIRECTIONAL STABILITY CHARACTERISTICS

"INTERNAL" TYPE FINAL STAGE

SUBSONIC

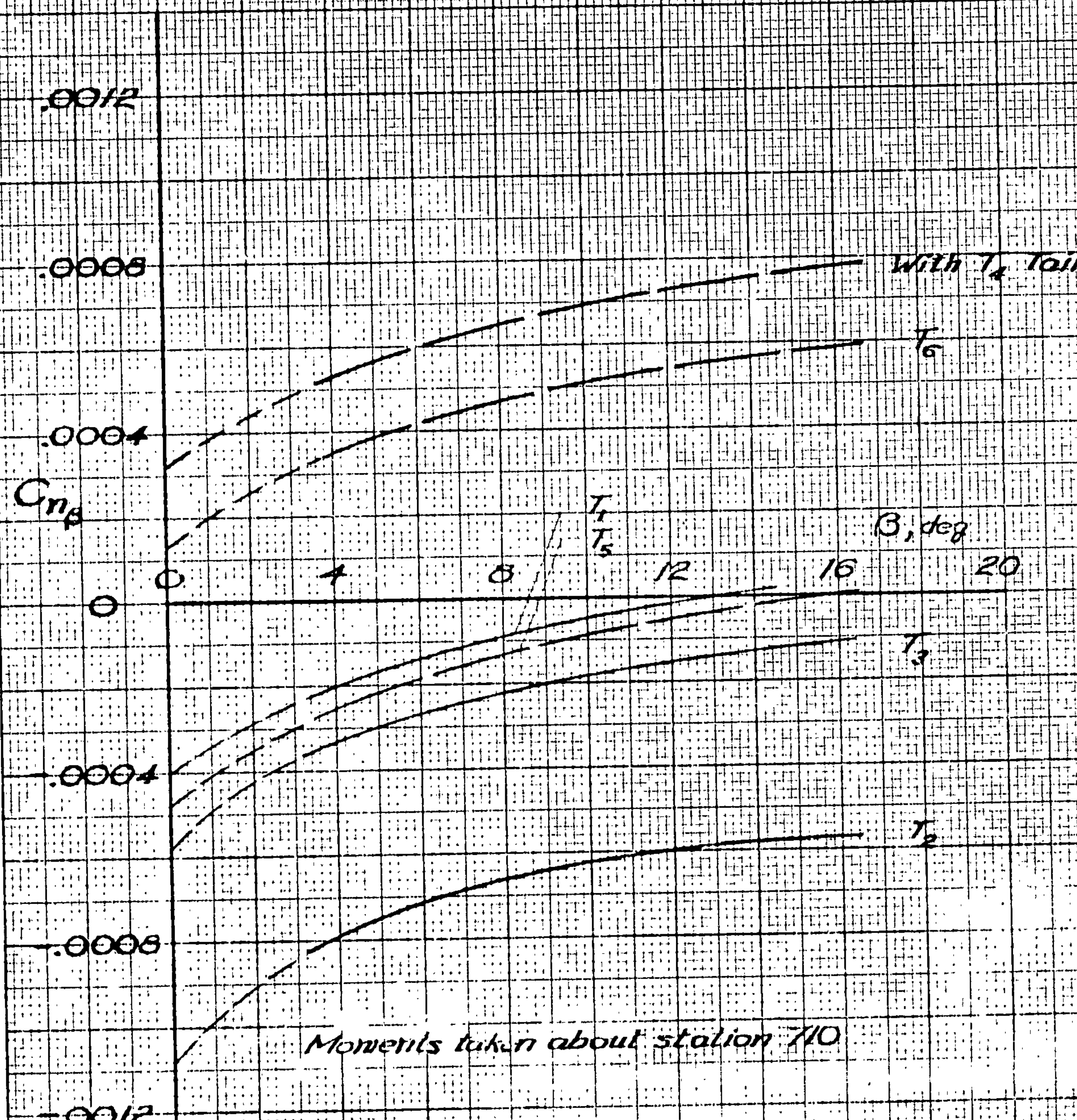

SECRET

4.12 AERODYNAMIC HEATING DURING UNPOWERED FLIGHT

4.12.1 GLIDE

Two glide flight plans, Figures 4.12-1 and 2 were examined very briefly in order to determine the equilibrium temperatures for two conditions. Figures 4.12-3 and 4 give the equilibrium temperatures for a one foot location using laminar flow which is representative of temperatures on the bottom of the wing and body forward of transition, and the equilibrium temperatures for a ten foot location using turbulent flow which is representative of the temperatures that would be experienced aft of the transition region. These, of course, are similar to the results reported in Reference 4.12.1. Complete temperature profiles for the glide portion would have been rather repetitious of earlier work.

The two flight plans are very similar as far as temperature profiles are concerned. For these particular conditions the temperatures are below 2000°F at the start of the glide and generally decrease from that point.

Figure 4.12-5 illustrates the effect of variation of the initial glide altitude on the equilibrium wall temperature for the same one foot and ten foot stations.

4.12.2 RAPID DESCENTS

Recovery of the vehicles or a capsule in case of a major malfunction has been examined from a design standpoint. Several zero lift trajectories from various burnout conditions, see Figures 4.5-1 through 4.5-6, have been examined. A one foot location on a five degree body has been examined for each of these flight plans for both laminar and turbulent flow, see Figures

4.12-6 through 4.12-11. It can be seen from these curves that if the flow is turbulent which it is likely to be in the region of maximum temperature, a drag parameter of 0.2 to 0.3 must be obtained in order to maintain the temperatures over the major portion of the vehicle below 2000°F for this array of initial conditions.

4.12 REFERENCES

4.12.1 Reconnaissance Aircraft Weapon System - Aerodynamics. Bell Aircraft Corporation, Report No. D143-945-024, December 1955

SECRET

Time Histories of Altitude, Velocity and Angle of Attack During the Glide

Flight Plan 7
"External" Type

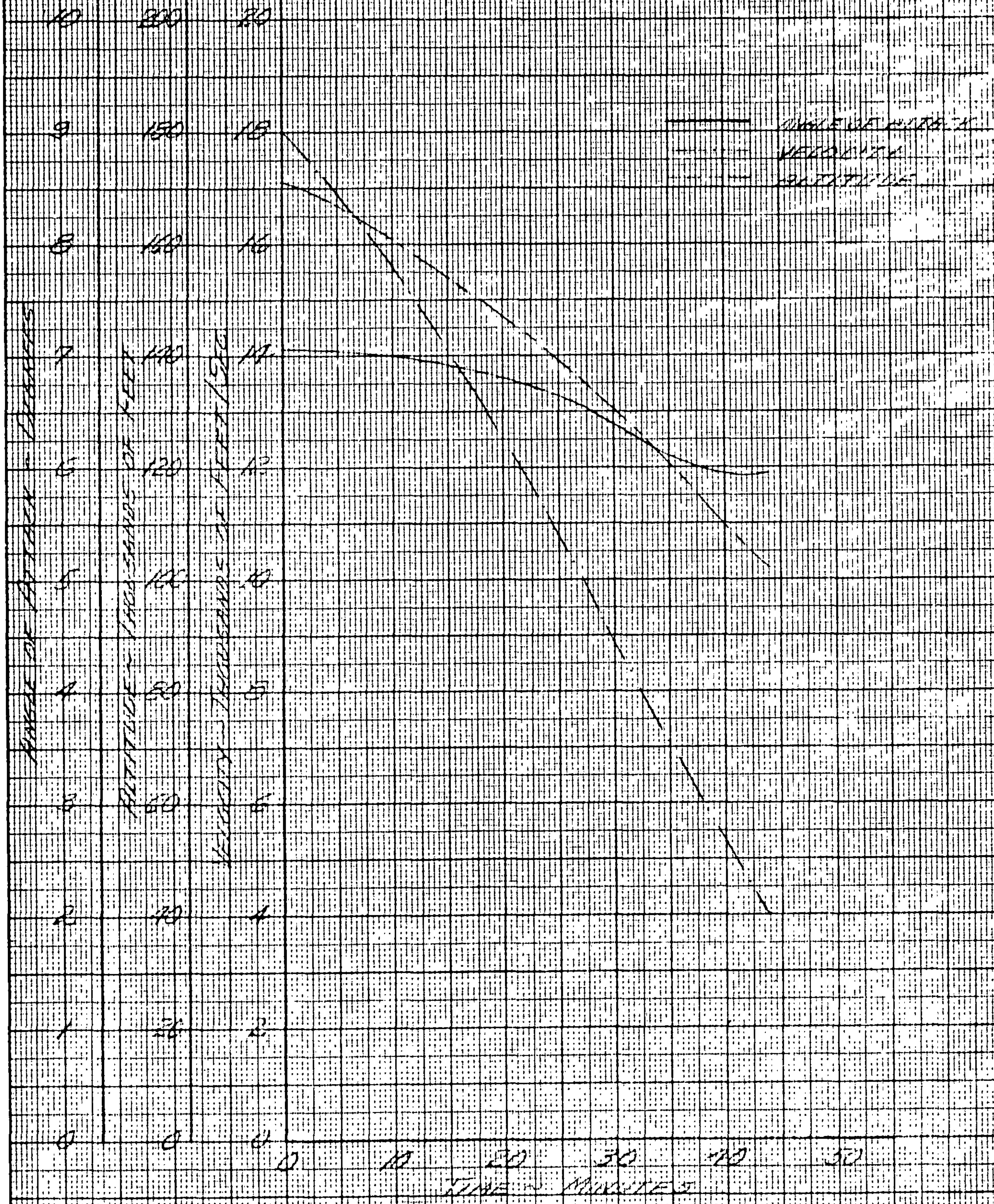

SECRET

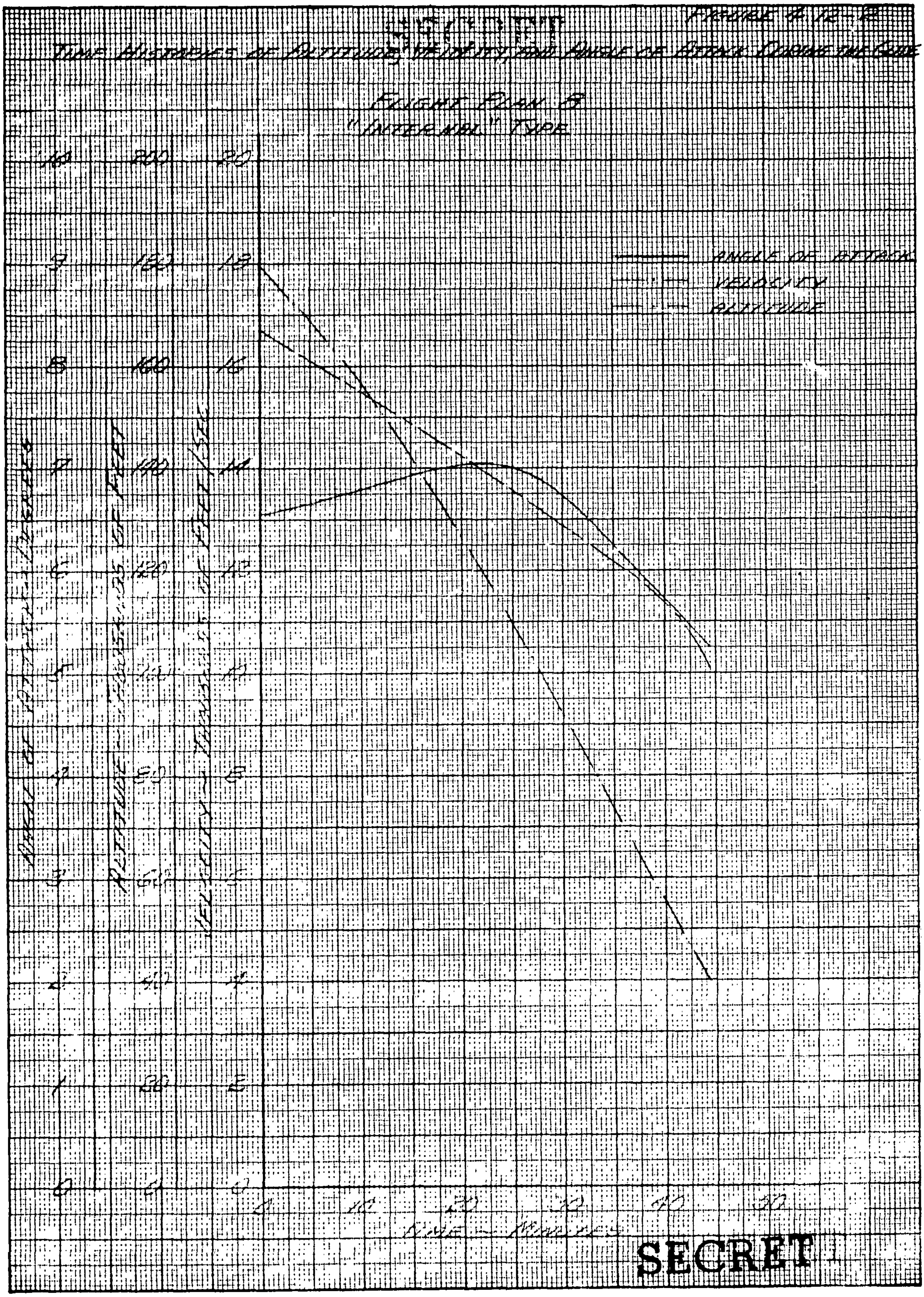
SECRET
FIGURE 4.12-2
TIME HISTORIES OF ALTITUDE, VELOCITY AND ANGLE OF ATTACK DURING THE GLIDE
FLIGHT PLAN B
"INTERNAL" TYPE
ANGLE OF ATTACK
VELOCITY
ALTITUDE
ANGLE OF ATTACK ~ DEGREES
ALTITUDE ~ THOUSANDS OF FEET
VELOCITY ~ THOUSANDS OF FEET/SEC
TIME ~ MINUTES
SECRET

SECRET

TIME HISTORIES OF EQUILIBRIUM WALL TEMPERATURES

FLIGHT PLAN 7

EXTERNAL TUBE

$\epsilon = 0.9$

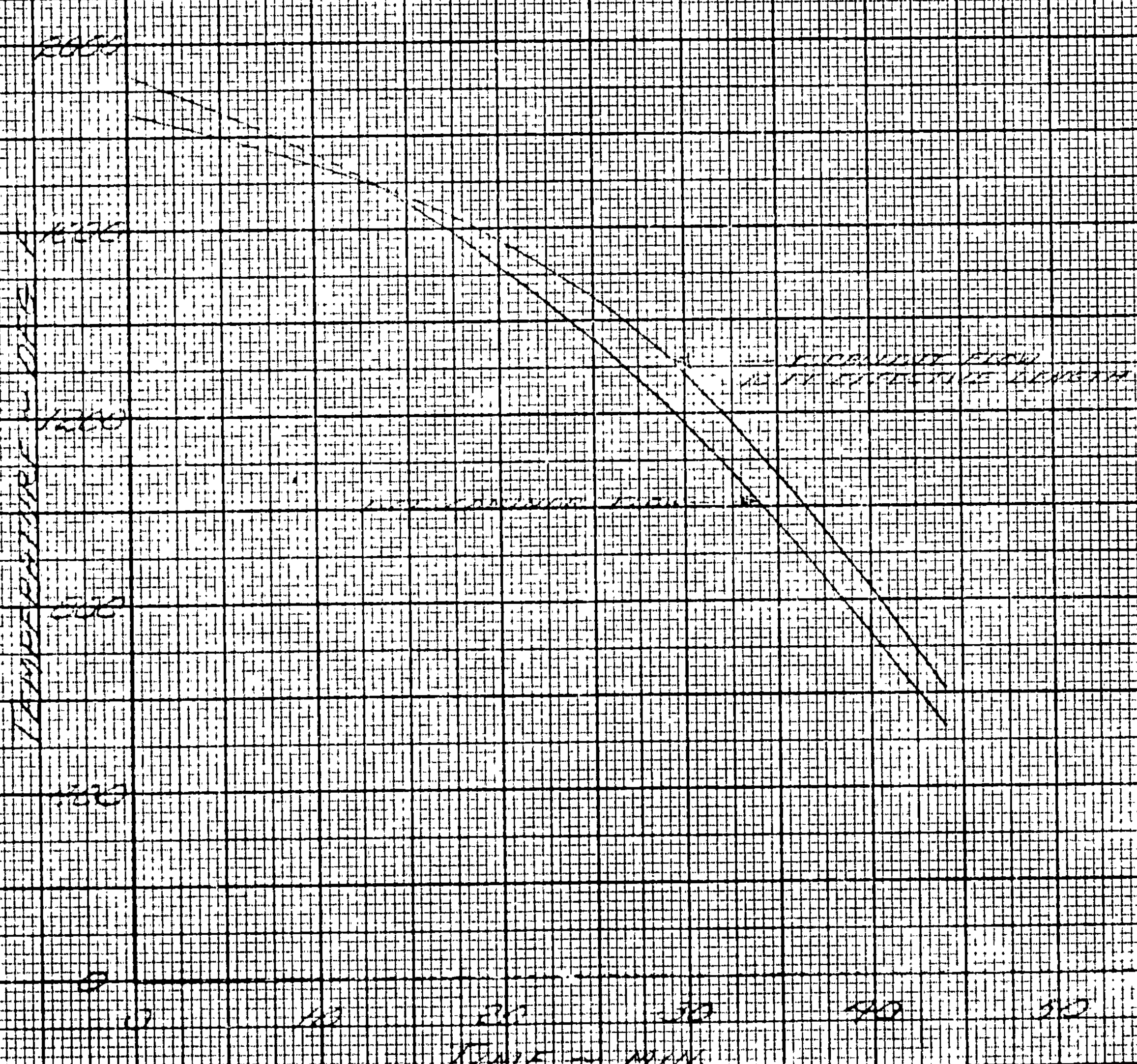

SECRET

SECRET

FIGURE 4.12-4

TIME HISTORIES OF EQUILIBRIUM WALL TEMPERATURES

FLIGHT PLAN B
"INTEGRAL" TYPE
ε = 0.9

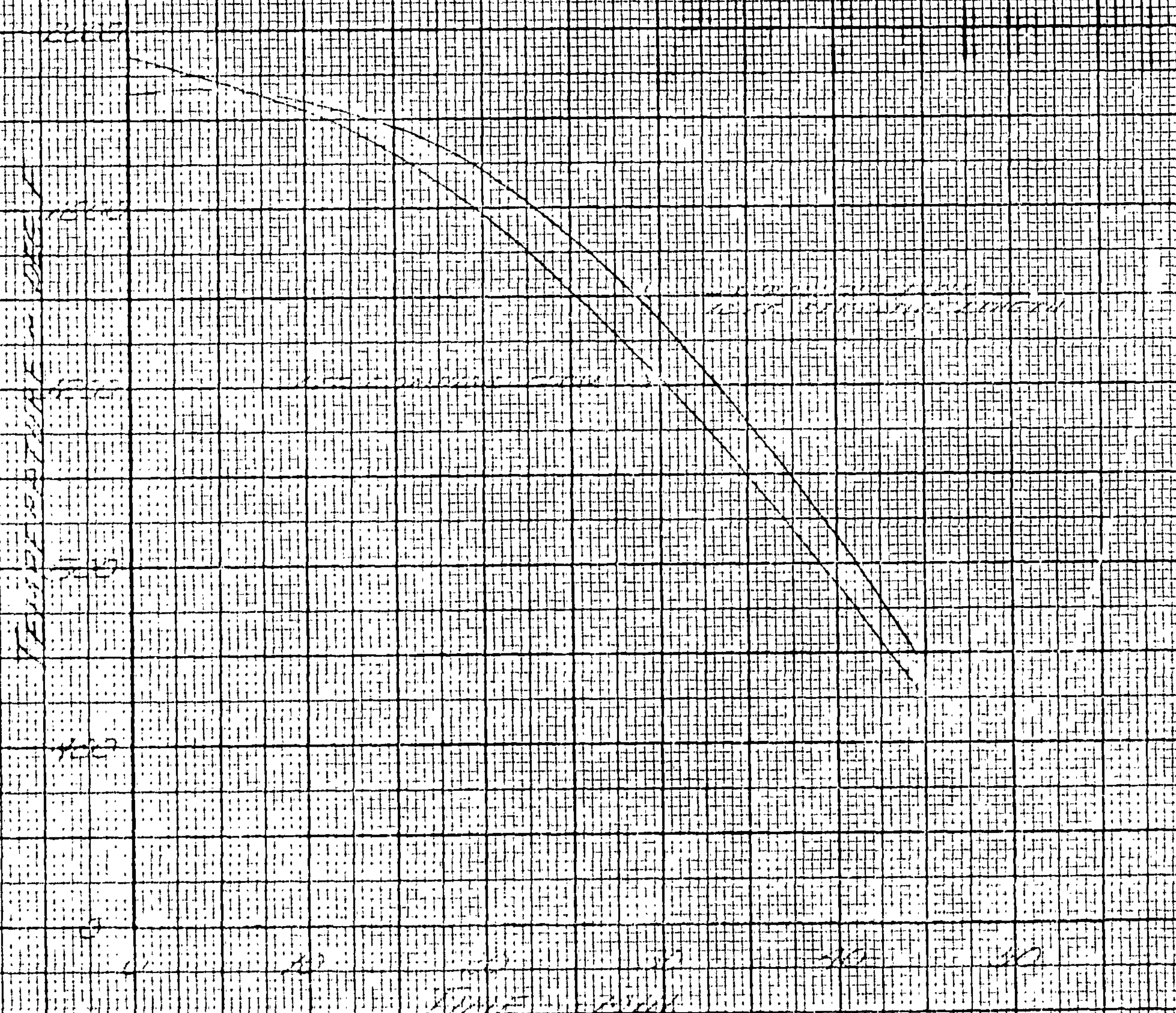

SECRET

SECRET

Figure 4.12-5

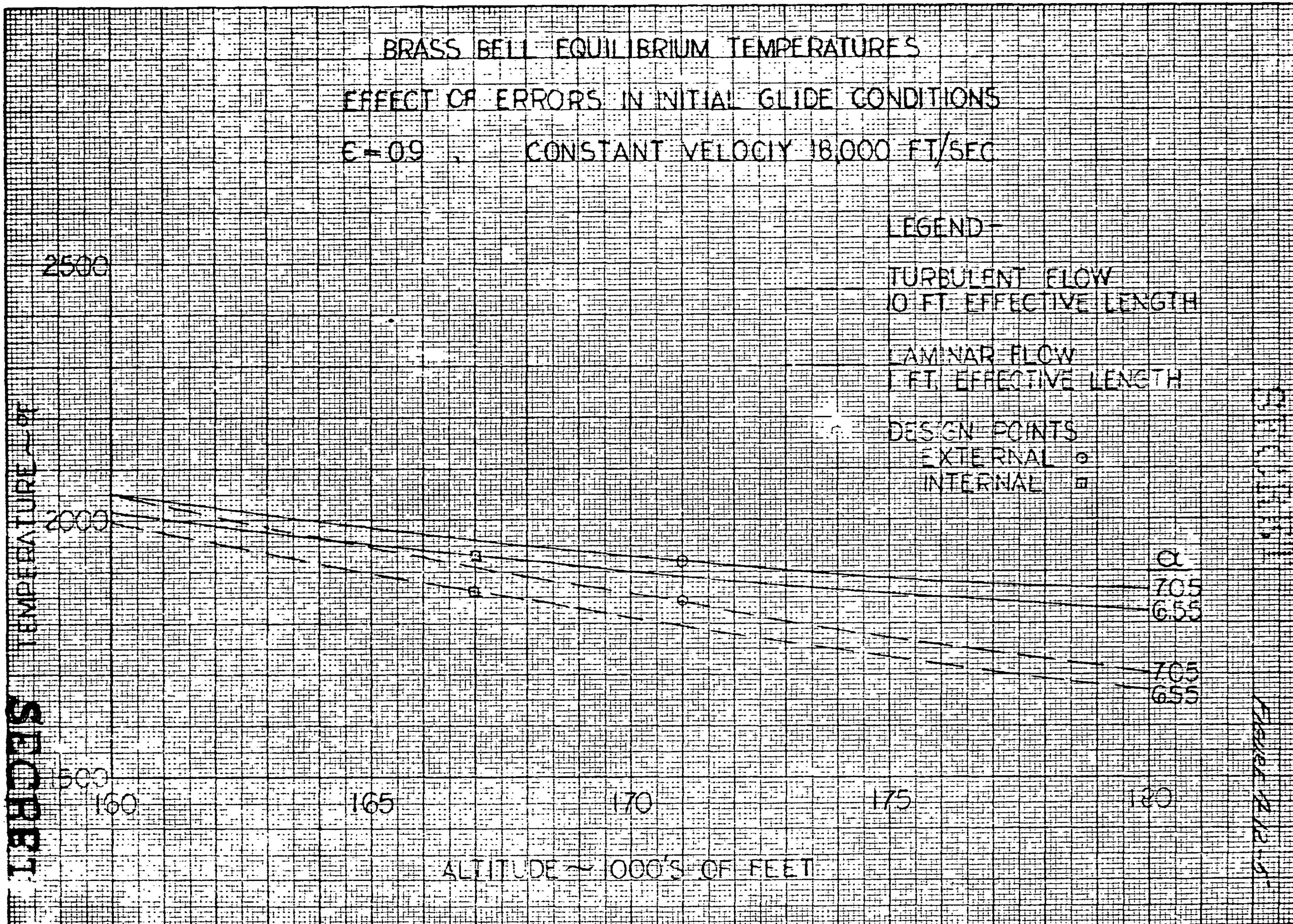

SECRET

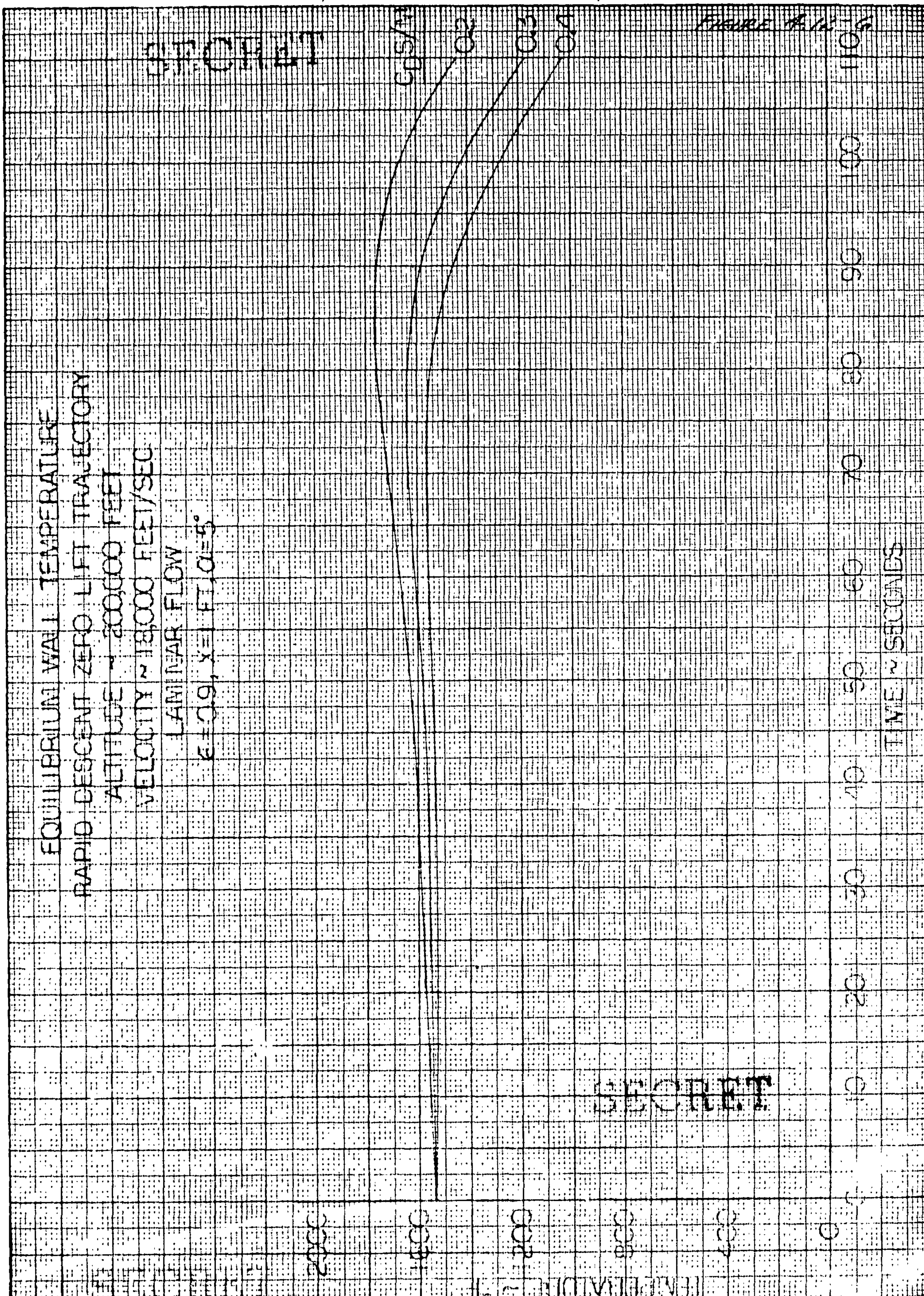
SECRET
EQUILIBRIUM WALL TEMPERATURE
RAPID DESCENT ZERO LIFT TRAJECTORY
ALTITUDE ~ 200,000 FEET
VELOCITY ~ 18,000 FEET/SEC
LAMINAR FLOW
ε = 0.9, x = 1 FT, α = 5°
$C_D S/W$
0.2
0.3
0.4
2000
1600
1200
800
400
0
0
10
20
30
40
50
60
70
80
90
100
110
TIME ~ SECONDS
SECRET

SECRET

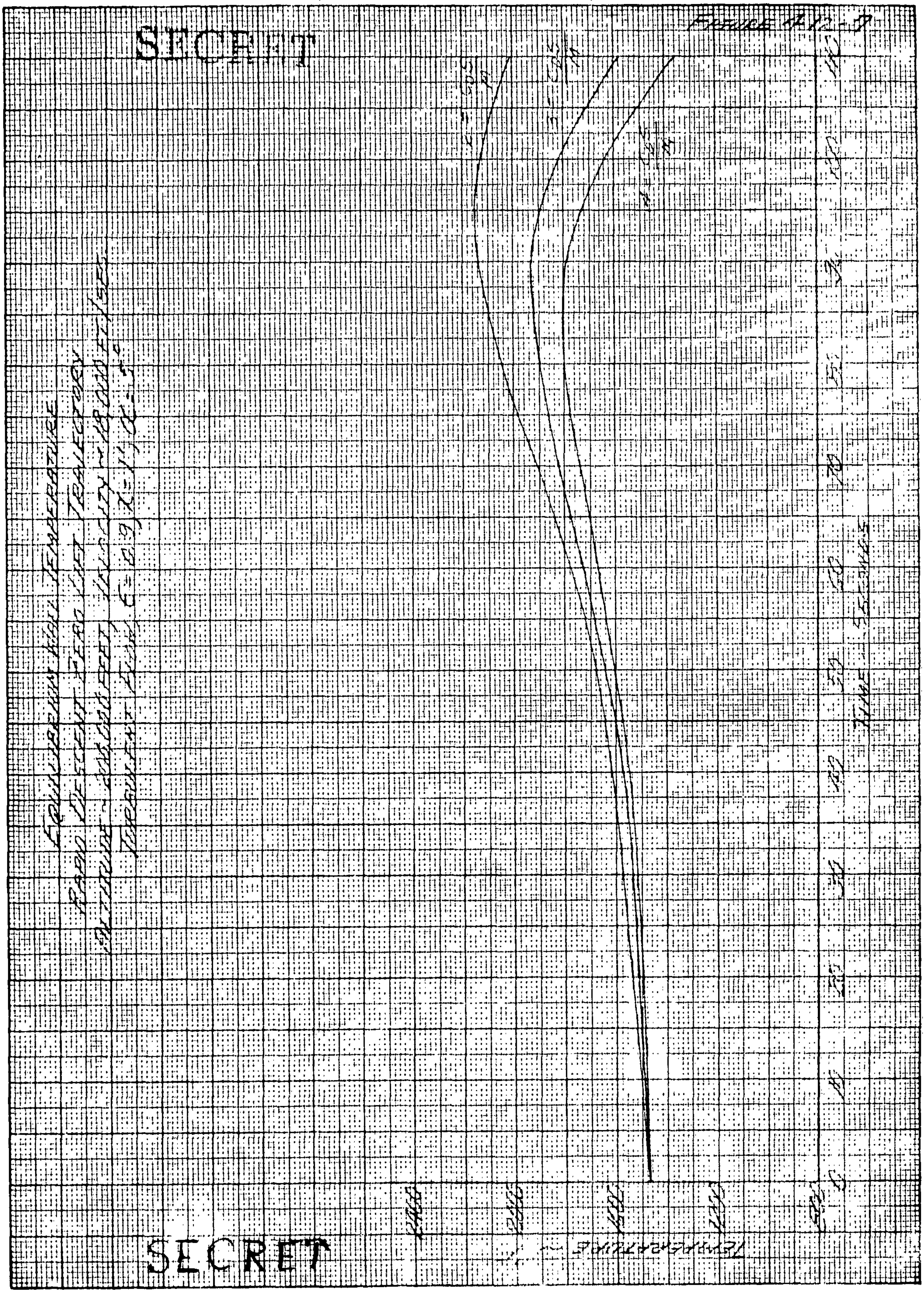

SECRET

SECRET

Figure 4.12.8

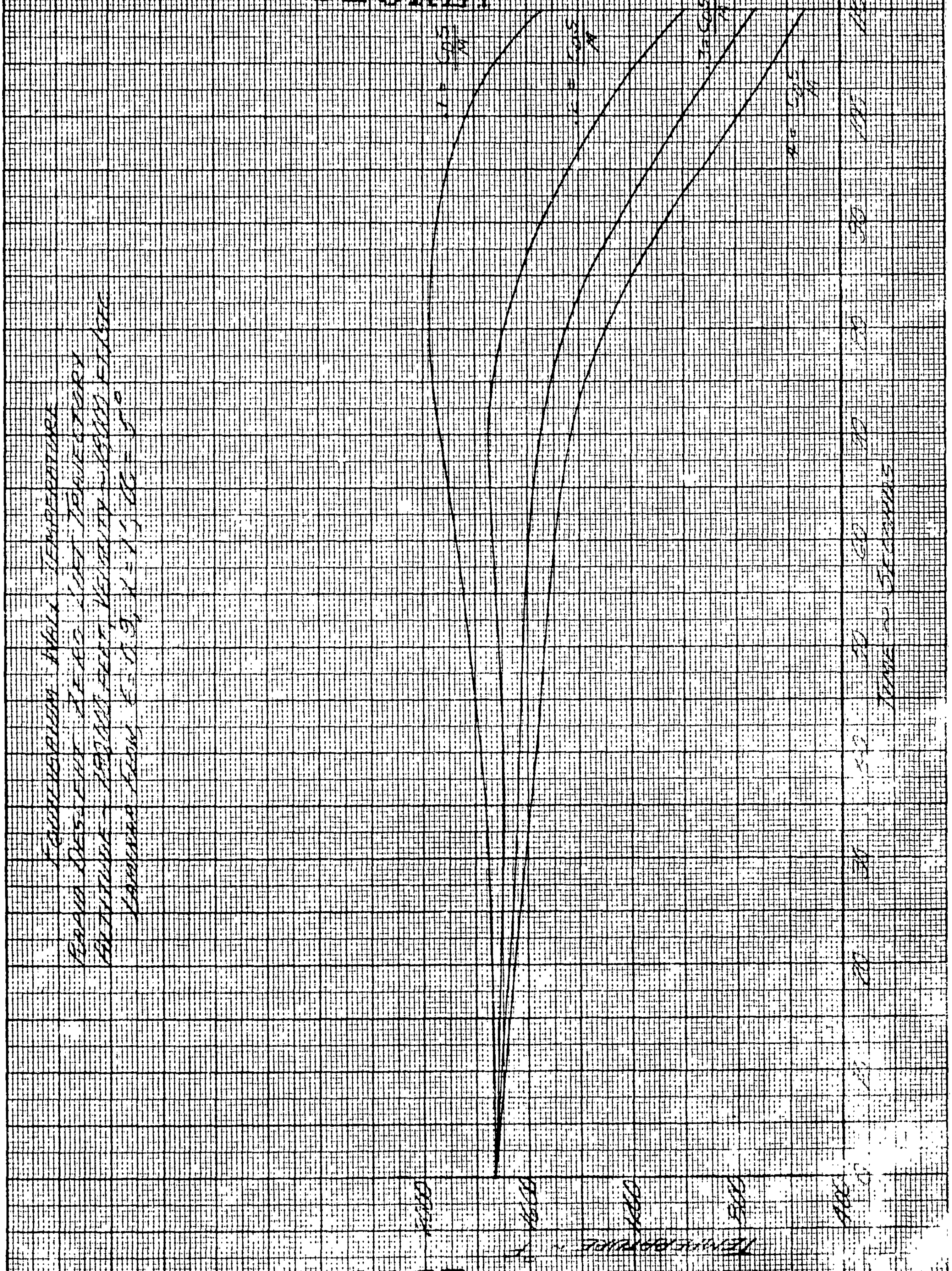

SECRET

SECRET

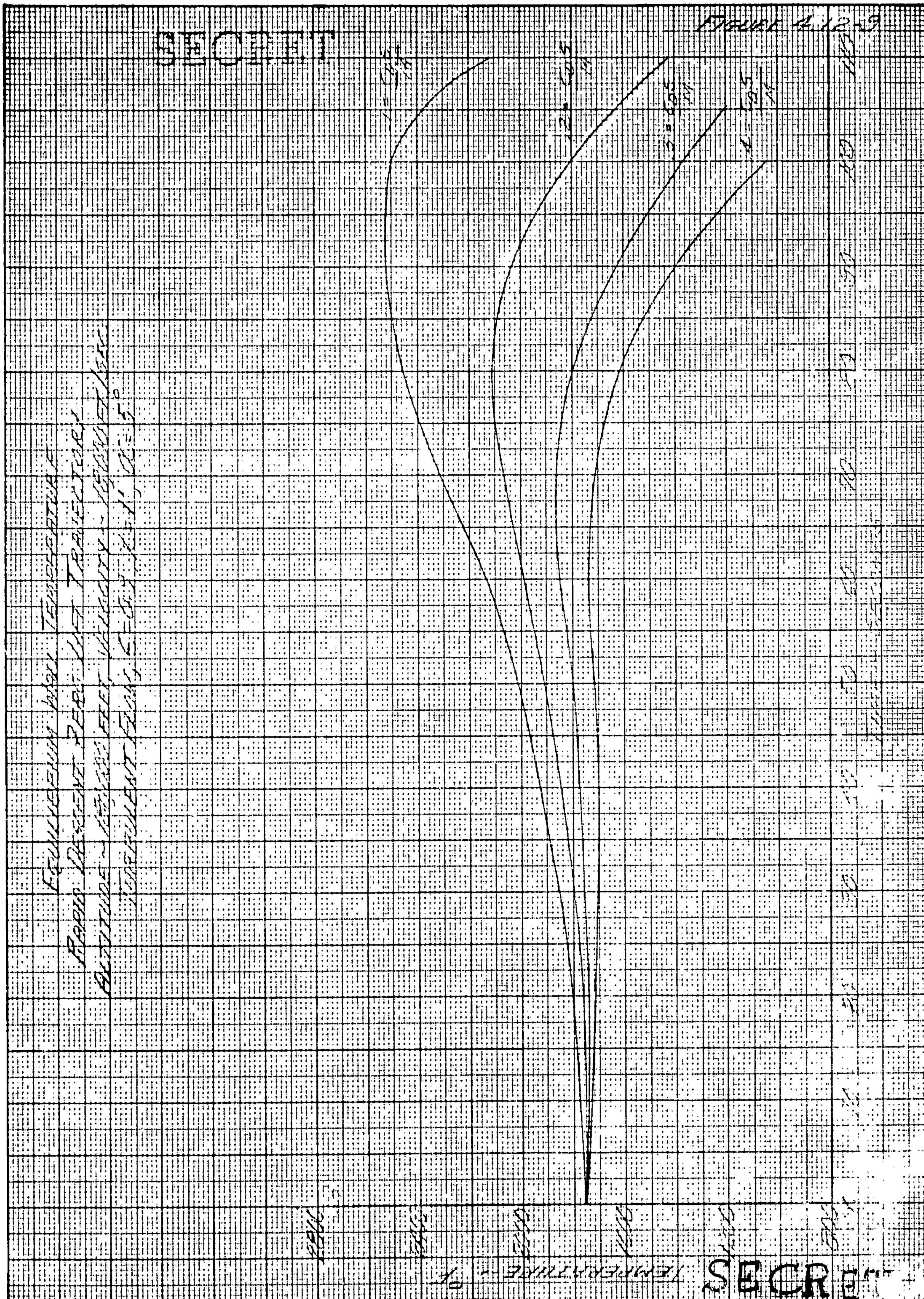

SECRET

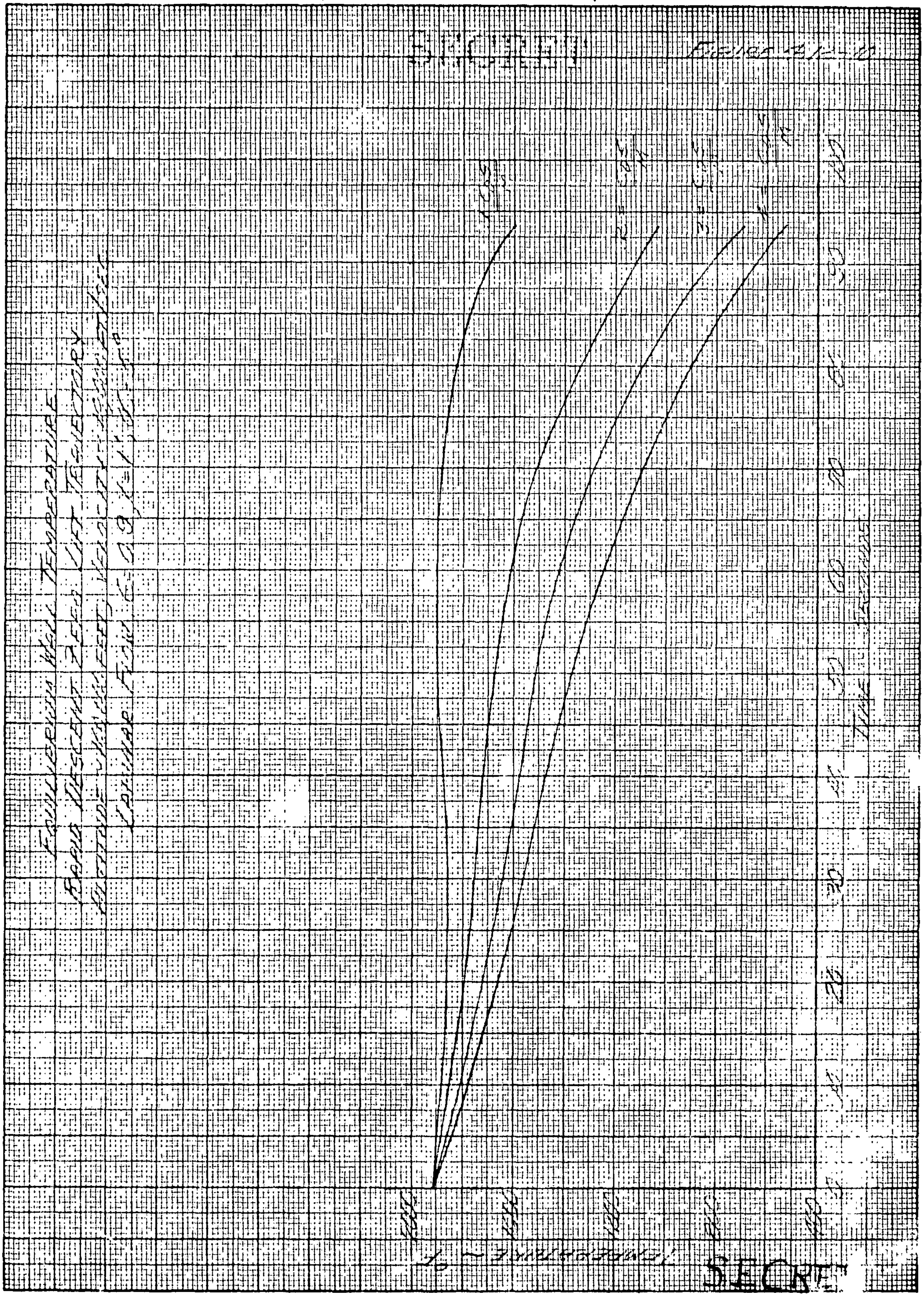
SECRET
EQUILIBRIUM WALL TEMPERATURE
RAPID DESCENT ZERO LIFT TRAJECTORY
TIME ~ SECONDS
0
10
20
30
40
50
60
70
80
90
100
SECRET

BY ____________ DATE ____________ CHECKED ____________ DATE ____________

BELL Aircraft CORPORATION

MODEL ____________ PAGE 4-130
SHIP ____________ REPORT D143-945-033

SECRET

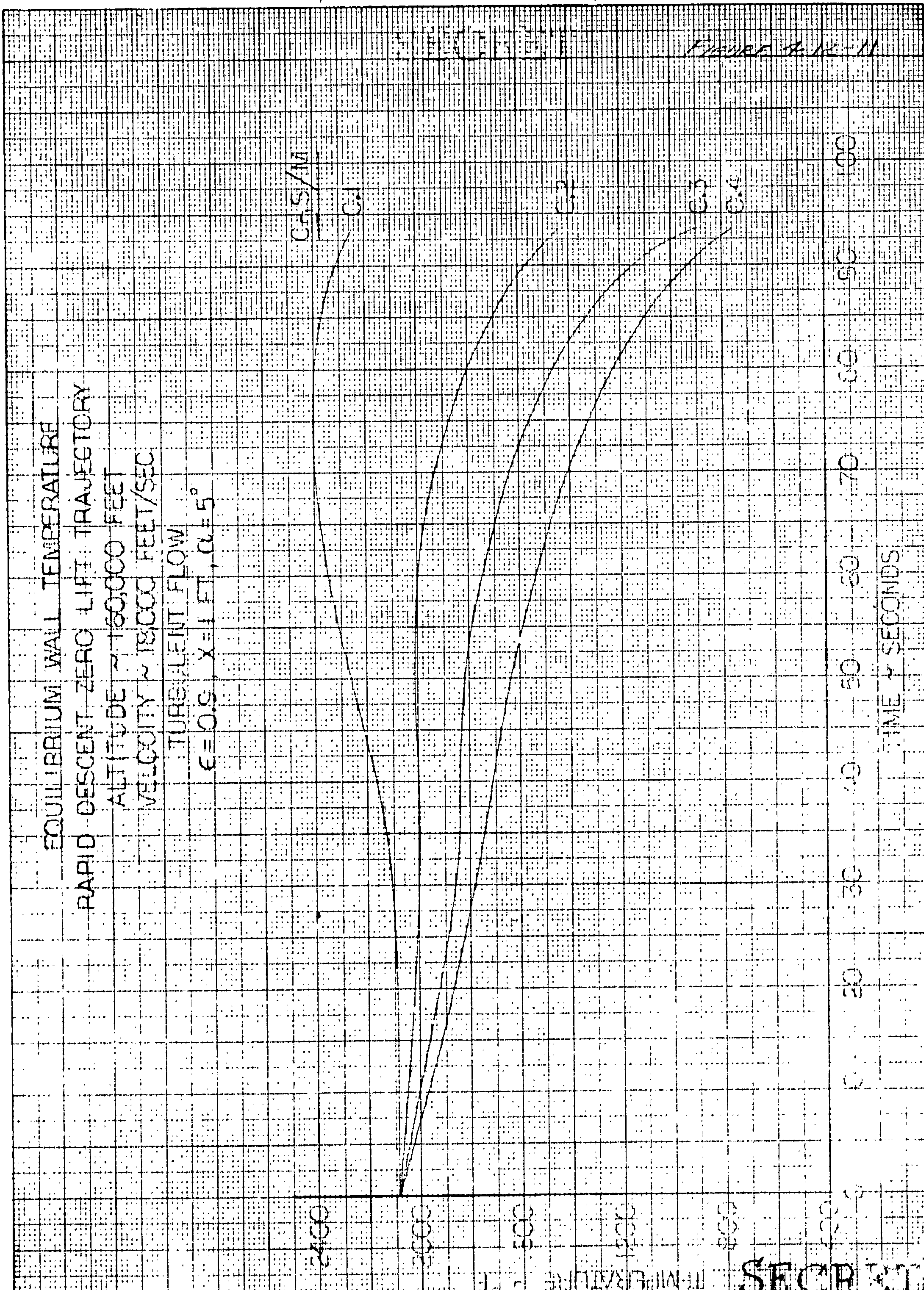

SECRET

4.13 DESCENT PATHS

A problem area of extreme importance for nonpowered aircraft is the determination of the flight regime from which the aircraft can be navigated to a given landing site. To provide a basis for the definition of such a regime for Brass Bell, a study was made of descent paths incorporating sustained bank angles. It was assumed that equilibrium flight would be maintained at all times, i.e. that the vertical component of the lift would always equal the effective weight of the aircraft. Flight at the angle of attack for maximum lift to drag ratio was also assumed; thus producing maximum range along the flight path.

The specific paths which were examined were those resulting from bank angles of 0, 10, 20, 30, and 40 degrees. Lift coefficient values of .2, .3, and .4 were selected. For this range of coefficients, maximum lift to drag ratios of 4 and 5 were considered representative of the Brass Bell configuration.

The development of the equations which make it possible to estimate the performance of a nonpowered aircraft executing coordinated turns is given in Reference 4.13.1. Those equations were developed in terms of lateral maneuvering accelerations. By substituting the expressions

$$1. \quad \cos\phi = \frac{L_e}{L} = \frac{W}{L}\left[1 - \frac{V^2}{g(r_o+h)}\right]$$

$$2. \quad \sin\phi = \frac{L_m}{L} = \frac{n_m W}{L}$$

where ϕ is the bank angle and the other notation is as given in the reference, the equations will describe coordinated turns effected by bank angles.

The descent paths were computed for an initial velocity of 4000 feet per second and a constant weight of 18,017 pounds. It was assumed that initially, the aircraft was at zero bank angle so that altitude at the beginning of each descent was obtained for each value of C_L from the equilibrium condition with $\phi = 0°$ (expression 1 above). Subsequent altitude-velocity correspondences were then computed for each combination of C_L, ϕ, and selected values of velocity. Atmospheric data was obtained from Reference 4.13.2. Integration of the expressions for X, the down range distance, and Y, the off course distance, then provided coordinates from which ground tracks and altitude profiles could be plotted. These curves are shown in Figures 4.13-1 through 4.13-6 for each combination of C_L and $(L/D)_{max}$. Points of constant velocity have been joined to produce a pseudo-carpet from which paths for intermediate values of ϕ can be estimated. The plots have been shown only to velocities of 500 feet per second since by that time the descent spirals were of such small diameter that no significant range increments were being obtained.

As indicated by the curves, straight-in approaches can carry the aircraft to landing sites 280 nautical miles from the point of descent initiation for $(L/D)_{max} = 5$ or 220 nautical miles for $(L/D)_{max} = 4$. If turns with constant bank angles are made, landings at sites 100 nautical miles to either side of the initial descent azimuth are possible, with, of course, a corresponding reduction in the down range distance. If the curves are

interpreted without regard to the differences which exist along the constant velocity lines, segments of the various constant bank angle curves can be combined to produce programmed bank angle descents. With such a program, the attainable off course distances may be increased by as much as 50 percent over the constant bank angle tracks.

That the altitude differences which occur along the constant velocity curves can be desregarded is an assumption which must to some extent temper the use of the curves as suggested above. The altitude variations with velocity and bank angle are shown on the Off Course and Down Range Profiles. At the lower velocities and smaller bank angles, the differences are quite small and, consequently, descent programs composed of segments in these regions should be fairly reliable. The altitude differences are more significant at the higher velocities so that flight paths which include programming at these speeds must be considered, at best, rough estimates.

It is apparent from a cursory examination of the curves that there will be areas around the point of descent initiation and along the initial descent azimuth which cannot be reached flying the type of paths considered in this study, i.e. equilibrium flight at maximum lift to drag ratio. Some less efficient (in terms of range) landing approaches, such as zero or negative lifting flight, will extend the attainable area and should therefore be examined in conjunction with bank angle programming.

Although representative values of the parameters were selected for this study, the results are still of a fairly general nature. A similar analysis using the lift coefficients and lift to drag ratios determined in Sections 3.15 and 4.8 of this report would provide a more practical basis

for defining the flight regime from which the Brass Bell can reach a given landing site.

4.13 REFERENCES

4.13.1 Postle, R. S., et al: MX-2276 Reconnaissance Aircraft Weapon System - Aerodynamics. Bell Aircraft Corporation Report No. D143-945-024, December 1, 1955

4.13.2 The Standard Atmosphere Sea Level to 300,000 Feet. Bell Aircraft Corporation - Aerodynamics Information Note #3, June 1956

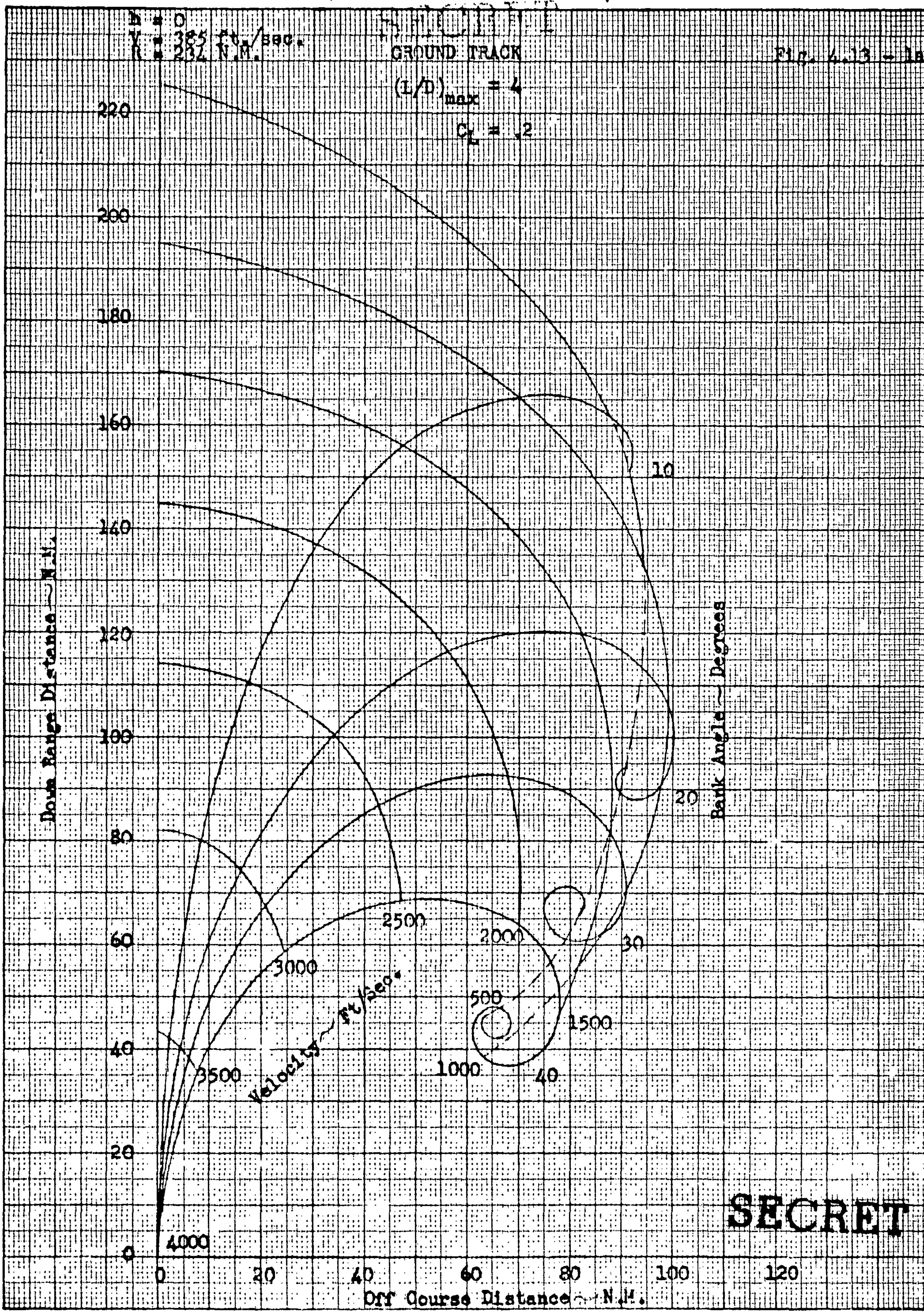
h = 0
V = 385 ft./sec.
R = 232 N.M.
GROUND TRACK
(L/D)max = 4
CL = .2
Fig. 4.13 - 1a
Down Range Distance ~ N.M.
220
200
180
160
140
120
100
80
60
40
20
0
10
20
30
40
Bank Angle ~ Degrees
2500
2000
3000
500
1500
1000
3500
4000
Velocity ~ Ft/Sec.
0
20
40
60
80
100
120
Off Course Distance ~ N.M.

SECRET

SECRET

Fig. 4.13 - D

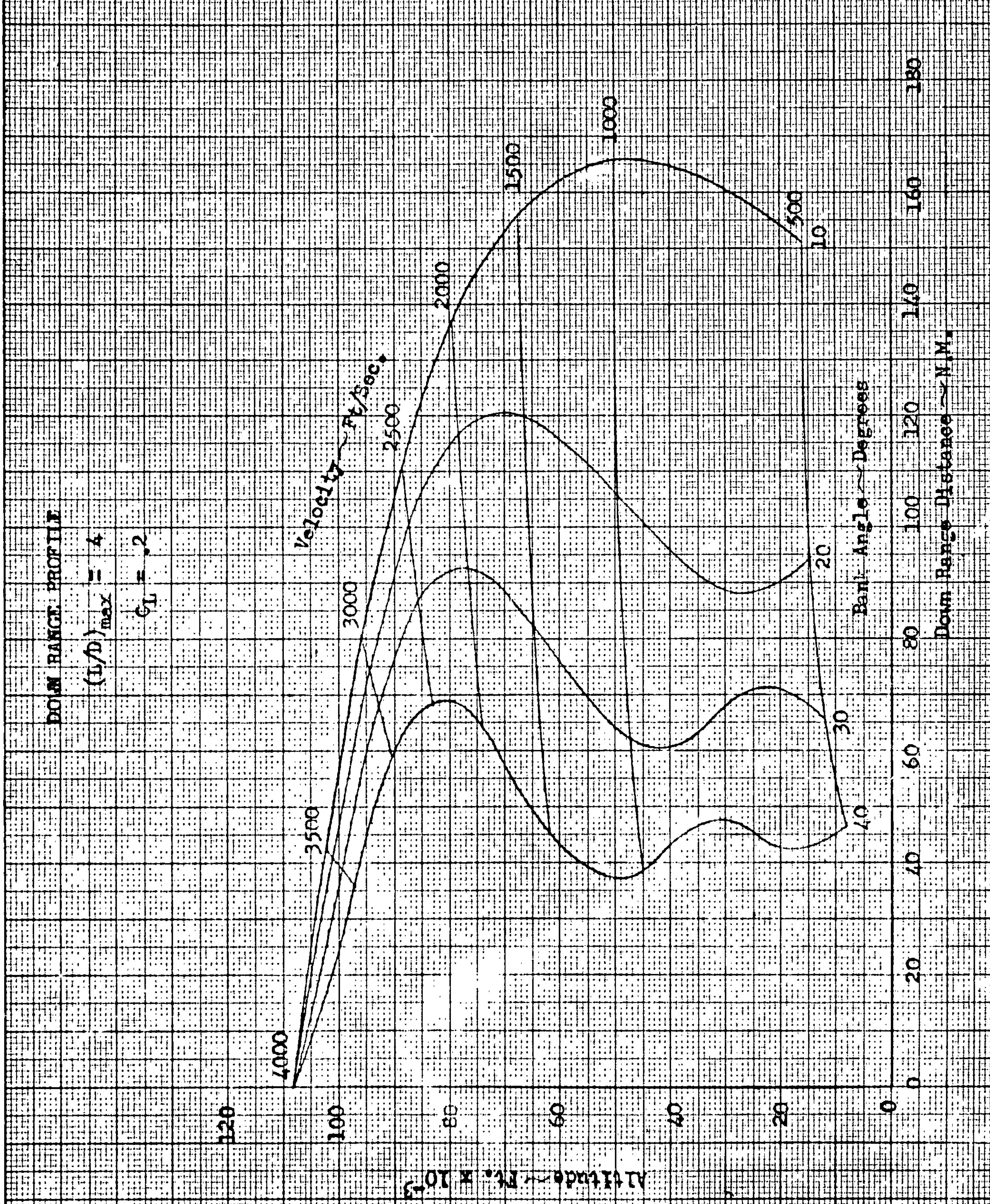

SECRET

SECRET

Fig. 4.13 - 1c

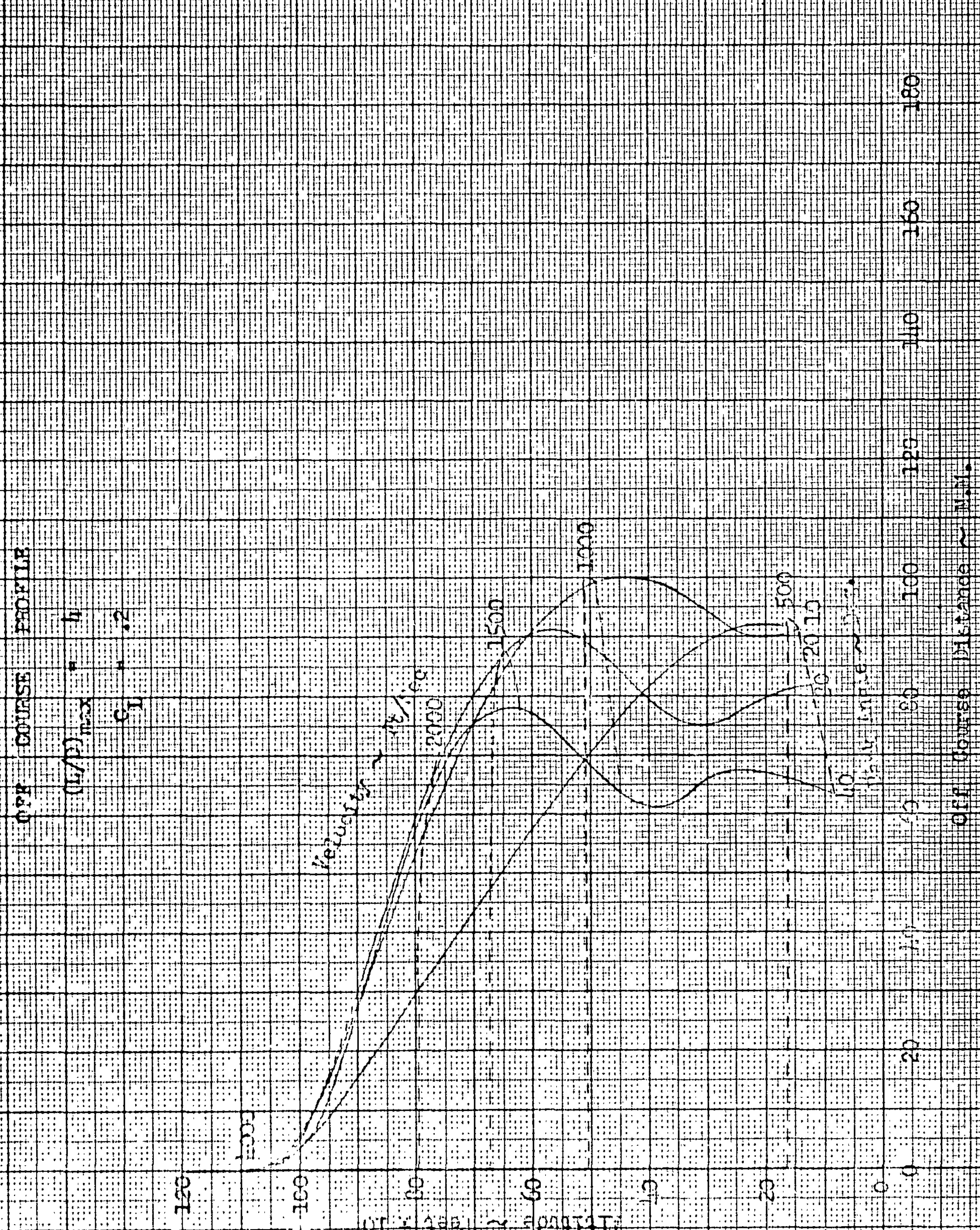

SECRET

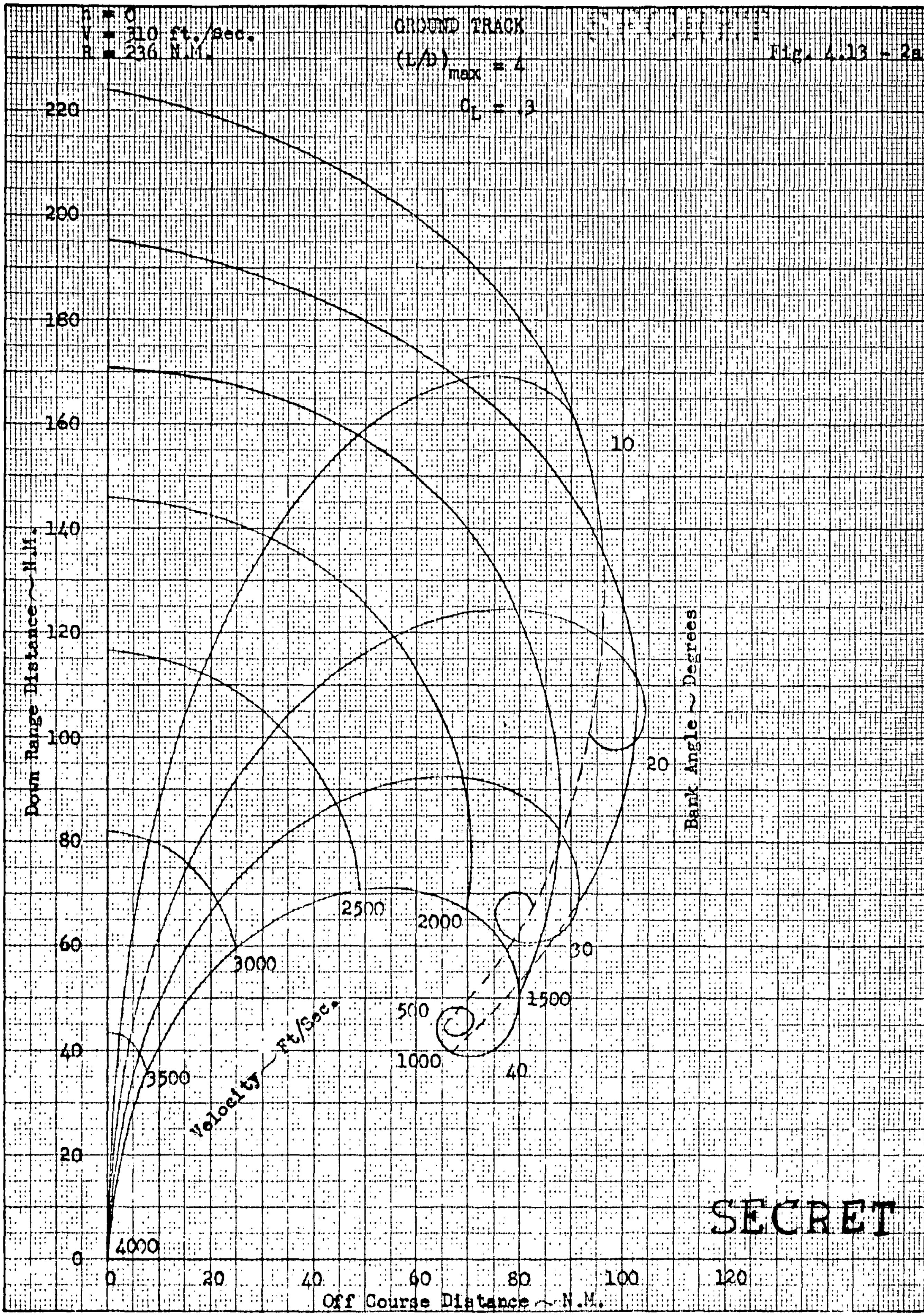
h = 0
V = 310 ft./sec.
R = 236 N.M.
GROUND TRACK
$(L/D)_{max} = 4$
$C_L = .3$
Fig. 4.13 - 2a
Down Range Distance ~ N.M.
Off Course Distance ~ N.M.
Bank Angle ~ Degrees
Velocity ~ Ft/Sec.
0
20
40
60
80
100
120
140
160
180
200
220
10
20
30
40
4000
3500
3000
2500
2000
1500
1000
500
SECRET

SECRET

Fig. 4.13 - 26

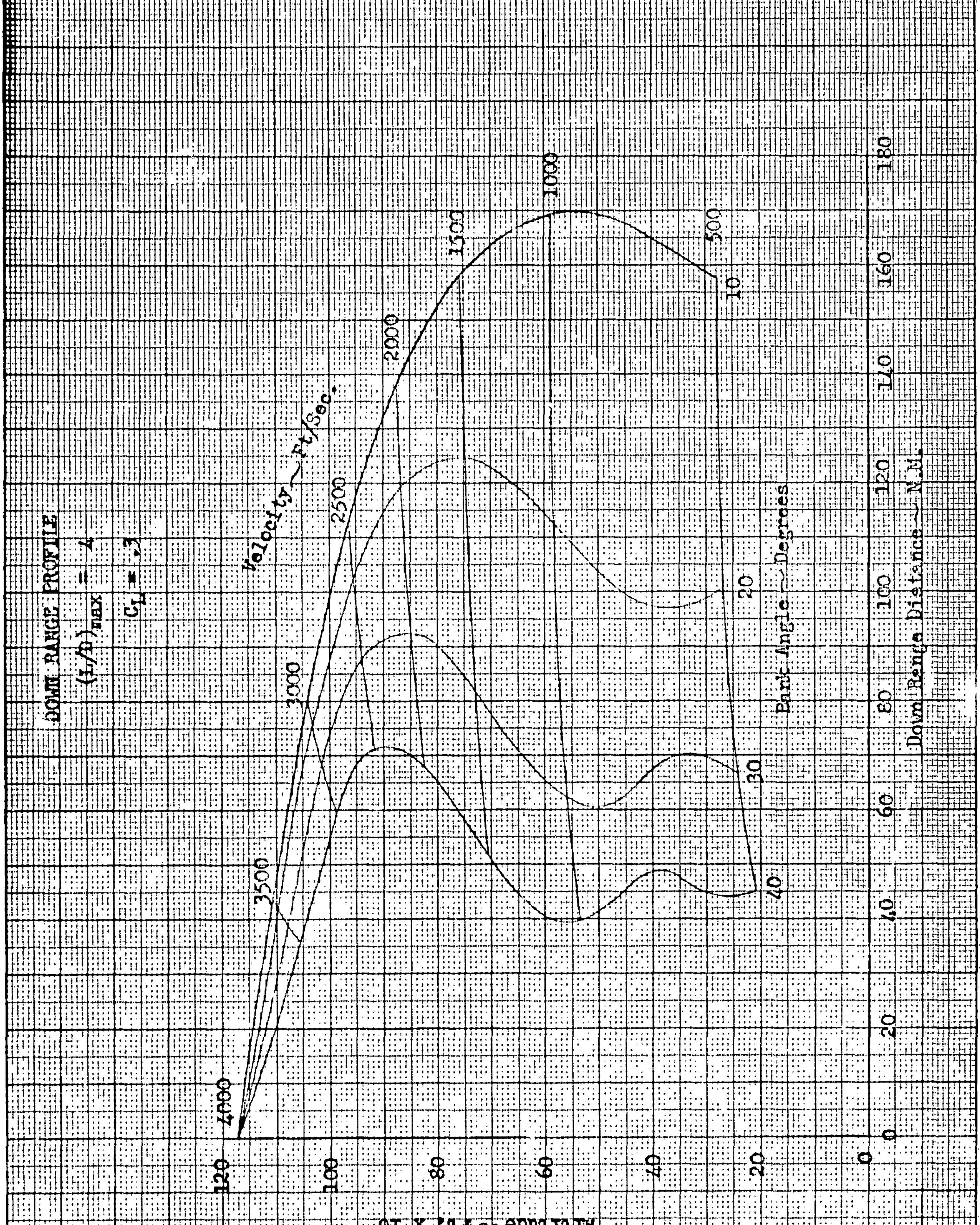

SECRET

SECRET

Fig. 4.13 - 2c

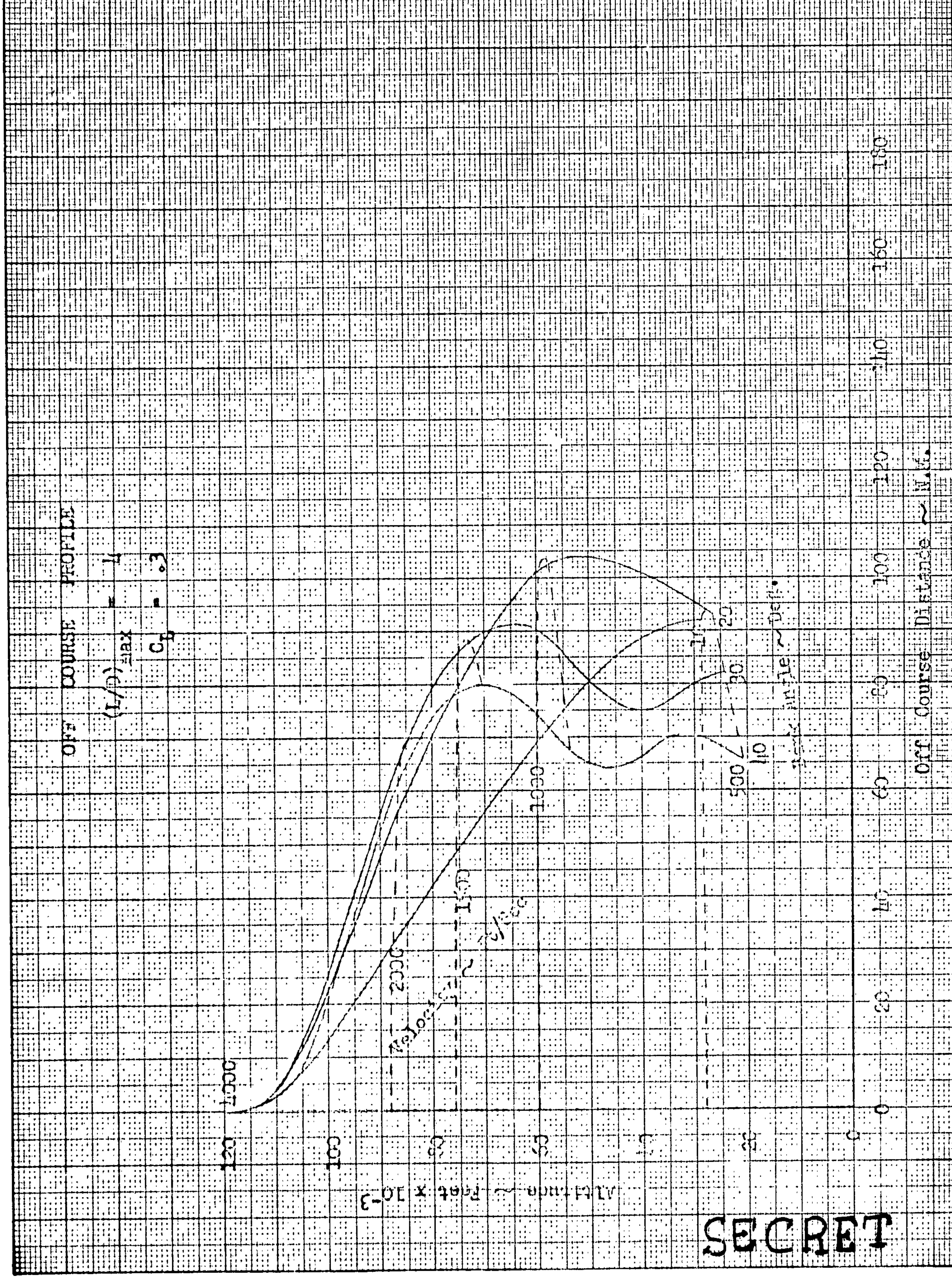

SECRET

SECRET

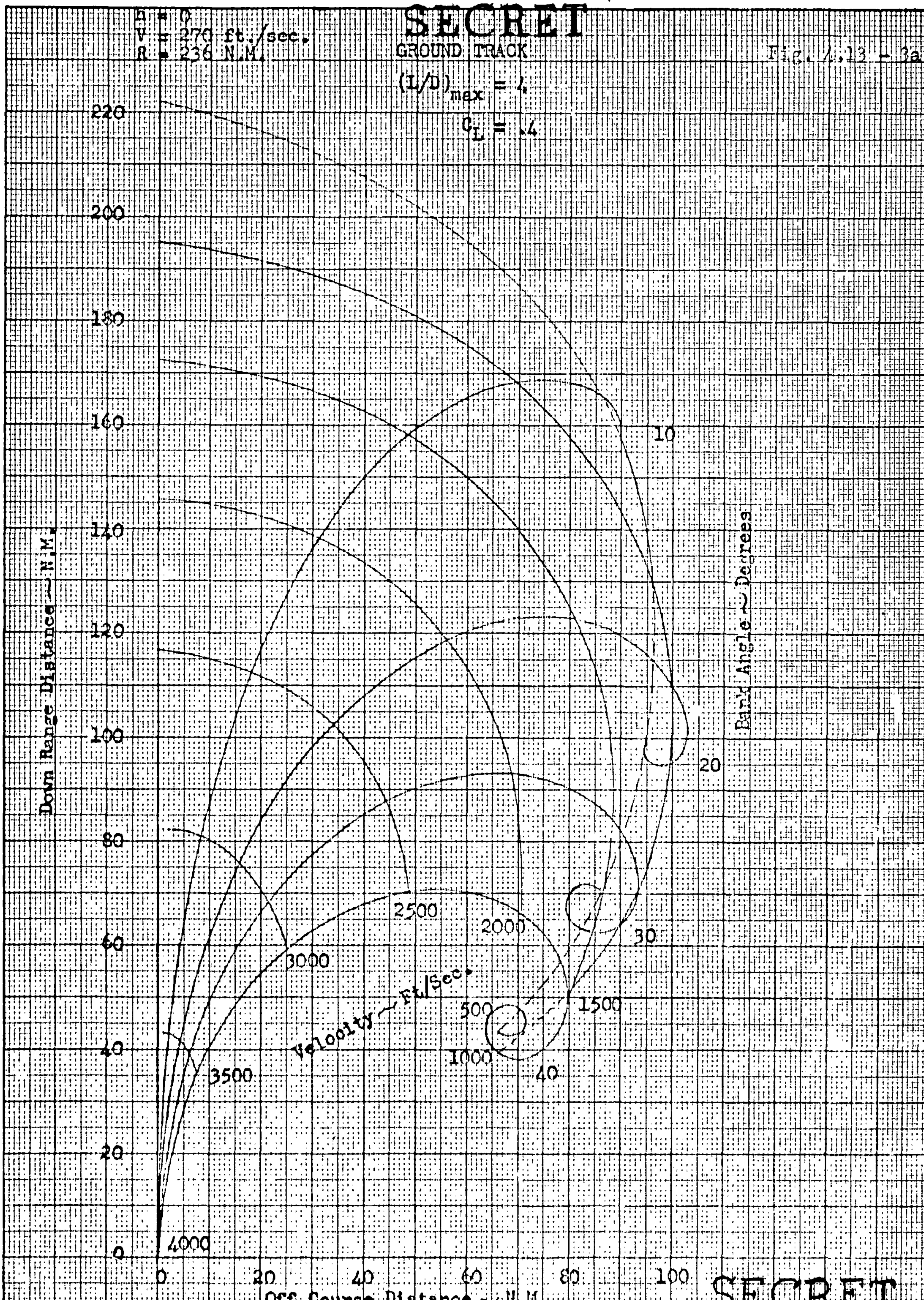
h = 0
V = 270 ft./sec.
R = 236 N.M.
GROUND TRACK
$(L/D)_{max} = 4$
$C_L = .4$
Fig. 4.13 - 3a
Down Range Distance ~ N.M.
Off Course Distance ~ N.M.
Bank Angle ~ Degrees
Velocity ~ Ft/Sec.
0
20
40
60
80
100
120
140
160
180
200
220
10
20
30
40
500
1000
1500
2000
2500
3000
3500
4000
SECRET

SECRET

Fig. 4.13 - 3b

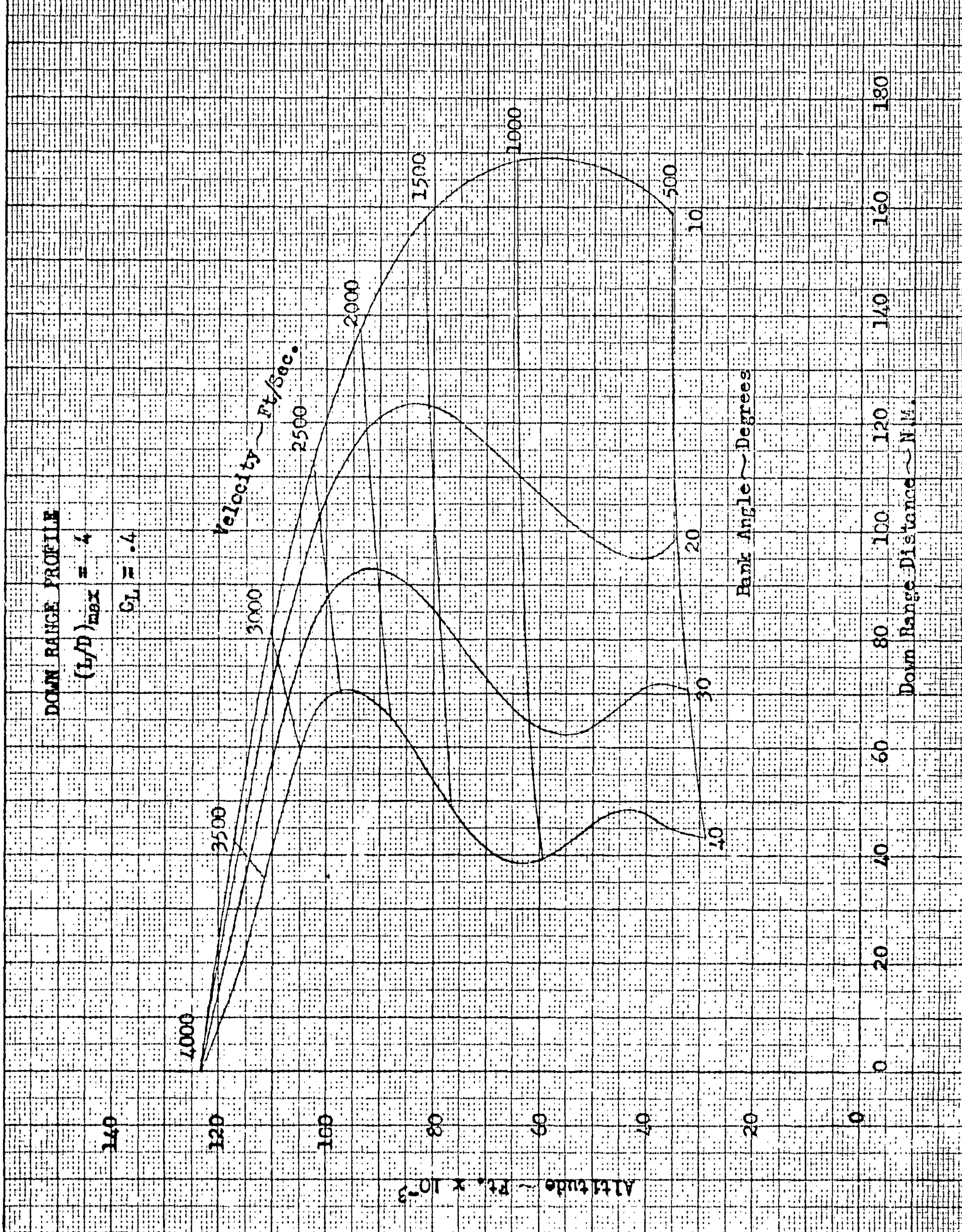

SECRET

SECRET

Fig. 4.13 - 3a

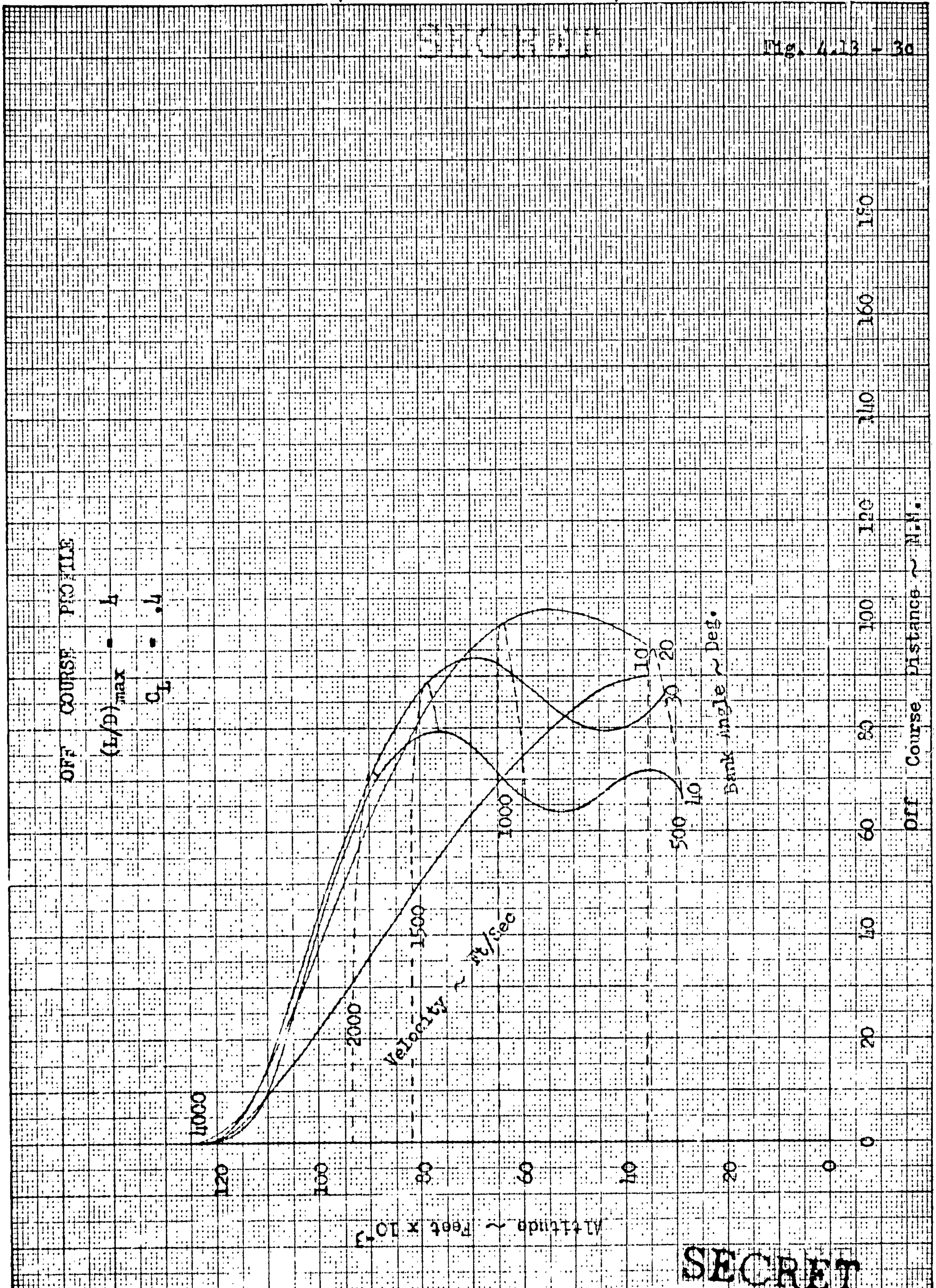

SECRET

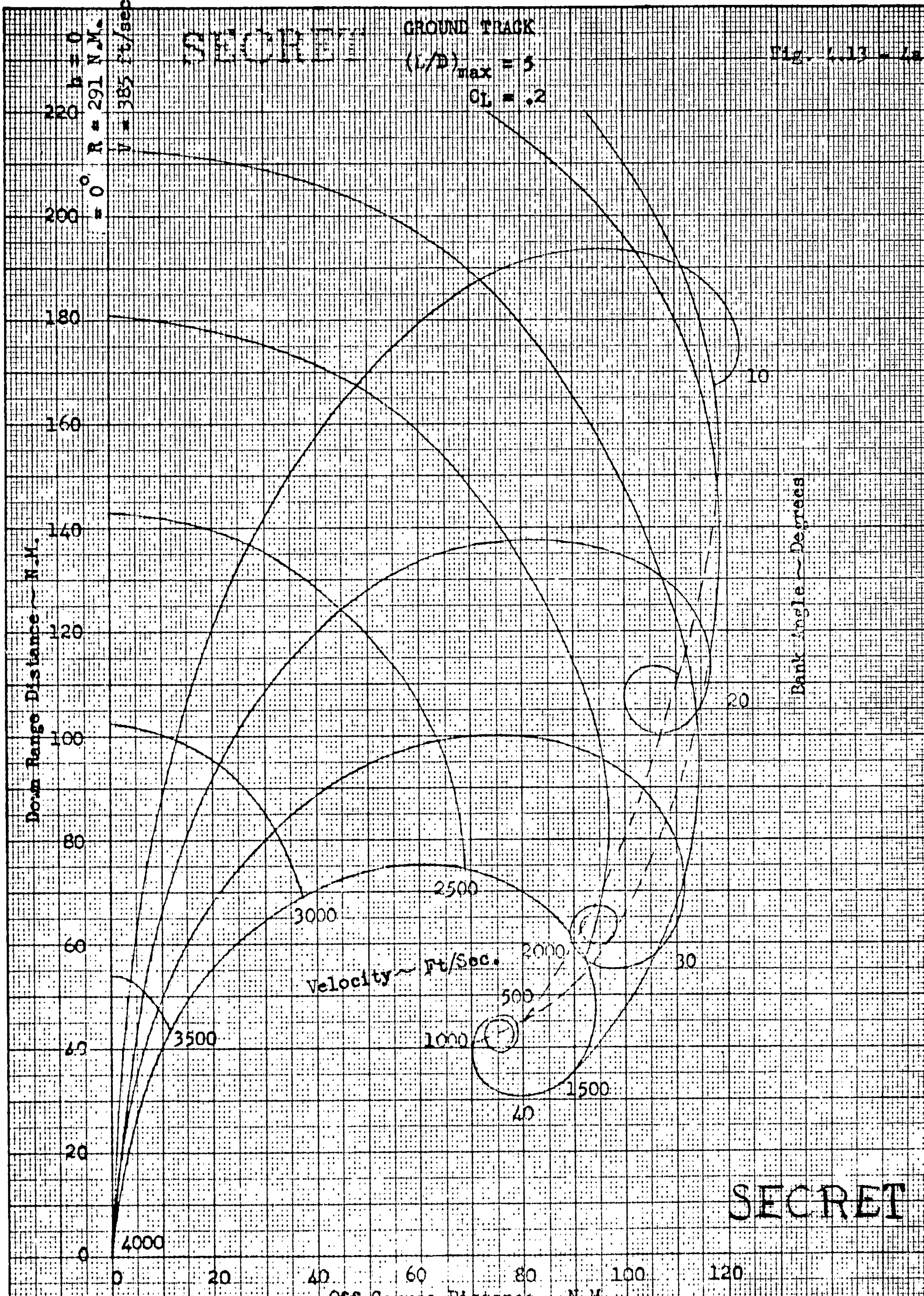
SECRET
GROUND TRACK
$(L/D)_{max} = 5$
$C_L = .2$
Fig. 4.13 - 4a
$\theta = 0°$ $b = 0$
R = 291 N.M.
V = 385 ft/sec
Down Range Distance ~ N.M.
Off Course Distance ~ N.M.
Bank Angle — Degrees
Velocity ~ Ft/Sec.
10
20
30
40
500
1000
1500
2000
2500
3000
3500
4000
0
20
40
60
80
100
120
140
160
180
200
220
SECRET

SECRET

Fig. 4.13 - 4b

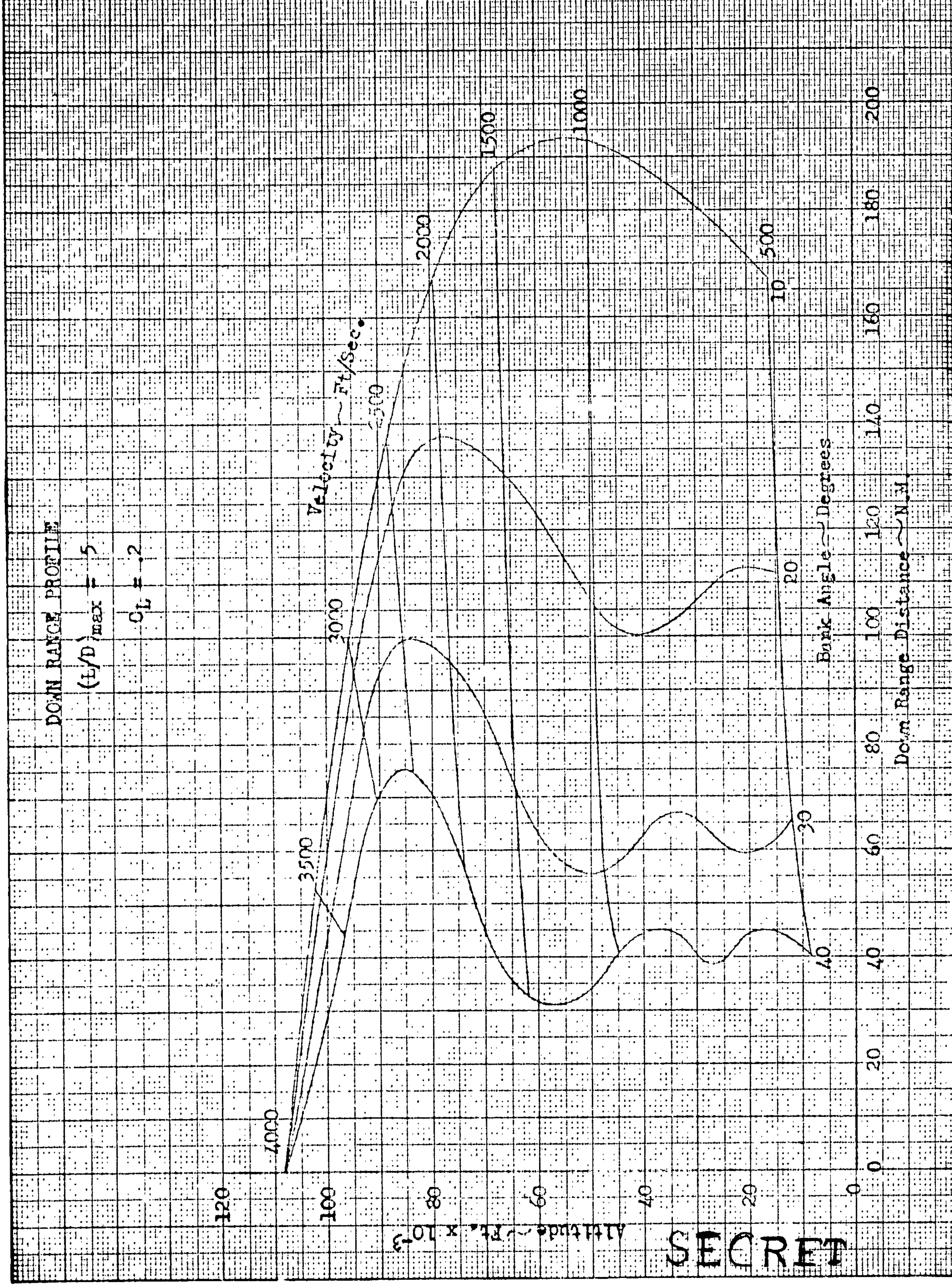

SECRET

BY ______ DATE ______ | **BELL** *Aircraft* CORPORATION | MODEL ______ PAGE 4-146

CHECKED ______ DATE ______ | | SHIP ______ REPORT D143-945-033

SECRET

Fig. 4.13-4c

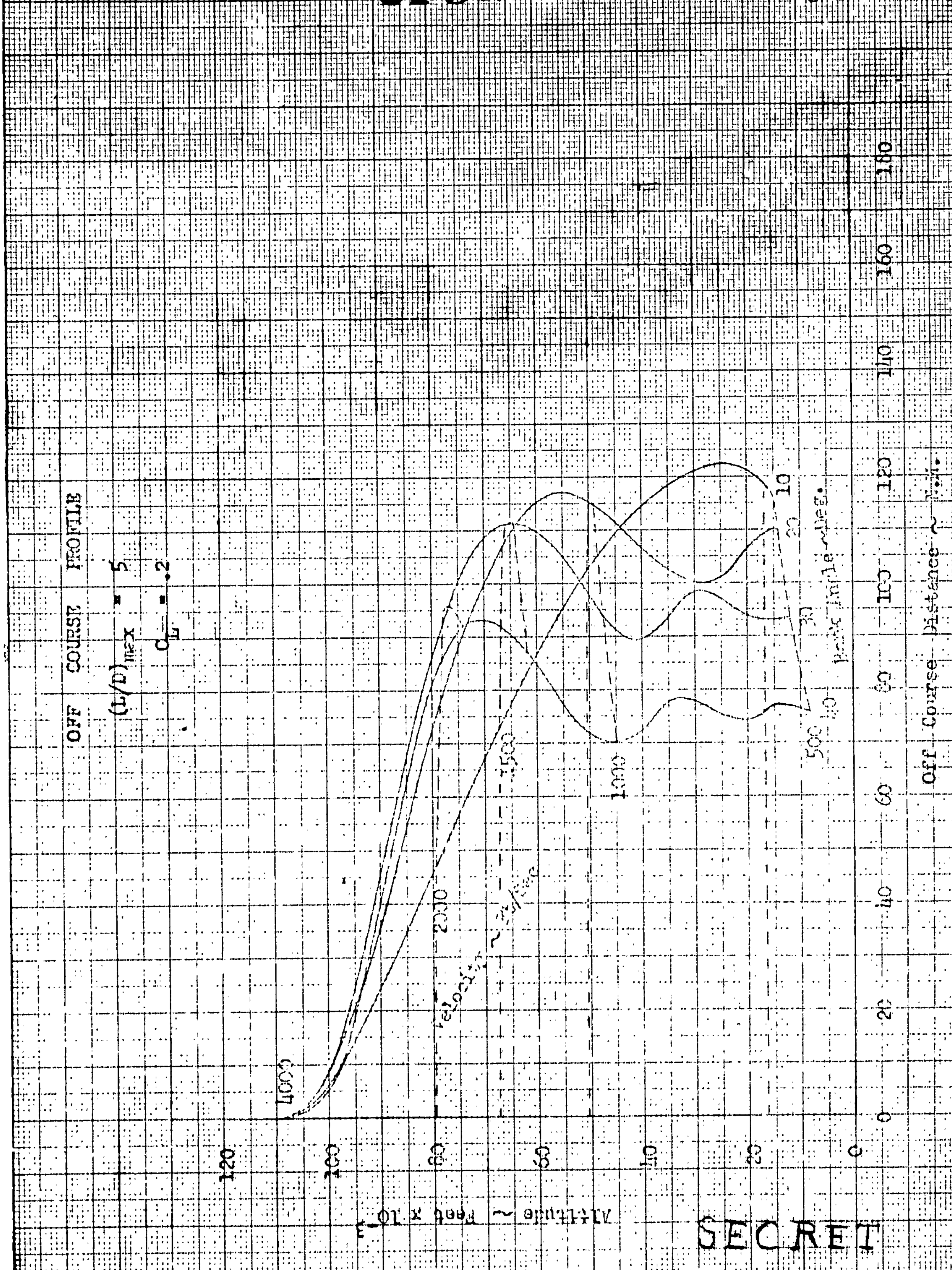

SECRET

SECRET

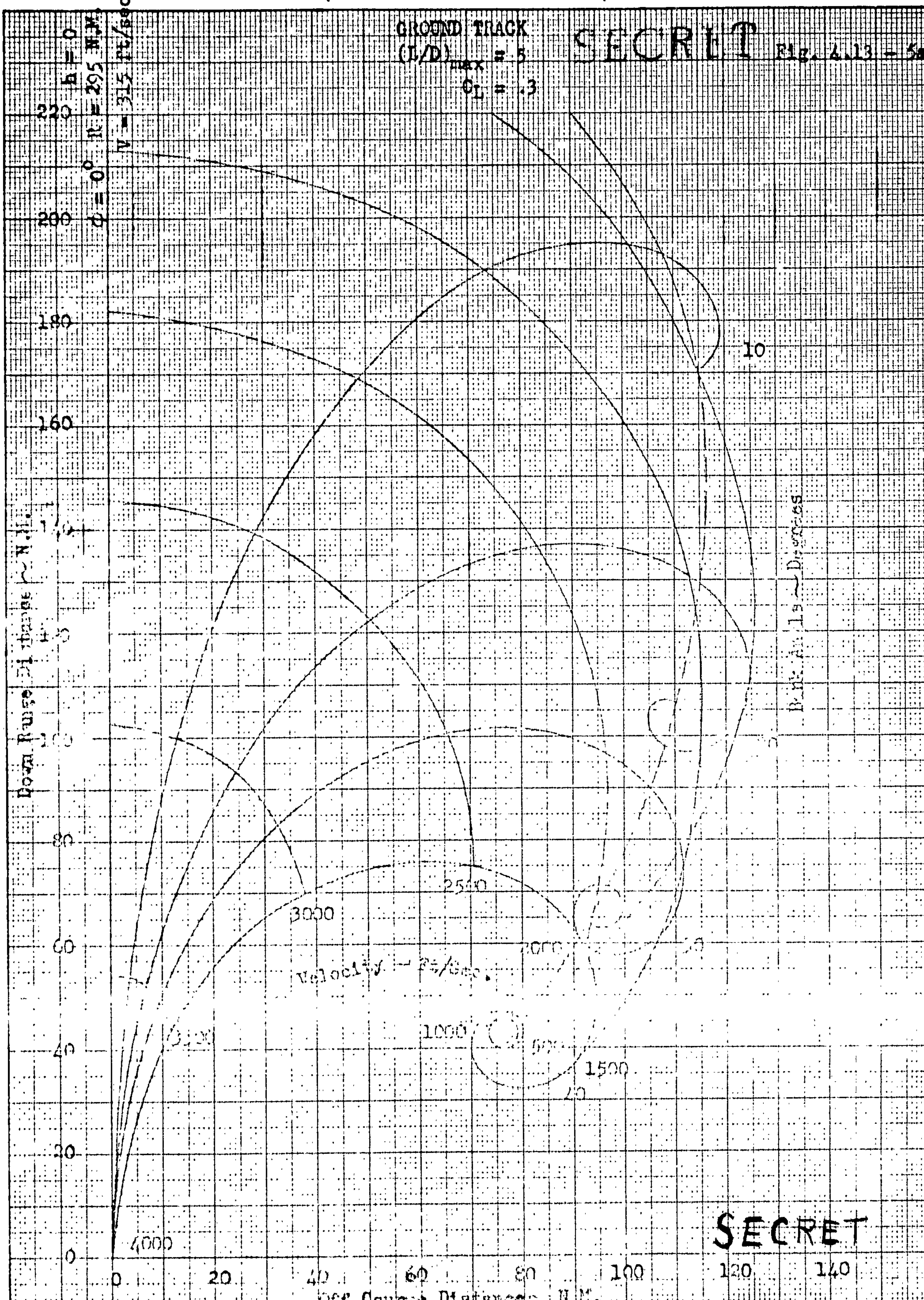

SECRET

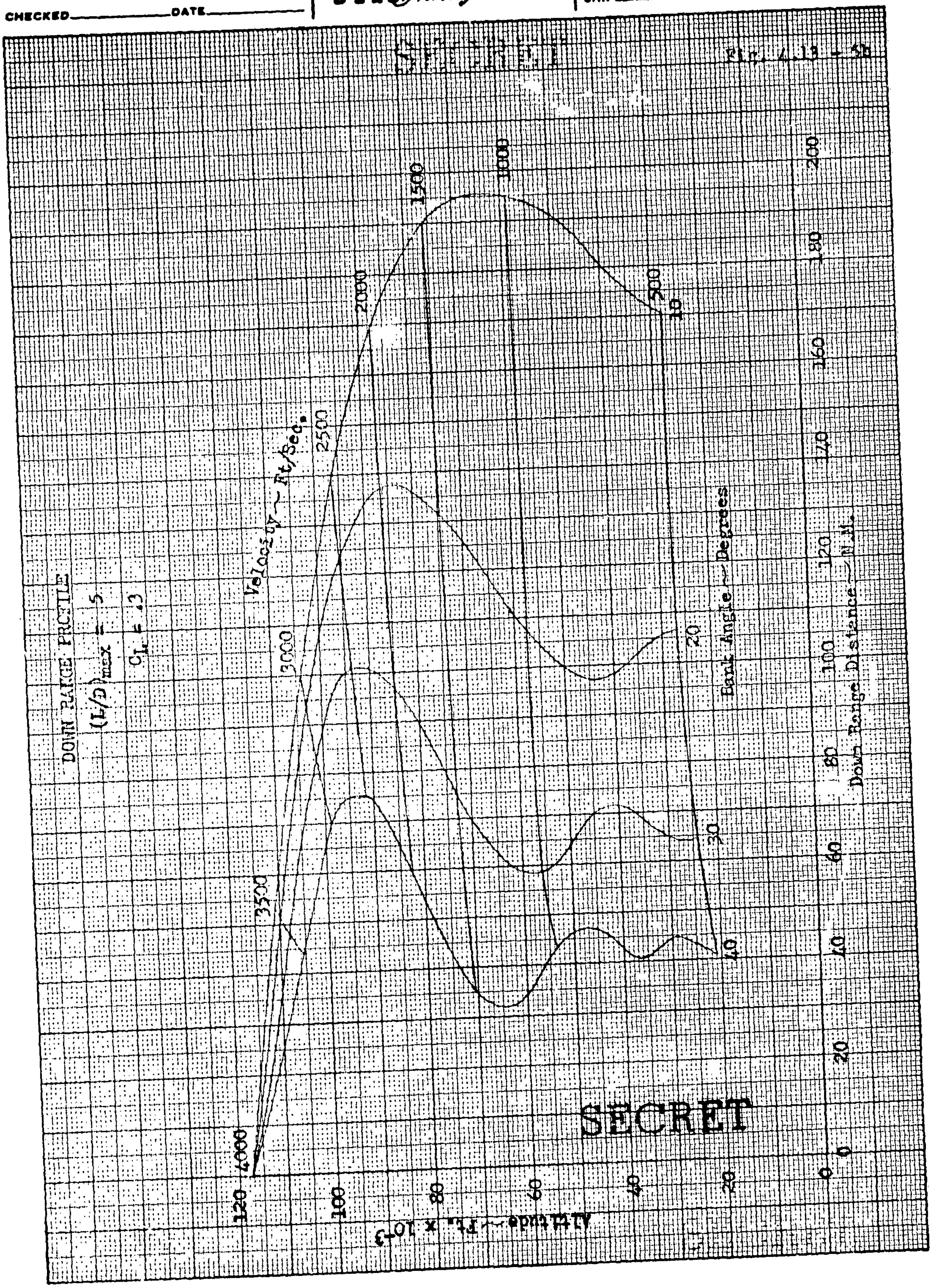
SECRET
Fig. 4.13 - 5b
DOWN RANGE PROFILE
(L/D)max = 5
CL = .3
Velocity ~ Ft/Sec.
4000
3500
3000
2500
2000
1500
1000
500
Bank Angle ~ Degrees
10
20
30
40
Down Range Distance ~ N.M.
0
20
40
60
80
100
120
140
160
180
200
Altitude ~ Ft. x 10-3
120
100
80
60
40
20
SECRET

SECRET

Fig. 4.13 - 50

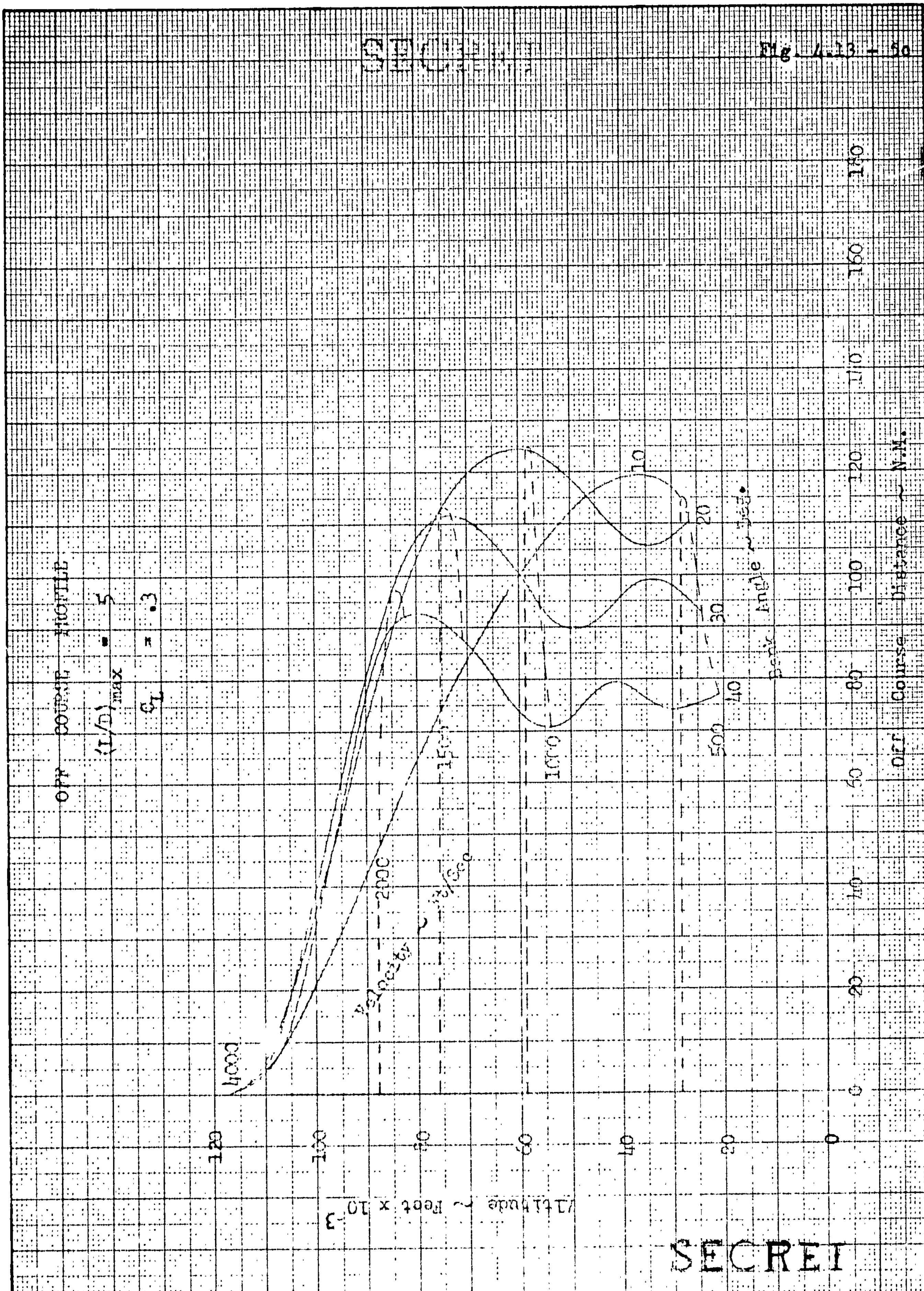

SECRET

SECRET

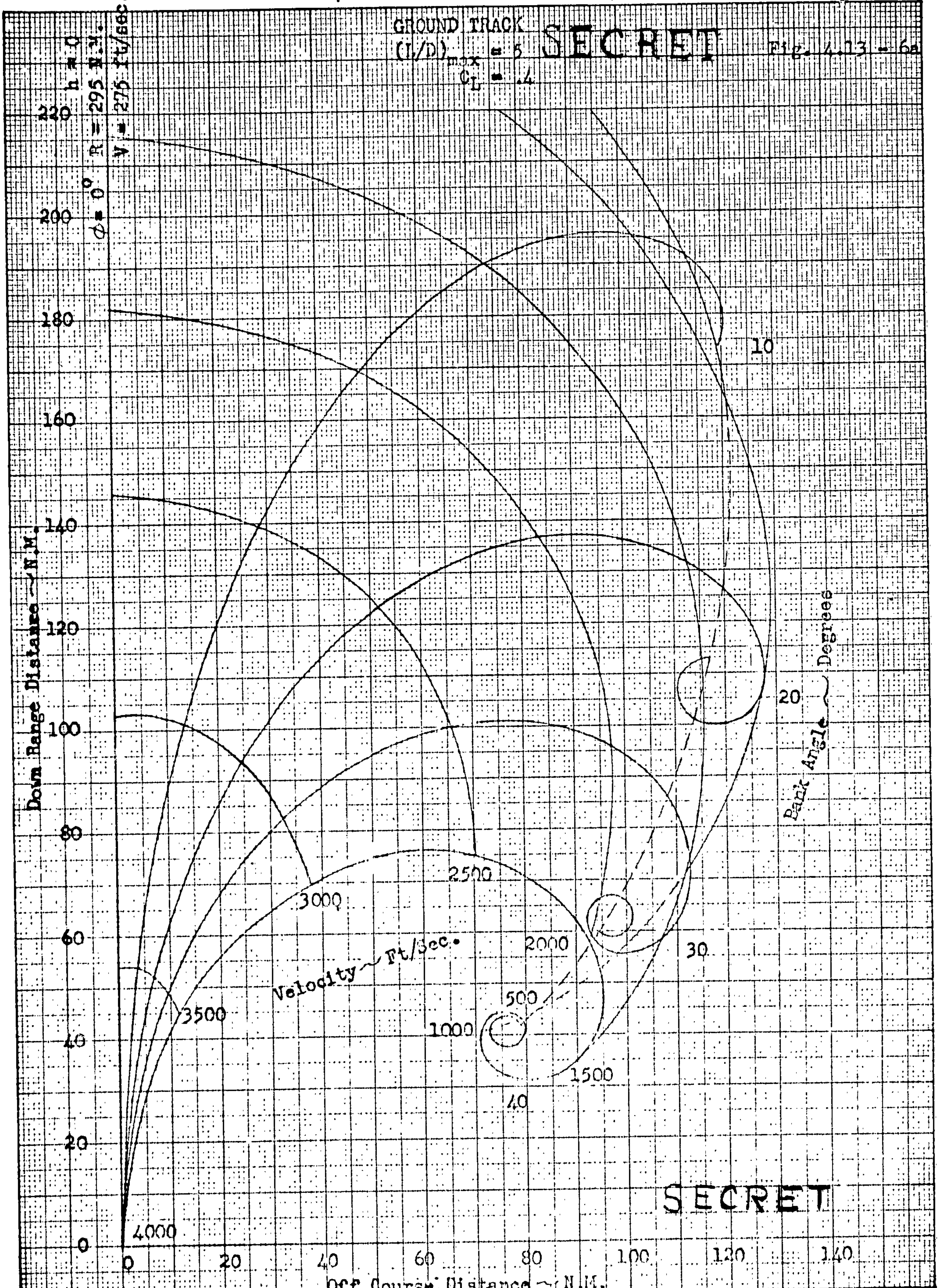

SECRET

SECRET

Fig. 4.13 - 6b

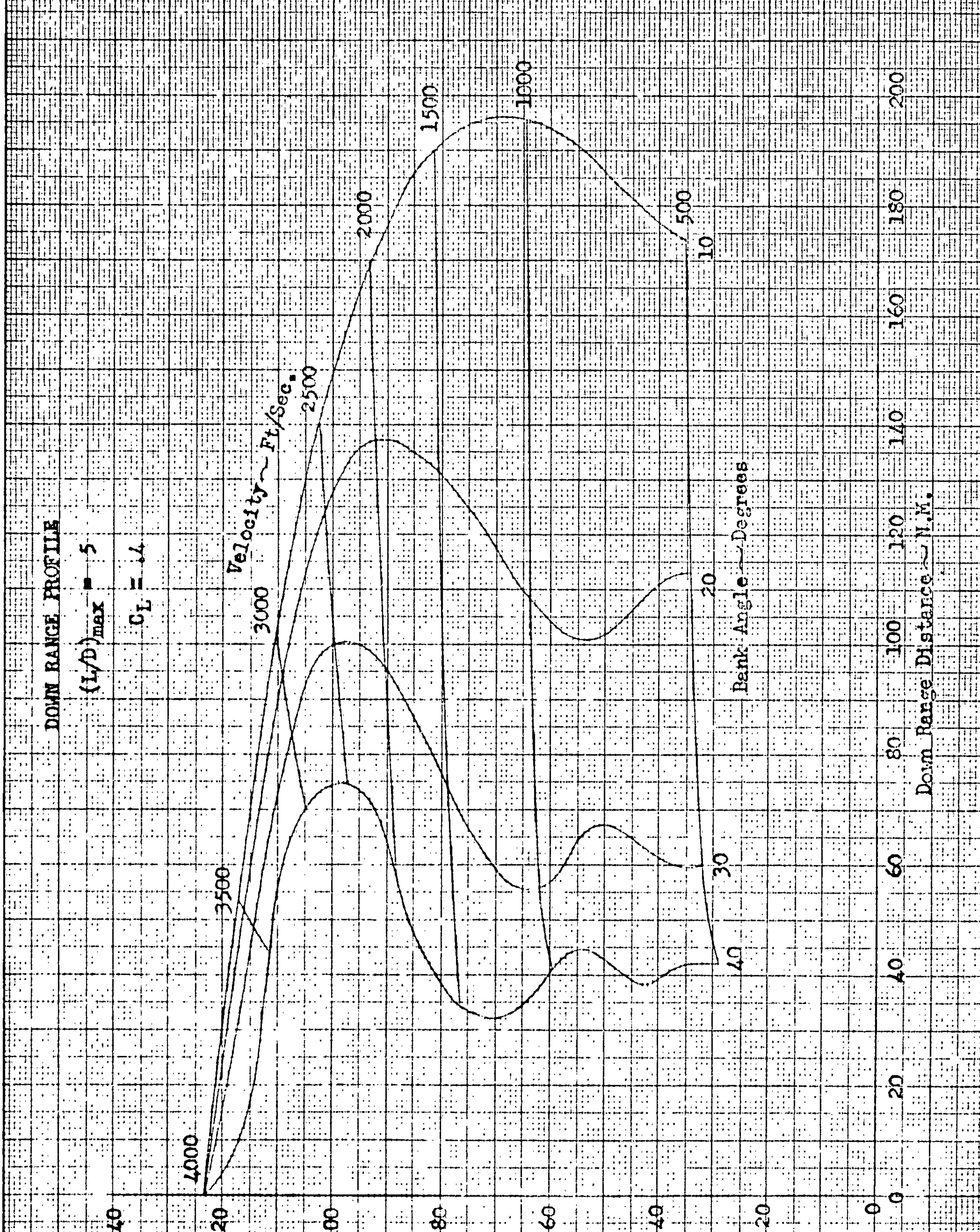

SECRET

SECRET

Fig. 4.13 - 6c

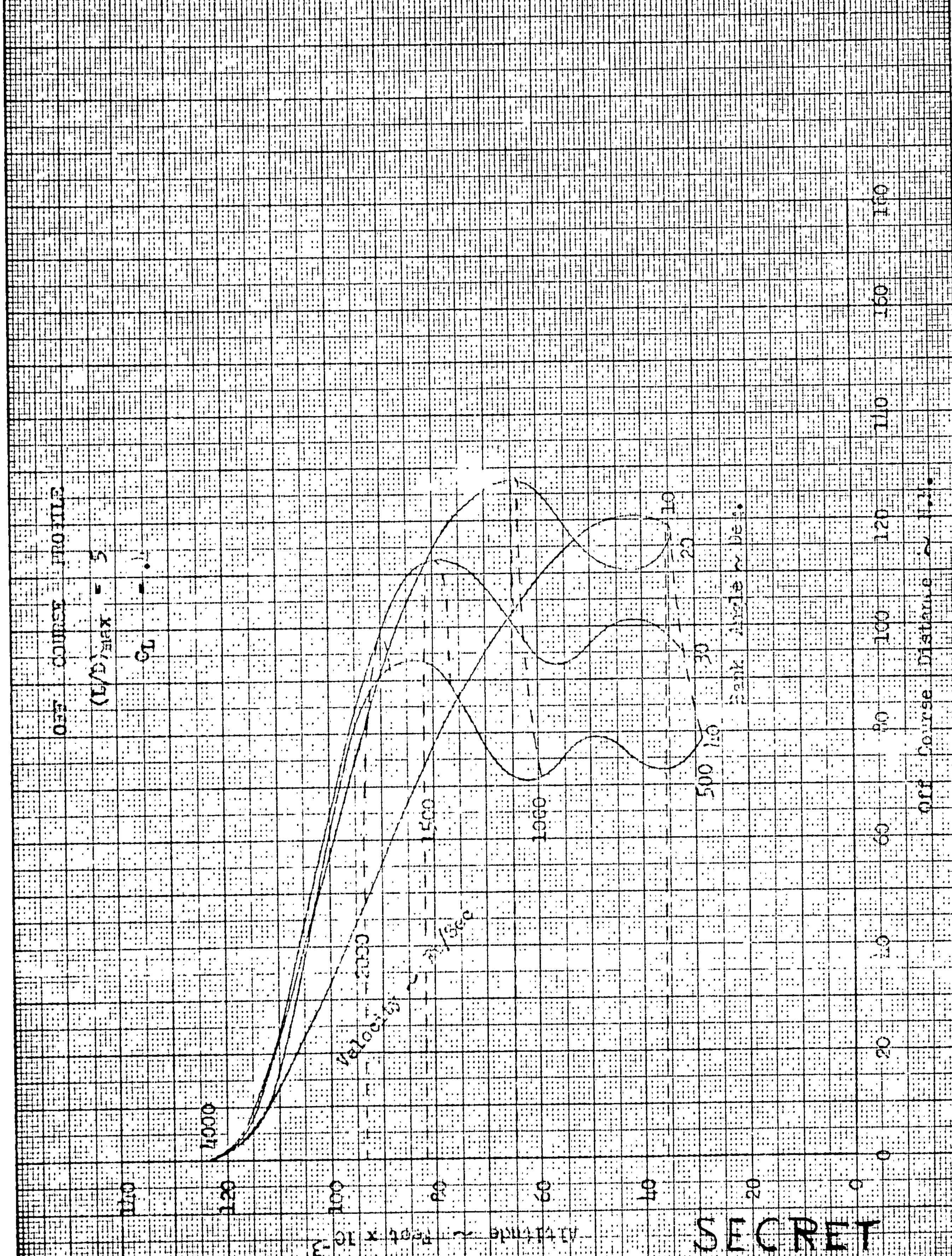

SECRET

SECTION 5

CONCLUSIONS AND RECOMMENDATIONS

5.1 INTRODUCTION

The conclusions and recommendations presented in this section are based not only on material presented in the body of this report but also on the results of the work of others. This work was often far removed from that of aerodynamics, however, the interdependence of the many fields of endeavor involved in a design of a system such as Brass Bell often necessitates compromises to be made to aerodynamic design. In some instances the results of this other work will require that additional aerodynamic studies be conducted before final conclusions can be drawn and final recommendations made.

5.2 AERODYNAMIC CONFIGURATION

In the course of the studies pertaining specifically to the preliminary configurations of this report several points of interest to aerodynamic design have been uncovered. These are presented below:

1) The wing sweep should be increased. This will result in a lighter structural wing weight per square foot which will in turn decrease the required wing area. This decrease in dead weight will be reflected in a lower gross weight at take-off. Increasing the wing sweep will also decrease the drag of the rounded wing leading edge and thereby increase the glide range.
2) Static longitudinal stability can be achieved over the entire speed range for the required lift conditions. The use of an autopilot will permit the slightly inherent instability at the low angles of attack.
3) It is necessary to use lower vertical surfaces to provide static directional stability at the high Mach numbers, as they are the most effective and least costly means in terms of drag.
4) Adequate longitudinal control can be provided by wing trailing edge surfaces. It appears feasible to design to very low static margins at flight conditions and achieve low trim requirements at high speeds by permitting unstable pitching characteristics at angles of attack below flight angles.
5) Reaction controls may be necessary to provide control and increased stability in yaw. The small span of the lower vertical surfaces, necessitated by the ground clearance requirements,

makes the attachment of adequate rudder surfaces impractical. Exhausting coolants and the exhaust of auxiliary power unit could be used to provide all or part of the necessary side force.

6) The proposed aircraft can achieve a range of approximately 5500 nautical miles. It will be necessary to fix more exactly the trim requirements and attendant control surface drag before a more accurate estimate of range can be calculated. However, the small trim requirements at Mach numbers above 10 (where the largest range increment is attained) would serve to indicate only a slight variation between the range as calculated using untrimmed lift to drag ratios and that to be estimated using values of trimmed lift to drag ratios.

7) The ascent configuration of the vehicle using the "internal" type final stage is acceptable. However, the drag of the "external" type final stage during the early part of the final boost period is too high. It will be necessary to redesign this vehicle in order to reduce this drag, so required ascent performance can be attained.

An over-all conclusion can be drawn from the results of the various aerodynamic design studies of this report and applied in general to configurations. It does not appear necessary to use unusual or extreme aerodynamic configurations in order to accomplish the Brass Bell mission. This conclusion is the outcome of experience with designs which were necessarily compatible with flight conditions encountered over the entire speed range of the Brass Bell System and applicable to the manned system concept. It

SECRET

Classified only when data are entered

has been found unnecessary to make design compromises of such magnitude as to depreciate seriously the feasibility and acceptability of the configurations within any of the flight regimes. No optimization of the configuration design has yet been attempted, because the required "tools" are not yet available for this task. It is anticipated that future design work will be directed chiefly towards improving the hypersonic aspects of Brass Bell vehicles. However, on the basis of this and previous work, it is felt that this optimization for the hypersonic conditions will in any way endanger the achievement of the ultimate aim, namely: a manned hypersonic reconnaissance vehicle which is capable of operating successfully throughout the entire flight range from subsonic to hypersonic conditions.

As an aid to future configuration and design studies it is strongly recommended that "semi-development" type of testing be initiated. Sufficient experience has been gained through this and previous work to permit reasonably good selections to be made concerning various configurations and components that would prove feasible for Brass Bell application. True, tests concerning the hypersonic aspects are of prime importance, but it would be advantageous to start a process of weeding out those hypersonic concepts impractical for use at lower speeds. Even today, many problems of control, stability, and wing characteristics of extremely low aspect ratio configurations are unknown. Tests of final stage plus booster combinations from subsonic to supersonic conditions would prove extremely helpful to their aerodynamic design and invaluable to the design of an ascent path control system.

Without a doubt, the most important unknowns lie within the hypersonic speed range. But there are at least as many within the speed regimes that can be investigated using presently available facilities. Eventually such testing must be done; it would seem only reasonable to expect saving in time and money to initiate it as soon as possible.

5.3 POWERED FLIGHT

5.3.1 INTRODUCTION

The values of the over-all specific impulses of the propulsion systems of each of the two stages are based upon more complete data than in previous studies.

It is recommended that information regarding possible variations in these over-all specifics be attained. The effects of these variations on performance must be ascertained for much the same design purpose as in jet aircraft design wherein the effects of engine characteristics varying with hot and cold dry conditions are considered.

5.3.2 STAGING REQUIREMENTS

The proposed propellants allow attainment of initial glide flight conditions employing only two stages of boost without requiring propellant loading ratios that are outside the realm of present day design capabilities.

Requiring the initial stage to carry the vehicle to a specified altitude permits a more realistic prediction of staging requirements in that the specific impulse of the succeeding stage can be predicted more accurately.

The method employed in determining the staging requirements is a convenient one for rapidly estimating the effects of various design parameters upon the ascent performance. The new flight path angle programming results in an improved ascent performance and significantly reduces the required maneuvering loads of the vehicle during the initial boost phase.

Effects of other propellants upon the ascent performance should be investigated in case those proposed should prove undesirable for some reason.

Additional ascent path programming should be studied. It has been suggested that programming of the attitude angle during the ascent might prove a simpler path to control. The problems involved in instrumentation for control of a flight path angle program presently appear more complex than those required for other types of ascent paths.

5.3.3 TAKE-OFF WEIGHT

Within the limits of accuracy imposed by preliminary weight estimates, it appears reasonable to expect a vehicle capable of performing the Brass Bell mission to weigh approximately 200,000 to 250,000 pounds at take-off. The initial stage propulsion units required will be available in the near future and power plant units of the same order of magnitude of thrust as required in the final stage are presently under development.

This investigation clearly indicates the importance of reducing the dead weight of the final stage. An erroneous choice in the selection of the staging of preliminary configuration could be serious in consequence. For example, the addition, of only 500 pounds to one of the "internal" type configurations completely removed it from any further consideration. Thus, it is strongly recommended that growth capability be afforded an important position in the selection of preliminary configuration.

A take-off thrust level at 300,000 pounds is sufficient for Brass Bell application. The maximum axial acceleration imposed by this thrust

upon the proposed vehicles is not serious enough to cause undue concern for the crew.

The lower take-off weight of the two stage vehicle employing an "external" type final stage is indicitive of the advantages to be realized with even "unpowered staging". So long as weight is carried, expendable coolant has to be provided. (This is a direct analogy to providing additional propellants, as in the case of powered cruising flight, to account for additional dead weight.) It is recommended, as an effective means to reduce take-off weight, that all weight be jettisoned as soon as it ceases to be of importance to the performance of the system. As a source of weight in this category there are such things as: propulsion units, propellant tankage, coolant tankage, coolants, pressurizing gases, etc.

5.3.4 ASCENT FLIGHT PATH

The ascent paths of the proposed vehicles are such as to require small lifting forces on the vehicles. This should prove advantageous to achieving the low structural weight required for vehicles of this type. By the addition of only small amounts of take-off thrust it is possible to retain a particular schedule of staging with its attendant ascent path characteristics even though the final stage weight increases. This is an important finding because at some later time the reduction of the problems involved in controlling the vehicle along selected ascent paths may gain importance over weight and thrust considerations.

5.3.5 TRANSIENT HEATING

The transient temperature at a ten foot effective length, turbulent flow boundary layer is less than 1500°F during the entire ascent. However,

maximum rates of temperature rise of as high as 40°F/sec occurs during the first boost.

The temperature gradient across a sandwich skin can be reduced by increasing the density of the core, increasing the emissivity of the faces, and/or decreasing the depth of the core.

The heat transmittance coefficient across the sandwich varies considerably during the ascent, hence it is not feasible to choose an effective transmittance coefficient.

A method is presented for computing the effects of both viscous heating and conduction on the transient heating of a leading edge. Conduction reduces the temperature at the stagnation point by as much as 850°F.

The maximum temperature for the radome and the camera lens are 2000°F and 1700°F, respectively. Temperature gradients in the radome are less than 20°F, however gradients of as much as 450°F exist in the camera lens.

5.3.6 MODIFYING THE FLIGHT PATH ANGLE PROGRAM DURING THE FINAL BOOST PERIOD

It is possible to reduce the aerodynamic lifting load upon the final stage by modifying its deflection program during the final boost period. This will prove doubly beneficial by reducing the aerodynamic drag and lessening the angle of attack change required immediately after initial stage separation.

5.3.7 EFFECT OF WING LOADING ON TAKE-OFF WEIGHT

Reducing the wing loading sufficiently so as to permit flight at altitudes above 200,000 feet at a velocity of 18,000 feet per second will increase the take-off weight appreciably. This is largely due to the added dead weight in the guise of additional wing weight.

It is recommended that wing loadings of 35 to 40 pounds per square foot of exposed wing (based upon the weight at the start of the glide) be used for glide vehicles of the Brass Bell System.

5.3.8 CHANGE IN BURNOUT WEIGHT

Small changes in burnout weight of the final stage will not alter the range appreciably.

It is recommended that the secondary effects (i.e. center of gravity shift, trim, and altered glide altitude conditions) also be investigated in an effort to place a practical limit upon allowable weight variations.

5.3.9 COMPLETE LOSS OF THRUST

The premature loss of thrust can more seriously affect the range than an increase of burnout weight. The propellant flow control is very important and every effort should be spent to guarantee the full burning time.

As in the case of the change in burnout weight the secondary effects should be studied. However, in the case of propellants, it is feasible to jettison them after the power plant is shut down. In this way the changes in trim, etc would only be limited to a short time period.

5.3.10 INCREASING THE SPECIFIC IMPULSE OF THE INITIAL STAGE'S PROPULSION SYSTEM

A small decrease in take-off weight can be realized by increasing the specific impulse from 245 seconds to 254 seconds. However, this increase in specific impulse is attained by using a single thrust chamber.

It is recommended that the two chamber propulsion unit be used as it can more easily provide satisfactory control moments. The estimated saving in weight is too small to be of consequence at this phase of the design.

5.3.11 INITIAL STAGE PROPELLANT LOADING RATIO

A reasonable change in the dead weight of the initial stage booster (propellant weight constant) can alter the estimates of the take-off weight by approximately five percent.

The weight estimates of the initial stage booster should soon be afforded the same degree of refinement that the final stage has received in the course of this study.

5.3.12 FINAL STAGE PERFORMANCE

Since the over-all study has indicated the advantages of employing a final stage having a large propellant loading ratio, it is possible to achieve good performance (altitude and velocity) from the final stage alone. However, this would necessitate air launching the vehicle from some appropriate carrier.

More severe air loads will be encountered during this air launch than in a normal operational flight. The extent and effects of the necessary structural weight increases must be fully evaluated before an operational vehicle design is compromised. In addition, designing for acceptable low speed stability characteristics of a fully loaded final stage can result in a configuration completely incompatible with high speed requirements.

5.3.13 MAXIMUM PERMISSIBLE BURNOUT WEIGHT OF A FINAL STAGE

The maximum addition to the dead weight of a specific final stage is limited by the available thrust at take-off. When the take-off thrust is limited to 300,000 pounds the permissible increase to the dead weight of the proposed "internal" type final stage is about 3000 pounds. Increasing the dead weight beyond this point without increasing the propellant weight will make it impossible to reach the required initial glide conditions when using only 300,000 pounds of thrust at take-off.

Additional investigations should be undertaken to determine the effects of employing greater thrust at take-off as might be provided by an auxiliary propulsion system. At some time during the initial boost phase when the primary propulsion has increased its thrust due to the altitude effects this system could be jettisoned. It is anticipated that use of short time auxiliary thrust could prove beneficial by allowing a greater weight growth potential for the Brass Bell System.

5.3.14 CONDITIONS AT INITIAL STAGE SEPARATION

The initial stage booster separates rapidly from the final stage of the two stage vehicle employing an "internal" type final stage. It will be necessary to add drag or a thrust device to the cylindrical first stage booster of the other type of proposed vehicle to insure the same positive separating force.

The present design and/or thrust level of the "external" type final stages is unacceptable. At the instant of separation the drag is of the same

order of magnitude as the thrust available, thereby preventing the necessary acceleration. This condition can be alleviated by increasing the final stage level of thrust, altitude of initial separation, and decreasing the drag of its external propulsion package.

It has been clearly demonstrated that removal of dead weight and wetted area of the glide vehicle, even after the termination of the boost phase, can be highly effective in reducing take-off weight. What does remain is to design a vehicle which allows this to be accomplished efficiently without an appreciable increase in the ratio of drag to thrust available as was the case in this investigation.

5.3.15 THRUST REQUIREMENTS DURING THE LANDING PHASE

There are small turbojet engines which can provide sufficient thrust to permit a powered landing.

However, the increased take-off weight, possible loss of glide performance, and difficulties of installation would suggest using drag devices to control the descent rather than thrust.

This is another example wherein data vital to the Brass Bell System could be attained. Flight tests of an unpowered configuration similar to ones proposed for Brass Bell could be conducted to prove the feasibility of unpowered landings under operational conditions.

5.4 UNPOWERED FLIGHT

5.4.1 INTRODUCTION

Additional work concerning the flight mechanics of a maximum range glide path is required. However, the convenient manner in which the glide range is calculated for a maximum L/D glide path enables quick comparisons to be made between configurations.

Present day methods and the extensions of these methods into the hypersonic regime are useful in the qualitative comparison of configurations. They have been and it is felt still will be convenient tools for employing in the "weeding out" still to come.

It is during the unpowered portion of flight wherein the problems most seriously affecting the aerodynamic design of the Brass Bell vehicle are encountered. As the more advanced theory and data become available, feasible and practical hypersonic vehicles will evolve only as a result of design studies and methods which have kept pace with advanced research. In the immediate future, more detailed and exact design analyses must be undertaken in order to incorporate recent research findings into the Brass Bell design. It is therefore strongly recommended that aerodynamic design studies be directed almost entirely to this unpowered portion of the vehicle's flight at the earliest possible time.

5.4.2 EFFECT OF NOSE DROOP ON THE AERODYNAMIC CHARACTERISTICS OF THE FINAL STAGE

The drooped nose fuselage penalizes the over-all design by reducing the trim lift coefficient as well as requiring greater control deflections

for trim. Both of these effects will decrease the important trim lift-drag ratio. The lower trim lift coefficient of the drooped nosed configuration will increase the heat input to the rest of the airframe for flight at the same altitude as an undrooped nose configuration.

On the basis of the above mentioned conclusions it is recommended that an undrooped nose fuselage design be incorporated into the Brass Bell design. It is further recommended that additional studies be undertaken to investigate a nose whose center line is at a greater angle of attack than the afterbody center line and extend the investigations to include possible nose-wing and nose-tail interference effects.

5.4.3 AIRFOIL THICKNESS RATIO

At the present time selection of an airfoil thickness ratio rests primarily upon structural considerations. Use of the four percent airfoil is satisfactory to the aerodynamic design of the Brass Bell glide vehicle.

So far in this design a constant thickness ratio airfoil has been used in the wing design. The effects of using a varying thickness ratio between wing root and tip should be investigated. Such future studies should also account for leading edge, boundary layer, and three dimensional effects which are especially important during the high Mach number, low Reynolds number flight.

5.4.4 LOCATION OF THE AERODYNAMIC CENTER OF LOW ASPECT RATIO WINGS

For the purposes of preliminary design work the empirical method of Reference 4.4.3 appears more applicable to clipped delta wings.

Low speed tests of wings representative of those pertinent to Brass Bell design application should be initiated. It is further recommended to include ground and body interference effects in such tests.

5.4.5 CREW SURVIVAL

The problem of crew survival is indeed a serious one and requires considerable additional investigation before final conclusions and recommendations can be made. However, on the basis of this preliminary investigation an escape vehicle should be designed to possess as large a value of the parameter C_DS/m as possible. It is possible to employ the entire glide aircraft as the escape vehicle as it is already provided with all the necessary elements of crew protection and because of its low weight (after propellant expulsion) a reasonably high value of the design drag parameter can be easily attained. In addition, the problem of stabilizing an escape "capsule" may prove very difficult, whereas the aircraft must already possess adequate static stability.

The modifications to the glide aircraft design, if any, necessitated by employing the vehicle itself the means of escape should be investigated.

5.4.6 ERRORS IN INITIAL GLIDE ALTITUDE

It does not appear as if reasonable errors in attaining the correct pressure altitude for the initiation of the glide will cause serious variations in range.

By merely controlling the aircraft such that the maximum L/D is continually attained, it will be possible to fly a path resulting in near

maximum glide range. Since the aircraft tends to seek the correct pressure altitude corresponding to the lift coefficient for maximum L/D it will be unnecessary to sense ambient pressure for glide path control.

However, a further study is warranted. The combined effect of γ as well as $\dot{\gamma}$ being other than zero at the initiation of the glide requires investigation as this preliminary study assumed the glide to start with $\gamma = 0$. As a result of this study it is felt that initial glide conditions wherein the flight path angle is other than zero will more seriously alter the glide range.

5.4.7 APPROXIMATING FUNCTION FOR THE LIFT TO DRAG RATIO

This function approximates the actual lift-drag ratio characteristics of a typical vehicle very closely. It is a simple expression which should prove helpful in the simulation of the glide flight.

5.4.8 GLIDE PERFORMANCE

Both of the glide vehicles investigated in this report were capable of attaining a ground to ground range of at least 5500 nautical miles. Very little difference in range existed between the two types. The "external" type glider covers the glide portion of the range at altitudes higher than the "internal" type and therefore would be subjected to slightly lower temperatures. This was due to the slightly lower glide wing loading of the former configuration (based upon exposed wing area).

In the course of the drag calculations, it became apparent that reduction of the sweepback of the wing leading edge appreciably reduced the range.

A preliminary estimate of the glide range had been made by extrapolating previous calculations for a configuration with a 75 degree sweptback wing to an initial velocity of 18,000 feet per second. This preliminary work indicated a glide range of 5500 nautical miles as compared with the present calculated results of 5000 nautical miles. It is therefore recommended that the wing sweep be increased to 75 degrees. This will reduce the drag of the rounded leading edge as well as increase the lifting effectiveness of the fuselage afterbody. (The area of fuselage included between the wing root chords is assumed to be subjected to the same pressures as the wing. Thus, increasing the wing root chord effectively increases the wing area without additional exposed wing area.) As a result of this increased sweep the glide range should be increased approximately 300 nautical miles for the same initial glide velocity.

5.4.9 STATIC LONGITUDINAL STABILITY

Both configurations can be designed for reasonable static margins at the conditions encountered in the unpowered portion of flight. The effects of boundary layer - shock wave interaction upon the results have not been fully investigated. It is expected this effect would move the neutral point forward, but would decrease in importance as the angle of attack increased and speed decreased.

The aft travel of the center of gravity during the glide was helpful in preventing extreme changes in the static margin from the hypersonic to subsonic conditions.

It appears that the wing positions shown for both configurations (see Figures 2-1 and 2-2) were slightly too far aft for the actual range of center of gravity position extimated for each. It is therefore recommended that the wings of each glider configuration be moved forward by an amount equal to five percent of the exposed wing mean aerodynamic chord. This will reduce the trimming moments required during flight while still maintaining a reasonable static margin for stability at the flight C_L's. An autopilot can easily accommodate the unstable characteristics at low angles of attack, but just as present day aircraft are not allowed to enter the unstable regions usually associated with flight at high angles of attack this aircraft should be kept from the low angles during those portions of flight where unstable moments are encountered.

As the cg travel associated with consumption of coolants is appreciable, ways should be investigated to advantageously program the storage of the unused quantities so as to improve both stability and trim characteristics of the aircraft.

5.4.10 CONTROL DEFLECTIONS FOR TRIM DURING GLIDE

Carefully designing of the travel of the center of gravity during the glide can result in configurations which require small deflections of the controls for trim during the high Mach number portion of the glide. As a result, the glide range lost due to additional control surface drag can be held to a minimum. Hence, the forward location of the center of gravity of a Brass Bell vehicle at the start of the glide must be determined not only by stability but control requirements as well. With an inclusion of an

autopilot in the aircraft, it might not be necessary to have inherent static stability. Under these circumstances forward location of the center of gravity would best be determined to keep trim control deflections to a minimum.

5.4.11 STATIC DIRECTIONAL STABILITY

The "external" and "internal" type glider configurations exhibit a constant degree of positive static directional stability throughout the subsonic speed regime. At supersonic speeds the "external" type configuration is shown to possess positive static directional stability at zero angle of attack to about a Mach number of 8.0 whereas the "internal" type configuration because neutrally stable directionally at about M = 3.0. It has been estimated that the internal type configuration would require about an 85 percent increase in total tail area to give positive static directional stability up to Mach number of about 8.0. The movement of center of gravity due to expulsion of coolant has been shown to have little effect on the static directional stability for Mach numbers less than 8.0. It is estimated that for Mach numbers greater than 8.0 the variation of cg with Mach number will have a significant effect on the directional stability. The present studies have assumed that the ratio of local dynamic pressure to free stream dynamic pressure, q_L/q_∞, is unity at the tail location for angles of attack near zero. Additional studies to determine the effect of q_L/q_∞ at angle of attack should be conducted in order to gain a better perspective of the stability contribution of the ventral fin in relation to that of the upper vertical tail. Studies conducted by the NACA for the X-15 project (Reference 4.11.1) have indicated large effectiveness for the ventral

fin because of the high ratios of q_L/q_∞ generated on the compression side of the wing at angle of attack. Likewise, it is shown that the effectiveness of the upper vertical tail may approach zero at the high angles of attack that may be encountered during the glide portion of the flight.

5.4.12 AERODYNAMIC HEATING DURING UNPOWERED FLIGHT

Temperatures during the glide phase of flight are less than 2000°F for both laminar and turbulent flow.

An error in the initial glide altitude will cause a change in the initial equilibrium temperature for turbulent flow of about 17°F per 1000 feet of altitude and somewhat less for laminar flow.

For a zero lift trajectory a drag parameter of 0.2 to 0.3 must be obtained in order to maintain temperatures of less than 2000°F over the major portion of the vehicle or a capsule.

5.4.13 DESCENT PATHS

The equations which were developed in Reference 4.13-1 which make it possible to evaluate the performance of a nonpowered aircraft executing a coordinated turn under constant lateral accelerations have been modified to made them applicable to constant bank angle programs. These equations have been employed to obtain curves from which it is possible to estimate the ability of the Brass Bell to reach a given landing site with a program of bank angles.

Straight-in approaches to landing sites at distances up to 280 nautical miles are possible. With bank-angle programming, landings at distances up

to 150 nautical miles to either side of the initial descent azimuth can be made. There are, however, areas close to the point of descent initiation which cannot be reached by flying with maximum lift to drag ratios.

The descent study which was made was of a general nature. A similar analysis using the lift coefficients and lift to drag ratios determined in Sections 3.15 and 4.8 of this report would provide a more practical definition of the flight regime from which the Brass Bell can reach a given landing site. The determination of such a regime should be made not only assuming maximum lift to drag ratio flights but also less efficient descents such as zero or negative lifting paths.

SECTION 6.0

FUTURE DESIGN STUDIES

6.1 INTRODUCTION

As a result of the work pertaining to the Brass Bell System reported herein and elsewhere, it appears worthwhile to affect changes to the configurations studied in this report. Although many of these changes are required primarily for other than aerodynamic reasons, it will be necessary to continue the aerodynamic analyses of new configurations in order to evaluate the importance of such changes to the aerodynamic design of a Brass Bell vehicle.

With more applicable data and better methods of analyses becoming available it will be necessary to apply them as soon as possible to the over-all design. In this manner, a more rapid evaluation of a feasible design will be achieved with the least chance of having incorrectly evaluated a design aspect of the Brass Bell System from the aerodynamic point of view.

So far, most of the aerodynamic design effort has been expended in an effort to attain a broad and general aerodynamic picture of the Brass Bell System. During the interim wherein the aerodynamic research program continues to gather data and evolve methods pertinent to the high Mach number flight regime of a Brass Bell vehicle, more detailed design analyses of representative vehicles within the more known regions of flight could profitably be undertaken.

It is not the purpose of this section to present completely an aerodynamic design program. As it is anticipated that the aerodynamic research

program will and should represent the major portion of the effort during the immediate future it is felt that this description of a few worthwhile design studies that could be initiated during this same time period will suffice.

6.2 AERODYNAMIC CONFIGURATION

The design analyses of the configurations illustrated in Figures 2.2-1, 2.2-2, 2.3-1, and 2.3-2 have indicated that the estimated weights of these configurations were low. Therefore, means were explored by which configurational changes could affect a measurable decrease in dead weight. It was found the most important weight saving could be attained through increasing the sweepback of the wing leading edge. Since this reduced the aspect ratio of the wing, decreased the taper ratio, and increased the depth of the root chord a lighter wing structure resulted. In addition, the increased length of the root chord would increase the amount of fuselage lift (from increased wing-body interaction) so that less exposed wing area would be required to attain the same effective wing loading at landing.

In addition, the increased sweep will tend to increase the L/D ratio so that it will not be necessary to reach a velocity of 18,000 ft/sec at the termination of boost in order to attain the same range as estimated for the configurations investigated herein.

A more detailed and exact evaluation of the static directional stability requirements of the Brass Bell vehicle (see Section 4.11) will be required in order to estimate more accurately the size and hence the weight of the vertical surfaces. This resultant tail size should also be checked by investigating the dynamic stability characteristics of the airframe within those regions of flight wherein present day methods are applicable.

On the other hand, it is advisable to investigate completely different configurations than previously so as to have a basis for a more general

comparison. To accomplish this purpose it will be necessary to start from scratch to design, analyze, and evaluate the configurations in much the same manner as in present and past studies.

As mentioned in Section 2.0 many of the configurational aspects of the vehicle were rather arbitrarily selected; for example, the fineness ratio of the nose. It will be necessary in the future to return to some of these general features and examine them more closely with regard to their effects on over-all vehicle design. Likewise, many of the components (i.e. wings, bodies, controls, etc) thought to be applicable to hypersonic aircraft design could be subjected to actual testing at subsonic and low supersonic speeds so that a backlog of design data concerning them would be available for future use.

6.3 POWERED FLIGHT

It is within this powered portion of the Brass Bell flight that the most productive aerodynamic design of the immediate future can be accomplished.

The study of ascent flight and attendant control requirements can proceed essentially independent of any aerodynamic effects important to successful sustained hypersonic flight. Thus, work of this nature can be of great importance to the Brass Bell System regardless of the eventual aerodynamic configuration.

In Section 3.5 studies of transient aerodynamic heating, important to structural design, have been initiated. These studies should be continued. Also, in this same section, evidence of the suitability of a temperature sustaining leading edge has been reported. This phase of study should be pursued further so that a more exact comparison can be obtained of this design with the presently proposed leading edge which is cooled using liquid metals.

A study should be initiated to investigate the aerodynamic design aspects of crew safety during the ascent. In conjunction with this more detailed study of the motion of the initial stage during separation is necessary. An investigation of the initial stage's trajectory after separation would also be of interest. The falling initial stage represents quite a hazard to personnel on the ground and an accurate prediction of its location when it hits the ground is required.

Some of the studies, discussed above, would necessarily be of a general nature, but their results would be applicable to the Brass Bell System and therefore well worth undertaking during the next phase of design work.

6.4 UNPOWERED FLIGHT

The major portion of design work pertaining to this phase of the Brass Bell flight will necessarily have to wait on the research program. However, work can be initiated which would concern itself with the lower speed range of the unpowered flight of the vehicle. Landing, low speed control and stability (static and dynamic), ground run, and investigations pertinent to landing gear design are a few of the studies which would be benificial to undertake during the immediate future.

As data and advanced methods for analyses become available they would be applied to past as well as any current studies involving the hypersonic design aspects of the Brass Bell vehicle. In this manner a more rapid evaluation of designs could be achieved rather than by waiting until the research program was completed. As the experimental research wanes it will be necessary to begin the development type testing required in any design work. Hence, this continuing familiarity with applying the results of the research program will facilitate an efficient and early start to the experimental development work.